



University
of Antwerp

Faculty of Science
Department of Biology

Elucidating the molecular mechanisms underlying grassland species in response to more persistent precipitation regimes

Thesis submitted for the degree of Doctor of Science: Biology
at the University of Antwerp

Lin Zi

Supervisor(s):
Prof. Dr. Han Asard
Prof. Dr. Hamada Abd Elgawad
Prof. Dr. Kris Laukens

Antwerp, 2024

Disclaimer

The author allows to consult and copy parts of this work for personal use. Further reproduction or transmission in any form or by any means, without the prior permission of the author is strictly forbidden.

Table of contents

List of Abbreviations.....	5
Summary.....	9
Samenvatting.....	12
Chapter 1 General introduction.....	15
1 Persistent precipitation regimes.....	16
2 Plant stress responses to altered precipitation patterns.....	17
3 Legacy effect and stress memory.....	20
4 Grassland ecosystem and species.....	22
5 Application of omics technologies to understand plant responses under climate change.....	23
6 Framework of regime shift project.....	26
7 Thesis outline.....	28
Chapter 2 Ecometabolomic analysis of the effect of more persistent precipitation regimes reveals common and tolerance related metabolic adjustments in four grassland species ..	32
Abstract.....	33
1 Introduction.....	33
2 Material and Methods.....	36
2.1 Experimental design and treatments.....	36
2.2 Fv/Fm measurement.....	38
2.3 Sample harvesting and metabolite extraction for liquid chromatography-mass spectrometry (LC-MS) analysis.....	39
2.4 HPLC-MS analysis.....	39
2.5 Processing of LC-MS Data.....	41
2.6 Statistical analysis.....	41
3 Results.....	42
3.1 Effects of increasingly persistent PRs on the mean Fv/Fm of four grassland species.....	42
3.2 Effects of increasingly persistent precipitation regimes on the metabolome of four grassland species.....	43
3.3 Identification of key metabolites that respond to increasingly persistent precipitation regimes using VIP score.....	49
3.4 Identification of metabolic pathway responses to more persistent precipitation regimes.....	53
4 Discussion.....	55
4.1 Is there a tipping point in the metabolic responses to changing PRs, and does this differ between sensitive and tolerant species?.....	55
4.2 Dry or wet start influences the impact of PRs.....	56
4.3 Increasing of amino acids is a general response across species.....	57
4.4 Responses in other chemical classes showed species-specific changes.....	59
5 Conclusion.....	61
6 Supplementary materials.....	62

Table of contents

Chapter 3 Biochemical composition changes can be linked to the tolerance of four grassland species under more persistent precipitation regimes	104
Abstract	105
1 Introduction	105
2 Materials and methods	108
2.1 Experimental design and treatments	108
2.2 Biomass measurements	110
2.3 Measurements of cell wall composition	110
2.4 Measurements of other biochemical components	112
2.5 Statistical analysis	112
3 Results	113
3.1 Effects of increasingly persistent precipitation regimes on soil water characteristics	113
3.2 Effect of increasingly persistent precipitation regimes on the biomass of four grassland species	114
3.3 Effect of increasingly persistent precipitation regimes on biochemical components of four grassland species	115
3.4 Relationship between PR, soil water characteristics, biochemical components and biomass..	120
4 Discussion	124
4.1 More persistent PRs decreased nonstructural sugars but increased lignin biosynthesis.....	124
4.2 Intrinsic and PR-induced differences between sensitive and tolerant species....	125
4.3 The associations between PR, soil water characteristics, biochemical components and biomass	127
5 Conclusion	128
6 Supplementary Data	128
Chapter 4 Does previous exposure to extreme precipitation regimes result in acclimated grassland communities?	134
Abstract	135
1 Introduction	136
2 Methods & Materials	141
2.1 Experimental setup	141
2.2 Microclimate measurements	144
2.3 Biochemical measurements	146
2.4 Statistical analysis	148
3 Results	149
3.1 Acclimation effects in productivity and species composition	149
3.2 Acclimation effects in plant macromolecular composition and stress-metabolism	152
3.2.1 Structural sugars, lipids and proteins	152
3.2.2 Non-structural sugars	154
3.2.3 Proline	155
3.2.4 Polyphenols and flavonoids.....	156
4 Discussion	157

Table of contents

4.1	Acclimation effects in community structure.....	159
4.2	Acclimation effects in productivity and stress-metabolism.....	160
4.3	Interactions between acclimation effects	164
5	Conclusion.....	166
6	Supplementary.....	167
Chapter 5 Soil microbiome legacy shifts cell wall composition and hormonal response to more persistent precipitation regimes across multiple northern European grassland species		
Abstract.....		
1	Introduction	178
2	Material and methods	182
2.1	Experimental Design	182
2.2	Soil water content measurement	183
2.3	Biomass, DW/FW and Fv/Fm measurement.....	184
2.4	RNA Extraction and Next-Generation Sequencing.....	184
2.5	Data Acquisition and Quality Control	185
2.6	Creating De Novo Transcriptomes.....	185
2.7	Annotation of Transcriptomes.....	186
2.8	Differential Expression and GO enrichment analysis.....	186
2.9	Clustering analysis and interpretation.....	187
2.10	Plant cell wall composition analysis.....	188
2.11	Analysis of enzymes related to cell wall composition	190
2.11.1	Cinnamyl alcohol dehydrogenase (CAD) activity.....	190
2.11.2	Peroxidase (POD) activity.....	190
2.11.3	Chitinase activity assay.....	190
2.11.4	Callose synthase assay	191
2.12	Plant Hormone analysis	191
2.13	Statistical analysis	194
3	Results.....	194
3.1	Patterns of soil water content induced by different precipitation regimes	194
3.2	Plant phenotypes in response to different precipitation regimes and soil background	195
3.3	RNA Seq	199
3.3.1	Transcriptome Assembly.....	199
3.3.2	Annotation	200
3.3.3	Differential Expression.....	200
3.4	Clustering.....	201
3.4.1	Effect of drought	201
3.4.2	Shift in 1W plants induced by soil history	203
3.4.3	Shift in 5W plants induced by soil history	204
3.5	Cell wall modification and plant hormone changes induced by different precipitation regimes and soil legacy.....	209
4	Discussion	214
4.1	More persistent PR reduced plant productivity and fitness	214
4.2	Soil legacy affected plant responses to the subsequent PR at transcriptome and biochemical level.....	215

Table of contents

4.3 Comparisons between different functional group and species 219

5 **Conclusion** 220

6 **Supplementary**..... 221

Chapter 6 Discussion 222

1 **Discern potential tipping point (threshold) in plant responses to prolonged dry/wet period** 223

2 **Amino acids, cell wall modification, and hormone signaling pathways are highly involved in responses to more persistent PRs**..... 224

3 **Different strategies of species with varied sensitivity in response to more persistent PRs**..... 226

4 **Acclimation potential of grassland ecosystem to more persistent weather** 227

5 **Soil-plant interactions** 228

6 **Challenges**..... 230

7 **Perspectives**..... 232

Acknowledgement 235

Bibliography..... 237

List of Abbreviations

AA	amino acid
AAA	aromatic amino acid
ABA	abscisic acid
ABC	ATP binding cassette
ABCG	G sub-family of ABC transporters
ABM	aboveground biomass
ABR	abscisic acid repressor
AC	<i>Agrostis capillaris</i> L.
ACC	1-aminocyclopropane-1-carboxylic acid
ACN	acetonitrile
ACS	acetyl-CoA synthetase
AFP	ABI five binding protein
AMP	adenosine monophosphate
ANOVA	analysis of variance
ANPP	aboveground net primary productivity
AO	<i>Anthoxanthum odoratum</i> L.
APX	ascorbate peroxidase
ATAF	<i>Arabidopsis thaliana</i> activating factor
ATP	adenosine triphosphate
AZF	azoospermia factor
BCAA	branched-chain amino acid
BEH	ethylene bridged hybrid
BLAST	basic local alignment search tool
BRH	brassinosteroid-responsive RING-H2
BSA	bovine serum albumin
CAD	cinnamyl alcohol dehydrogenase
CAT	catalase
CDPK	calcium-dependent protein kinase
CFI	comparative fit index
CHIT5	class V chitinase
CI	confidence interval
CJ	<i>Centaurea jacea</i> L.
CMP	cytidine monophosphate
CRK	cysteine-rich receptor-like kinases

List of abbreviations

CWI	cell wall integrity
DAD	diode-array detector
DC	<i>Deschampsia cespitosa</i> (L.) P. Beauv.
DEG	differentially expressed gene
DNA	deoxyribonucleic acid
DW	dry weight
EDAC	1-Ethyl-3-(3-dimethylaminopropyl)carbodiimide
EDR	enhanced disease resistance
EDTA	ethylenediaminetetraacetic acid
ERF	ETS domain-containing transcription factor
FA	fatty acid
FC	field capacity
FDR	false Discovery Rate
FW	fresh weight
GABA	gamma-aminobutyric acid
GAMM	generalized additive mixed model
GC-MS	gas chromatography-mass spectrometry
GFI	goodness-of-fit index
GNPS	global natural products social molecular networking
GO	gene ontology
GR	glutathione reductase
HC	hemicellulose
HESI	heated electrospray ionization
HL	<i>Holcus lanatus</i> L.
HPLC	high-performance liquid chromatography
JA	jasmonic acid
KEGG	Kyoto Encyclopedia of Genes and Genomes
LC	<i>Lotus corniculatus</i> L.
LMM	linear mixed effect models
MACPF	membrane Attack Complex/Perforin
MAPK	mitogen-activated protein kinase
MAPKK	mitogen-activated protein kinase kinase
MAPKKK	mitogen-activated protein kinase kinase kinase
MEV	multiple experiment viewer
ML	maximum likelihood
MS	mass spectrometry
MSE	mean square error
MYB	myeloblastosis
NADP	nicotinamide adenine dinucleotide phosphate

List of abbreviations

NGS	next-generation sequencing
NMR	nuclear magnetic resonance spectrometry
ORA	over-representation analysis
ORF	open reading frame
PAL	phenylalanine ammonia-lyase
PAR	photosynthetically active radiation
PCA	principal component analysis
PERMANOVA	permutational multivariate analyses of variance
PHP	<i>Phleum pratense</i> L.
PL	<i>Plantago lanceolata</i> L.
PLS-DA	partial least squares discriminant analyses
POD	peroxidase
POP	<i>Poa pratensis</i> L.
PR	precipitation regime
PUFA	polyunsaturated fatty acid
PVP	polyvinylpyrrolidone
PWP	permanent wilting point
REW	relative extractable water
RH	relative humidity
RLK	receptor Like Kinase
RMSEA	root mean square error of approximation
RNA	ribonucleic acid
ROS	reactive oxygen species
RT	retention time
SA	salicylic acid
SAPK	stress-activated protein kinase
SE	standard error
SEM	structural equation modeling
SF	<i>Lychnis flos-cuculi</i> L.
SIK	salt-inducible protein kinase
SRK	s locus receptor kinase
SWC	soil water content
TCA	tricarboxylic acid
TEW	total extractable water
TF	transcription factors
TM	<i>Trifolium medium</i> L.
TP	<i>Trifolium pratense</i> L.
UGT	UDP-glucuronosyltransferase
UPLC	ultra performance liquid chromatography

List of abbreviations

VIP	variable importance in projection
VPD	vapor pressure deficit
WAK	wall associated kinase
WRK	wound-induced receptor-like protein kinase
ZAT	zinc transporter
ZIP	zinc-regulated, iron-regulated transporter-like proteins

Summary

One aspect of climate change is the increased persistence of precipitation regime (PR), featuring both longer dry and wet periods. This more persistent PR (alternated longer dry/wet cycle) not only induces notable extremes such as drought and flooding but also results in more complex patterns than with a single extreme event. Studies on the impact of a single extreme event on ecosystems have boomed in the last few decades, but few studies have investigated the immediate and legacy effect of the emerging more persistent PR, particularly at the plant molecular level.

The purpose of my PhD thesis is to address this knowledge gap through a large-scale outdoor experiment and an indoor study, where the PRs are experimentally altered from short to long dry/wet cycles. Multiple treatment levels were applied to open-air grassland mesocosms, which allows us to discern non-linearity and tipping points in the grassland ecosystem's response. By applying ecometabolomics and biochemical analysis, I explored the metabolome (Chapter 2) and some important biochemical components (Chapter 3) changes of several grassland species with varied sensibilities towards the increasingly persistent PR. I found that the metabolome of a relatively sensitive species *Centaurea jacea* shifted already under a mild PR (10-day dry/wet cycle), while the metabolome of the other less sensitive species changed only from 20-day PR onwards. Accumulation of amino acids, lignin, and decreased non-structural sugar levels are universal responses across species to the increasing PR extremity, while changes in other metabolite classes are exhibited in a more species-specific manner. I have also found that

the sensitive species are less capable of inducing sufficient changes on some important molecules such as lignin, and phenylalanine, which may partly explain its sensitivity in response to more persistent PR.

Except for the immediate effect, the acclimation potential of the grassland community in the next growing season (Chapter 4) and soil microbiome legacy induced plant responses to subsequent PR (Chapter 5) were further investigated. In Chapter 4, the grassland communities that were exposed to more persistent or historically normal PR in year 1 were further exposed to an identical PR or an opposite PR in year 2. The results showed that previous exposure to more persistent PR resulted in acclimated grassland communities in the following year. These communities showed increased aboveground productivity and structural sugar content, reduced molecular stress responses but altered diversity. In Chapter 5, we cultivated four grassland species in a sterile substrate inoculated with soil conditioned by either a more persistent PR or historically normal PR from the previous mesocosm experiment. The plants were then exposed to increasingly longer dry/wet cycles in a growth room. The more persistent PR significantly reduced all four species' survival, productivity, and photosynthesis activity. Through transcriptomic and biochemical analysis, we found that pathways related to hormone synthesis (e.g. jasmonic acid, abscisic acid, salicylic acid, ethylene), oxidative stress, cell wall modification (e.g. lignin deposition, callose synthesis, cell wall thickening, pectin metabolic process), and chitin catabolic processes were affected under more persistent PR. Moreover, soils conditioned by more persistent PR promoted the upregulation of these processes, which may provide potential beneficial effects for plants.

Summary

In conclusion, by combining ecological, biochemical, metabolomic, and transcriptomic analyses, this thesis elucidates the impact of forthcoming more persistent PR on grassland ecosystems through a molecular mechanisms angle. We have shown that the more persistent PR could induce significant changes in plant metabolome and biochemical compositions. Although these changes may improve the acclimation of grassland species, they may decrease the nutritive value thereby possibly changing its role in feeding of organisms. Species or individuals unable to induce sufficient protective changes may be excluded from the community, leading to a loss of diversity in the ecosystem.

Samenvatting

Eén aspect van de klimaatverandering is de toegenomen persistentie van het neerslagregime (precipitation regime, PR), met zowel langere droge als natte perioden. Deze meer persistente PR (afwisselende langere droge/natte cyclus) resulteren niet alleen in extremen zoals droogte en overstromingen, maar vormen een veel complexere blootstelling dan met één enkele extreme gebeurtenis. Onderzoek naar de impact van één enkel extreem op het ecosysteem zijn de afgelopen decennia enorm toegenomen. Maar, weinig studies hebben het onmiddellijke en historische effect onderzocht, bij planten, op moleculair niveau van de opkomende meer persistente PR.

Het doel van mijn proefschrift is om deze kenniskloof aan te pakken met een grootschalige, buiten- en binnenstudie, waarbij de PR experimenteel wordt gewijzigd van korte naar lange droog/nat cycli. Er zijn meerdere behandelniveaus toegepast op artificieel samengestelde graslanden in de open lucht, waardoor we niet-lineariteit en omslagpunten in de reactie van het graslandecosysteem kunnen identificeren. Door ecometabolomics en biochemische analyses toe te passen, heb ik de veranderingen in het metabool (Hoofdstuk 2) en enkele belangrijke biochemische componenten (Hoofdstuk 3) onderzocht van verschillende graslandsoorten met uiteenlopende gevoeligheden voor de steeds persistenter wordende PR. Ik ontdekte dat het metabool van een relatief gevoelige soort, *Centaurea jacea*, al veranderde onder een mild PR (10-daagse droog/nat-cyclus), terwijl het metabool van de andere, minder gevoelige soorten pas veranderden vanaf een PR van 20 dagen. Accumulatie van aminozuren en lignine, en verminderde

gehalten niet-structurele suikers zijn universele reacties bij verschillende soorten op de toenemende PR-extremiteit, terwijl de veranderingen in andere metabolietenklassen meer soortspecifiek optreden. Ik heb ook ontdekt dat in de gevoelige soorten minder veranderingen optreden in enkele belangrijke moleculen zoals lignine en fenylalanine, wat de gevoeligheid voor meer aanhoudende PR gedeeltelijk kan verklaren.

Behalve het onmiddellijke effect werden ook het acclimatisatiepotentieel van de graslandgemeenschap in het volgende groeiseizoen (Hoofdstuk 4), en de door het bodemmicrobioom veroorzaakte reacties van planten op daaropvolgende PR (Hoofdstuk 5) onderzocht. In Hoofdstuk 4 werden graslandgemeenschappen blootgesteld aan meer persistente of historisch normale PR in jaar 1, gevolgd door blootstelling aan een identieke PR of tegenovergestelde PR in jaar 2. De resultaten lieten zien dat voorgaande blootstelling aan meer persistente PR, resulteerde in geacclimatiseerde graslandgemeenschappen in het daaropvolgende jaar. Deze gemeenschappen hebben een verhoogde bovengrondse productiviteit en gehalte aan structurele suikers, verminderde moleculaire stressreacties en een veranderde diversiteit onder toekomstige klimaatextremen. Voor de resultaten van Hoofdstuk 5, kweekten we vier graslandsoorten in een gesterilliseerde bodem geïnoculeerd met grond geconditioneerd door een meer persistent PR of historisch normaal PR uit het vorige mesocosmos-experiment. We onderwierpen de planten aan steeds langere droog/nat cycli in een geconditioneerde plantenkweekkamer. De meer aanhoudende PR verminderde de overleving, productiviteit en fotosynthese-activiteit van vier soorten aanzienlijk. Via transcriptoom en biochemische analyse hebben we ontdekt dat routes gerelateerd aan hormoonsynthese (bijv. jasmijnzuur, abscisinezuur, salicylzuur, ethyleen),

Summary

oxidatieve stress, celwandmodificatie (bijv. lignine-afzetting, callose-synthese, celwandverdikking, pectine-metabolisch proces), en katabole processen van chitine werden beïnvloed onder meer aanhoudende PR. Bovendien bevorderde de bodem met een meer persistente PR-geschiedenis, de opregulatie van deze processen, wat potentiële gunstige effecten voor planten kan opleveren.

In conclusie, door het combineren van ecologische, biochemische, metabolische en transcriptoom analyses, draagt dit proefschrift bij aan het begrijpen van de moleculaire mechanismen die optreden bij blootstelling van graslandecosystemen aan meer persistente PR. Ik heb aangetoond dat de meer persistente PR significante veranderingen in het metaboloom en de biochemische samenstelling van planten kan veroorzaken. Hoewel deze veranderingen de acclimatisatie van graslandsoorten kunnen verbeteren, kunnen ze de voedingswaarde verlagen, waardoor mogelijk de rol ervan in de voeding van organismen verandert. Soorten en individuen die onvoldoende bescherming kunnen genereren, verdwijnen mogelijk uit de gemeenschap en leiden tot verlies van diversiteit in het ecosysteem.

Chapter 1

General introduction

1 Persistent precipitation regimes

Due to the accelerated warming in the Arctic compared to lower latitudes regions, the reduction in equator-to-pole temperature difference has a profound impact on atmospheric circulations and hydrologic processes, leading to more persistent extreme weather in the mid-latitude (Coumou et al. 2018; Kornhuber and Tamarin-Brodsky 2021; Cohen et al. 2019; Francis et al. 2020; Easterling et al. 2000). The more extreme weather has been changing regarding intensity, frequency, and duration in the last few decades, and the increase in the occurrence and severity is already apparent (Smith 2011; Ummenhofer and Meehl 2017). According to a report by the United Nations Office for Disaster Risk Reduction (UNDRR) in 2020, extreme climate events have “come to dominate the disaster landscape in the 21st century” (UNDRR 2020). Examples include heatwaves in Europe in 2003 (Garcia-Herrera et al. 2010), 2010 (Barriopedro et al. 2011), 2018, and 2019 (Xuebang Liu et al. 2020), as well as flooding in Europe, China and India during July 2021 (Kreienkamp et al. 2021).

One of the key predictions of hydrological alteration is more extreme precipitation regimes (PRs) characterized by large rainfall events and longer dry intervals (IPCC 2021; Knapp et al. 2008; Zeppel et al. 2014; Breinl et al. 2020). The size and timing of rain events are strong drivers of ecological processes (Osvaldo and Sala 2004). A shift to more extreme precipitation patterns with more heavy rainfall and longer dry intervals decreases the rain use efficiency and water quality across biomes (Tebaldi et al. 2006; Ummenhofer and Meehl 2017). While the effects of individual extreme climate events such as drought and flooding have been extensively investigated (dos Santos et al. 2022; Fàbregas and Fernie 2019; Allen et al. 2010; Mutava et al. 2015), the responses to precipitation redistribution are likely to differ from responses to individual

drought/flooding events (Y. Luo et al. 2011; Zeppel et al. 2014). Moreover, changes in precipitation during warm and dry seasons may have larger effects than changes during cool and wet seasons (Zeppel et al. 2014). Previous studies have shown that more extreme rainfall patterns without changes in total rainfall quantity reduced the aboveground net primary productivity (ANPP) of native grassland (Knapp et al. 2002); enhanced interannual precipitation variation decreases grass and increases shrub-productivity (Gherardi and Sala 2015); Heisler-White et al. (2009) found contingent responses to more extreme precipitation regimes across a grassland biome. These studies focused on precipitation redistribution with more intense peak precipitation (single large rainfall event) interspersed with longer drought (Knapp et al. 2002; Zeppel et al. 2014). However, the new trend of alternation of both longer consecutive dry periods and wet periods has been scarcely studied. Therefore, there is an urgent need to assess the consequences of persistent PRs on natural and agricultural ecosystems and understand the changes at multiple levels of organisms towards the increasingly persistent PRs.

2 Plant stress responses to altered precipitation patterns

While the recent pattern of extended sequences of both dry and wet periods has received limited attention, the comprehensive studies on plant stress responses to drought and flooding offer a solid foundation for understanding the potential effects. Drought and flooding disrupt plant functions by impacting turgor and water potential, thereby causing changes in the morphological, physiological, and molecular characteristics of plants (Chaudhry and Sidhu 2021; Farooq et al. 2009; Y. Fang and Xiong 2015).

Plants generally reduce the number and the size of leaves under water deficit environment (Oladosu et al. 2019). The root characters such as length, density are the key components of drought avoidance (Farooq et al. 2009). Many plant species accumulate wax, cuticle on the leaf surface and rapidly close their stomata to reduce water transpiration when the water is limited, which decreases the CO₂ influx (Y. Fang and Xiong 2015). The reduction in CO₂ not only directly impacts carboxylation but also directs more electrons to generate reactive oxygen species (ROS)(Cornic and Massacci 1996; Farooq et al. 2009). ROS can interact with proteins, lipids and DNA, leading to oxidative damage and impairing the normal functions of cells (Foyer and Fletcher 2001). By activating the antioxidant defense system, which includes both enzymatic and non-enzymatic components, plant cells can eliminate ROS and therefore protect their functions (Farooq et al. 2009). In addition to the antioxidant system, another common strategy for drought stress tolerance involves osmotic adjustment achieved through the accumulation of various compatible solutes, including soluble sugar, soluble alcohols, proline, glycinebetaine, organic acids, etc (Gurrieri et al. 2020; Barchet et al. 2014; Y. Fang and Xiong 2015). Except the above strategies, phytohormones play vital roles in drought tolerance of plants. For instance, plants accumulate ABA under drought to increase the root-to-shoot ratio and regulate stomata closure (Onyemaobi et al. 2021; Muhammad Aslam et al. 2022). Jasmonic acid has been reported to effectively improved the drought resistance of plants by increasing the organic osmoprotectants and antioxidative enzyme activity (Ali and Baek 2020). Synthesis stress proteins is another important response to cope with drought stress (Farooq et al. 2009). For example, heat shock proteins, membrane-stabilizing proteins, calcium-dependent proteins have been shown for

conferring drought tolerance by prevent protein denaturation, transduce stress signals, etc (He et al. 2018).

Depending on the intensity, duration and timing, moderate rainfall can be seen as a favorable/recovery period for plant growth (Z. Xu et al. 2010). After cessation of the drought stress, process of recovery includes damage repair and growth resumption (Rangani et al. 2020). It is of particular importance that leaves and roots recover quickly after drought to assure water and nutrient uptake and to continue photosynthesis (Wedeking et al. 2018). In addition, plants sometimes need to maintain acclimation to make themselves 'alert' for the future stress exposure (Wedeking et al. 2018). However, heavy rainfall may lead to waterlogging stress, which drastically influences the soil properties, most notably soil redox potential, pH and O₂ level (Parent et al. 2008). The lack of O₂ inhibits mitochondria respiration, ATP synthesis, photosynthesis and root permeability (Parent et al. 2008), which is one of the major constraints that plants suffer under flooding conditions (Striker 2012). Plants develop multiple mechanisms to cope with this condition, with the generation of aerenchyma and adventitious roots being among the most common anatomical responses (Seago et al. 2005; Grimoldi et al. 2005; Striker 2012). To further prevent the leakage of oxygen, suberin is deposited in the cell walls of the outer root cortex and/or the exodermis, serving as a physical barrier. (Striker 2012). As O₂ is limited, plants also shift their metabolism from aerobic respiration to anaerobic fermentation, and accelerated glycolysis to compensate the deficit in energy (Parent et al. 2008).

3 Legacy effect and stress memory

Climate change applies selective pressures on ecosystems, supporting the development of some coping strategies to enhance acclimation or adaptation to the constantly changing environments (Xiliang Li et al. 2022; Gessler et al. 2020; terHorst and Zee 2016). These coping strategies may maintain for long periods even after the initial ‘driver’ ceases, and these persisting effects are called legacy effects or stress memory (Wurst and Ohgushi 2015; Cuddington 2011). Legacy effects play a vital role in shaping ecosystems’ function under future stressors through multiple levels such as community restructuring, plant acclimation, and plant-soil interactions (Gessler et al. 2020; Meisner et al. 2018; Xiliang Li et al. 2022; Barnard et al. 2013; Walter et al. 2013). For instance, extreme soil water depletion often filters out drought-sensitive species and selects for species with increased resistance to future droughts, thus reducing diversity but stabilizing key ecosystem processes such as productivity (De Boeck et al. 2018; Engelbrecht et al. 2007; H. Liu et al. 2018; Harrison et al. 2018). This process, where primarily abiotic factors prevent the (re-)establishment or persistence of specific species (or species traits) in a particular environment, is known as ‘environmental filtering’ (Kraft et al. 2015). At the plant individual level, one possible response of plants from repeated exposure to stress is that they become more tolerant to future exposure through the acquisition of memory, a response referred to as hardening, priming, conditioning, or acclimation (Crisp et al. 2016; Kinoshita and Seki 2014; van Loon 2016). Plant stress memory involves a broad range of mechanisms, from epigenetic regulation, phytohormone regulation to the alteration of signaling metabolites (Hilker and Schmölling 2019; Crisp et al. 2016). The stress memories may allow plants to react more rapidly or strongly to recurrent stress, and even can persist

between generations (Hilker and Schmülling 2019; Crisp et al. 2016). It has been observed that there were significant increases in the osmoprotectants including sugar, organic acids and amino acids levels in primed plants (Kambona et al. 2023; Tugizimana et al. 2018). The levels of amino acids, such as proline, glycine, histidine, alanine, GABA, and tryptophan, were higher in plants subjected to multiple drought cycles compared to those exposed to a single stress event (Kambona et al. 2023). Another important aspect is soil abiotic and biotic legacy effects. Due to the precipitation redistribution, changes in soil moisture affect the soil mineral N, P availability (S. Yu and Ehrenfeld 2009; Cavagnaro 2016), and impact the biomass, activity, and diversity of soil microbial communities (Cavagnaro 2016). As plants grow and react with the varied environment, they also shape the soil environment (De Long et al. 2023). For example, the rooting patterns change soil structure, and root exudation recruits soil microbial community. In turn, the altered soil characteristics and microbiome affect the subsequent growth of plants, termed plant-soil feedback (De Long et al. 2023). It has been reported that the altered microbial community induced by extreme weather history can modify the performance of plant species, but depending on the type, frequency and timing of extreme events (Meisner et al. 2013; 2018). Beneficial microbiomes in the soil contribute to plant stress tolerance by facilitating nutrient uptake, modulating phytohormones for root development, aiding in osmotic adjustment, and enhancing the antioxidant system under both abiotic and biotic stress (Gachara et al. 2023). Due to the complexity and broad range of legacy effects, it is challenging and of key importance to dissect the multiple levels of legacy effects and understand how the interacting different levels determine the outcome of the ecosystem.

4 Grassland ecosystem and species

Grasslands are among the most widely distributed terrestrial biomes on earth, accounting for 41% of the global land area (Sala 2001; Y. Zhao et al. 2020; Revenga 2001; Petermann and Buzhdygan 2021). Grasslands are considered to play a key role in greenhouse gas mitigation and contribute significantly to food security through providing the feed requirements of ruminants (O'Mara 2012).

Grasslands are dominated by grasses (*Poaceae*), but variable proportions of clovers and other forbs can be found. Given they are water-limited ecosystems, grasslands are highly sensitive to precipitation variation (Felton et al. 2020; Craine et al. 2012). Thus, understanding the physiological, and molecular mechanisms of different grassland species responding to precipitation variation is important for determining how climate change will impact these essential ecosystems. Evidence has shown that the temporal variability of rainfall patterns can alter grassland productivity and biodiversity (Felton et al. 2020). Some grassland species can produce deep root systems to increase water uptake, therefore inducing a competitive advantage over other species (Grieu et al. 2001; Signarbieux and Feller 2012). On the other hand, the capacity of plants to recover from drought stress is another aspect of competitive growth and survival (Signarbieux and Feller 2012). It has been reported that there are differences between forb and grass species in photosynthesis under drought, and the drought tolerance of forbs is partially due to increased water use efficiency (Signarbieux and Feller 2012). Rhizomatous and bunch grasses showed rapid recovery after drought, possibly restricting the forbs' growth (W. Luo et al. 2023). Except for the differences in physiological responses, different strategies in molecular regulations under stress conditions were also observed in different grassland species. Abdelgawad et al. (2015) found that under stress

conditions, the glutamate pathway leading to proline production, is predominantly activated in grasses while the ornithine pathway for proline synthesis is activated in the forbs. This is probably related to differences in N-nutritional status. Proline content contributes to variation in salinity stress resistance among C₃ grass species (Soliman et al. 2018). Elevated CO₂ increased ascorbate and glutathione levels and their redox status in grassland-model species *Lolium perenne L.* and *Medicago lupulina L.*, although to different levels (Farfan-Vignolo and Asard 2012). By comparing two *Plantago* species, Yang et al. (2015) found that *P. fengdouensis* were more tolerant to waterlogging stress in terms of free proline levels and activities of catalase (CAT), ascorbate peroxidase (APX), and glutathione reductase (GR) than *P. asiatica*, especially in root systems. However, studies on the comparison of different grassland species in response to varied precipitation regime is still rare, the underlying molecular changes need to be further depicted in future studies.

5 Application of omics technologies to understand plant responses under climate change

Multiple “omics” approaches have been applied successfully to elucidate plant responses under climate change over the last few decades (Y. Yang et al. 2021). These techniques, such as genomics, transcriptomics, proteomics, metabolomics, phenomics and ionomics are valuable to explore the genetic and molecular basis of plant development against various environmental stresses (Muthamilarasan et al. 2019; Y. Yang et al. 2021). Integration of multi-omics datasets enhances our understanding of molecular regulatory networks that link phenotype to genotype (or vice versa)(Y. Yang et al. 2021).

Metabolomics aims at investigation of the complete metabolome of an organism at a given time point. Compared with targeted analysis which focuses

on some well-characterized metabolites, non-targeted metabolomics provides a comprehensive, unbiased view of the plant's metabolic responses towards varying environments (Peters et al. 2018; Schweiger et al. 2014; Fiehn 2002). Gas chromatography-mass spectrometry (GC-MS), liquid chromatography-mass spectrometry (LC-MS) and nuclear magnetic resonance spectrometry (NMR) are the most frequently used platforms in plant metabolomics (Sardans et al. 2020; Fiehn 2002). Ecometabolomics, as a rapidly developing transdisciplinary domain, connects the distinct spatiotemporal scales between ecology and biochemistry and is increasingly employed to study the effects of global climate changes (Peters et al. 2018; Sardans et al. 2011). Several studies illustrate the relevance and type of results that can be obtained. Earlier metabolomic studies reported that plant shoots generally accumulate osmoprotectants like monosaccharides, polyols, and some amino acids under drought stress (Sardans et al. 2020; Fàbregas and Fernie 2019). Upregulation of secondary metabolites such as phenolics provides antioxidative defense during drought stress (Rivas-Ubach et al. 2014; Rangani et al. 2020). The accumulation of osmotic compounds and the enhancement of energy and secondary antioxidant metabolism under drought stress are the mechanisms responsible for drought tolerance in some drought-tolerant species such as soybean (Wang et al. 2019). Similar to drought, heat stress induces plants to accumulate amino acids, soluble carbohydrates, and associated derivatives in foliar tissue (Sardans et al. 2020). It is clear from these studies that ecometabolomic analyses provide a powerful tool to study the effects of climate change (include altered PRs) on plant metabolism, and further allow distinction between general patterns and species-specific responses.

Since the development of next-generation sequencing (NGS), transcriptomics has been much more widely used to gain insight into the molecular mechanisms by which plant species respond to biotic and abiotic stresses (Kang et al. 2020). For example, NGS studies have revealed the potential role of genes related to jasmonic acid, ethylene, peroxidase, and the phenylpropanoid pathway in response to bacterial infections (Soniya et al. 2022). Jasmonic acid mediated resistance was detected as the critical component of defense against fungus *F. fujikuroi* in rice plants (Cheng et al. 2020). Chevilly et al. (2021) discovered increased levels of methionine and abscisic acid and decreased levels of urea, quinic acid, and gluconic acid lactone in drought-tolerant broccoli cultivars. In soybean, drought-response TFs such as WRKY, MYB and bZIP may play an important role in drought resistance (M. Li et al. 2022). It has also been reported that the general transcriptional responses greatly differed between genotypes, the sensitive genotypes showed a higher number of stress-regulated genes compared with tolerant genotypes (Harb et al. 2020; Ereful et al. 2020; Janiak et al. 2019), but the genes that could confer drought tolerance were either specifically induced or greatly upregulated in the tolerant genotype (Harb et al. 2020).

The omics studies have greatly improved our understanding on the regulatory mechanisms of plants to varied stress, which provide an important basis to explore the effect of changed PR. Considering the complexity of changing PR (alternated longer dry and wet duration), species variation, the differences between controlled and field environments, future studies are needed to reveal the common and different responses at omics level among different species.

6 Framework of regime shift project

To investigate the impact of the ongoing more persistent PR on grassland species, we built up a large-scale, open-air multidisciplinary project named 'regime shift'. The project scope ranges from plants to soil biota, and from ecosystem processes to metabolism and genetic regulation assessed with bioinformatics. Four PhD students are collaborating on these different aspects and combining analyses at the ecosystem, organism and molecular level. Simon Reynaert performed measurements at ecosystem scale, such as plant survival, biomass, green cover, photosynthesis efficiency, etc. Lingjuan Li is responsible for soil microbiome community analysis. Chase Donnelly conducted transcriptomic analysis. As for my role, I am responsible for studying plants at the biochemical level, focusing on metabolomics and stress responses.

This project utilized an experimental platform named 'FATI', constructed at the University of Antwerp under the framework of AnaEE (Analysis and Experimentation on Ecosystems, www.anaee.com). The FATI platform comprises eight open-air exposure units (FATIs, Figure 1A). Each FATI is equipped with a screen that is automatically deployed during rain to eliminate natural rainfall, and the plants will experience unaltered sunlight more than 95% of the time (Figure 1B). We constructed 256 identical grassland mesocosms using gray PVC containers with dimensions of 30 cm and 50 cm depth. These mesocosms were then evenly distributed across eight FATIs, with each FATI containing 32 mesocosms (Figure 1C). Mesocosm provides a relatively controlled and replicable environment, allowing us to manipulate specific variables (e.g. PR) (Stewart et al. 2013). In the meantime, it maintains a natural community under natural exposure conditions. Mesocosms can also be designed to mimic longer-term ecological processes, which is important for

gaining insights into the resilience and adaptability of grasses in dynamic environments (Fry et al. 2017). In this project, mesocosms were subjected to a range of 8 PRs, with alternating dry/wet periods of 1, 3, 6, 10, 15, 20, 30 and 60 consecutive wet and dry days (referred to as '1-day PR', '3-day PR', etc.). For each PR, half of the mesocosms started with dry period, while the other half started with wet period. The desired PR can be imposed through computer-controlled drippers (Figure 1C). The soil's field capacity (FC) was estimated at $0.26 \text{ m}^3 \text{ m}^{-3}$ and the permanent wilting point (PWP) at $0.05 \text{ m}^3 \text{ m}^{-3}$. Three individuals of 12 common perennial temperate C3 grassland species were planted in each mesocosm (Figure 1D; E). Species were planted to maximize interspecies interactions and covered 3 functional groups: 6 grasses (*Agrostis capillaris* L., *Anthoxanthum odoratum* L., *Deschampsia cespitosa* (L.) P. Beauv., *Phleum pratense* L., *Poa pratensis* L., *Holcus lanatus* L.); 3 N-fixing forbs (N-fixers) (*Lotus corniculatus* L., *Trifolium pratense* L., *Trifolium medium* L.); and 3 non-N-fixing forbs (*Centaurea jacea* L., *Lychnis flos-cuculi* L., *Plantago lanceolata* L.). For the practical reasons of irrigation supply, four replicates of all short cycle PRs (1, 3, 6, 10) or long cycle PRs (15, 20, 30, 60) were grouped per FATI. Therefore, four FATIs are designated for short-cycle PRs, and an additional four FATIs are allocated for long-cycle PRs (Figure 1E). The specific positions of the replicates were randomly allocated across the four FATIs to account for potential edge effects (Figure 1E). As a result, there were a total of 16 replicated mesocosms per treatment, evenly spread across four FATIs.

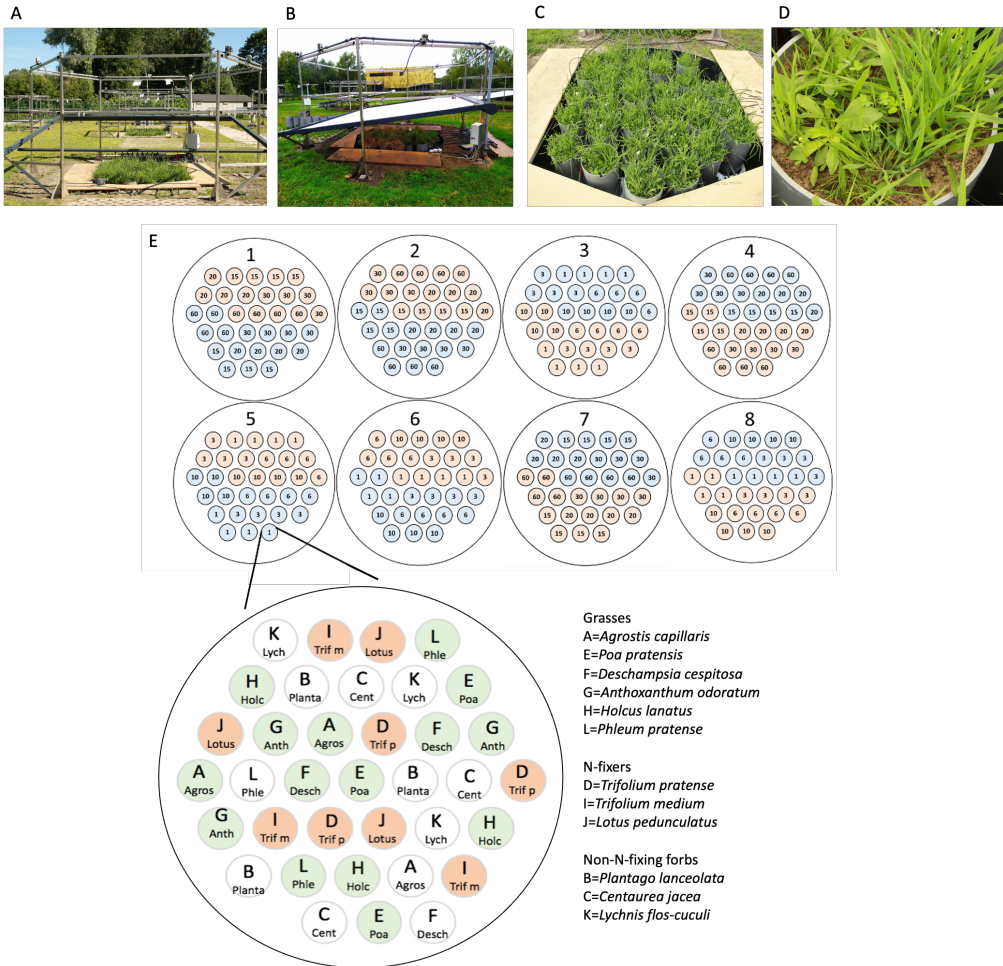


Figure 1 FATI experimental platform at the University of Antwerp to study the effect of more persistent precipitation regime. (A) One FATI with rolled-up screen. (B) One FATI with rolled-down screen. (C) Mesocosms of one FATI with drippers. (D) Example of one mesocosm. (E) There are eight FATIs (1-8) in total, and each FATI contains 32 mesocosms. Treatments starting with a dry or wet period are indicated in brown and blue, respectively. Three individuals of 12 temperate grassland species (A-L) were planted in each mesocosm according to the same pattern.

7 Thesis outline

The aim of this thesis is to investigate the impact of more persistent PR (prolonged consecutive days of dry/wet period) on grassland mesocosms, specifically focusing at the molecular-level effects. In the year 1 FATI experiment (02/07/2019 – 25/06/2020, 360 days), mesocosms were subjected

to a range of 8 PRs, with alternating dry/wet periods of 1, 3, 6, 10, 15, 20, 30 and 60 consecutive wet and dry days (referred to as '1-day PR', '3-day PR', etc.). In year 2 (26/06/2020 - 23/10/2020, 120 days), the 3-day PR and 20-day PR were selected as normal and extreme PR, respectively, and the mesocosms were exposed to an identical PR or the opposite PR to study PR history effects (legacy effect). Among the legacy effects, soil microbial communities play a crucial role in influencing host nutrition, development, and immunity (Xiaogang Li et al. 2019). Therefore, we further conducted a growth room experiment to investigate the soil microbiome legacy and the transcriptome changes in plants under different PRs. In this experiment, soils from 1-day and 30-day PR treatment were collected from year 1 mesocosm experiment and separately inoculated into plants. The plants were further exposed to a range of alternating dry/wet cycle. Through the above outdoor and indoor growth room experiments, this thesis provides insight on the impact of more persistent PRs and the potential legacy effect at the grassland community, species, biochemical, metabolomics, transcriptomics level.

This dissertation contains six chapters. Apart from this Introduction (Chapter 1), in Chapter 2, I analyze the metabolomic profiles of four grassland species with varying sensitivity to more persistent PRs (*Holcus lanatus*, *Phleum pratense*, *Centaurea jacea*, *Plantago lanceolata*) from the year 1 FATI experiment. Stress sensitivity was determined as the slope of the survival decline in response to increasing stress (decreasing of Fv/Fm) (Reynaert et al. 2021). Based on my colleague Simon Reynaert's research, the stress sensitivities of these four species towards the altered PRs were *Centaurea jacea* > *Holcus lanatus* > *Plantago lanecolata* > *Phleum pratense*, with *Phleum pratense* also being the least sensitive species among the 12 species used in the mesocosms (Fig. S12B,

S13, S14 in Reynaert et al. 2021). I chose to study *Centaurea jacea* instead of *Lychnis flos-cuculi* (the most sensitive species among the 12) because *Lychnis* did not produce enough leaf material for metabolomic analysis, particularly under severe PRs. The goals of this research were to: 1) investigate at what dry-wet cycle duration the metabolome of grassland species significantly changes (is there a tipping point?); 2) identify key metabolites that drive the shift of the metabolome as potential biomarkers; 3) identify the most influenced metabolic pathways in response to more persistent PRs; 4) compare similar and divergent responses of the four species differing in sensitivity towards the altered PR.

In Chapter 3, the biochemical composition (soluble sugar, starch, lipids, proteins, cell wall constituents) of four grassland species with varying sensitivity to PR persistency (*Holcus lanatus*, *Phleum pratense*, *Lychnis flos-cuculi*, *Plantago lanceolata*) from the year 1 experiment were analyzed. It should be noted that in this chapter, I investigated the most sensitive species, *Lychnis flos-cuculi*, while the other three species remained the same as in Chapter 2. The objectives were to determine: 1) how increasingly persistent PRs affect grassland species biomass, cell wall composition and other biochemical composition; 2) the relationship between biochemical composition and biomass under more persistent PRs; 3) potential drivers of differences between grassland species.

In Chapter 4, based on the year 2 experiment, I investigated differences in exposure to extreme or historically normal PR induced legacy effects at the level of community (e.g., species composition), plant (e.g., biomass), and molecular composition (e.g., sugars, lipids, stress markers). We hypothesized that plant communities which were subjected to the same PR in year 2 versus

year 1 would consistently outperform (in terms of productivity, richness stability, plant fitness) communities subjected to a different PR in year 2.

In Chapter 5, based on the indoor experiment, the physiological, biochemical and transcriptomic changes of four species (*Holcus lanatus*, *Phleum pratense*, *Plantago lanceolata*, *Lotus corniculatus*) were studied, and the goal of this research is to study: 1) what are the molecular mechanisms of different grassland species in response to the increasingly long dry/wet cycle? 2) does an adaptation of microbial community to previous precipitation frequency modify plant responses to subsequent regimes and what are the underlying mechanisms?

Finally, in the general discussion (Chapter 6), I discuss the highlights of this research, the challenges and the future perspective.

Chapter 2

Ecometabolomic analysis of the effect of more persistent precipitation regimes reveals common and tolerance related metabolic adjustments in four grassland species

Published as: Zi, Lin, Albert Gargallo-garriga, Michal Oravec, Hamada AbdElgawad, Ivan Nijs, Hans J De Boeck, Simon Reynaert, et al. 2023. "Ecometabolomic Analysis of the Effect of More Persistent Precipitation Regimes Reveals Common and Tolerance Related Metabolic Adjustments in Four Grassland Species." *Environmental and Experimental Botany* 215 (August): 105489. <https://doi.org/10.1016/j.envexpbot.2023.105489>.

Lin Zi ^{a,*}, Albert Gargallo-Garriga ^{b,c}, Michal Oravec ^b, Hamada AbdElgawad ^{a,d}, Ivan Nijs ^e, Hans J. De Boeck ^{e,f}, Simon Reynaert ^e, Chase Donnelly ^g, Lingjuan Li ^e, Gerrit T.S. Beemster ^a, Otmar Urban ^b, Han Asard ^a

a Integrated Molecular Plant Physiology Research (IMPRES), Department of Biology, University of Antwerp, B-2020 Antwerp, Belgium

b Global Change Research Institute, Czech Academy of Sciences, Břelidla 986/4a, CZ-60300 Brno, Czech Republic

c Universitat Autònoma de Barcelona, Bellaterra, 08193 Catalonia, Spain

d Botany and Microbiology Department, Faculty of Science, Beni-Suef University, Beni-Suef 62511, Egypt

e Plants and Ecosystems (PLECO), Department of Biology, University of Antwerp, B-2610 Wilrijk, Belgium

f School of Ecology and Environmental Sciences, Yunnan University, Kunming 650091, China

g Adrem Data Lab (Adrem), Department of Computer Science, University of Antwerp, B-2020 Antwerp, Belgium

*Corresponding author

For this chapter, L. Z performed the metabolomic data analysis, data interpretation and wrote the manuscript.

Abstract

Climate change is inducing more persistent precipitation regimes (PRs) in the mid-latitudes, characterized with both longer dry and longer wet periods. Such PRs could potentially result in water deficiency, as well as water logging stress. However, the effects of persistent PRs on plant metabolism remain largely unknown. We applied an 8-level PR of increasingly longer alternating dry and wet periods over 120 days to grassland mesocosms and analysed the metabolomic profiles of four species with varying sensitivity to PRs (*Holcus lanatus*, *Phleum pratense*, *Centaurea jacea*, *Plantago lanceolata*). The metabolome of the most sensitive species *Centaurea* showed a clear tipping point at a mild PR (10-day dry/wet), while in the other species this happened at more persistent PRs. Amino acids accumulation was a general response across all species. This was more evident in the tolerant species *Phleum*. Phenylalanine metabolism, alanine, aspartate and glutamate metabolism pathways were highly involved in PR responses in four species. Fewer phenylpropanoids were changed significantly under more persistent PRs in *Centaurea* than in the remaining species. These results suggest that the accumulation of amino acids and modulation of secondary metabolism may be key factors limiting metabolic acclimation of sensitive species in response to more persistent PRs.

1 Introduction

Weather is becoming more persistent in the mid-latitudes, including the shift of precipitation regimes (PRs) towards more extreme patterns with both longer dry and longer wet periods (Pfleiderer et al. 2019; Breinl et al. 2020). Single longer dry or wet spells caused profound impacts on terrestrial ecosystems such as agricultural yield losses, increased mortality in forests, and reduced

production and biodiversity of grassland communities (De Boeck et al. 2016; Breinl et al. 2020; Allen et al. 2010; Brookshire and Weaver 2015). In addition, the alternating longer dry and longer wet periods result in stronger fluctuations of soil water contents (SWC). Such fluctuations may induce water deficiency, a certain degree of recovery from drought stress and potentially water surplus, depending on the length and intensity of the dry and wet periods. While effects of drought and waterlogging on plant physiology and biochemistry have been extensively investigated, the influence of alternating longer dry and longer wet periods remains poorly understood (Reynaert et al. 2021).

Our previous studies primarily focused on community-level responses and have shown that the persistent PR reduces plant diversity (Reynaert et al. 2021), select for acclimated communities with increased productivity and attenuated molecular stress responses (Reynaert et al. 2022). However, the effects of persistent PRs on species/individual level, and the comparison between different species on metabolic responses and stress acclimation have been scarcely studied.

As a rapidly developing transdisciplinary domain, ecometabolomics allows investigation of the complete metabolome of an organism at a given time point. Compared with targeted analysis which focuses on some well-characterized metabolites, non-target metabolomics provides a comprehensive, unbiased view of the plant's metabolic responses towards varying environments (Fiehn 2002; Peters et al. 2018; Schweiger et al. 2014). Ecometabolomics connects the distinct spatiotemporal scales between ecology and biochemistry and is increasingly employed to study the effects of global climate changes (Peters et al. 2018; Sardans et al. 2011). Earlier metabolomic studies reported that plant shoots generally accumulate osmoprotectants like monosaccharides, polyols,

and some amino acids under drought stress (Sardans et al. 2020; Fàbregas and Fernie 2019). Upregulation of secondary metabolites such as phenolics provides antioxidative defence during drought stress (Rivas-Ubach et al. 2014; Rangani et al. 2020). Metabolic pathways including the tricarboxylic acid (TCA) cycle, glycolysis, galactose metabolism, glutamate-mediated proline biosynthesis and shikimate-mediated secondary metabolisms have been reported to be altered under drought stress in various species (Guo et al. 2018; Yobi et al. 2013; Shahbazy et al. 2020). Re-watering often (partially) reversed the changes of many metabolites induced by drought stress. However, notable differences were found between species (Liang et al. 2023; Shen et al. 2022; Warren et al. 2012). For instance, in some *Eucalyptus* species, further increases of some metabolites such as fructose, glucose and proto-quercitol decrease osmotic potential during re-watering, which are considered as helping plants cope with future water stress (Warren et al. 2012). Similar to drought, heat stress induces plants to accumulate amino acids, soluble carbohydrates, and associated derivatives in foliar tissue (Sardans et al. 2020). It is therefore clear that ecometabolomic analyses provide a powerful tool to study the effects of altered PRs on plant metabolism, and further allow distinction between general patterns and species-specific responses.

In this study, we applied alternating dry and wet periods over 120 days to grassland mesocosms, composed of 12 temperate grassland species covering three functional groups (grasses, non-N-fixing forbs and N-fixers). Grasslands are characterized by generally high biodiversity and their existence depends strongly on precipitation and temperature (Sala et al. 2013). They are therefore ideal model ecosystems for PR studies. We exposed the mesocosms to a gradient of eight PRs, ranging from 1 to 60 days consecutive dry and consecutive wet periods (Figure S1). The gradient design allows investigation of

how increasingly persistent PR affect plant metabolism (i.e. through gradual changes and/or threshold responses). Knowledge about this will help to better understand the mechanisms behind changes in ecosystem properties (e.g. resilience/resistance of productivity, responses to subsequent extremes, etc.) under climate change and differences in the acclimation potential of individual species. Our previous results on these mesocosms showed that an alternation of longer dry and longer wet periods led to a severe loss of species richness and diversity, and that the 12 grassland species exhibited different sensitivities to the altered PR (Reynaert et al. 2021). In the current study, two grasses (*Holcus lanatus* and *Phleum pratense*), two forbs (*Centaurea jacea* and *Plantago lanceolata*) were subjected to metabolomic studies. These four species prefer mesic to moist conditions but can tolerate some degree of water limitation (Britten 1871; Jonavičienė et al. 2012; Wright et al. 2021; Benson-Evans 1950; Orians et al. 2019; Cavers et al. 1980). Based on our previous research, the stress sensitivities of these four species towards the altered PRs were *Centaurea jacea* > *Holcus lanatus* > *Plantago lanceolata* > *Phleum pratense*, with *Phleum pratense* also being the least sensitive species among the 12 species used in the mesocosms (Figure S12B, S13, S14 in Reynaert et al. 2021). We hypothesized that the metabolome of four species shifted at different PRs, and that the four species share some common metabolomic responses towards PRs, but also exhibit species-specific patterns that may partly explain the different sensitivities.

2 Material and Methods

2.1 Experimental design and treatments

The experiment took place at the Drie Eiken Campus of the University of Antwerp in Belgium (51°09'41"N, 04°24'9"E). We used the same study site and

experimental setup as Reynaert et al. ((2021): Grassland mesocosms (256) were distributed across eight experimental units (32 mesocosms per unit). Each unit was equipped with a rain screen which automatically covered the plants during rain periods, and with automatic irrigation through drippers to mimic different PRs (including different regimes within a single unit). The mesocosms (50 cm depth and 30 cm diameter) were filled with sandy-loam soil with a pH between 7.0 and 7.2. The soil's field capacity (FC) was estimated at $0.26 \text{ m}^3 \text{ m}^{-3}$ and the permanent wilting point (PWP) at $0.05 \text{ m}^3 \text{ m}^{-3}$. Seeds of 12 common perennial temperate C3 grassland species were first sown in small seedling containers in April 2019. Three individuals of each species were transplanted into each mesocosm in May. All mesocosms were well watered before the start of experiment (in July). Species were planted to maximize interspecies interactions and covered 3 functional groups: 6 grasses (*Agrostis capillaris* L., *Anthoxanthum odoratum* L., *Deschampsia cespitosa* (L.) P. Beauv., *Phleum pratense* L., *Poa pratensis* L., *Holcus lanatus* L.); 3 N-fixing forbs (N-fixers) (*Lotus corniculatus* L., *Trifolium pratense* L., *Trifolium medium* L.); and 3 non-N-fixing forbs (*Centaurea jacea* L., *Lychnis flos-cuculi* L., *Plantago lanceolata* L.).

From July 2, 2019, to October 28, 2019 (120 days), mesocosms were subjected to a gradient of 8 PRs, with alternating dry/wet periods of 1, 3, 6, 10, 15, 20, 30 and 60 consecutive wet and dry days (referred to as '1-day PR', '3-day PR', etc.). As watering cycles can start with either a wet or dry period, half of the mesocosms were exposed to a dry start (shortened as '1D', '3D', etc.), and the other to a wet start (shortened as '1W', '3W', etc.). The detailed PRs scheme is available in Figure S1. Each regime had 16 replicate mesocosms spread over four units. On wet days, mesocosms were irrigated between 10:30 am and 11:00 am with 6.87 L m^{-2} stored rainwater. This volume is 1.5 times the daily Belgian average precipitation to account for additional evapotranspiration in

the mesocosms compared to open field conditions. All regimes had the same total number of irrigation days (60 days) and total water amount (412 L m^{-2}) after 120 days. During the whole experimental period, the average volumetric soil water content (SWC) over 30 cm depth soil was measured automatically every half-hour by a CS650-DS Reflectometer (Campbell Scientific INC). The different PRs strongly influenced soil water contents (SWC; Figure S2). More persistent PRs with longer dry/wet periods such as 30D, 30W, 60D, 60W generally resulted in longer periods during which the SWC was below the permanent wilting point (Reynaert et al. 2021)(Figure S2). Because the mesocosms can drain, no water logging stress was induced, but the PRs with longer alternating dry/wet periods almost reached field capacity ($0.26 \text{ m}^3 \text{ m}^{-3}$) during the wet period (Figure S2).

At day 120, two grasses (*Holcus lanatus*; *Phleum pratense*) and two forbs (*Centaurea jacea*; *Plantago lanceolata*) were harvested to study metabolic changes.

2.2 Fv/Fm measurement

To estimate plant physiological stress level, we measured chlorophyll fluorescence with the Plant Efficiency Analyser (Hansatech Ltd, Pentney, England) as an indicator of photosystem II efficiency. We measured the Fv/Fm every two weeks over the course of 120 days, randomly selecting one mature green leaf from each species in three replicate mesocosms. Leaves were dark adapted for 30 min prior to measurement. We calculated average values of Fv/Fm per treatment on each species.

2.3 Sample harvesting and metabolite extraction for liquid chromatography-mass spectrometry (LC-MS) analysis

Among the 16 replicate mesocosms assigned to each PR, six replicates of each species were randomly chosen for the metabolomic analysis. We sampled all the leaves of that individual between 10:30-15:30. Leaf material from *Holcus lanatus* and *Centaurea jacea* under 60-day PR had largely vanished, therefore we couldn't perform metabolomic analysis on this treatment of these two species. There are four and five replicates under 60-day PR instead of six replicates for *Phleum pratense* and *Plantago lanceolata* due to shortage of material.

After being frozen in liquid nitrogen, leaves (approx. 300 mg) were lyophilized (at a temperature of -110°C , and pressure of ≤ 1 Pa) for at least 48 hours. Lyophilized samples were ground with a ball mill at 1500 rpm for 3 min and a fine powder produced was stored at -80°C in Eppendorf tubes. The precisely weighted homogenized samples (70 mg) were then extracted using a methanol: H_2O solution (1:1). After adding the extraction solvent (1 ml), the tubes were vortexed for 5 min and sonicated for 25 min at room temperature (22°C). To separate the supernatant and pellet, the samples were centrifuged at 14000 g for 5 min at 4°C . Consequently, 700 μl of the metabolite-containing supernatant was transferred to a new vial and the whole process was repeated. Finally produced supernatant was transferred to a labelled set of high-performance liquid chromatography (HPLC) vials and kept at -20°C till the HPLC analysis.

2.4 HPLC-MS analysis

Samples were analysed for metabolomics twice on the system of high-performance liquid chromatography (HPLC) coupled with a mass spectrometer (MS) using the positive and negative polarity of MS. Recordings from both the

diode array detector (DAD) and the high-resolution MS were monitored and saved to verify system function and to evaluate subsequent results.

A Dionex Ultimate 3000 (ThermoFisher Scientific, USA/Dionex RSLC, Dionex, USA) was used for the HPLC part. The injection volume was 5 μl . The separation column used was a C18 Hypersil Gold column (150 mm x 2.1 mm, 3 μm particle size; ThermoFisher Scientific, USA). The flow rate of mobile phases was 0.3 ml min^{-1} and the column temperature was set up on 30°C. The HPLC mobile phase consisted of (A) acetonitrile and (B) water containing 0.1 % acetic acid. Both mobile phases (A) and (B) were filtrated and degassed for 10 min in an ultrasonic bath prior to use. Gradient elution chromatography was performed starting with 10% acetonitrile (A) and 90% water (0.1 % acetic acid) (B) and held for 5 minutes. Within the time interval (5-20 minutes), A% composition was increased to 90%. This composition was then maintained for 5 min, after which the system was 5 min equilibrated to initial conditions (10% acetonitrile (A) and 90% water (0.1 % acetic acid)). The following wavelengths 254, 272, 274, and 331 nm from DAD detector were monitored.

MS and MS^n were performed using an LTQ Orbitrap XL- high-resolution mass spectrometer LTQ Orbitrap XL (ThermoFisher Scientific, USA) equipped with a HESI II (Heated electrospray ionization) source. The high-resolution mass spectrometer (orbitrap) was operated in full scan with resolution 60000. Full scan spectra were acquired over the mass range m/z 50-1000 in positive mode and 65-1000 in negative mode. The resolution and sensitivity of the Orbitrap were controlled by injection of mixed standard (phenolic compounds) after analyzing each of the 25 samples, and resolution was also checked by using lock masses (phthalates). Blanks were also analyzed during the sequence. The

compounds were searched in the mass library, which was created from the measurement of standards in MS and MSⁿ modes of Orbitrap.

2.5 Processing of LC-MS Data

LC-MS instrument-specific raw data (.raw) were converted to a common data format (.mzML) before processing in MZmine 2 (Pluskal et al. 2010). Chromatograms were baseline corrected, deconvoluted, aligned, filtered and normalized. The resulting numerical database containing the peak area of each feature was exported in “csv” format (see Table S1 for details). The peak area represents the abundance of each metabolite. Normalized peak areas were used for quantification, and their values were log₂ transformed before statistical analysis. The missing values in the dataset were replaced by the values that were half the minimum nonzero value of that specific metabolite (Grace and Hudson 2016). Metabolite identifications were assigned by two methods: a) by comparing the retention time (RT) and mass spectrum of analysed standards; b) the MS/MS data were submitted to GNPS (Global Natural Products Social Molecular Networking; <http://gnps.ucsd.edu>; Wang (2016)) and identified by reference libraries of known molecules in GNPS (see Table S2 for details).

2.6 Statistical analysis

Statistical analyses were performed with R programming language (version 4.0.4). Effects were considered significant with *p*-values < 0.05.

Seasonal mean F_v/F_m of each species were subjected to two-way ANOVA, with dry or wet start, PRs and their interactions as fixed factors. Tukey HSD pairwise comparisons were further utilised to test the significant differences between different groups. The processed LC-MS data were subjected to permutational

multivariate analyses of variance (PERMANOVA), with species, PR, dry or wet start and their interactions as fixed factors, and experiment unit as a random factor. Unsupervised principal component analysis (PCA) was performed to elucidate the metabolome differences among different species and treatments. For each species, both PCA and supervised partial least squares discriminant analyses (PLS-DA) were carried out to further detect patterns of sample ordination in the metabolomic dataset. Through VIP (variable importance in projection) analyses, metabolites with a VIP score > 1 are considered as the most important metabolites responsible for separating the defined groups of samples in PLS-DA (Sebastiana et al. 2021). The component scores of the cases in PCA were further subjected to one-way ANOVA and Tukey HSD comparison to determine the statistical differences among groups with different PR. PCA, PLS-DA, VIP analyses were performed by the mixOmics package (Rohart et al. 2017). PERMANOVA was performed with the ADONIS function in the Vegan package (OKSANEN 2007). Correlation analysis between each metabolite and PR levels (dry start and wet start respectively) was conducted by the *rcorr* function in the Hmisc package (Harrell 2023). The Pheatmap package (Kolde 2012) was used to generate heatmaps. The pathway analysis was constructed using the MetaboAnalyst 5.0 (Xia et al. 2009) with the reference metabolic pathways of *A. thaliana*. All remaining graphs were created by the R package ggplot2 (Wickham 2016).

3 Results

3.1 Effects of increasingly persistent PRs on the mean Fv/Fm of four grassland species

The more persistent PRs with longer alternating dry/wet durations significantly reduced the mean Fv/Fm of all four species ($p < 0.001$ in four species; Figure 1).

Dry or wet start also significantly affected Fv/Fm in *Holcus lanatus*, *Centaurea jacea* and *Plantago lanceolata* ($p < 0.05$), but not in *Phleum pratense* ($p = 0.076$).

Under dry start regimes, *Holcus lanatus* and *Centaurea jacea* exhibited significantly decreased Fv/Fm values from 30-day PR and 20-day PR respectively compared with the short dry/wet cycle PRs, while in *Phleum pratense* and *Plantago lanceolata*, a decrease of Fv/Fm was evident only under the 60-day PR (Figure 1; Table S3). Under wet start regimes, all species showed significantly reduced Fv/Fm at 30-day PR, but showed non-significantly altered Fv/Fm under 60-day PR (Figure 1; Table S3). This is probably because under the 60-day wet start PR (60W), plants were well watered during July and August (Figure S2), which maintained a relatively high mean Fv/Fm during the experiment.

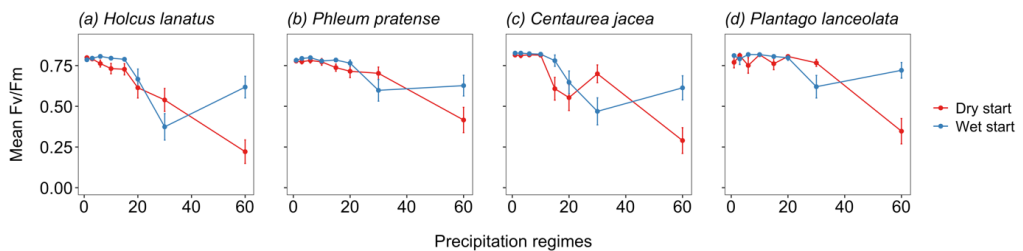


Figure 1 Seasonal mean Fv/Fm of four species induced by increasingly persistent precipitation regimes. Data are represented as mean \pm SE ($n=3$).

3.2 Effects of increasingly persistent precipitation regimes on the metabolome of four grassland species

For the metabolomic analysis, as a first step we performed a global analysis of the metabolomic differences between the four species and treatments. Metabolome of four species were distinctly different based on PERMANOVA (Table S4) and principal component analysis (PCA, Figure 2a). PC1 separated *Holcus lanatus*, *Plantago lanceolata* from *Centaurea jacea* and *Phleum pratense*, and explained 31% of the variance (Figure 2a). PC2 separated

Centaurea jacea from the other three species, and accounted for 20% of the variance (Figure 2a). PRs significantly influenced the metabolism (Table S4), and species, PRs, dry or wet start significantly interacted (Table S4), indicating that the impact of cycle length in the PR was species-specific and also depended on the start with a dry or wet period. Coinciding with PERMANOVA results, *Centaurea jacea* showed slightly more separation between less and more persistent PR along PC2, while the other three species did not show any clear separation between PRs (Figure 2a). Dry or wet start had an edge significant effect (Table S4), yet the effect was not observed in PCA with four species together (Figure 2a). The variance of the PC2 scores were highest in *Centaurea jacea* (42.3), and lowest in *Phleum pratense* (10.7), which indicate that the variability of the metabolome was lower in *Phleum pratense* than the other three species (Figure 2a). Differences in phenylpropanoids seems the primary factor driven the distinction among four species metabolome profiles (Figure 2b). Amino acids contribute to drive the separation of *Holcus lanatus* from other three species (Figure 2b).

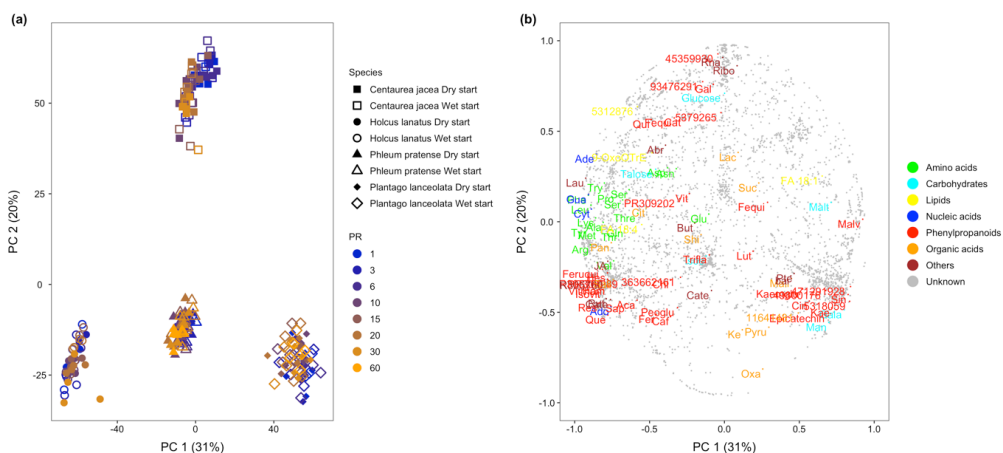


Figure 2 Global impact of increasingly persistent precipitation regimes (PRs) on the metabolome of four grassland species. Principal component analysis (PCA) conducted on metabolomic variables of four species using PC1 vs PC2: (a) The samples are categorized by species, PRs and dry or wet start. (b) Loadings of the metabolomic variables in PC1 and PC2. The identified

metabolites are classified into seven chemical classes, and unassigned metabolites are represented by small grey points. The full names of variables are listed in Table S2.

In order to further study the metabolome changes of each species induced by different PRs, we conducted both PCA and partial least-squares discriminant analysis (PLS-DA) on the metabolome of the individual species. There were 1022 features detected in *Holcus lanatus*. Among them, 92 compounds were identified by comparisons of retention times, mass-to-charge ratio and secondary mass spectrum. In *Phleum pratense*, 746 features were detected and 71 compounds were identified. There were 1004 and 1080 detected features in *Centaurea jacea* and *Plantago lanceolata*, and 80, 97 compounds were identified, respectively. Under PCA (Figure S3), *Holcus lanatus*, *Phleum pratense* showed separation between less and more persistent PRs along PC2. *Centaurea jacea* exhibited a clearer separation along PC1 (Figure S3). However, *Plantago lanceolata* did not show separation between less and more persistent PRs (Figure S3).

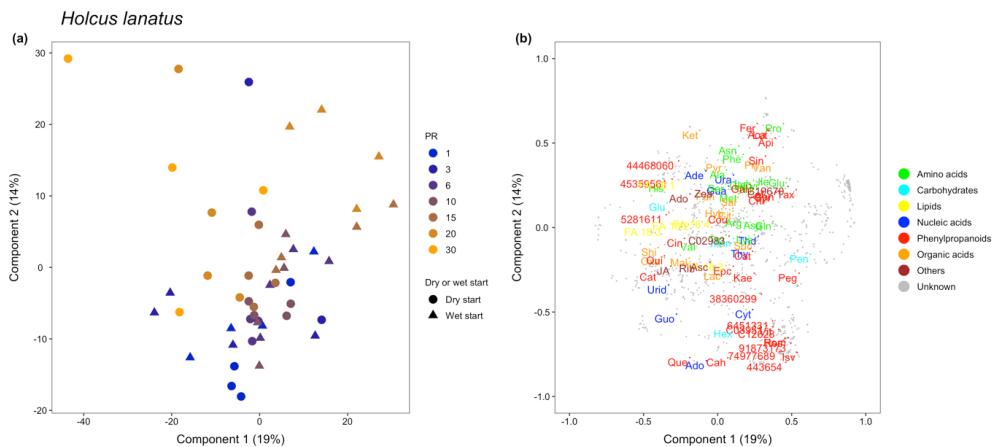
To investigate if a potential tipping point could be identified in the metabolome changes along the PR gradient, we subjected the component score coordinates from the PCA (irrespective dry or wet start) to one-way ANOVA and Tukey's HSD analysis for each species. There was a significant difference between PRs on *Holcus lanatus* (PC2: $p < 0.01$), *Phleum pratense* (PC2: $p < 0.001$), and *Centaurea jacea* (PC1: $p < 0.001$). For *Plantago lanceolata*, there was an edge significant difference on PC1 scores between different PRs ($p = 0.060$). Post hoc analysis of the score coordinates from different PRs revealed that the metabolome differed at 20-day PR in *Holcus lanatus*, *Phleum pratense*, and *Plantago lanceolata* showed edge significant differences between 20-day PR and 3-day PR (Table S5). For *Centaurea jacea*, the comparison of coordinates

indicates that the metabolome already significantly differed from 10-day PR onward (10, 15, 20, 30) compared to short-cycle PRs (1, 3, 6) (Table S5).

Using the PLS-DA which is a supervised method for classification, four species exhibited a more clear separation between different PRs (Figure 3). Component 2 of PLS-DA, which explained 14% and 11% of the variance, separated less and more persistent PR of *Holcus lanatus* and *Phleum pratense*, respectively (Figure 3a, c). In *Centaurea jacea* and *Plantago lanceolata*, less and more persistent PR separated along component 1, which accounted for 25% and 13% of the variance, respectively (Figure 3e, g). For the more persistent PR (15-day PR onwards) *Holcus lanatus* samples separated between dry and wet start along component 1 (Figure 3a). *Phleum pratense* showed separation between dry and wet start along component 2 under less persistent PR (until 10-day PR), with the metabolome of wet start short-cycle PR closer to long-cycle PR (Figure 3c). In contrast, no separation between dry or wet start occurred for *Centaurea jacea* and *Plantago lanceolata*, irrespective of less or more persistent PRs (Figure 3e, g). The 60W PR separated from other PRs along component 2 in *Plantago lanceolata* (Figure 3g), which suggests that the metabolome changed significantly and was no longer comparable with other PRs.

The variable plots derived from PLS-DA (Figure 3b, d, f, h) further illustrate the contributions of metabolites to the separation of metabolomes among different PRs. The PLS-DA indicates that amino acids showed higher concentrations in more persistent PRs (Figure 3b, d, f, h). Consistent with the PLS-DA indication, correlation analysis between metabolites and PR gradient (dry and wet start respectively) showed that in *Holcus lanatus*, several amino acids such as alanine, leucine, proline, phenylalanine, glutamine and tyrosine, have a significant positive correlation with the wet start PR gradient (Table S6,

Figure 3b). Proline showed the highest correlation coefficient ($r = 0.78$). However, the amino acids were not significantly positively correlated with dry start PRs (Table S6, Figure 3b). In *Phleum pratense*, amino acids alanine, phenylalanine, arginine, glutamine, serine, lysine, leucine, proline, tyrosine, methionine was positively correlated with both dry and wet start PRs (Table S6, Figure 3d). Similar in *Centaurea jacea*, phenylalanine, tryptophan, proline, alanine, asparagine, valine, arginine, leucine, threonine, glutamine, histidine increased along both dry and wet start PR gradient (Table S6, Figure 3f). In *Plantago lanceolata*, only lysine, phenylalanine, and tyrosine exhibited a positive correlation with both dry and wet start PRs (Table S6, Figure 3h). The other chemical classes displayed divergent patterns, with both up- and down-regulated changes, and no evident alterations were observed under more persistent PRs in different species. For *Plantago lanceolata*, organic acids and carbohydrates were negatively correlated with more persistent PRs, especially under dry start PRs (Table S6, Figure 3h).



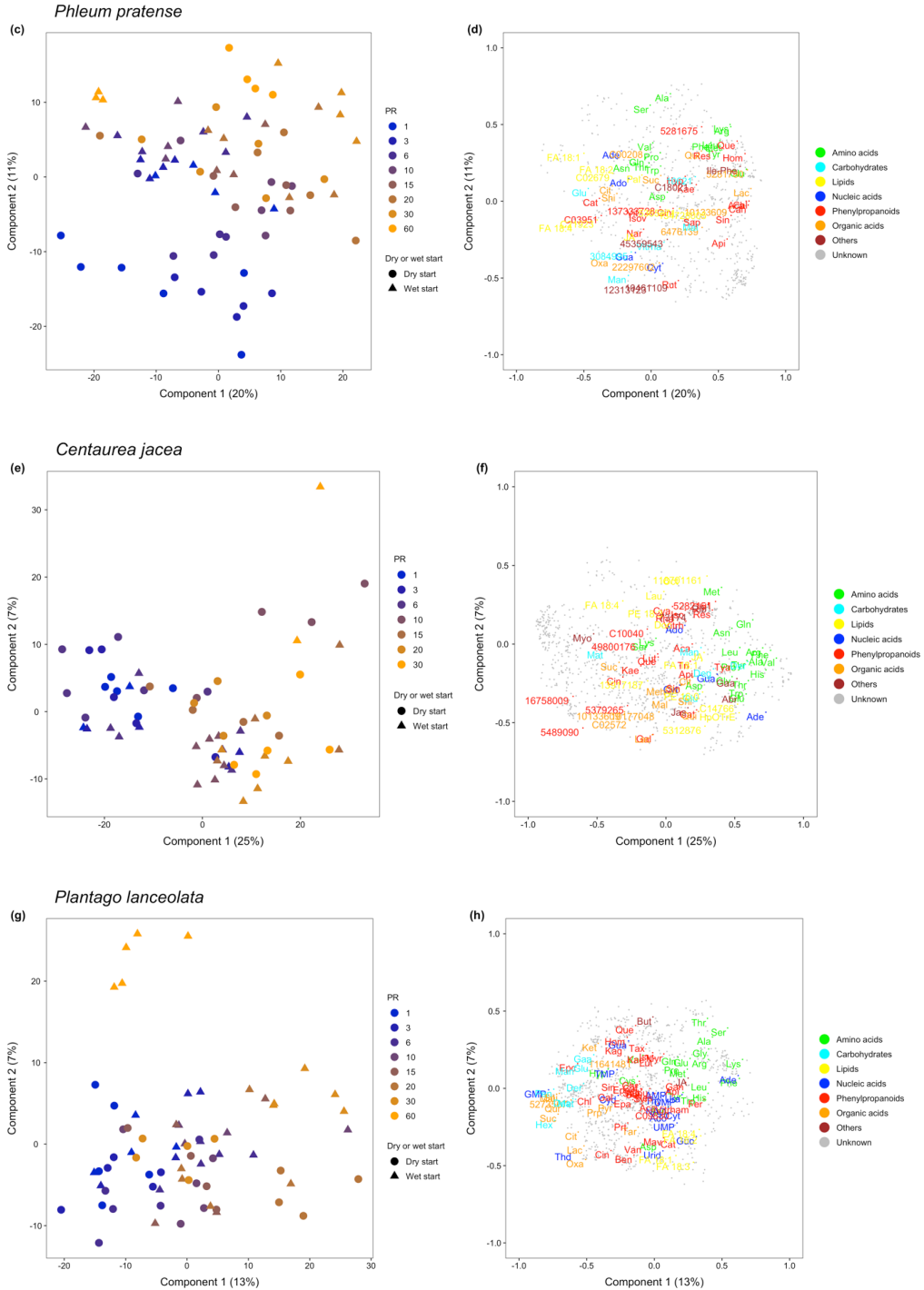


Figure 3 Impact of increasingly persistent precipitation regimes (PRs) on the individual metabolomes of four grassland species. Partial least-squares discriminant analysis (PLS-DA) conducted with metabolomic variables of individual species using component 1 versus

component 2. (a, c, e, g) The cases are categorized by PR and dry or wet start. (b, d, f, h) Loadings of the metabolomic variables in component 1 and component 2. The identified metabolites are classified in seven chemical classes, and unassigned metabolites are represented by small grey points. The full names of variables are listed in Table S2.

3.3 Identification of key metabolites that respond to increasingly persistent precipitation regimes using VIP score

According to VIP analysis, in total 28 identified metabolites have VIP scores > 1 in *Holcus lanatus* (Figure 4a), mainly including phenylpropanoids (Figure S4). Among these metabolites, catechol, peonidin-3-glucoside, isovitexin, guanosine, neoeriocitrin, quercetin, homoorientin, adenosine, vitexin, vitexin 2''-O-rhamnoside, luteolin-7-glucoside, resveratrol, pentose had lower contents at more persistent PR (20D, 30D, 20W). At the same time, proline, ferulic acids, acacetin, 9-octadecenamamide, caffeic acid, apigenin, asparagine, sinapic acids, phenylalanine, protocatechuic acid, vanillic acid, pyruvic acid, syringic acid were upregulated under more persistent PR (Figure 4a).

In *Phleum pratense*, 23 metabolites were identified with VIP > 1 (Figure 4b), which were dominated by phenylpropanoids and amino acids (Figure S4). The amino acids alanine, serine, arginine, lysine, glutamic acid, leucine, phenylalanine, and phenylpropanoids luteolin-8-C-glucoside, quercetin, homoorientin, acacetin, quinic acid, catechol, chlorogenic acid, 3,4-dicaffeoylquinic acid were upregulated under more persistent PR (with a few exceptions at 60W). The organic acid oxaloacetic acid, and lipids FA 18:4+2O, FA 18:1+3O were downregulated in response to more persistent PR (with exceptions at 60D/W; Figure 3b).

There were 18 metabolites that showed VIP >1 for *Centaurea jacea* (Figure 4c), including mainly primary metabolites such as amino acids, lipids and carbohydrates (Figure S4). Their contents were all increased from 10-day PR, especially in the dry start treatment (with a few exceptions at 30W; Figure 4c).

There were 34 metabolites with VIP scores >1 in *Plantago lanceolata* (Figure 4d). They were more evenly distributed in the different chemical classes compared with the other three species (Figure S4). The levels of the amino acids lysine, phenylalanine, serine, histidine, alanine, tyrosine, and hydroxy-proline were all higher under more persistent PR (with exceptions at 60W). In contrast, organic acids levels, i.e., malic acid, shikimic acid, succinic acid, citric acid, lactic acid, propionic acid, oxaloacetic acid, sinapic acid, α -ketoglutaric acid and protocatechuic acid, as well as carbohydrates pentose and hexose, were reduced at more persistent PR (with some exceptions at 60W; Figure 4d). Specifically, phenylalanine showed a VIP > 1 among four species and alanine had a VIP > 1 in three species (except *Holcus lanatus*), and they were generally increased under more persistent PRs (Figure 4).

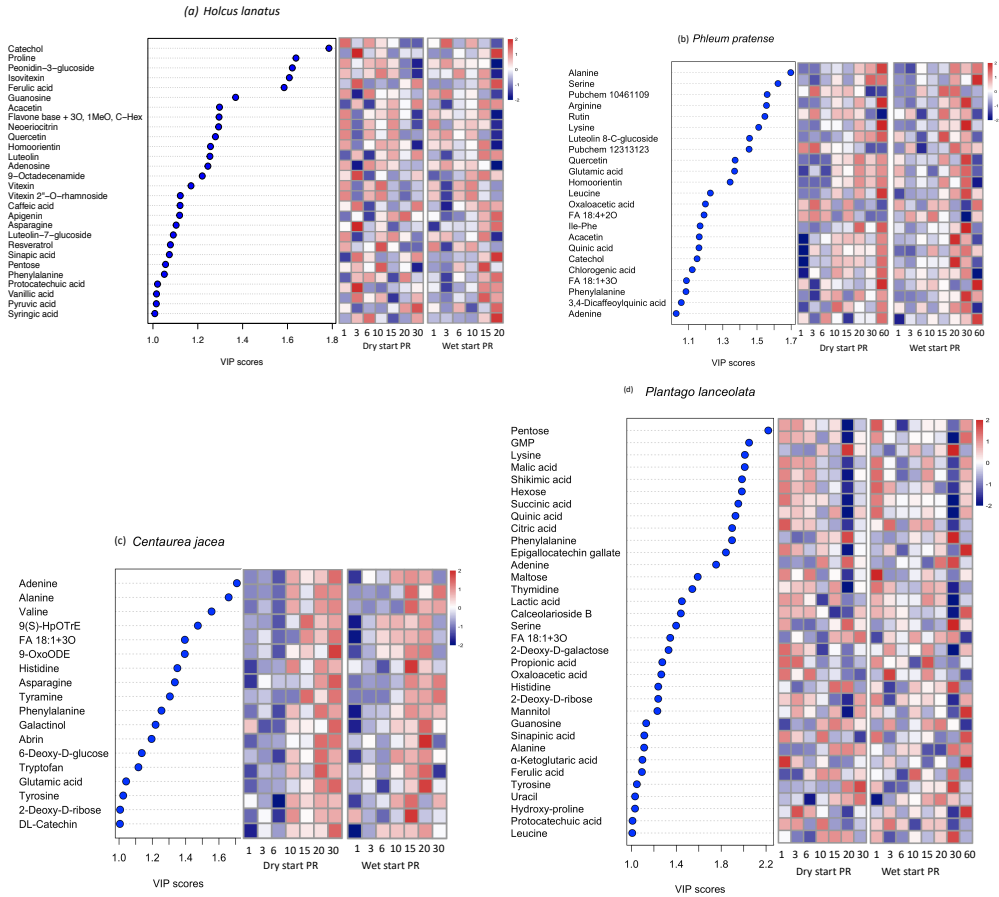


Figure 4 The impact of increasingly persistent precipitation regimes (PRs) on the selected metabolites (VIP > 1) in four grassland species. The VIP score plots of four species showing the most significantly changed metabolites under different PRs. The heatmaps indicate up (red colours) and down regulations (blue colours) of metabolites in respective PR groups.

We further compared the extend of phenylalanine and alanine increases under long-cycle PRs among different species (Figure 5). The separation of PRs into short-cycle and long-cycle PRs was based on the PCA (Figure S3) and the potential tipping point suggested by component score coordinate comparison (Table S5). On the other hand, since only two species have materials at 60-day PR for metabolomic analysis and the PR gradient is highly skewed because of a large gap between 30-day and 60-day PR gradient, the 60-day PR was not included in the long-cycle PRs group. As a result, the short-cycle PRs group included 1, 3, 6, 10, 15-day PR, and the long-cycle PRs group included 20, 30-

day PR for *Holcus lanatus*, *Phleum pratense* and *Plantago lanceolata*, while 1, 3, 6-day PR were short-cycle PR and 10, 15, 20, 30-day PR were long-cycle PR for *Centaurea jacea*. As shown in Figure 5a-d, phenylalanine showed significant differences between short-cycle and long-cycle PRs in the tolerant species *Phleum pratense* and *Plantago lanceolata*, especially under a wet start (Figure 5a-d). Notably, the phenylalanine content was generally higher in *Phleum pratense* and *Plantago lanceolata*. With regard to alanine, only the most tolerant species *Phleum pratense* exhibited significant differences between short and long-cycle PRs (Figure 5e-h).

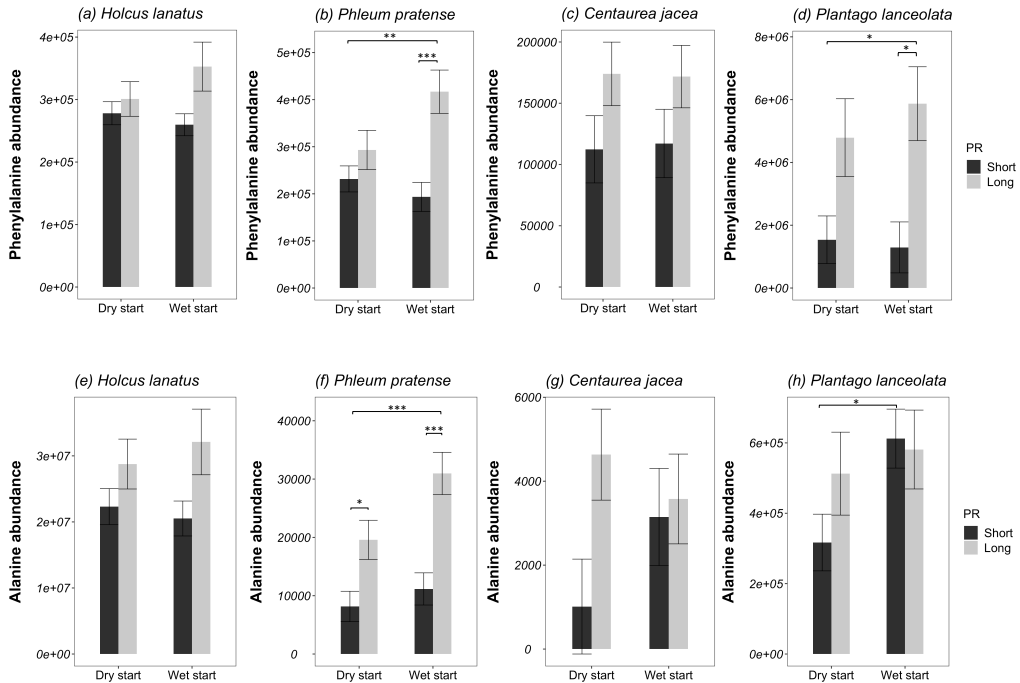


Figure 5 The effect of increasingly persistent precipitation regimes (PRs) on phenylalanine and alanine abundance of four species. Short or long-cycle PRs are defined by the potential ‘tipping point’ observed in this study, i.e. short-cycle PRs includes 1, 3, 6, 10, 15-day PR and the long-cycle PRs includes 20, 30-day PR for *Holcus lanatus*, *Phleum pratense* and *Plantago lanceolata*; for *Centaurea jacea*, the short-cycle PR includes 1, 3, 6-day PR and the long-cycle PR includes 10, 15, 20, 30-day PR. Error bars indicate mean \pm SE. The number of replicates depends on the combined treatments, which varies between 25-60. Asterisks depict significant two-by-two differences with Tukey HSD correction (*: $p < 0.05$; **: $p < 0.01$; ***: $p < 0.001$).

3.4 Identification of metabolic pathway responses to more persistent precipitation regimes

To determine the significantly affected metabolic pathways under long-cycle PRs compared with short-cycle PRs, we performed a pathway enrichment and topology analysis. To this end, we used the KEGG database, which restricted the analysis to identified metabolites which mapped with KEGG IDs. The metabolic pathways are presented as a circle based on their score from pathway topology analysis (pathway impact, horizontal axis) and pathway enrichment analysis ($-\log P$, vertical axis) (Figure 6). The darker red indicates more significant changes of metabolites in the respective pathway (higher $-\log P$ value), and the circle size indicates the pathway impact value. The pathway impact value is determined based on the importance of the metabolites within the pathway (i.e., changes in more important positions of a network will have a more prominent effect on pathway function than changes occurring in marginal or relatively isolated positions (Rangani et al. 2020). Long-cycle PRs significantly affected both the primary and secondary metabolism of the four grassland species under both dry and wet start (Figure 6; Table S7). In *Holcus lanatus*, long-cycle PRs under dry start mainly influenced the primary metabolism, with glycolysis as the most significantly affected pathway (Figure 6a; Table S7a). More pathways were significantly influenced by the long-cycle PRs under wet start in *Holcus lanatus* compared to the dry start, with phenylpropanoid biosynthesis as the most significantly influenced pathway under wet start (Figure 6b; Table S7b). In *Phleum pratense*, alanine, aspartate and glutamate metabolism pathway was significantly affected by long-cycle PRs and also showed high impact under both dry and wet start PRs (Figure 6c, d; Table S7c, d). In *Centaurea jacea*, the long-cycle PRs also significantly affected alanine, aspartate and glutamate metabolism (highest $-\log P$ and impact, Figure

6e; Table S7e), while starch and sucrose biosynthesis were the most affected by long-cycle PRs under wet start (Figure 6f; Table S7f). In *Plantago lanceolata*, glyoxylate and dicarboxylate metabolism pathway was the most affected pathway induced by long-cycle PRs under dry start and phenylalanine metabolism pathway was the most affected pathway under wet start (Figure 6g, h; Table S7g, h). Long-cycle PRs induced significantly changes on phenylalanine metabolism and alanine, aspartate and glutamate metabolism in all four species (Figure 6). The detailed pathway view with the identified changes in metabolites can be found in the supplementary (Figure S5).

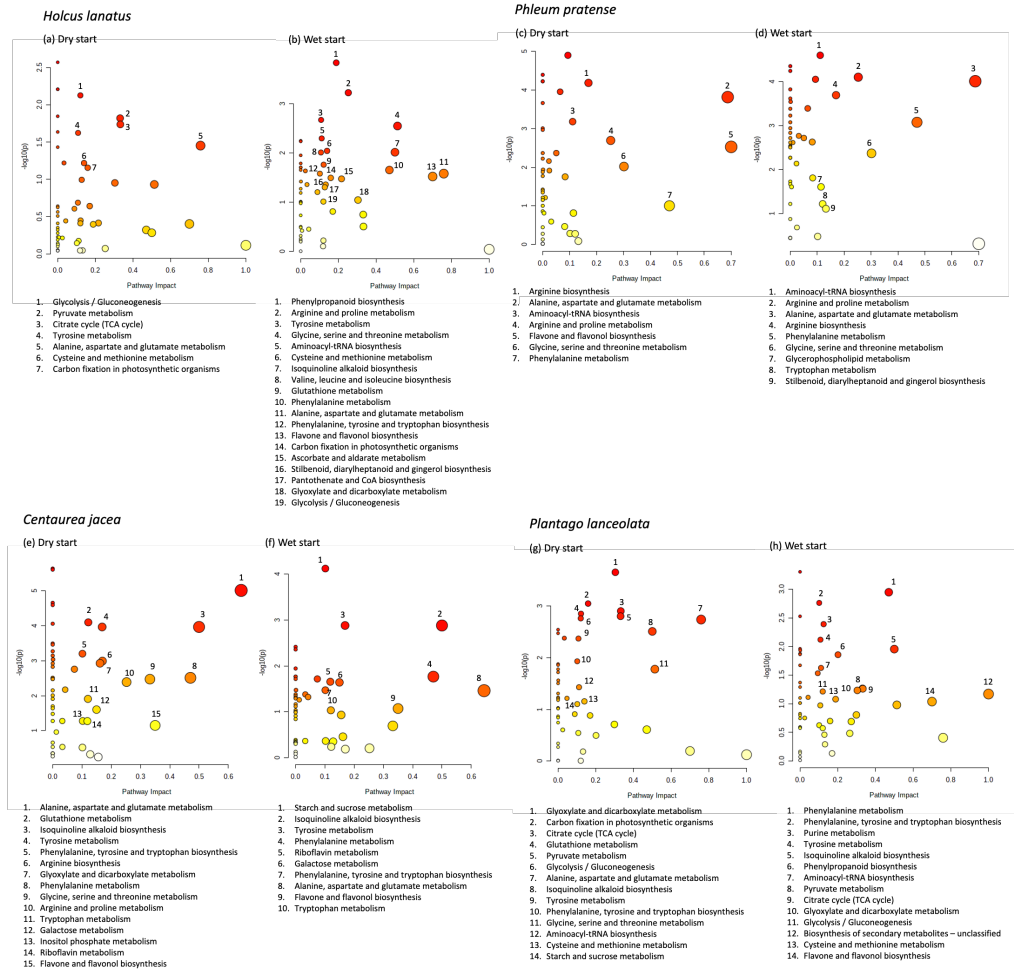


Figure 6 The effects of long-cycle compare with short-cycle PRs under dry and wet start on metabolic pathways in four grassland species. The color gradient from red to yellow reflects the magnitude of alterations of compounds in the respective pathway (red = most, yellow = least). The circle size represents the pathway impact value. Pathways that have both $-\text{Log}_{10} p > 1$ and $\text{impact} > 0.1$ were labeled.

4 Discussion

As a consequence of global climate change, precipitation regimes are predicted and have already been observed to become more persistent with both longer dry and longer wet periods (Pfleiderer et al. 2019; Breinl et al. 2020). To unravel the effects of these changing PRs and understand how plants with different tolerance capacities respond to such adverse conditions, we analysed the metabolic changes of four grassland species subjected to a range of PRs. The four species have contrasting sensitivities to these conditions, with *Centaurea jacea*, *Holcus Lanatus*, *Plantago lanceolata*, *Phleum pratense* being increasingly tolerant based on survival and photochemistry data (Reynaert et al. 2021).

4.1 Is there a tipping point in the metabolic responses to changing PRs, and does this differ between sensitive and tolerant species?

At the metabolome level, we found that the four species have distinct metabolomic profiles, with the sensitive species *Centaurea jacea* showed longest metabolomic distances to the other species (Figure 2). The observed variability of the metabolome across the PR range was lowest in *Phleum pratense* (Figure 2), which suggest that this most tolerant species has a more stable and homeostatic metabolism than the relative sensitive species. The metabolome of the most sensitive species *Centaurea jacea* showed clearly tipping point at 10-day PR as opposed to only changed from the 20-day PR in the other three species (Figure 3; Table S5). This further confirms that sensitive species more rapidly lose metabolic homeostasis. On the other hand, we should

be aware that plants have some degree of flexibility to alter their metabolism in response to the changing environment. Therefore, the tolerance capacity is likely an outcome of a trade-off (balance) between adaptive capacity (flexibility) and stability (homeostasis) (Gargallo-Garriga et al. 2020). We speculated that during the experiment, the more tolerant species may have faster and more efficient plasticity responses such as metabolic and morphological adjustment, and a stronger accumulation of key metabolites (e.g., phenylalanine, alanine; Figure 5). These features may provide enough protection and help them to return to normal metabolism at the end of the experimental period. On the other hand, in the sensitive species the continued investment on metabolic reprogramming may come at the cost of lower productivity. The metabolome of three species shifted at 20-day PR coincided with the reduction of the biodiversity in the mesocosm (Reynaert et al. 2021) suggests that the 20-day dry/wet regime is an extreme response threshold that may cause irreversible changes to the grassland ecosystem. Notably, Gargallo-Garriga et al. (2018) also reported that a period of drought (around 18 days) caused an irreversible effect on root exudate metabolomes, as the exudates could not return to the pre-drought composition even after six weeks of re-watering. Hence, temperate grassland ecosystems are at risk of changing irreversibly under increasing summer weather persistence, leading to long(er) term changes in aboveground plant performance (e.g., stress metabolism), biodiversity and ecosystem provisioning (e.g., fodder production and quality).

4.2 Dry or wet start influences the impact of PRs

The timing of dry and wet spells influenced the impact of PR on metabolome changes. Because all PRs were set up to have the same overall precipitation, the start and end were always opposite, thereby confounding their effects. This

makes it impossible to discriminate the relative effects of early and late dry and wet phases. Nevertheless, we observed that in some key metabolites (e.g., phenylalanine), the differences between short-cycle and long-cycle PR were more evident under a wet start (dry end) (Figure 3). This is probably because, at the time of harvesting, the PR ended in a dry period with lower soil water content (SWC), especially for the long-cycle PR (Figure S2), which intensifies the stress responses. The different impact of dry and wet start PR may also link to the developmental stage of the plants (Prasad et al. 2008; Ihsan et al. 2016). For instance, the timing of dry or wet periods may coincide with sensitive phenological stages, or with a hot period that exacerbates drought. The separation between dry and wet start was more evident in grasses (*Holcus lanatus* and *Phleum pratense*; Figure 3), which may imply that compared with forbs, the metabolome of grasses is more influenced by current SWC, but less shaped by previous and longer-term stimulus (e.g., PRs). This flexibility of adjusting the metabolome based on undergoing condition may partly explain why grasses are generally showing higher resilience (recover fast in favourable condition) compared with other functional groups (Elst et al. 2017).

4.3 Increasing of amino acids is a general response across species

Accumulation of amino acids in plants exposed to various forms of abiotic stress has been described in many studies (Krasensky and Jonak 2012; Rivas-Ubach et al. 2014; Sardans et al. 2020; Fàbregas and Fernie 2019; Gargallo-Garriga et al. 2015). In this study, aromatic amino acids (AAAs) phenylalanine, tryptophan and tyrosine were increased under long-cycle PRs and showed higher VIP scores (with phenylalanine having $VIP > 1$ in all four species; (Figure 4; Table S6). Their metabolisms were significantly affected and showed high impact in the pathway analysis, with phenylalanine metabolism affected in all four species

(Figure 6). This strongly suggests a critical role of AAAs in response to the changing PR. The underlying molecular mechanism may lie in their role in secondary metabolism. AAAs serve as precursors for a significant number of secondary metabolites which have defence functions. Noticeably, in the tolerant species *Phleum pratense* and *Plantago lanceolata*, the accumulation of phenylalanine under long-cycle PRs was more prominent and the concentration was higher than in the sensitive species *Holcus lanatus* and *Centaurea jacea* (Figure 5a-d). This indicates that insufficient accumulation of phenylalanine may be a limiting factor for the sensitive species in response to altered PR. Similarly, earlier findings also showed that higher phenylalanine is associated with drought tolerance of plants (Rangani et al. 2020). AAAs have been shown to be the most accumulated amino acids in maize leaves under stress (Fàbregas and Fernie 2019; Vogt 2010; Obata et al. 2015). On the other hand, the branched-chain amino acids (BCAAs) valine, leucine, isoleucine showed VIP > 1 in all species except *Holcus lanatus* (Figure 4). However, the related metabolic pathways were not significantly affected in most of them (Figure 6). This means that other metabolites involved in this pathway did not change significantly, and the pathway remained relatively static. This is supported by earlier studies showing that the elevated BCAAs were only significant under severe drought stress in rice (Todaka et al. 2017), and the response occurred later than AAAs (Fàbregas and Fernie 2019). We have also found that alanine and glutamate generally increased under long-cycle PRs and showed VIP > 1 at least in two species (Figure 4; 6). Consistently, the alanine, aspartate and glutamate metabolism pathway were highly activated under long-cycle PRs in four species, especially in dry start regimes (Figure 6). This may be related to alanine, glutamate and aspartate being precursors for various protective compounds such as β -alanine betaine, proline, glutamine, GABA,

asparagine, which are well-known for their anti-stress functions (osmoprotection, stomata regulation, tissue repairing, etc.)(Sardans et al. 2020; Llanes et al. 2018). The accumulation of alanine under long-cycle PRs was more evident in the most resistant species *Phleum pratense* (Figure 5e-h), which may contribute to its tolerance capacity. In that regard, Rangani et al. (2020) found that alanine, aspartate and glutamate metabolism significantly altered during drought stress recovery. Thus, our results that this pathway was more activated in dry start regimes, may indicate that plants showed signs of recovery in wet periods during harvest. However, it should be noted that earlier findings indicate that during osmotic stress, the accumulated amino acids in *Arabidopsis* are mainly the result of protein degradation (T. Huang and Jander 2017). Therefore, despite the anti-stress functions, the increased amino acids found in this study may also imply protein degradation and cell damage induced by more persistent PRs. Nevertheless, the overall accumulation of amino acids in four species indicates that amino acids probably have a more prominent role than other metabolites in more persistent PR responses.

4.4 Responses in other chemical classes showed species-specific changes

Unlike amino acids which generally increased under long-cycle PR in all four species, other metabolites changed in a more species-specific manner. For example, TCA cycle intermediates such as citric acid, oxaloacetic acid, malic acid, and succinic acid were considerably more affected in *Plantago lanceolata* than in the other species, with five TCA intermediates generally decreasing under long-cycle PRs and showing higher VIP scores (Figure 4; Table S6). Consistently, the TCA cycle pathway was affected in both dry and wet start long-cycle PR in this species (Figure 6). In the same species, carbohydrates (pentose, hexose, maltose, etc.) generally decreased under long-cycle PRs (Figure 4; Table S6).

The TCA cycle utilizes carbohydrates as fuel molecules for the oxidative decarboxylation of pyruvate and generation of energy-rich molecules. Simultaneously, carbohydrates are also involved in defence responses such as osmoprotection and ROS scavenging during stress acclimation. Therefore, the down-regulated TCA intermediates may reflect a shortage of carbohydrates for energy metabolism. In the other three species, the changes of TCA intermediates were not evident. This is in agreement with previous studies, which showed different results of TCA responses induced by stress among different species (Sardans et al. 2020; Fàbregas and Fernie 2019). Due to the relatively small numbers of carbohydrates that we were able to identify in this study, it's difficult to conclude the general responses of carbohydrates towards the altered PRs in all four species. However, as discussed earlier about *Plantago lanceolata*, the decreased carbohydrates under long dry/wet cycle PRs may be the outcome of the decreased photosynthesis efficiency as reflected by the seasonal Fv/Fm (Figure 1). It should be noted that since carbohydrates and polyalcohol play important roles in osmotic potential adjustment, signal transduction, etc., their depletion may impair the tolerance of plants towards stress (Rosa et al. 2009; Naudts et al. 2013).

Species specific PR-induced changes were also observed in lipids. Polyunsaturated fatty acids (PUFAs) have multiple roles, such as the storage of carbon and energy, precursors of various defence molecules and modulators of stress signalling (He and Ding 2020). In our study, the increase of particular PUFAs under long-cycle PRs was evident in the sensitive species *Centaurea jacea*, while the tolerant species *Phleum pratense* showed decreasing PUFAs levels (Figure 4; Figure S5). However, previous research reported that stress-sensitive plants generally showed decreased levels of PUFA, and elevated PUFA improved the tolerance of tobacco to salt and drought stress (Upchurch 2008;

Zhang et al. 2005). This may be due to the different strategies and/or stress levels combating the changing PR between tolerant and sensitive species. We found that except *Centaurea jacea*, phenylpropanoids (secondary metabolites) accounted for a major proportion of the high VIP-score metabolites in response to long-cycle PR in the other three species (Figure S4). This suggests that *Centaurea jacea* was less capable of modulating secondary metabolism (defence response), but more dependent on changing of primary metabolism (amino acids, lipids, carbohydrates). Consequently, this species' growth and development was likely more affected by the altered PR. Phenylpropanoids generally exhibit increased concentrations under various levels of stress according to previous studies (Sardans et al. 2020; Fàbregas and Fernie 2019). In our study, although the flavone and flavonoids biosynthesis pathway were generally affected by the altered PR in four species (Figure 6), no particular phenylpropanoid compound showed higher VIP in at least three species, and no universal up or down regulation of any compound was found among the four species (Figure 4; Figure S5). This observation reflects the high species-specificity in the synthesis of secondary metabolites during PR responses. We assume that since plants were exposed to repeated stress (dry)/recovery (wet) cycles, it is more efficient for plants to store upstream metabolites (such as amino acids mentioned above), and only further synthesize downstream anti-stress molecules when necessary.

5 Conclusion

This study is the first to document changes in the metabolome of contrasting grassland species subjected to a range of PRs with increasing duration of alternating dry and wet periods (i.e., increasing summer weather persistence). We confirmed both our hypotheses by showing that 1) the metabolome of a

relatively sensitive species *Centaurea jacea* shifted already under a mild PR (10-day PR), while the metabolome of the other less sensitive species changed only from 20-day PR onwards; 2) increasing levels of amino acids, particularly aromatic amino acids in all four species is a universal response to increasing PR extremity. Moreover, phenylalanine metabolism, alanine, aspartate and glutamate metabolism pathways were highly involved in more persistent PR responses for all species; 3) changes in other classes of metabolites exhibited in a more species-specific manner; 4) insufficient accumulation of AAs (e.g. phenylalanine, alanine) and deficient induction of secondary metabolism may be the limiting factors for sensitive species in response to more persistent PRs. Likely these changes will affect plant composition and thereby possibly changing its role in feeding of organisms. These findings could aid in predicting the impact of future precipitation regimes on grassland ecosystems and provide fundamental information on how species respond at the metabolome level to the increasing persistent weather conditions.

6 Supplementary materials

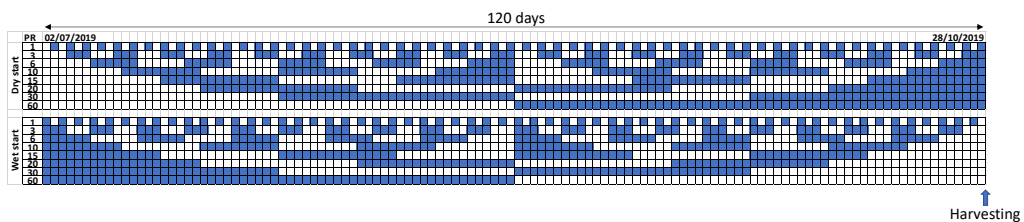


Figure S1 Scheme of precipitation regimes (PRs) applied in this study. Blue squares represent wet days, and blank squares represent dry days. All PRs received same amount of water by the end of 120 days.

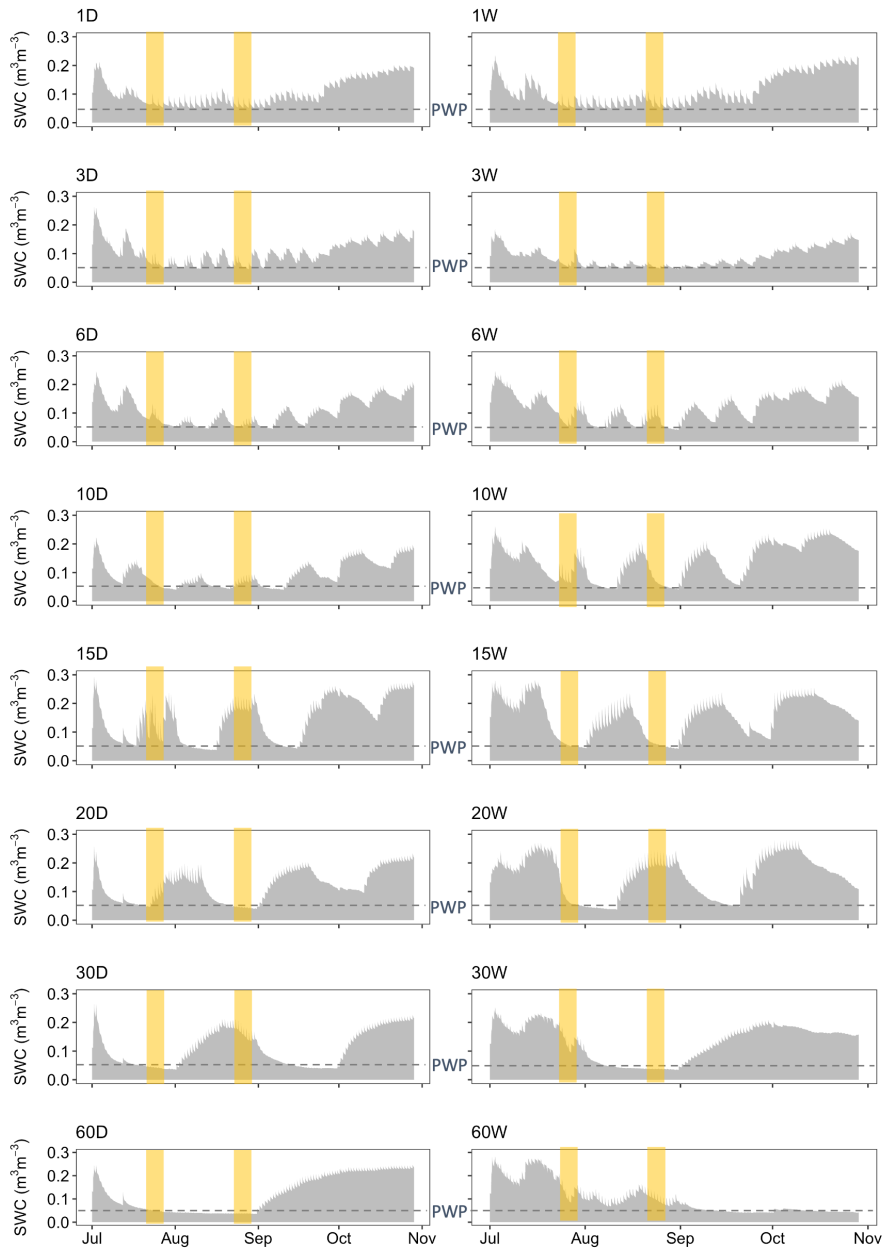


Figure S2 Soil water contents (SWC) induced by increasingly persistent PR during the experiment period. 'D' and 'W' represent dry or wet start treatments, respectively. The spiky nature of the profiles represents the daily irrigation events during the wet periods. The dashed line indicates the permanent wilting point (PWP) at $0.05 \text{ m}^3\text{m}^{-3}$. Heatwaves, indicated in orange blocks, were defined as a period of three or more days with average temperature $>25^\circ\text{C}$. This graph is modified based on Figure 2 in L. Li, Nijs, et al. (2023) with permission from the publisher.

Table S1 Processing parameters of the LC-MS chromatograms using MZmine 2 (Pluskal et al. 2010).

	(+H) Chromatograms	(-H) Chromatograms
Baseline correction		
Chromatogram type	TIC	TIC
MS level	1	1
Smoothing	10 ^{E6}	10 ^{E6}
Asymmetry	0.001	0.001
Mass detection (Centroid)		
Noise level	5.0 ^{E5}	5.0 ^{E5}
ADAP chromatogram builder		
Min group size in # of scans	5	5
Group intensity threshold	5.0 ^{E2}	5.0 ^{E2}
Min highest intensity	1.0 ^{E3}	1.0 ^{E3}
m/z tolerance	0.001 m/z or 0.0 ppm	0.001 m/z or 0.0 ppm
Smoothing		
Filter width	5	5
Chromatogram deconvolution		
Chromatographic threshold	70%	70%
Search minimum in RT range (min)	0.1	0.1
Minimum relative height	7.0%	7.0%
Minimum absolute height	30000	30000
Min ratio of peak top/edge	2	2
Peak duration range	0.0-2.0	0.0-2.0
Group isotopes		
m/z tolerance	0.001 m/z or 0.0 ppm	0.001 m/z or 0.0 ppm
RT tolerance	30 relative (%)	30 relative (%)
Maximum charge	3	3
Chromatogram alignment (RANSAC alignment)		
m/z tolerance	0.001	0.001
RT tolerance	0.2	0.2
RT tolerance after correction	0.05	0.05
Gap filling (Peak finder, multithreaded)		
Intensity tolerance	20%	20%
m/z tolerance	0.001	0.001

RT tolerance	0.1	0.1
Filtering (Feature list rows filter)		
Minimum peaks in a row	4	4
Normalization		
Normalization type	Total raw signal	Total raw signal
Peak measurement type	Peak area	Peak area

Table S2 Metabolites that were defined after the comparison with our standard compound library or by a matching of MS/MS data with the GNPS library.

Library	RT	M/Z	Identity	Abbreviation
Internal standard	1.43	76.039	Glycine	Gly
Internal standard	1.43	90.054	Alanine	Ala
Internal standard	1.53	118.086	Valine	Val
Internal standard	1.76	132.101	Leucine	Leu
Internal standard	1.7	132.101	Isoleucine	Ile
Internal standard	1.47	106.049	Serine	Ser
Internal standard	1.43	120.065	Threonine	Thr
Internal standard	1.46	122.026	Cysteine	Cys
Internal standard	1.59	150.058	Methionine	Met
Internal standard	1.32	147.112	Lysine	Lys
Internal standard	1.5	134.044	Aspartic acid	Asp
Internal standard	1.46	133.06	Asparagine	Asn
Internal standard	1.47	148.06	Glutamic acid	Glu
Internal standard	1.46	147.076	Glutamine	Gln
Internal standard	1.34	175.119	Arginine	Arg
Internal standard	1.5	156.076	Histidine	His
Internal standard	1.91	166.086	Phenylalanine	Phe
Internal standard	2.49	205.097	Tryptophan	Trp
Internal standard	1.49	116.07	Proline	Pro
Internal standard	1.54	182.081	Tyrosine	Val
Internal standard	1.46	132.065	Hydroxy-proline	Hypro
Internal standard	1.39	183.0865	D-Mannitol	Man
Internal standard	3.16	355.1027	Chlorogenic acid	Chl
Internal standard	1.75	193.0337	Citric acid (monohydrate)	Cit
Internal standard	4.8	181.0497	trans-Caffeic acid	Caf
Internal standard	11.29	187.0366	3-coumaric acid	Cou
Internal standard	16.4	345.0966	5,7-dihydroxy-3,4,5-trimethoxyflavone	6250403

Chapter 2

Internal standard	16.87	285.0755	Acacetin	Aca
Internal standard	14.63	271.0601	Apigenin	Api
Internal standard	4.82	181.0551	Caffeic acid	Caf
Internal standard	3.44	291.0863	DL-catechin	Cat
Internal standard	17.1	271.06	Galangin	Gala
Internal standard	1.83	171.0224	Gallic acid	Gal
Internal standard	9.45	449.1078	Homoorientin	Hom
Internal standard	11.1	433.1125	Isovitexin	Isov
Internal standard	14.82	287.0552	Kaempferol	Kaem
Internal standard	13.68	287.0551	Luteolin	Lut
Internal standard	12.47	319.0446	Myricetin	Myr
Internal standard	2.58	155.0215	Protocatechuic acid	Prt
Internal standard	13.72	303.0498	Quercetin	Que
Internal standard	1.51	193.0707	Quinic acid	Qui
Internal standard	13.09	229.0857	Resveratrol	Res
Internal standard	15.95	317.0654	Rhamnetin	Rha
Internal standard	8.83	595.1657	Saponarin	Sap
Internal standard	4.9	199.0597	Syringic acid	Syr
Internal standard	11.09	305.0649	Taxifolin	Tax
Internal standard	14.28	149.059	trans-Cinnamic acid	Cin
Internal standard	10.57	217.0476	Trans-Ferulic acid	Fer
Internal standard	4.65	169.0429	Vanillic acid	Van
Internal standard	1.42	136.0614	Adenine	Ade
Internal standard	1.75	268.1038	Adenosine	Ado
Internal standard	1.45	348.0704	Adenosine monophosphate	(AMP)
Internal standard	1.44	324.0591	Cytidine monophosphate	(CMP)
Internal standard	1.35	244.0929	Cytidine	Cytd
Internal standard	1.31	112.0501	Cytosine	Cyt
Internal standard	1.45	152.0563	Guanine	Gua
Internal standard	1.49	284.0989	Guanosine	Guo
Internal standard	1.78	364.0654	Guanosine monophosphate disodium salt hydrate	(GMP)
Internal standard	1.49	80.04897	Pyridine	Pyr
Internal standard	1.81	243.0978	Thymidine	Thyd
Internal standard	1.73	127.0498	Thymine	Thy
Internal standard	1.5	113.0341	Uracil	Ura
Internal standard	1.77	245.077	Uridine	Uri
Internal standard	1.5	177.039	Ascorbic acid	Asc
Internal standard	14.81	211.1324	Jasmonic acid	(JA)

Chapter 2

Internal standard	5.02	377.1453	Riboflavin	Ribo
Internal standard	1.42	341.1089	2-Deoxy- D-glucose	Deoglu
Internal standard	1.65	87.00892	L-(-)-Malic acid	Mal
Internal standard	3.11	353.0884	Lactic acid	Lac
Internal standard	1.77	191.0196	Oxalacetic acid	Oxa
Internal standard	1.77	191.0196	Pyruvic acid	Pyr
Internal standard	1.51	133.0143	Shikimic acid	Shi
Internal standard	1.78	117.0194	Succinic acid	Suc
Internal standard	1.52	89.02454	α -Ketoglutaric acid	Ket
Internal standard	16.87	283.0613	Catechol (Pirocatequina)	Cate
Internal standard	1.41	181.0719	2-Deoxy-D-ribose	Deorib
GNPS	2.43	188.07	Spectral Match to Abrine from NIST14	Abr
GNPS	23.5	256.262	Spectral Match to Palmitamide from NIST14	Pal
GNPS	11.01	579.171	Massbank:CE000153 Vitexin-2 »-O-rhamnoside	Vitrha
GNPS	19.56	200.201	Spectral Match to Lauric acid leelamide from NIST14	Lau
GNPS	11.41	449.108	luteolin-7-glucoside	Pubchem 45933934
GNPS	11.99	607.167	NCGC00385120-0117-[(2S,3R,4S,5S,6R)-4,5-dihydroxy-6-(hydroxymethyl)-3-[(2S,3R,4R,5R,6S)-3,4,5-trihydroxy-6-methyloxan-2-yl]oxyoxan-2-yl]oxy-5-hydroxy-2-(4-hydroxy-3-methoxyphenyl)chromen-4-one	91873173
GNPS	2.42	291	ReSpect:PM003725 Epicatechin	Epica
GNPS	10.94	577.156	MoNA:2925606 Vitexin-2''-rhamnoside	Vitrha
GNPS	19.05	277.23	Spectral Match to 9S-Hydroxy-10E,12Z,15Z-octadecatrienoic acid from NIST14	13917187
GNPS	2.86	337.129	coumaroylquinic acid	14158103

Chapter 2

GNPS	3.96	447.093	Massbank:PR305828 Luteolin-8-C-glucoside	PR305828
GNPS	11.97	611	ReSpect:PM000505 Rutin	Rut
GNPS	10.87	563.141	NCGC00384911-01!6-[(2S,3R,4S,5S,6R)-4,5-dihydroxy-6-(hydroxymethyl)-3-[(2S,3R,4S,5S)-3,4,5-trihydroxyoxan-2-yl]oxyoxan-2-yl]-5,7-dihydroxy-2-(4-hydroxyphenyl)chromen-4-one	44468060
GNPS	12.84	755.204	5,7-dihydroxy-2-[4-[(2S,3R,4S,5S,6R)-3,4,5-trihydroxy-6-(hydroxymethyl)oxan-2-yl]oxyphenyl]-3-[(2S,3R,4S,5S,6R)-3,4,5-trihydroxy-6-[[[(2R,3R,4R,5R,6S)-3,4,5-trihydroxy-6-methyloxan-2-yl]oxymethyl]oxan-2-yl]oxychromen-4-one	44559783
GNPS	1.25	543.135	Polysaccharide Hexose x3	Hex
GNPS	13.66	287.055	Massbank:PR302254 Luteolin	Lut
GNPS	3.28	367.103	(1R,3R,4S,5R)-1,3,4-trihydroxy-5-[(E)-3-(4-hydroxy-3-methoxyphenyl)prop-2-enoyl]oxycyclohexane-1-carboxylic acid	6451331
GNPS	0.52	279.169	Spectral Match to Ile-Phe from NIST14	Ilephe
GNPS	3.8	611	ReSpect:PM002819 C-Hexosyl-luteolin O-hexoside	PM002819
GNPS	18.85	275.202	Spectral Match to 9S-Hydroxy-10E,12Z,15Z-octadecatrienoic acid from NIST14	13917187
GNPS	12.21	491.119	Massbank:PR305609 Malvidin-3-O-glucoside	PR305609
GNPS	19.71	291.198	Spectral Match to 9-OxoOTrE from NIST14	9-OxoOTrE

Chapter 2

GNPS	15.11	329.231	Massbank:PR309108 FA 18:1+3O	FA 18:1
GNPS	2.47	179.055	Spectral Match to. alpha.-D- (+)-Talose from NIST14	Tal
GNPS	13.37	593.151	2-(3,4-dihydroxyphenyl)-5- hydroxy-7-[(2S,3R,4S,5S,6R)- 3,4,5-trihydroxy-6- [[[(2R,3R,4R,5R,6S)-3,4,5- trihydroxy-6-methyloxan-2- yl]oxymethyl]oxan-2- yl]oxychromen-4-one	25245356
GNPS	13.17	611	ReSpect:PM000505 Rutin	Rut
GNPS	12.55	493.093	methoxy-myricetin-3-O- hexoside	73196016
GNPS	10.09	621.109	Massbank:PR309281 Flavone base + 3O, O-HexA-HexA	PR309281
GNPS	14.29	563.141	trihydroxyflavone-C-hexoside- C-pentoside	137333728
GNPS	14.74	677.425	(10E,15E)-9,12,13- trihydroxyoctadeca-10,15- dienoic acid	FA 18:2
GNPS	12.99	593.151	2-(3,4-dihydroxyphenyl)-5- hydroxy-3,7- bis[[[(2S,3R,4R,5R,6S)-3,4,5- trihydroxy-6-methyloxan-2- yl]oxy]chromen-4-one	15953752
GNPS	13.58	639.156	NCGC00385604-01!5,7- dihydroxy-2-(4- hydroxyphenyl)-6,8-bis[3,4,5- trihydroxy-6- (hydroxymethyl)oxan-2- yl]chromen-4-one	3084407
GNPS	27.49	338.343	Spectral Match to 13- Docosenamide, (Z)- from NIST14	5365369
GNPS	10.86	565.155	NCGC00384957-01!8-[3,5- dihydroxy-6-(hydroxymethyl)- 4-(3,4,5-trihydroxyoxan-2- yl)oxyoxan-2-yl]-5,7-dihydroxy-	45359561

Chapter 2

			3-(4-hydroxyphenyl)chromen-4-one	
GNPS	23.7	282.278	Spectral Match to 9-Octadecenamide, (Z)- from NIST14	C19670
GNPS	12.23	461.108	Massbank:PR306342 Peonidin-3-O-glucoside	PR306342
GNPS	11.78	447.093	5,7-dihydroxy-2-[4-hydroxy-3-[(2S,3R,4S,5R)-3,4,5-trihydroxyoxan-2-yl]oxyphenyl]-3-methoxychromen-4-one	38360299
GNPS	12.27	575.139	Massbank:PR309291 Flavone base + 4O, C-(dehydro-dHex)-dHex	PR309291
GNPS	10.11	461.108	Massbank:PR309289 Flavone base + 3O, 1MeO, C-Hex	PR309289
GNPS	11.46	593.151	2-(3,4-dihydroxyphenyl)-5-hydroxy-7-[(2S,3R,4S,5S,6R)-3,4,5-trihydroxy-6-[[[(2R,3R,4R,5R,6S)-3,4,5-trihydroxy-6-methyloxan-2-yl]oxymethyl]oxan-2-yl]oxychromen-4-one; Luteolin 7-rutinoside	10461109
GNPS	11.58	623.162	5,7-dihydroxy-2-(4-hydroxy-3-methoxyphenyl)-3-[3,4,5-trihydroxy-6-[[[(2R,3R,4R,5R,6S)-3,4,5-trihydroxy-6-methyloxan-2-yl]oxymethyl]oxan-2-yl]oxychromen-4-one	12313123

Table S3 *p*-values of the post-hoc Tukey's HSD test comparing seasonal mean Fv/Fm between PR of each species. Significant differences ($p < 0.05$) are highlighted in bold.

<i>Holcus lanatus</i>	3D	6D	10D	15D	20D	30D	60D
1D	1.0000	0.9992	0.9640	0.9510	0.0725	0.0013	<.0001
3D		0.9998	0.9824	0.9744	0.1011	0.0022	<.0001
6D			0.9997	0.9993	0.2732	0.0112	<.0001
10D				1.0000	0.5844	0.0524	<.0001
15D					0.6276	0.0625	<.0001
20D						0.9373	<.0001
30D							<.0001

<i>Holcus lanatus</i>	3W	6W	10W	15W	20W	30W	60W
1W	1.0000	1.0000	1.0000	1.0000	0.5791	<.0001	0.1533
3W		1.0000	1.0000	1.0000	0.4641	<.0001	0.1000
6W			1.0000	1.0000	0.3507	<.0001	0.0624
10W				1.0000	0.4637	<.0001	0.0998
15W					0.5335	<.0001	0.1286
20W							0.9947
30W							0.0035

<i>Phleum pratense</i>	3D	6D	10D	15D	20D	30D	60D
1D	1.0000	1.0000	1.0000	0.9924	0.9122	0.7988	<.0001
3D			1.0000	0.9957	0.9346	0.8363	<.0001
6D			1.0000	0.9874	0.8858	0.8523	<.0001
10D				0.9968	0.9435	0.8523	<.0001
15D					0.9998	0.9969	<.0001
20D						1.0000	<.0001
30D							<.0001

<i>Phleum pratense</i>	3W	6W	10W	15W	20W	30W	60W
1W	1.0000	1.0000	1.0000	1.0000	1.0000	0.0058	0.0391
3W		1.0000	1.0000	1.0000	0.9990	0.0025	0.0194
6W			0.9999	1.0000	0.9976	0.0017	0.0144
10W				1.0000	1.0000	0.0079	0.0508
15W					0.9999	0.0052	0.0360
20W						0.0197	0.1046
30W							0.9991

Chapter 2

<i>Centaurea jacea</i>	3D	6D	10D	15D	20D	30D	60D
1D	1.0000	1.0000	1.0000	0.0674	0.0056	0.7274	<.0001
3D		1.0000	1.0000	0.0740	0.0064	0.7485	<.0001
6D			1.0000	0.0645	0.0053	0.7173	<.0001
10D				0.0685	0.0057	0.7311	<.0001
15D					0.9942	0.8968	0.0002
20D						0.4286	0.0050
30D							<.0001

<i>Centaurea jacea</i>	3W	6W	10W	15W	20W	30W	60W
1W	1.0000	1.0000	1.0000	0.9980	0.1794	<.0001	0.0527
3W		1.0000	1.0000	0.9980	0.1794	<.0001	0.0527
6W			1.0000	0.9988	0.2004	<.0001	0.0608
10W				0.9992	0.2190	<.0001	0.0683
15W					0.5588	0.0003	0.2578
20W						0.1822	0.9997
30W							0.4454

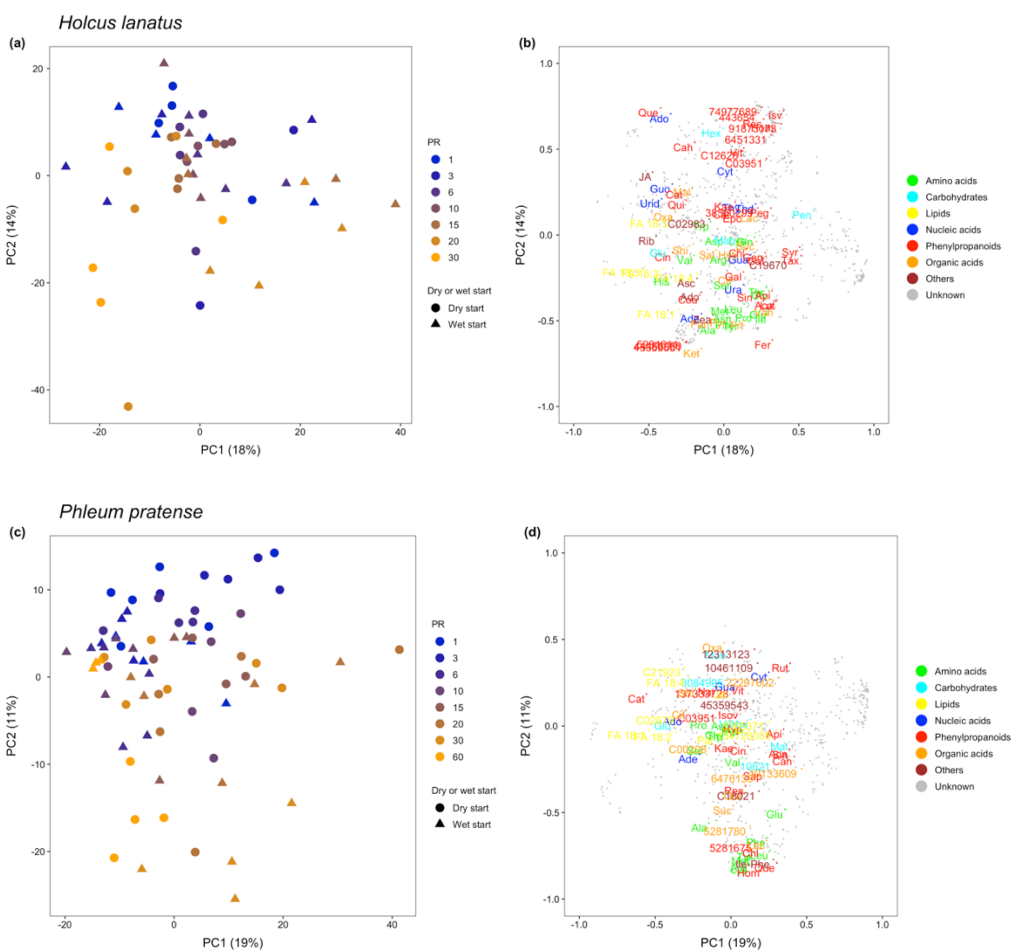
<i>Plantago lanceolata</i>	3D	6D	10D	15D	20D	30D	60D
1D	1.0000	1.0000	0.9843	1.0000	1.0000	1.0000	<.0001
3D		1.0000	1.0000	0.9756	1.0000	0.9869	<.0001
6D			0.9023	1.0000	0.9584	1.0000	<.0001
10D				0.9603	1.0000	0.9769	<.0001
15D					0.9876	1.0000	<.0001
20D						0.9941	<.0001
30D							<.0001

<i>Plantago lanceolata</i>	3W	6W	10W	15W	20W	30W	60W
1W	1.0000	1.0000	1.0000	1.0000	1.0000	0.0045	0.6287
3W		0.9995	0.9995	1.0000	1.0000	0.0182	0.8639
6W			1.0000	1.0000	0.9999	0.0027	0.5387
10W				1.0000	1.0000	0.0028	0.5466
15W					1.0000	0.0066	0.7003
20W						0.0114	0.7941
30W							0.4873

Table S4 PERMANOVA model of four species metabolomes with species, precipitation regimes (PRs), dry or wet start (Start) and interactions as fixed factors, and experiment unit as a random factor. Asterisks depict significant differences (*: $p < 0.05$; **: $p < 0.01$; ***: $p < 0.001$).

Chapter 2

Factor	Df	F	Pr (>F)
Species	3	283.5747	0.001 ***
PRs	7	2.5555	0.001 ***
Start	1	2.1992	0.055
Species:PRs	19	2.2831	0.001 ***
Species:Start	3	2.0469	0.017 *
PRs:Start	7	2.2138	0.001 ***
Species:PRs:Start	17	1.738	0.002 **



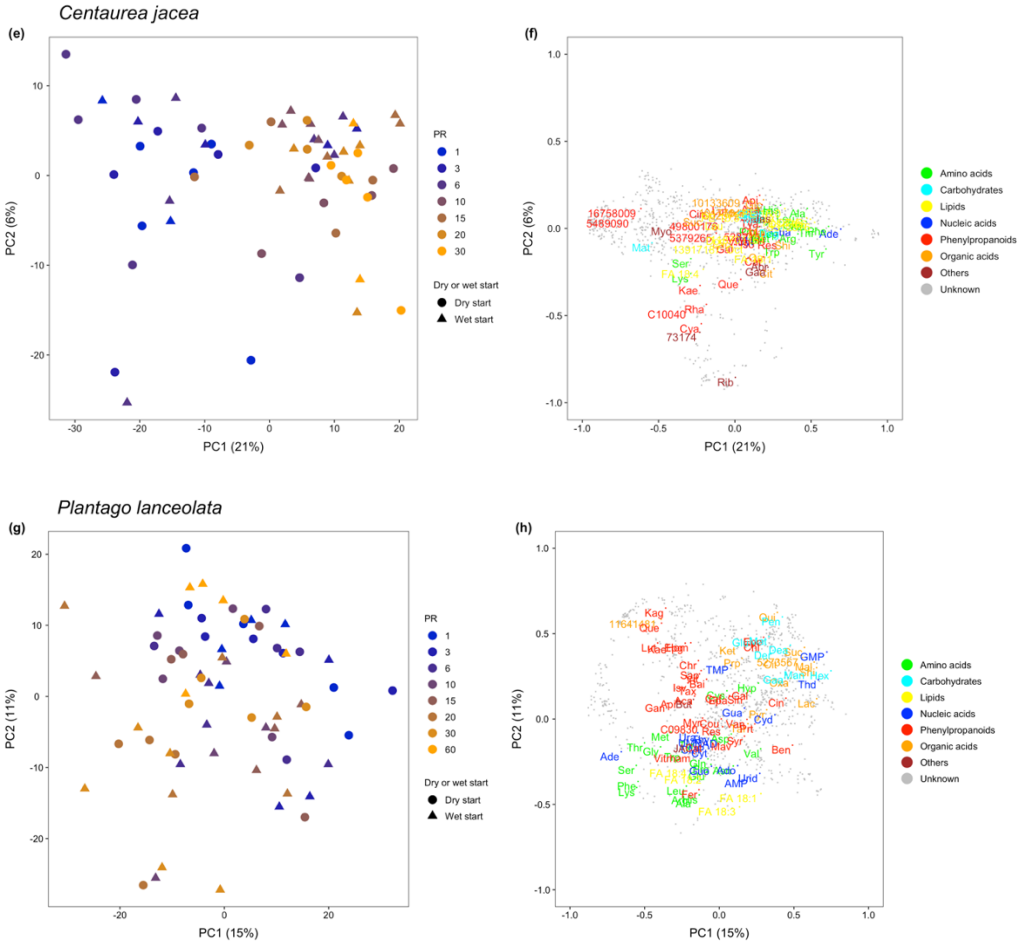


Figure S3 Impact of increasingly persistent precipitation regimes (PRs) on the individual metabolomes of four grassland species analyzed by principal component analysis (PCA). PCA conducted on metabolomic variables of four species using PC1 vs PC2: (a) The samples are categorized by species, PR and dry or wet start. (b) Loadings of the metabolomic variables in PC1 and PC2. The identified metabolites are classified into seven chemical classes, and unassigned metabolites are represented by small grey points. The full names of variables are listed in Table S2.

Table S5 Investigation of potential tipping point in metabolome changes of four grassland species subjected to increasingly persistent precipitation regimes (PRs). Tukey's HSD test to identify significant differences of component score coordinates in PCA among different precipitation regimes (PRs). $p < 0.05$ are marked in bold.

Chapter 2

Adjusted <i>p</i> value of PC2	3	6	10	15	20	30
score of <i>Holcus lanatus</i>						
1	0.891	0.794	0.999	0.891	0.015	0.089
3		1.000	0.967	0.990	0.371	0.620
6			0.997	1.000	0.124	0.348
10				0.970	0.032	0.149
15					0.239	0.510
20						1.000

Adjusted <i>p</i> value of PC2	3	6	10	15	20	30	60
score of <i>Phleum pratense</i>							
1	0.997	0.955	0.737	0.729	0.060	0.001	0.003
3		0.660	0.345	0.360	0.012	0.000	0.000
6			0.999	0.998	0.515	0.028	0.053
10				1.000	0.872	0.141	0.199
15					0.944	0.259	0.321
20						0.862	0.886
30							1.000

Adjusted <i>p</i> value of PC1	3	6	10	15	20	30
score of <i>Centaurea jacea</i>						
1	0.868	0.986	0.001	0.002	0.001	0.000
3		0.996	0.036	0.038	0.027	0.002
6			0.002	0.004	0.002	0.000
10				0.999	1.000	0.868
15					1.000	0.938
20						0.939

Adjusted <i>p</i> value of PC1 score	3	6	10	15	20	30	60
of <i>Plantago lanceolata</i>							
1	0.999	0.999	0.776	0.995	0.208	0.515	0.969
3		0.979	0.453	0.921	0.067	0.223	0.830
6			0.939	0.999	0.394	0.763	0.997
10				0.994	0.977	0.999	0.999
15					0.682	0.943	0.999
20						0.998	0.953
30							0.998

Table S6 Correlations between metabolites and PR gradient of four species. Spearman correlation coefficient and p value are displayed. $p < 0.05$ are marked in bold.

<i>Holcus lanatus</i>	Metabolites	Dry start PRs		Wet start PRs	
		cor	p	cor	p
Nucleic acids	Cytosine	-0.31	0.13	-0.09	0.67
	Thymine	-0.37	0.06	0.22	0.30
	Guanine	-0.03	0.90	0.13	0.53
	Uracil	0.09	0.66	0.60	0.00
	Adenosine	-0.24	0.23	-0.35	0.09
	Guanosine	-0.32	0.11	-0.46	0.02
	Thymidine	-0.37	0.06	0.31	0.14
	Uridine	-0.35	0.08	-0.38	0.06
	Adenine	-0.06	0.77	0.16	0.45
Amino acids	Glycine	0.23	0.26	0.01	0.97
	Alanine	0.01	0.96	0.59	0.00
	Leucine	0.01	0.96	0.61	0.00
	Isoleucine	-0.18	0.38	0.54	0.01
	Serine	-0.10	0.64	0.51	0.01
	Threonine	-0.21	0.31	0.45	0.03
	Methionine	0.23	0.25	0.51	0.01
	Lysine	0.10	0.63	0.37	0.08
	Aspartic acid	-0.13	0.52	0.41	0.05
	Asparagine	-0.30	0.13	0.59	0.00
	Glutamic acid	0.27	0.19	0.53	0.01
	Arginine	0.14	0.51	0.48	0.02
	Histidine	-0.05	0.81	0.30	0.15
	Proline	0.00	0.99	0.78	0.00
	Valine	-0.43	0.03	-0.30	0.16
	Phenylalanine	0.10	0.64	0.53	0.01
	Tryptophan	-0.36	0.07	0.36	0.09
	Glutamine	-0.56	0.00	0.57	0.00
	Tyrosine	0.09	0.68	0.71	0.00
	Organic acid	α -Ketoglutaric acid	0.11	0.60	0.21
Pyruvic acid		0.35	0.08	0.29	0.18
Shikimic acid		-0.32	0.12	-0.29	0.17
Citric acid		-0.25	0.21	0.03	0.90
L-(-)-Malic acid		-0.35	0.08	0.02	0.92
Succinic acid		-0.66	0.00	0.08	0.71
	Oxalacetic acid	-0.03	0.89	-0.31	0.14

Chapter 2

	Lactic acid	-0.18	0.37	0.17	0.43
	Salicylic acid	0.02	0.93	0.53	0.01
	Protocatechuic acid	-0.08	0.69	0.60	0.00
	Vanillic acid	0.07	0.72	0.63	0.00
Phenylpropanoids	Coumaric acid	0.05	0.82	-0.11	0.62
	Gallic acid	0.25	0.22	0.39	0.06
	Caffeic acid	0.43	0.03	0.47	0.02
	Ferulic acid	0.14	0.50	0.79	0.00
	Syringic acid	-0.01	0.96	0.46	0.02
	Sinapic acid	0.18	0.39	0.51	0.01
	Chlorogenic acid	0.19	0.34	0.28	0.19
	Apigenine	0.15	0.48	0.66	0.00
	Galangine	0.14	0.49	0.35	0.10
	Kaempferol	-0.01	0.95	0.32	0.12
	Epicatechin	0.01	0.94	-0.21	0.33
	DL-catechin	-0.21	0.30	0.12	0.57
	Taxifolin	-0.23	0.27	0.55	0.01
	Isovitexin	-0.44	0.03	-0.02	0.93
	Acacetin	0.40	0.05	0.63	0.00
	Homoorientin	-0.34	0.09	-0.16	0.45
	Resveratrol	-0.36	0.07	-0.36	0.08
	Quercetin	-0.24	0.24	-0.56	0.00
	Luteolin	0.39	0.05	0.61	0.00
	luteolin.7.glucoside	-0.24	0.23	-0.22	0.30
	Massbank.CE000153.Vitexin.2...	-0.27	0.19	-0.13	0.54
	O.rhamnoside				
	NCGC00384957.01.8..3.5.dihydr	0.47	0.02	-0.56	0.00
	oxy.6..hydroxymethyl..4..3.4.5.tr				
	ihydroxyoxan.2.yl.oxyoxan.2.yl..				
	5.7.dihydroxy.3..4.hydroxyphen				
	yl.chromen.4.one				
	NCGC00385120.01.7...2S.3R.4S.	-0.49	0.01	-0.17	0.42
	5S.6R..4.5.dihydroxy.6..hydroxy				
	methyl..3...2S.3R.4R.5R.6S..3.4.5				
	.trihydroxy.6.methyloxan.2.yl.ox				
	yoxan.2.yl.oxy.5.hydroxy.2..4.hy				
droxy.3.methoxyphenyl.chrome					
n.4.one					

Chapter 2

	Massbank.PR309289.Flavone.ba se...3O..1MeO..C.Hex	-0.43	0.03	-0.15	0.49
	X5.7.dihydroxy.2..4.hydroxy.3... 2S.3R.4S.5R..3.4.5.trihydroxyoxa n.2.yl.oxyphenyl..3.methoxychr omen.4.one	0.07	0.72	-0.10	0.65
	trihydroxyflavone.C.pentoside.C .pentoside	-0.12	0.55	-0.22	0.31
	Massbank.PR306342.Peonidin.3 .O.glucoside	-0.57	0.00	-0.27	0.20
	NCGC00384911.01.6...2S.3R.4S. 5S.6R..4.5.dihydroxy.6..hydroxy methyl..3...2S.3R.4S.5S..3.4.5.tri hydroxyoxan.2.yl.oxyoxan.2.yl..5 .7.dihydroxy.2..4.hydroxyphenyl .chromen.4.one	0.47	0.01	-0.07	0.74
	MoNA.2925606.Vitexin.2	-0.28	0.16	-0.20	0.36
	Catechol	-0.77	0.00	-0.53	0.01
	X.1R.3R.4S.5R..1.3.4.trihydroxy. 5...E..3..4.hydroxy.3.methoxyph enyl.prop.2.enoyl.oxycyclohexa ne.1.carboxylic.acid	-0.13	0.51	-0.13	0.54
	Spectral.Match.to....Quinic.acid. from.NIST14	-0.14	0.50	-0.25	0.24
	DL.catechin	-0.14	0.51	-0.21	0.33
	trans.Cinnamic.acid	-0.10	0.62	0.05	0.81
	Massbank.PR306342.Peonidin.3 .O.glucoside	-0.02	0.92	0.18	0.41
Carbohydrates	Pentose	-0.30	0.14	0.19	0.38
	Hexose	-0.35	0.08	-0.16	0.45
	Glucose	0.31	0.13	0.10	0.63
	D.Mannitol	-0.45	0.02	0.10	0.63
Lipids	Spectral.Match.to.9.OxoOTrE.fr om.NIST16	0.15	0.46	0.11	0.60
	Spectral.Match.to.9S.Hydroxy.1 0 ^E .12Z.15Z.octadecatrienoic.acid .from.NIST14	0.03	0.90	0.13	0.53
	X.10 ^E .15 ^E ..9.12.13.trihydroxyoct adeca.10.15.dienoic.acid	0.43	0.03	-0.01	0.95

Chapter 2

Others	Massbank.PR309108.FA.18.1.3O	-0.02	0.93	-0.12	0.58
	Massbank.PR309076.FA.18.4.2O	-0.19	0.35	0.19	0.36
	Spectral.Match.to.Abrine.from. NIST17	-0.42	0.03	0.34	0.11
	Riboflavin	0.00	0.99	-0.16	0.46
	Ascorbic acid	-0.40	0.05	-0.33	0.11
	Adonitol	-0.03	0.87	0.17	0.44
	Jasmonic acid (JA)	0.13	0.54	-0.06	0.77
	Trans-Zeatin	-0.09	0.67	0.01	0.95
	Spectral.Match.to.9.Octadecena mide...Z...from.NIST14	-0.04	0.86	0.61	0.00

<i>Phleum pratense</i>	Metabolites	Dry start PRs		Wet start PRs	
		cor	p	cor	p
Nucleic acids	Adenosine	-0.01	0.96	-0.47	0.01
	Adenine	0.14	0.40	0.47	0.01
	Cytosine	-0.43	0.01	-0.07	0.72
	Guanine	-0.52	0.00	-0.10	0.58
Amino acids	Alanine	0.74	0.00	0.64	0.00
	Phenylalanine	0.40	0.01	0.70	0.00
	Valine	0.29	0.07	0.57	0.00
	Arginine	0.63	0.00	0.46	0.01
	Glutamine	0.39	0.01	0.52	0.00
	Serine	0.68	0.00	0.60	0.00
	Lysine	0.53	0.00	0.63	0.00
	Asparagine	0.11	0.49	0.71	0.00
	Glutamic.acid	0.61	0.00	0.15	0.41
	Leucine	0.47	0.00	0.75	0.00
	Tryptophan	0.15	0.37	0.47	0.01
	Proline	0.49	0.00	0.70	0.00
	Aspartic.acid	0.06	0.70	0.27	0.13
	Threonine	0.30	0.06	0.50	0.00
	Tyrosine	0.55	0.00	0.48	0.01
Methionine	0.46	0.00	0.34	0.05	
Phenylpropanoids	Chlorogenic.acid	0.45	0.00	-0.05	0.78
	Homoorientin	0.77	0.00	0.10	0.60
	Quercetin	0.71	0.00	0.10	0.59
	DL.catechin	-0.10	0.53	-0.48	0.01
	Kaempferol	0.46	0.00	0.08	0.65

Chapter 2

	Saponarin	-0.01	0.94	0.16	0.38
	trihydroxyflavone.C.hexoside.C.pentoside	-0.14	0.37	-0.15	0.40
	Massbank.PR302125.Acacetin	0.46	0.00	0.23	0.21
	Spectral.Match.to.Narcissin.from.NIST14	-0.37	0.02	0.13	0.47
	Rutin	-0.47	0.00	0.14	0.45
	hyperoside	0.08	0.63	-0.04	0.83
	Catechol..Pirocatequina.	0.42	0.01	0.28	0.12
	luteolin.7.glucoside	-0.35	0.03	-0.07	0.70
	Massbank.PR305828.Luteolin.8.C.glucoside	0.82	0.00	0.05	0.78
	Cinnamic.acid	0.27	0.10	0.05	0.79
	Apigenin	-0.03	0.86	0.38	0.03
	Isovitexin	0.06	0.70	-0.17	0.36
	Resveratrol	0.59	0.00	0.16	0.40
	Vitexin	0.00	0.99	0.04	0.84
	Sinapic.acid	0.24	0.14	0.29	0.11
Organic acid	Shikimic.acid	0.00	0.98	0.04	0.83
	Oxalacetic.acid	-0.42	0.01	-0.09	0.61
	Lactic.acid	0.38	0.01	0.05	0.79
	Quinic.acid	0.30	0.06	0.55	0.00
	methyl.chlorogenate	-0.15	0.37	0.07	0.71
	X.1R.3R.4S.5R..1.3.4.trihydroxy.5..E..3..4.hydroxy.3.methoxyphenyl.prop.2.enoyl.oxycyclohexane.1.carboxylic.acid	-0.05	0.74	0.21	0.26
	NCGC00179718.03..1S.3R.4R.5R..3.4.bis...E..3..3.4.dihydroxyphenyl.prop.2.enoyl.oxy..1.5.dihydroxycyclohexane.1.carboxylic.acid	0.32	0.04	0.08	0.67
	Spectral.Match.to.9.Octadecanamide...Z...from.NIST14	0.32	0.04	0.26	0.15
	Massbank.PR310799.Licoagroside.B..not.validate	-0.12	0.45	-0.06	0.75
	Citric.acid	0.12	0.48	0.08	0.67
	Succinic.acid	0.27	0.09	0.32	0.08
Carbohydrates	D.....Maltosa	0.05	0.74	-0.01	0.96

Chapter 2

	Massbank.TY000206.Hesperidin.C irantin.Hesperidoside..2S..7...6.O.. 6.Deoxy.alpha.L.mannopyranosyl. .beta.D.glucopyranosyl.oxy..2.3.di hydro.5.hydroxy.2..3.hydroxy.4.m ethoxyphenyl..4H.1.benzopyran.4 .one..2S..5.hydroxy.2..5	0.52	0.00	0.50	0.00
	Massbank.FIO00720.Isoschaftosid e	-0.27	0.09	-0.37	0.04
	Massbank.PB006222.Vitexin.2...O .rhamnoside.8...2S.3R.4S.5S.6R..4. 5.dihydroxy.6..hydroxymethyl..3... 2S.3R.4R.5R.6S..3.4.5.trihydroxy.6 .methyloxan.2.yl.oxyoxan.2.yl..5.7 .dihydroxy.2..4.hydroxyphenyl.chr omen.4.one	-0.19	0.25	0.05	0.79
	Glucose	-0.07	0.69	-0.42	0.02
	Mannitol	-0.40	0.01	-0.53	0.00
Lipids	Massbank.PR309108.FA.18.1.3O	0.20	0.21	0.19	0.31
	Massbank.PR309076.FA.18.4.2O	-0.39	0.01	-0.30	0.10
	Spectral.Match.to.Palmitamide.fr om.NIST14	0.05	0.75	0.40	0.02
	Spectral.Match.to.9S.Hydroxy.10 ^E .12Z.15Z.octadecatrienoic.acid.fro m.NIST14	-0.29	0.07	-0.20	0.26
	Spectral.Match.to.Lauric.acid.leel amide.from.NIST14	0.03	0.87	-0.27	0.14
	Spectral.Match.to.13.Docosenami de...Z...from.NIST14	0.02	0.90	0.34	0.05
	Massbank.UT001936.Phosphatidy lethanolamine.lyso.18.2	0.22	0.17	0.35	0.05
	X.10 ^E .15 ^E ..9.12.13.trihydroxyocta deca.10.15.dienoic.acid	0.23	0.16	0.16	0.37
Others	Jasmonic.acid	-0.30	0.06	-0.01	0.95
	Pheophorbide.A	0.47	0.00	0.37	0.04
	Spectral.Match.to.Ile.Phe.from.NI ST14	0.50	0.00	0.32	0.08
	NCGC00385377.01_C19H32O7_4. .2.6.6.Trimethyl.4.oxo.2.cyclohex	-0.15	0.36	-0.01	0.95

Chapter 2

en.1.yl..2.butanyl.beta.D.glucoypyr anoside					
X2..3.4.dihydroxyphenyl..5.hydrox y.7...2S.3R.4S.5S.6R..3.4.5.trihydr oxy.6....2R.3R.4R.5R.6S..3.4.5.trih ydroxy.6.methyloxan.2.yl.oxymet hyl.oxan.2.yl.oxychromen.4.one	-0.50	0.00	0.21	0.25	
X5.7.dihydroxy.2..4.hydroxy.3.me thoxyphenyl..3..3.4.5.trihydroxy.62R.3R.4R.5R.6S..3.4.5.trihydrox y.6.methyloxan.2.yl.oxymethyl.ox an.2.yl.oxychromen.4.one	-0.67	0.00	0.31	0.09	

<i>Centaurea jacea</i>	Metabolites	Dry start PRs		Wet start PRs	
		cor	p	cor	p
Nucleic acids	Adenine	0.61	0.00	0.29	0.12
	Adenosine	0.05	0.79	-0.05	0.80
	Cytosine	0.27	0.14	0.22	0.26
	Guanine	0.54	0.00	-0.05	0.80
Amino acids	Phenylalanine	0.55	0.00	0.73	0.00
	Tryptophan	0.50	0.00	0.37	0.05
	Proline	0.42	0.01	0.46	0.01
	Glutamic acid	0.53	0.00	0.19	0.32
	Alanine	0.66	0.00	0.49	0.01
	Asparagine	0.52	0.00	0.57	0.00
	Valine	0.65	0.00	0.58	0.00
	Arginine	0.49	0.00	0.67	0.00
	Aspartic acid	0.16	0.37	0.19	0.33
	Glycine	0.44	0.01	0.28	0.14
	Leucine	0.44	0.01	0.38	0.04
	Serine	-0.39	0.02	0.44	0.02
	Threonine	0.42	0.01	0.38	0.04
	Methionine	0.22	0.21	0.20	0.30
	Lysine	-0.34	0.05	0.56	0.00
	Glutamine	0.53	0.00	0.37	0.05
Histidine	0.60	0.00	0.52	0.00	
Tyrosine	0.46	0.01	0.33	0.08	
Phenylpropanoids	Rhamnetin	0.01	0.95	0.14	0.45

Chapter 2

	X5.7.dihydroxy.3.4.5.trimethoxy flavone	-0.01	0.94	0.02	0.91
	DL.catechin	0.12	0.50	0.10	0.61
	Apigenine	0.38	0.03	-0.10	0.61
	Gallic.acid	0.21	0.25	-0.30	0.12
	Cyanidin.chloride	-0.06	0.73	0.17	0.39
	Quercetin	-0.20	0.26	0.13	0.49
	Tyramine	0.43	0.01	0.61	0.00
	Trihydroxy.Flavone	0.08	0.66	0.15	0.44
	NCGC00385512.01.5.hydroxy.2.3.hydroxy.4.methoxyphenyl.3.6.dimethoxy.7...2S.3R.4S.5S.6R.3.4.5.trihydroxy.6..hydroxymethyl.oxan.2.yl.oxychromen.4.one	-0.56	0.00	-0.48	0.01
	NCGC00385218.01.7.hydroxy.2.4.hydroxy.3.5.dimethoxyphenyl.5...2S.3R.4S.5S.6R..3.4.5.trihydroxy.6..hydroxymethyl.oxan.2.yl.oxychromen.4.one	0.02	0.92	-0.08	0.66
	X5.hydroxy.3..5.hydroxy.2.4.dimethoxyphenyl..6.methoxy.7..3.4.5.trihydroxy.6..hydroxymethyl.oxan.2.yl.oxychromen.4.one	-0.48	0.01	-0.55	0.00
	MoNA.2925606.Vitexin.2	0.08	0.66	0.19	0.33
	X5.7.dihydroxy.3.4.5.trimethoxy flavone.1	-0.18	0.31	-0.03	0.90
	Chlorogenic.acid	0.04	0.81	0.18	0.35
	Cinnamic.acid	-0.28	0.11	-0.44	0.02
	Sinapic.acid	0.08	0.67	-0.10	0.59
	Kaempferol	0.03	0.88	-0.14	0.48
	Resveratrol	0.14	0.45	0.19	0.33
	Isovitexin	0.08	0.66	-0.13	0.51
	Vitexin.2...O.rhamnoside	0.20	0.26	NA	NA
	Luteolin	-0.04	0.82	-0.14	0.46
	Acacetin	-0.01	0.95	0.11	0.58
Organic acids	Shikimic.acid	0.07	0.68	-0.13	0.49
	Succinic.acid	-0.21	0.24	-0.22	0.26
	D.Gluconic.acid	0.24	0.18	-0.13	0.52
	X.DL.Malic.acid.	-0.03	0.89	0.00	0.98

Chapter 2

	Citrate	0.02	0.93	-0.21	0.27
	NCGC00380877.01_C17H20O9_	0.22	0.21	-0.26	0.17
	Cyclohexanecarboxylic.acid..1.3				
	.5.trihydroxy.4....2 ^E ..3..4.hydrox				
	y.3.methoxyphenyl..1.oxo.2.pro				
	pen.1.yl.oxy.....1alpha.3alpha.4				
	alpha.5beta..				
	Massbank.PR309020.Feruloyl.q	0.03	0.85	-0.36	0.06
	uinic.acid..isomer.of.886..888.				
	X.1R.3R.4S.5R..1.3.4.trihydroxy.	-0.07	0.71	-0.26	0.18
	5...E..3..4.hydroxy.3.methoxyph				
	enyl.prop.2.enoyl.oxy cyclohexa				
	ne.1.carboxylic.acid				
	X...Quinic.acid	0.16	0.38	0.16	0.41
	X2.Methylmalate	-0.24	0.17	-0.39	0.04
	Lactic.acid	0.21	0.24	-0.30	0.11
Carbohydrates	X2.Deoxy.D.ribose	0.41	0.02	0.32	0.09
	D.....Maltose	-0.19	0.29	-0.79	0.00
	X6.Deoxy.D.glucose	0.28	0.11	0.43	0.02
	Glucose	0.11	0.54	0.25	0.19
	Mannitol	0.09	0.63	0.01	0.96
Lipids	X9S.Hydroxy.10E.12Z.15Z.octad	-0.27	0.13	-0.08	0.69
	ecatrenoic.acid				
	X13.Docosenamide	-0.01	0.96	-0.05	0.80
	Spectral.Match.to.9.Oxo.10 ^E .12	0.48	0.00	0.14	0.48
	Z.octadecadienoic.acid.from.NI				
	ST18				
	X.2S.3R.5R.10R.13R.14S.17S..2.	-0.02	0.89	-0.13	0.51
	3.14.trihydroxy.10.13.dimethyl.				
	17...2R.3R..2.3.6.trihydroxy.6.m				
	ethylheptan.2.yl..2.3.4.5.9.11.1				
	2.15.16.17.decahydro.1H.cyclop				
	enta.a.phenanthren.6.one				
	Massbank.PR309108.FA.18.1.3	0.24	0.19	0.13	0.51
	O				
	X.10 ^E .15 ^E ..9.12.13.trihydroxyoct	0.63	0.00	0.24	0.20
	adeca.10.15.dienoic.acid				
	X.9.Octadecenamide	-0.06	0.72	0.09	0.64
	PE.16.0.0.0.	0.24	0.18	0.28	0.15

Chapter 2

	PE.18.3.0.0.	-0.31	0.08	0.02	0.91
	Spectral.Match.to.9.S..HpOTrE.f rom.NIST14	0.48	0.00	0.14	0.48
Others	Spectral.Match.to.Lauric.acid.le elamide.from.NIST14	-0.22	0.22	0.19	0.31
	Jasmonic.acid	0.51	0.00	0.11	0.57
	Massbank.PR309076.FA.18.4.2 O	-0.43	0.01	-0.06	0.78
	Riboflavin	0.15	0.39	0.28	0.14
	myo.Inositol	-0.23	0.20	-0.26	0.17
	X.Abrine	0.51	0.00	0.46	0.01
	MoNA.3475533.Dehydrocostus. lactone	0.11	0.55	0.29	0.12
	Jasmonic.acid..JA.	0.18	0.31	0.10	0.59
	Spectral.Match.to.Galactinol.fro m.NIST16	0.42	0.02	0.48	0.01

<i>Plantago lanceolata</i>	Metabolites	Dry start PRs		Wet start PRs	
		cor	p	cor	p
Amino acids	Glycine	0.25	0.16	0.21	0.27
	Alanine	0.45	0.01	0.05	0.78
	Valine	0.18	0.32	-0.03	0.87
	Leucine	0.24	0.17	0.29	0.11
	Serine	0.17	0.36	0.34	0.06
	Threonine	0.20	0.27	0.22	0.22
	Cysteine	0.20	0.25	0.23	0.22
	Methionine	-0.23	0.19	0.31	0.10
	Lysine	0.39	0.03	0.45	0.01
	Aspartic acid	0.33	0.06	-0.01	0.98
	Asparagine	0.02	0.92	0.16	0.39
	Glutamic acid	0.39	0.02	0.04	0.82
	Glutamine	0.08	0.65	-0.22	0.23
	Arginine	0.05	0.78	0.48	0.01
	Histidine	0.17	0.35	0.32	0.08
	Phenylalanine	0.36	0.04	0.53	0.00
	Tryptophan	0.17	0.33	0.24	0.20
	Proline	0.08	0.64	0.37	0.04
	Tyrosine	0.36	0.04	0.44	0.01

Chapter 2

Organic acids	Hydroxy.proline	-0.20	0.28	-0.17	0.37
	.Ketoglutaric.acid	-0.50	0.00	-0.07	0.70
	Pyruvic.acid	-0.51	0.00	-0.26	0.16
	Shikimic.acid	-0.45	0.01	-0.34	0.06
	Citric.acid	-0.64	0.00	-0.33	0.07
	L.....Malic.acid	-0.53	0.00	-0.44	0.01
	Succinic.acid	-0.58	0.00	-0.46	0.01
	Oalacetic.acid	-0.65	0.00	-0.15	0.41
	Tartaric.acid	-0.05	0.77	-0.07	0.69
	Lactic.acid	-0.46	0.01	-0.36	0.05
	Propionic.acid	-0.32	0.07	-0.42	0.02
	Quinic.acid	-0.15	0.39	-0.42	0.02
	NCGC00169106.02...2R.3S.4S. 5R.6R..6..2..3.4.dihydroxyphen yl.ethoxy..3.4.5.trihydroxyan.2. yl.methyl..E..3..3.4.dihydroxy phenyl.prop.2.enoate	-0.19	0.30	-0.39	0.03
	2S.3S.4S.5R.6S..6..2..3.4.dihyd roxyphenyl..5.hydroxy.4.oochro men.7.yl.oxy.3.4.5.trihydroxyoa ne.2.carboxylic.acid	-0.23	0.19	-0.01	0.94
	Nucleic acids	Adenine	0.40	0.02	0.50
Cytosine		0.13	0.47	0.25	0.18
Thymine		0.06	0.74	-0.31	0.08
Guanine		0.11	0.54	-0.34	0.06
Uracil		0.21	0.25	0.45	0.01
Adenosine		0.03	0.86	0.00	0.98
Guanosine		0.51	0.00	0.18	0.34
Cytidine		0.08	0.66	0.02	0.92
Thymidine		-0.21	0.25	-0.32	0.08
Uridine		0.13	0.47	0.06	0.73
AMP.		0.00	0.99	0.24	0.20
UMP.		0.11	0.55	0.14	0.45
CMP.		0.10	0.57	0.15	0.41
Guanosine.monophosphate.di sodium.salt.hydrate.GMP.		-0.42	0.02	-0.37	0.04
TMP.		-0.11	0.54	-0.14	0.45
Phenylpropanoids	3.hydroxybenzoic.acid	0.32	0.07	-0.04	0.82
	protocatechuic.acid	-0.29	0.10	-0.17	0.37

Chapter 2

	3.coumaric.acid	-0.03	0.88	0.28	0.12
	Vanillic.acid	-0.04	0.82	-0.04	0.85
	Gallic.acid	-0.24	0.18	-0.32	0.08
	Caffeic.acid	0.13	0.48	-0.09	0.65
	Ferulic.acid	0.34	0.05	0.27	0.15
	Syringic.acid	0.08	0.66	0.04	0.83
	Sinapic.acid	-0.38	0.03	-0.24	0.20
	Resveratrol	-0.06	0.74	0.08	0.68
	Chlorogenic.acid	-0.14	0.44	-0.31	0.09
	Chrysin	-0.05	0.76	0.11	0.55
	Apigenin	0.25	0.17	0.37	0.04
	Galangin	0.30	0.09	0.40	0.03
	Luteolin	-0.13	0.48	0.38	0.04
	Kaempferol	-0.08	0.66	0.07	0.71
	...epicatechin	0.10	0.58	-0.31	0.09
	DL.catechin	-0.28	0.12	0.13	0.49
	Quercetin	-0.20	0.27	0.05	0.79
	Taifolin	-0.08	0.68	-0.10	0.61
	...epigallocatechin	-0.49	0.00	-0.07	0.70
	Myricetin	0.26	0.14	0.18	0.34
	Isovitain	0.04	0.84	-0.05	0.78
	Homoorientin	-0.13	0.46	-0.24	0.19
	...epigallocatechin.gallate	0.03	0.85	-0.06	0.77
	Saponarin	-0.02	0.90	0.05	0.78
	Malvidin.chloride	0.11	0.55	0.18	0.32
	Massbank.PR305760.isosakur	0.17	0.35	-0.02	0.93
	anetin.7.O.neohesperidoside				
	Kaempferol.3.glucuronide	-0.14	0.45	0.02	0.92
	baicalin	0.07	0.68	0.05	0.78
	trans.Cinnamic.acid	-0.09	0.60	-0.42	0.02
	MoNA.2925606.Vitein.2	-0.17	0.36	-0.01	0.94
	Acacetin	-0.10	0.60	0.05	0.77
	Massbank.CE000153.Vitein.2..	0.17	0.34	0.33	0.07
	.O.rhamnoside				
Carbohydrates	Pentose	-0.75	0.00	-0.30	0.10
	Hexose	-0.63	0.00	-0.46	0.01
	D.Mannitol	0.03	0.85	-0.07	0.69
	2.Deoy.D.ribose	-0.22	0.22	-0.24	0.20
	D.Maltose	-0.40	0.02	-0.30	0.10

Chapter 2

	2.Deoy.D.galactose	-0.33	0.06	-0.23	0.22
	GALACTITOL	0.00	0.98	-0.11	0.55
	Glucose	-0.30	0.08	-0.08	0.65
Lipids	Massbank.PR309108.FA.18.1. 30	0.25	0.17	0.15	0.43
	10 ^E .15 ^E ..9.12.13.trihydroocta deca.10.15.dienoic.acid	0.48	0.00	0.54	0.00
	Spectral.Match.to.9.OoOTrE.fr om.NIST14	0.14	0.43	0.31	0.09
	Massbank.PR309076.FA.18.4. 20	0.21	0.25	0.38	0.04
	Spectral.Match.to.Butyrylcarn itine.from.NIST14	-0.02	0.90	0.24	0.18
Others	Jasmonic.acid	0.19	0.28	0.55	0.00

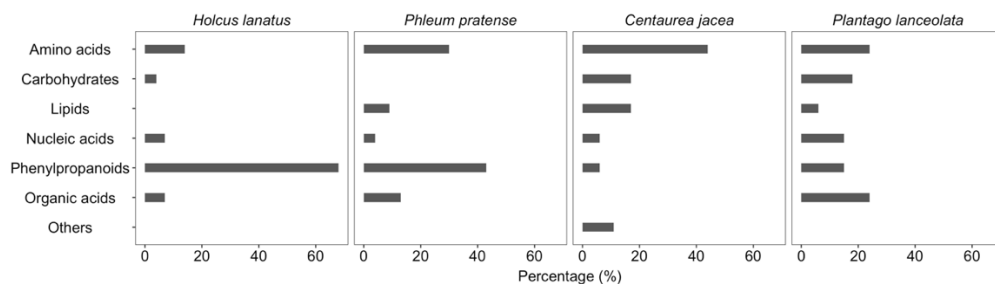


Figure S4 Percentage of chemical classes associated with annotated metabolites discriminating short-cycle PR from long-cycle PR (VIP > 1) of four species.

Table S7 List of pathways responsive to persistent PRs in four species identified by pathway analysis.

a) Dry start PR of *Holcus lanatus*

Pathway	Total Cmpd	Hits	Raw p	log p	FDR	Impact
Butanoate metabolism	17	4	0,00	2,57	0,10	0,00
C5-Branched dibasic acid metabolism	6	1	0,01	2,21	0,10	0,00
Terpenoid backbone biosynthesis	30	1	0,01	2,21	0,10	0,00
Glycolysis / Gluconeogenesis	26	3	0,01	2,13	0,10	0,12
Thiamine metabolism	22	2	0,01	1,85	0,13	0,00
Pyruvate metabolism	22	4	0,02	1,82	0,13	0,33
Citrate cycle (TCA cycle)	20	6	0,02	1,74	0,14	0,33
Monobactam biosynthesis	8	2	0,02	1,64	0,14	0,00

Chapter 2

Tyrosine metabolism	16	2	0,02	1,62	0,14	0,11
Alanine, aspartate and glutamate metabolism	22	9	0,04	1,45	0,18	0,76
Propanoate metabolism	20	1	0,04	1,43	0,18	0,00
Sulfur metabolism	15	2	0,06	1,22	0,24	0,03
Cysteine and methionine metabolism	46	4	0,06	1,22	0,24	0,14
Carbon fixation in photosynthetic organisms	21	5	0,07	1,16	0,26	0,16
Pantothenate and CoA biosynthesis	23	4	0,10	0,99	0,35	0,13
Glyoxylate and dicarboxylate metabolism	29	9	0,11	0,95	0,36	0,30
Glycine, serine and threonine metabolism	33	6	0,12	0,93	0,36	0,51
Valine, leucine and isoleucine biosynthesis	22	5	0,21	0,69	0,59	0,11
Arginine biosynthesis	18	5	0,23	0,64	0,59	0,17
Purine metabolism	63	4	0,23	0,64	0,59	0,00
Nitrogen metabolism	12	2	0,24	0,62	0,59	0,00
Pyrimidine metabolism	38	5	0,25	0,61	0,59	0,09
Sphingolipid metabolism	17	1	0,27	0,56	0,62	0,00
Selenocompound metabolism	13	1	0,31	0,51	0,67	0,00
Glutathione metabolism	26	3	0,36	0,45	0,67	0,12
Histidine metabolism	15	1	0,36	0,44	0,67	0,04
Ascorbate and aldarate metabolism	18	1	0,39	0,41	0,67	0,22
Tryptophan metabolism	28	1	0,39	0,41	0,67	0,12
Indole alkaloid biosynthesis	4	1	0,39	0,41	0,67	0,00
Flavone and flavonol biosynthesis	10	4	0,40	0,40	0,67	0,70
Phenylpropanoid biosynthesis	46	6	0,40	0,40	0,67	0,19
Porphyrin and chlorophyll metabolism	48	1	0,45	0,35	0,72	0,00
Phenylalanine metabolism	11	1	0,48	0,32	0,73	0,47
Tropane, piperidine and pyridine alkaloid biosynthesis	8	1	0,48	0,32	0,73	0,00
Isoquinoline alkaloid biosynthesis	6	1	0,52	0,28	0,76	0,50
Cyanoamino acid metabolism	29	5	0,53	0,28	0,76	0,00
alpha-Linolenic acid metabolism	28	1	0,59	0,23	0,82	0,00
Zeatin biosynthesis	21	2	0,60	0,22	0,82	0,01
Flavonoid biosynthesis	47	6	0,61	0,21	0,82	0,02
Nicotinate and nicotinamide metabolism	13	1	0,65	0,19	0,84	0,00

Chapter 2

Aminoacyl-tRNA biosynthesis	46	19	0,67	0,17	0,85	0,11
Phenylalanine, tyrosine and tryptophan biosynthesis	22	4	0,72	0,14	0,87	0,10
Glucosinolate biosynthesis	65	6	0,72	0,14	0,87	0,00
Ubiquinone and other terpenoid-quinone biosynthesis	38	2	0,75	0,12	0,89	0,00
Biosynthesis of secondary metabolites - unclassified	5	1	0,77	0,11	0,89	1,00
beta-Alanine metabolism	18	3	0,80	0,10	0,90	0,00
Arginine and proline metabolism	34	3	0,85	0,07	0,91	0,25
Lysine biosynthesis	9	2	0,89	0,05	0,91	0,00
Stilbenoid, diarylheptanoid and gingerol biosynthesis	8	1	0,90	0,05	0,91	0,13
Riboflavin metabolism	11	1	0,90	0,04	0,91	0,12
Lysine degradation	18	1	0,91	0,04	0,91	0,00
Valine, leucine and isoleucine degradation	37	3	0,91	0,04	0,91	0,00

b) Wet start PR of *Holcus lanatus*

Pathway	Total Cmpd	Hits	Raw p	log p	FDR	Impact
Phenylpropanoid biosynthesis	46,00	6,00	0,00	3,83	0,01	0,19
Arginine and proline metabolism	34,00	3,00	0,00	3,22	0,02	0,25
Tyrosine metabolism	16,00	2,00	0,00	2,67	0,04	0,11
Isoquinoline alkaloid biosynthesis	6,00	1,00	0,01	2,01	0,05	0,50
Aminoacyl-tRNA biosynthesis	46,00	19,00	0,01	2,29	0,04	0,11
Thiamine metabolism	22,00	2,00	0,01	2,24	0,04	0,00
Cyanoamino acid metabolism	29,00	5,00	0,01	2,23	0,04	0,00
Cysteine and methionine metabolism	46,00	4,00	0,01	2,04	0,05	0,14
Glycine, serine and threonine metabolism	33,00	6,00	0,00	2,54	0,04	0,51
Valine, leucine and isoleucine biosynthesis	22,00	5,00	0,01	2,01	0,05	0,11
Selenocompound metabolism	13,00	1,00	0,01	1,95	0,05	0,00
Sphingolipid metabolism	17,00	1,00	0,02	1,79	0,07	0,00
Glutathione metabolism	26,00	3,00	0,02	1,76	0,07	0,12
C5-Branched dibasic acid metabolism	6,00	1,00	0,02	1,70	0,07	0,00
Terpenoid backbone biosynthesis	30,00	1,00	0,02	1,70	0,07	0,00

Chapter 2

Phenylalanine metabolism	11,00	1,00	0,02	1,65	0,07	0,47
Tropane, piperidine and pyridine alkaloid biosynthesis	8,00	1,00	0,02	1,65	0,07	0,00
Flavonoid biosynthesis	47,00	6,00	0,02	1,63	0,07	0,02
Alanine, aspartate and glutamate metabolism	22,00	9,00	0,03	1,58	0,07	0,76
Phenylalanine, tyrosine and tryptophan biosynthesis	22,00	4,00	0,03	1,58	0,07	0,10
Flavone and flavonol biosynthesis	10,00	4,00	0,03	1,52	0,07	0,70
Carbon fixation in photosynthetic organisms	21,00	5,00	0,03	1,49	0,08	0,16
Ascorbate and aldarate metabolism	18,00	1,00	0,03	1,47	0,08	0,22
Ubiquinone and other terpenoid-quinone biosynthesis	38,00	2,00	0,04	1,42	0,08	0,00
Stilbenoid, diarylheptanoid and gingerol biosynthesis	8,00	1,00	0,04	1,36	0,09	0,13
Sulfur metabolism	15,00	2,00	0,04	1,36	0,09	0,03
Pantothenate and CoA biosynthesis	23,00	4,00	0,05	1,30	0,10	0,13
Glucosinolate biosynthesis	65,00	6,00	0,05	1,27	0,10	0,00
Pyrimidine metabolism	38,00	5,00	0,06	1,21	0,11	0,09
Monobactam biosynthesis	8,00	2,00	0,06	1,19	0,11	0,00
Glyoxylate and dicarboxylate metabolism	29,00	9,00	0,09	1,04	0,15	0,30
Glycolysis / Gluconeogenesis	26,00	3,00	0,10	1,01	0,15	0,12
Butanoate metabolism	17,00	4,00	0,10	1,01	0,15	0,00
Nitrogen metabolism	12,00	2,00	0,10	1,00	0,15	0,00
Valine, leucine and isoleucine degradation	37,00	3,00	0,10	1,00	0,15	0,00
Purine metabolism	63,00	4,00	0,11	0,98	0,15	0,00
Arginine biosynthesis	18,00	5,00	0,15	0,81	0,22	0,17
Pyruvate metabolism	22,00	4,00	0,18	0,75	0,24	0,33
Porphyrin and chlorophyll metabolism	48,00	1,00	0,18	0,73	0,25	0,00
Citrate cycle (TCA cycle)	20,00	6,00	0,31	0,51	0,40	0,33
beta-Alanine metabolism	18,00	3,00	0,31	0,50	0,40	0,00
Lysine degradation	18,00	1,00	0,33	0,49	0,40	0,00
Histidine metabolism	15,00	1,00	0,35	0,45	0,42	0,04
Zeatin biosynthesis	21,00	2,00	0,38	0,42	0,45	0,01
Propanoate metabolism	20,00	1,00	0,48	0,32	0,55	0,00

Chapter 2

Lysine biosynthesis	9,00	2,00	0,55	0,26	0,62	0,00
Tryptophan metabolism	28,00	1,00	0,60	0,22	0,65	0,12
Indole alkaloid biosynthesis	4,00	1,00	0,60	0,22	0,65	0,00
Nicotinate and nicotinamide metabolism	13,00	1,00	0,63	0,20	0,67	0,00
Riboflavin metabolism	11,00	1,00	0,78	0,11	0,81	0,12
Biosynthesis of secondary metabolites - unclassified	5,00	1,00	0,90	0,05	0,92	1,00
alpha-Linolenic acid metabolism	28,00	1,00	0,98	0,01	0,98	0,00

c) Dry start PR of *Phleum pratense*

Pathway	Total Cmpd	Hits	Raw p	log p	FDR	Impact
Glyoxylate and dicarboxylate metabolism	29,00	4,00	0,00	4,90	0,00	0,09
Selenocompound metabolism	13,00	1,00	0,00	4,39	0,00	0,00
Sphingolipid metabolism	17,00	1,00	0,00	4,22	0,00	0,00
Sulfur metabolism	15,00	1,00	0,00	4,22	0,00	0,00
Arginine biosynthesis	18,00	4,00	0,00	4,18	0,00	0,17
Carbon fixation in photosynthetic organisms	21,00	3,00	0,00	3,95	0,00	0,06
Arginine and proline metabolism	34,00	3,00	0,00	2,69	0,01	0,25
Nitrogen metabolism	12,00	2,00	0,00	3,66	0,00	0,00
Aminoacyl-tRNA biosynthesis	46,00	14,00	0,00	3,18	0,00	0,11
Cysteine and methionine metabolism	46,00	2,00	0,00	3,01	0,00	0,00
Pyrimidine metabolism	38,00	1,00	0,00	2,97	0,00	0,00
Glycine, serine and threonine metabolism	33,00	4,00	0,01	2,02	0,02	0,30
Phenylalanine metabolism	11,00	1,00	0,10	1,00	0,14	0,47
Glutathione metabolism	26,00	1,00	0,00	2,37	0,01	0,05
Butanoate metabolism	17,00	1,00	0,00	2,37	0,01	0,00
Cyanoamino acid metabolism	29,00	4,00	0,01	2,22	0,02	0,00
Porphyrin and chlorophyll metabolism	48,00	2,00	0,01	2,16	0,02	0,02
Alanine, aspartate and glutamate metabolism	22,00	6,00	0,00	3,82	0,00	0,69
Purine metabolism	63,00	3,00	0,01	1,93	0,03	0,00
Flavonoid biosynthesis	47,00	3,00	0,01	1,91	0,03	0,02
Pantothenate and CoA biosynthesis	23,00	1,00	0,01	1,88	0,03	0,00

Chapter 2

Valine, leucine and isoleucine degradation	37,00	2,00	0,02	1,77	0,03	0,00
Citrate cycle (TCA cycle)	20,00	1,00	0,02	1,75	0,03	0,08
Valine, leucine and isoleucine biosynthesis	22,00	3,00	0,04	1,42	0,07	0,00
Glucosinolate biosynthesis	65,00	4,00	0,04	1,39	0,07	0,00
Lysine degradation	18,00	1,00	0,04	1,35	0,08	0,00
Pyruvate metabolism	22,00	2,00	0,06	1,21	0,10	0,01
Glycolysis / Gluconeogenesis	26,00	2,00	0,06	1,21	0,10	0,00
Fatty acid biosynthesis	56,00	1,00	0,07	1,15	0,11	0,00
Flavone and flavonol biosynthesis	10,00	2,00	0,00	2,53	0,01	0,70
Tropane, piperidine and pyridine alkaloid biosynthesis	8,00	1,00	0,10	1,00	0,14	0,00
Lysine biosynthesis	9,00	2,00	0,14	0,86	0,19	0,00
Glycerophospholipid metabolism	37,00	1,00	0,15	0,81	0,20	0,11
Glycosylphosphatidylinositol (GPI)-anchor biosynthesis	13,00	1,00	0,15	0,81	0,20	0,00
Phenylpropanoid biosynthesis	46,00	2,00	0,25	0,59	0,33	0,03
Phenylalanine, tyrosine and tryptophan biosynthesis	22,00	3,00	0,34	0,47	0,43	0,08
alpha-Linolenic acid metabolism	28,00	1,00	0,36	0,45	0,43	0,00
Starch and sucrose metabolism	22,00	1,00	0,52	0,29	0,59	0,10
Tryptophan metabolism	28,00	1,00	0,53	0,28	0,59	0,12
Indole alkaloid biosynthesis	4,00	1,00	0,53	0,28	0,59	0,00
Zeatin biosynthesis	21,00	1,00	0,74	0,13	0,81	0,00
Stilbenoid, diarylheptanoid and gingerol biosynthesis	8,00	1,00	0,82	0,09	0,87	0,13
Monobactam biosynthesis	8,00	1,00	0,96	0,02	0,96	0,00
beta-Alanine metabolism	18,00	1,00	0,96	0,02	0,96	0,00
Nicotinate and nicotinamide metabolism	13,00	1,00	0,96	0,02	0,96	0,00

d) Wet start PR of *Phleum pratense*

Pathway	Total Cmpd	Hits	Raw p	log p	FDR	Impact
Aminoacyl-tRNA biosynthesis	46,00	14,00	0,00	4,60	0,00	0,11
Valine, leucine and isoleucine degradation	37,00	2,00	0,00	4,35	0,00	0,00

Chapter 2

Valine, leucine and isoleucine biosynthesis	22,00	3,00	0,00	4,24	0,00	0,00
Arginine and proline metabolism	34,00	3,00	0,00	4,10	0,00	0,25
Glyoxylate and dicarboxylate metabolism	29,00	4,00	0,00	4,05	0,00	0,09
Glycine, serine and threonine metabolism	33,00	4,00	0,00	2,37	0,01	0,30
Glucosinolate biosynthesis	65,00	4,00	0,00	3,82	0,00	0,00
Arginine biosynthesis	18,00	4,00	0,00	3,69	0,00	0,17
Selenocompound metabolism	13,00	1,00	0,00	3,62	0,00	0,00
Purine metabolism	63,00	3,00	0,00	3,54	0,00	0,00
Carbon fixation in photosynthetic organisms	21,00	3,00	0,00	3,39	0,00	0,06
Lysine degradation	18,00	1,00	0,00	3,38	0,00	0,00
Nitrogen metabolism	12,00	2,00	0,00	3,23	0,00	0,00
Phenylalanine metabolism	11,00	1,00	0,00	3,08	0,00	0,47
Tropane, piperidine and pyridine alkaloid biosynthesis	8,00	1,00	0,00	3,08	0,00	0,00
Cyanoamino acid metabolism	29,00	4,00	0,00	2,94	0,00	0,00
Lysine biosynthesis	9,00	2,00	0,00	2,84	0,00	0,00
Phenylpropanoid biosynthesis	46,00	2,00	0,00	2,77	0,00	0,03
Glutathione metabolism	26,00	1,00	0,00	2,72	0,00	0,05
Butanoate metabolism	17,00	1,00	0,00	2,72	0,00	0,00
Phenylalanine, tyrosine and tryptophan biosynthesis	22,00	3,00	0,00	2,63	0,00	0,08
Pyruvate metabolism	22,00	2,00	0,00	2,62	0,00	0,01
Glycolysis / Gluconeogenesis	26,00	2,00	0,00	2,62	0,00	0,00
Pantothenate and CoA biosynthesis	23,00	1,00	0,00	2,54	0,01	0,00
alpha-Linolenic acid metabolism	28,00	1,00	0,00	2,52	0,01	0,00
Fatty acid biosynthesis	56,00	1,00	0,00	2,50	0,01	0,00
Alanine, aspartate and glutamate metabolism	22,00	6,00	0,00	4,01	0,00	0,69
Sphingolipid metabolism	17,00	1,00	0,01	2,27	0,01	0,00
Sulfur metabolism	15,00	1,00	0,01	2,27	0,01	0,00
Porphyrin and chlorophyll metabolism	48,00	2,00	0,01	2,14	0,01	0,02
Citrate cycle (TCA cycle)	20,00	1,00	0,02	1,81	0,02	0,08
Cysteine and methionine metabolism	46,00	2,00	0,02	1,73	0,03	0,00
Pyrimidine metabolism	38,00	1,00	0,02	1,67	0,03	0,00

Chapter 2

Glycerophospholipid metabolism	37,00	1,00	0,02	1,61	0,03	0,11
Glycosylphosphatidylinositol (GPI)- anchor biosynthesis	13,00	1,00	0,02	1,61	0,03	0,00
Tryptophan metabolism	28,00	1,00	0,06	1,22	0,07	0,12
Indole alkaloid biosynthesis	4,00	1,00	0,06	1,22	0,07	0,00
Stilbenoid, diarylheptanoid and gingerol biosynthesis	8,00	1,00	0,08	1,11	0,09	0,13
Zeatin biosynthesis	21,00	1,00	0,13	0,88	0,15	0,00
Flavonoid biosynthesis	47,00	3,00	0,21	0,68	0,23	0,02
Starch and sucrose metabolism	22,00	1,00	0,33	0,48	0,36	0,10
Monobactam biosynthesis	8,00	1,00	0,36	0,45	0,37	0,00
beta-Alanine metabolism	18,00	1,00	0,36	0,45	0,37	0,00
Nicotinate and nicotinamide metabolism	13,00	1,00	0,36	0,45	0,37	0,00
Flavone and flavonol biosynthesis	10,00	2,00	0,48	0,31	0,48	0,70

e) Dry start PR of *Centaurea jacea*

Pathway	Total Cmpd	Hits	Raw p	log p	FDR	Impact
Selenocompound metabolism	13,00	1,00	0,00	5,64	0,00	0,00
Aminoacyl-tRNA biosynthesis	46,00	17,00	0,00	5,61	0,00	0,00
Arginine and proline metabolism	34,00	3,00	0,00	2,39	0,01	0,25
Carbon fixation in photosynthetic organisms	21,00	2,00	0,00	4,66	0,00	0,00
Zeatin biosynthesis	21,00	1,00	0,00	4,60	0,00	0,00
Glutathione metabolism	26,00	2,00	0,00	4,10	0,00	0,12
Pantothenate and CoA biosynthesis	23,00	1,00	0,00	4,06	0,00	0,00
Glycine, serine and threonine metabolism	33,00	4,00	0,00	2,47	0,01	0,33
Tyrosine metabolism	16,00	2,00	0,00	3,97	0,00	0,17
Ubiquinone and other terpenoid- quinone biosynthesis	38,00	1,00	0,00	3,49	0,00	0,00
Nitrogen metabolism	12,00	2,00	0,00	3,46	0,00	0,00
Valine, leucine and isoleucine degradation	37,00	2,00	0,00	3,27	0,00	0,00
Phenylalanine, tyrosine and tryptophan biosynthesis	22,00	4,00	0,00	3,20	0,00	0,10
Valine, leucine and isoleucine biosynthesis	22,00	4,00	0,00	3,15	0,00	0,00

Chapter 2

Purine metabolism	63,00	3,00	0,00	3,04	0,00	0,00
Arginine biosynthesis	18,00	4,00	0,00	2,99	0,00	0,17
Glyoxylate and dicarboxylate metabolism	29,00	5,00	0,00	2,93	0,00	0,16
Glucosinolate biosynthesis	65,00	5,00	0,00	2,92	0,00	0,00
Porphyrin and chlorophyll metabolism	48,00	1,00	0,00	2,83	0,00	0,00
alpha-Linolenic acid metabolism	28,00	2,00	0,00	2,76	0,00	0,07
Phenylalanine metabolism	11,00	1,00	0,00	2,51	0,01	0,47
Phenylpropanoid biosynthesis	46,00	1,00	0,00	2,51	0,01	0,00
Tropane, piperidine and pyridine alkaloid biosynthesis	8,00	1,00	0,00	2,51	0,01	0,00
Butanoate metabolism	17,00	2,00	0,00	2,48	0,01	0,00
Cyanoamino acid metabolism	29,00	4,00	0,00	2,47	0,01	0,00
Isoquinoline alkaloid biosynthesis	6,00	2,00	0,00	3,97	0,00	0,50
Alanine, aspartate and glutamate metabolism	22,00	6,00	0,00	5,01	0,00	0,64
Histidine metabolism	15,00	1,00	0,01	2,17	0,01	0,04
Lysine degradation	18,00	1,00	0,01	2,15	0,01	0,00
Thiamine metabolism	22,00	1,00	0,01	2,01	0,02	0,00
Tryptophan metabolism	28,00	1,00	0,01	1,91	0,02	0,12
Indole alkaloid biosynthesis	4,00	1,00	0,01	1,91	0,02	0,00
Lysine biosynthesis	9,00	2,00	0,02	1,70	0,03	0,00
Pentose phosphate pathway	19,00	2,00	0,02	1,64	0,04	0,00
Galactose metabolism	27,00	2,00	0,02	1,60	0,04	0,15
Pyrimidine metabolism	38,00	1,00	0,03	1,48	0,05	0,00
Inositol phosphate metabolism	28,00	1,00	0,05	1,28	0,07	0,10
Phosphatidylinositol signaling system	26,00	1,00	0,05	1,28	0,07	0,03
Ascorbate and aldarate metabolism	18,00	1,00	0,05	1,28	0,07	0,00
Riboflavin metabolism	11,00	1,00	0,05	1,27	0,07	0,12
Flavone and flavonol biosynthesis	10,00	2,00	0,07	1,15	0,09	0,35
Flavonoid biosynthesis	47,00	3,00	0,11	0,96	0,14	0,01
Fatty acid biosynthesis	56,00	1,00	0,22	0,66	0,27	0,00
Sulfur metabolism	15,00	1,00	0,29	0,53	0,34	0,03
Propanoate metabolism	20,00	1,00	0,29	0,53	0,34	0,00
Starch and sucrose metabolism	22,00	1,00	0,30	0,52	0,34	0,10
Monobactam biosynthesis	8,00	1,00	0,45	0,35	0,48	0,00
beta-Alanine metabolism	18,00	1,00	0,45	0,35	0,48	0,00

Nicotinate and nicotinamide metabolism	13,00	1,00	0,45	0,35	0,48	0,00
Cysteine and methionine metabolism	46,00	2,00	0,47	0,32	0,49	0,13
C5-Branched dibasic acid metabolism	6,00	1,00	0,54	0,27	0,55	0,00
Citrate cycle (TCA cycle)	20,00	2,00	0,57	0,25	0,57	0,16

f) Wet start PR of *Centaurea jacea*

Pathway	Total Cmpd	Hits	Raw p	log p	FDR	Impact
Starch and sucrose metabolism	22,00	1,00	0,00	4,12	0,00	0,10
Isoquinoline alkaloid biosynthesis	6,00	2,00	0,00	2,88	0,02	0,50
Tyrosine metabolism	16,00	2,00	0,00	2,88	0,02	0,17
Zeatin biosynthesis	21,00	1,00	0,00	2,42	0,05	0,00
Lysine degradation	18,00	1,00	0,00	2,36	0,05	0,00
Cyanoamino acid metabolism	29,00	4,00	0,01	1,94	0,09	0,00
Phenylalanine metabolism	11,00	1,00	0,02	1,77	0,09	0,47
Phenylpropanoid biosynthesis	46,00	1,00	0,02	1,77	0,09	0,00
Tropane, piperidine and pyridine alkaloid biosynthesis	8,00	1,00	0,02	1,77	0,09	0,00
alpha-Linolenic acid metabolism	28,00	2,00	0,02	1,72	0,09	0,07
Lysine biosynthesis	9,00	2,00	0,02	1,71	0,09	0,00
Riboflavin metabolism	11,00	1,00	0,02	1,65	0,09	0,12
Galactose metabolism	27,00	2,00	0,02	1,64	0,09	0,15
Purine metabolism	63,00	3,00	0,03	1,47	0,11	0,00
Phenylalanine, tyrosine and tryptophan biosynthesis	22,00	4,00	0,03	1,47	0,11	0,10
Alanine, aspartate and glutamate metabolism	22,00	6,00	0,03	1,46	0,11	0,64
Sulfur metabolism	15,00	1,00	0,04	1,38	0,12	0,03
Propanoate metabolism	20,00	1,00	0,04	1,38	0,12	0,00
Glucosinolate biosynthesis	65,00	5,00	0,05	1,35	0,12	0,00
Histidine metabolism	15,00	1,00	0,05	1,32	0,12	0,04
Aminoacyl-tRNA biosynthesis	46,00	17,00	0,05	1,31	0,12	0,00
Selenocompound metabolism	13,00	1,00	0,05	1,29	0,12	0,00
Flavonoid biosynthesis	47,00	3,00	0,05	1,26	0,12	0,01
Valine, leucine and isoleucine degradation	37,00	2,00	0,07	1,16	0,15	0,00
Pantothenate and CoA biosynthesis	23,00	1,00	0,08	1,12	0,16	0,00
Flavone and flavonol biosynthesis	10,00	2,00	0,08	1,07	0,17	0,35

Chapter 2

Tryptophan metabolism	28,00	1,00	0,09	1,03	0,17	0,12
Indole alkaloid biosynthesis	4,00	1,00	0,09	1,03	0,17	0,00
Butanoate metabolism	17,00	2,00	0,10	1,00	0,18	0,00
Valine, leucine and isoleucine biosynthesis	22,00	4,00	0,10	0,99	0,18	0,00
Citrate cycle (TCA cycle)	20,00	2,00	0,12	0,93	0,20	0,16
Carbon fixation in photosynthetic organisms	21,00	2,00	0,12	0,91	0,20	0,00
Ubiquinone and other terpenoid-quinone biosynthesis	38,00	1,00	0,14	0,84	0,23	0,00
Glycine, serine and threonine metabolism	33,00	4,00	0,20	0,69	0,31	0,33
Glyoxylate and dicarboxylate metabolism	29,00	5,00	0,35	0,46	0,52	0,16
Pentose phosphate pathway	19,00	2,00	0,41	0,39	0,55	0,00
Inositol phosphate metabolism	28,00	1,00	0,43	0,36	0,55	0,10
Phosphatidylinositol signaling system	26,00	1,00	0,43	0,36	0,55	0,03
Ascorbate and aldarate metabolism	18,00	1,00	0,43	0,36	0,55	0,00
Cysteine and methionine metabolism	46,00	2,00	0,44	0,35	0,55	0,13
Monobactam biosynthesis	8,00	1,00	0,46	0,34	0,55	0,00
beta-Alanine metabolism	18,00	1,00	0,46	0,34	0,55	0,00
Nicotinate and nicotinamide metabolism	13,00	1,00	0,46	0,34	0,55	0,00
Thiamine metabolism	22,00	1,00	0,47	0,33	0,55	0,00
C5-Branched dibasic acid metabolism	6,00	1,00	0,47	0,32	0,55	0,00
Porphyrin and chlorophyll metabolism	48,00	1,00	0,50	0,30	0,56	0,00
Glutathione metabolism	26,00	2,00	0,58	0,24	0,64	0,12
Arginine and proline metabolism	34,00	3,00	0,62	0,21	0,68	0,25
Arginine biosynthesis	18,00	4,00	0,65	0,19	0,69	0,17
Nitrogen metabolism	12,00	2,00	0,75	0,13	0,78	0,00
Pyrimidine metabolism	38,00	1,00	0,83	0,08	0,84	0,00
Fatty acid biosynthesis	56,00	1,00	0,97	0,01	0,97	0,00

g) Dry start PR of *Plantago lanceolata*

Pathway	Total Cmpd	Hits	Raw p	Log p	FDR	Impact
Glyoxylate and dicarboxylate metabolism	29,00	9,00	0,00	3,65	0,01	0,30
Carbon fixation in photosynthetic organisms	21,00	5,00	0,00	3,05	0,01	0,16
Citrate cycle (TCA cycle)	20,00	6,00	0,00	2,90	0,01	0,33
Glutathione metabolism	26,00	2,00	0,00	2,85	0,01	0,12
Pyruvate metabolism	22,00	4,00	0,00	2,80	0,01	0,33
Glycolysis / Gluconeogenesis	26,00	3,00	0,00	2,76	0,01	0,12
Alanine, aspartate and glutamate metabolism	22,00	9,00	0,00	2,74	0,01	0,76
Thiamine metabolism	22,00	2,00	0,00	2,54	0,02	0,00
Isoquinoline alkaloid biosynthesis	6,00	1,00	0,00	2,51	0,02	0,50
Butanoate metabolism	17,00	4,00	0,00	2,47	0,02	0,00
Sulfur metabolism	15,00	2,00	0,00	2,38	0,02	0,03
Tyrosine metabolism	16,00	2,00	0,00	2,37	0,02	0,11
Phenylalanine, tyrosine and tryptophan biosynthesis	22,00	4,00	0,01	1,93	0,04	0,10
Lysine degradation	18,00	1,00	0,01	1,88	0,05	0,00
Propanoate metabolism	20,00	2,00	0,01	1,86	0,05	0,00
Glycine, serine and threonine metabolism	33,00	6,00	0,02	1,78	0,05	0,51
Lysine biosynthesis	9,00	2,00	0,02	1,78	0,05	0,00
Cyanoamino acid metabolism	29,00	5,00	0,02	1,72	0,05	0,00
Ubiquinone and other terpenoid-quinone biosynthesis	38,00	3,00	0,03	1,56	0,07	0,00
Porphyrin and chlorophyll metabolism	48,00	1,00	0,03	1,51	0,08	0,00
Aminoacyl-tRNA biosynthesis	46,00	17,00	0,04	1,43	0,09	0,11
Selenocompound metabolism	13,00	1,00	0,05	1,31	0,11	0,00
Zeatin biosynthesis	21,00	1,00	0,06	1,23	0,12	0,00
Purine metabolism	63,00	4,00	0,06	1,22	0,12	0,05
C5-Branched dibasic acid metabolism	6,00	1,00	0,06	1,21	0,12	0,00
Terpenoid backbone biosynthesis	30,00	1,00	0,06	1,21	0,12	0,00
Monobactam biosynthesis	8,00	2,00	0,07	1,18	0,12	0,00

Chapter 2

Cysteine and methionine metabolism	46,00	4,00	0,07	1,16	0,12	0,14
Starch and sucrose metabolism	22,00	1,00	0,08	1,10	0,14	0,10
Nitrogen metabolism	12,00	2,00	0,09	1,03	0,15	0,00
Tropane, piperidine and pyridine alkaloid biosynthesis	8,00	1,00	0,09	1,03	0,15	0,00
Sphingolipid metabolism	17,00	1,00	0,10	1,02	0,15	0,00
Pyrimidine metabolism	38,00	4,00	0,12	0,91	0,19	0,09
Arginine biosynthesis	18,00	5,00	0,13	0,88	0,19	0,17
Pantothenate and CoA biosynthesis	23,00	3,00	0,14	0,87	0,19	0,00
beta-Alanine metabolism	18,00	2,00	0,14	0,84	0,20	0,00
Nicotinate and nicotinamide metabolism	13,00	1,00	0,18	0,75	0,24	0,00
Arginine and proline metabolism	34,00	4,00	0,19	0,71	0,26	0,30
Phenylalanine metabolism	11,00	2,00	0,25	0,61	0,31	0,47
Flavonoid biosynthesis	47,00	8,00	0,25	0,60	0,31	0,02
Valine, leucine and isoleucine biosynthesis	22,00	4,00	0,28	0,55	0,35	0,11
Phenylpropanoid biosynthesis	46,00	7,00	0,32	0,50	0,38	0,20
Pentose phosphate pathway	19,00	1,00	0,45	0,34	0,53	0,00
Glucosinolate biosynthesis	65,00	5,00	0,53	0,27	0,61	0,00
Flavone and flavonol biosynthesis	10,00	4,00	0,64	0,20	0,71	0,70
Stilbenoid, diarylheptanoid and gingerol biosynthesis	8,00	1,00	0,65	0,19	0,71	0,13
Biosynthesis of secondary metabolites - unclassified	5,00	2,00	0,75	0,13	0,80	1,00
Valine, leucine and isoleucine degradation	37,00	2,00	0,97	0,01	0,98	0,00
Tryptophan metabolism	28,00	1,00	0,98	0,01	0,98	0,12
Indole alkaloid biosynthesis	4,00	1,00	0,98	0,01	0,98	0,00

h) Wet start PR of *Plantago lanceolata*

Pathway	Total Cmpd	Hits	Raw p	Log p	FDR	Impact
Tropane, piperidine and pyridine alkaloid biosynthesis	8,00	1,00	0,00	3,30	0,03	0,00
Phenylalanine metabolism	11,00	2,00	0,00	2,95	0,03	0,47
Phenylalanine, tyrosine and tryptophan biosynthesis	22,00	4,00	0,00	2,76	0,03	0,10

Chapter 2

Zeatin biosynthesis	21,00	2,00	0,00	2,53	0,04	0,00
Purine metabolism	63,00	7,00	0,00	2,39	0,04	0,13
Tyrosine metabolism	16,00	2,00	0,01	2,12	0,06	0,11
Propanoate metabolism	20,00	2,00	0,01	1,96	0,06	0,00
Isoquinoline alkaloid biosynthesis	6,00	1,00	0,01	1,95	0,06	0,50
Ubiquinone and other terpenoid-quinone biosynthesis	38,00	3,00	0,01	1,93	0,06	0,00
Cyanoamino acid metabolism	29,00	6,00	0,01	1,88	0,06	0,00
Lysine degradation	18,00	1,00	0,01	1,86	0,06	0,00
Phenylpropanoid biosynthesis	46,00	7,00	0,01	1,86	0,06	0,20
Glucosinolate biosynthesis	65,00	5,00	0,02	1,67	0,08	0,00
Aminoacyl-tRNA biosynthesis	46,00	19,00	0,02	1,62	0,09	0,11
Sulfur metabolism	15,00	3,00	0,03	1,53	0,10	0,09
Sphingolipid metabolism	17,00	1,00	0,04	1,37	0,14	0,00
Lysine biosynthesis	9,00	2,00	0,05	1,29	0,15	0,00
Pyruvate metabolism	22,00	4,00	0,05	1,27	0,15	0,33
Citrate cycle (TCA cycle)	20,00	6,00	0,05	1,26	0,15	0,33
Glyoxylate and dicarboxylate metabolism	29,00	9,00	0,06	1,23	0,15	0,30
Glycolysis / Gluconeogenesis	26,00	3,00	0,06	1,21	0,15	0,12
Biosynthesis of secondary metabolites - unclassified	5,00	2,00	0,07	1,17	0,16	1,00
Histidine metabolism	15,00	1,00	0,08	1,11	0,17	0,04
Pantothenate and CoA biosynthesis	23,00	4,00	0,08	1,10	0,17	0,00
Cysteine and methionine metabolism	46,00	5,00	0,08	1,08	0,17	0,19
Flavone and flavonol biosynthesis	10,00	4,00	0,09	1,04	0,18	0,70
C5-Branched dibasic acid metabolism	6,00	1,00	0,10	1,01	0,18	0,00
Terpenoid backbone biosynthesis	30,00	1,00	0,10	1,01	0,18	0,00
Glycine, serine and threonine metabolism	33,00	6,00	0,11	0,98	0,18	0,51
Valine, leucine and isoleucine biosynthesis	22,00	4,00	0,11	0,97	0,18	0,11
Butanoate metabolism	17,00	4,00	0,15	0,83	0,25	0,00
Arginine and proline metabolism	34,00	4,00	0,16	0,80	0,25	0,30
Valine, leucine and isoleucine degradation	37,00	2,00	0,16	0,80	0,25	0,00

Chapter 2

Flavonoid biosynthesis	47,00	8,00	0,18	0,75	0,26	0,02
beta-Alanine metabolism	18,00	2,00	0,18	0,74	0,26	0,00
Carbon fixation in photosynthetic organisms	21,00	5,00	0,20	0,70	0,28	0,16
Thiamine metabolism	22,00	4,00	0,21	0,69	0,28	0,27
Starch and sucrose metabolism	22,00	1,00	0,24	0,62	0,32	0,10
Pentose phosphate pathway	19,00	1,00	0,26	0,59	0,33	0,00
Monobactam biosynthesis	8,00	2,00	0,26	0,59	0,33	0,00
Tryptophan metabolism	28,00	1,00	0,27	0,57	0,33	0,12
Indole alkaloid biosynthesis	4,00	1,00	0,27	0,57	0,33	0,00
Pyrimidine metabolism	38,00	8,00	0,33	0,48	0,39	0,26
Glutathione metabolism	26,00	3,00	0,35	0,46	0,40	0,13
Alanine, aspartate and glutamate metabolism	22,00	9,00	0,39	0,40	0,45	0,76
Stilbenoid, diarylheptanoid and gingerol biosynthesis	8,00	1,00	0,51	0,29	0,57	0,13
Porphyrin and chlorophyll metabolism	48,00	1,00	0,68	0,16	0,74	0,00
Nitrogen metabolism	12,00	2,00	0,73	0,13	0,77	0,00
Arginine biosynthesis	18,00	5,00	0,74	0,13	0,77	0,17
Selenocompound metabolism	13,00	1,00	0,85	0,07	0,87	0,00
Nicotinate and nicotinamide metabolism	13,00	1,00	0,98	0,01	0,98	0,00

Chapter 2

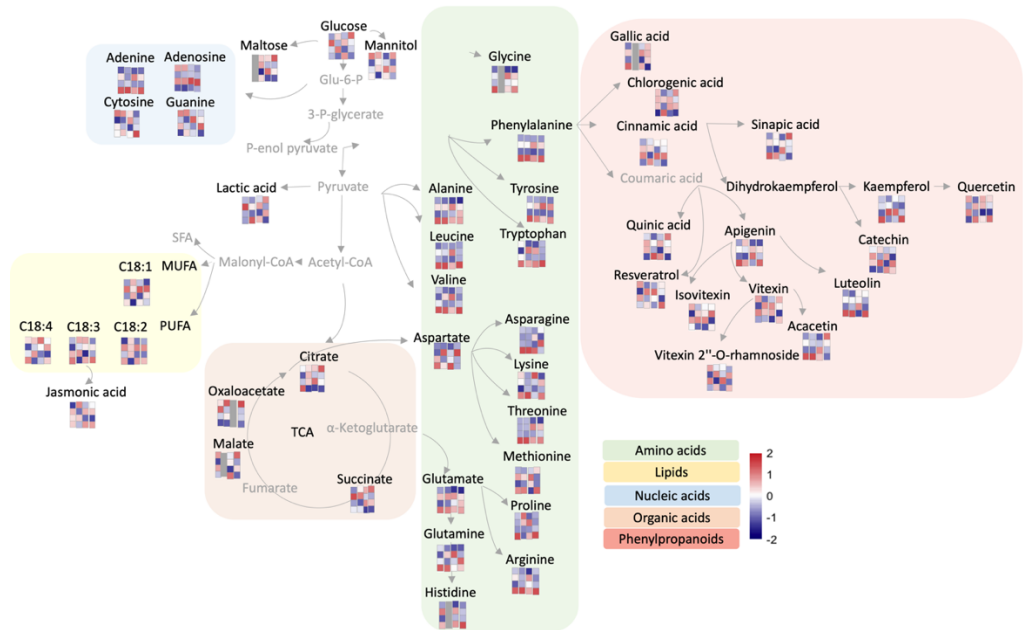


Figure S5 Representation of main metabolic pathways with the changed metabolites in response to short-cycle and long-cycle PRs of four species. The pathways were generated based on the KEGG database and literature. The heatmaps indicate up and down regulations of metabolites. Grey squares represent the metabolites that were non-detectable in a given species.

Chapter 3

Biochemical composition changes can be linked to the tolerance of four grassland species under more persistent precipitation regimes

Published as: Zi, Lin, Simon Reynaert, Ivan Nijs, Hans De Boeck, Erik Verbruggen, Gerrit T.S. Beemster, Han Asard, and Hamada AbdElgawad. 2023. "Biochemical Composition Changes Can Be Linked to the Tolerance of Four Grassland Species under More Persistent Precipitation Regimes." *Physiologia Plantarum* 175 (6). <https://doi.org/10.1111/PPL.14083>.

Lin Zi ^{a,*}, Simon Reynaert ^b, Ivan Nijs ^b, Hans De Boeck ^b, Erik Verbruggen ^b, Gerrit T.S. Beemster ^a, Han Asard ^a, Hamada AbdElgawad ^a

^a Integrated Molecular Plant Physiology Research (IMPRES), Department of Biology, University of Antwerp, B-2020 Antwerp, Belgium

^b Plants and Ecosystems (PLECO), Department of Biology, University of Antwerp, B-2610 Wilrijk, Belgium

*Corresponding author

For this chapter, L.Z performed the biochemical measurements, data interpretation and wrote the manuscript. L.Z carried out the data analysis with the support of S.R.

Abstract

Climate models suggest that the persistence of summer precipitation regimes (PRs) is on the rise, characterized by both longer dry and longer wet durations. These PR changes may alter plant biochemical composition and thereby their economic and ecological characteristics. However, impacts of PR persistence have primarily been studied at the community level, largely ignoring the biochemistry of individual species. Here, we analyzed biochemical components of four grassland species with varying sensitivity to PR persistence (*Holcus lanatus*, *Phleum pratense*, *Lychnis flos-cuculi*, *Plantago lanceolata*) along a range of increasingly persistent PRs (longer consecutive dry and wet periods) in a mesocosm experiment. The more persistent PRs decreased nonstructural sugars, whereas they increased lignin in all species, possibly reducing plant quality. The most sensitive species *Lychnis* seemed less capable of altering its biochemical composition in response to altered PRs, which may partly explain its higher sensitivity. The more tolerant species may have a more robust and dynamic biochemical network, which buffers the effects of changes in individual biochemical components on biomass. We conclude that the biochemical composition changes are important determinants for plant performance under increasingly persistent precipitation regimes.

1 Introduction

Climate change is inducing more persistent weather in the mid-latitudes, including a shift of precipitation regimes (PRs) towards more extreme patterns with longer dry and longer wet periods compared with historic averages (Pfleiderer et al. 2019; Breinl et al. 2020). These new regimes can be expected to prompt a range of plant stress responses. During dry periods, stomatal

closure typically inhibits photosynthesis, altering the central plant metabolism and growth (Melandri et al. 2020; Krasensky and Jonak 2012). Upon rewatering, plants exhibit a certain degree of species-specific recovery strongly depending on the preceding drought intensity and duration (Z. Xu et al. 2010). On the other hand, extensive rainfall events can result in various deleterious effects, including nutrient leaching and oxygen shortage in the root zone (Reyer et al. 2013; Salazar et al. 2014). It is therefore a challenge to understand and predict plant responses to repeated alternations of both longer dry and wet spells.

Previous studies have shown that more extreme rainfall patterns without changes in total rainfall quantity reduced the aboveground net primary productivity (ANPP) of native grassland (Knapp et al. 2002); enhanced interannual precipitation variation decreases grass and increases shrub-productivity (Gherardi and Sala 2015); Heisler-White et al. (2009) found contingent responses to more extreme precipitation regimes across a grassland biome. These studies focused on precipitation redistribution with more intense peak precipitation (single large rainfall event) intersperse with longer drought (Knapp et al. 2002; Zeppel et al. 2014; Reynaert et al. 2021). However, the new trend of alternation of both longer consecutive dry period and wet period has been scarcely studied so far. Our own previous research has shown that, at the community level, more persistent PRs reduce plant diversity in grassland ecosystems (Reynaert et al. 2021), and select for acclimated communities with increased productivity and attenuated molecular stress responses (Reynaert et al. 2022). In soils, more persistent PRs reduce fungal diversity and connectivity (L. Li, Nijs, et al. 2023), and moderately persistent PRs increase the stochasticity of microbial community assembly. However, the impact of persistent PRs on plant biochemical compositions are still unknown.

Given the paucity of available data on plant biochemistry under more persistent climate regimes, we turn to the knowledge base on the constituting events of such regimes: climate extremes. These are known to influence the biochemical composition of plants and thus their economic and ecological characteristics such as nutrition value and decomposition rate (AbdElgawad et al. 2014; Schmitz et al. 2020). For instance, plants can metabolize proteins and lipids as alternative respiratory substrates when carbohydrates are scarce (Araújo et al. 2011); starch biosynthesis contributes to maintaining leaf growth under drought stress and facilitates enhanced carbon acquisition upon recovery (AbdElgawad et al. 2020); soluble sugars provide carbon skeletons for defense compounds synthesis and can act as metabolic signaling molecules to induce defense genes (Jeandet et al. 2022). Plant cell wall is the first barrier of defense against adverse abiotic and biotic stress, and is an essential element to control the strength, rigidity and flexibility of the plant body (Johnson et al. 2018; Novaković et al. 2018). Polysaccharides such as cellulose, hemicellulose, callose, and pectin are the main components of cell walls, which represent around 50% of biomass (Doblin et al. 2010). The texture, nutritional and processing properties of plant-based products are highly influenced by cell wall characteristics (Doblin et al. 2010). In addition to cell wall polysaccharide, the phenolic polymer lignin is crucial to determine cell wall quality, as lignin deposition reinforces the strength and rigidity of the secondary cell wall and can be a key component of plant responses to environmental factors (Le Gall et al. 2015). It has been shown that lignification can occur prematurely to avoid cell wall damage when plants are exposed to water deficit for a long time (Le Gall et al. 2015), which could in turn reduce forage quality (Gallego-Giraldo et al. 2016). To assess the consequences of more persistent PRs on natural and

agricultural ecosystems, understanding the resulting changes in the biochemical composition of species with contrasting sensitivities towards those regime changes (in terms of stress response, survival and productivity), is of key importance.

To achieve this goal, we experimentally varied the temporal distribution of precipitation while keeping its total amount constant. A gradient of eight PRs was applied to experimental grassland mesocosms, with consecutive dry and wet periods ranging from 1 to 60 days (Reynaert et al. 2021). The gradient design allows investigation of how increasingly persistent PRs affect plant biomass and biochemical composition. Our previous results using this experimental setup showed that alternating longer dry and longer wet periods lead to a severe loss of species richness and diversity, and that grassland species exhibit different sensitivities in terms of stress response, survival and productivity, to the altered PRs (Reynaert et al. 2021). In the current study, four of these species (*Holcus lanatus* L., *Phleum pratense* L., *Lychnis flos-cuculi* L., *Plantago lanceolata* L.), with contrasting sensitivities were analyzed in detail. The objectives were to determine 1) how increasingly persistent PRs affect grassland species biomass, cell wall composition and other biochemical composition; 2) the relationship between biochemical composition and biomass under more persistent PRs; 3) potential drivers of differences between grassland species.

2 Materials and methods

2.1 Experimental design and treatments

The experiment took place at the Drie Eiken Campus of the University of Antwerp in Belgium (51°09'41"N, 04°24'9"E). We used the same study site and

experimental setup as Reynaert et al. (2021): grassland mesocosms (256) were distributed across eight experimental units (32 mesocosms per unit). Each unit was equipped with a rain screen which automatically covered the plants during natural rain, and automatic irrigation through drippers to add water according to different PRs. The mesocosms (50 cm deep and 30 cm diameter) were filled with sandy-loam soil with a pH between 7.0 and 7.2. The soil's field capacity (FC) was estimated at $0.26 \text{ m}^3 \text{ m}^{-3}$ and the permanent wilting point (PWP) at $0.05 \text{ m}^3 \text{ m}^{-3}$. Three individuals of 12 common perennial temperate C3 grassland species were planted in each mesocosm. Species were planted to maximize interspecies interactions and covered 3 functional groups: 6 grasses (*Agrostis capillaris* L., *Anthoxanthum odoratum* L., *Deschampsia cespitosa* (L.) P. Beauv., *Phleum pratense* L., *Poa pratensis* L., *Holcus lanatus* L.); 3 N-fixing forbs (N-fixers) (*Lotus corniculatus* L., *Trifolium pratense* L., *Trifolium medium* L.); and 3 non-N-fixing forbs (*Centaurea jacea* L., *Lychnis flos-cuculi* L., *Plantago lanceolata* L.).

From July 2, 2019, to October 28, 2019 (120 days), the mesocosms were subjected to a gradient of 8 PRs, with alternating dry/wet periods of 1, 3, 6, 10, 15, 20, 30 and 60 consecutive wet and dry days (referred to as '1-day PR', '3-day PR', etc.). As watering cycles can start with either a wet or dry period, half of the mesocosms were exposed to a dry start (shortened as '1D', '3D', etc.), and the other to a wet start (shortened as '1W', '3W', etc.). Each combination of PR and start type had 16 replicate mesocosms spread over four units. On wet days, mesocosms were irrigated between 10:30 am and 11:00 am with 6.87 L m^{-2} stored rainwater. This volume is 1.5 times the daily Belgian average precipitation to account for additional evapotranspiration in the mesocosms

compared with open field conditions. All regimes had the same total number of irrigation days (60 days) and total water amount (412 L m⁻²) after 120 days.

2.2 Biomass measurements

At the end of the experiment (120 days), all standing biomass above 4.5 cm from 12 out of 16 replicate mesocosms was cut and pooled in paper bags per species and per mesocosm. Materials were oven-dried at 70 °C for > 72 h and weighed to the closest 0.01 g. The average weight of 10 oven-dried empty bags was subtracted to determine plant dry weights. Two grasses (*Holcus lanatus* L.; *Phleum pratense* L.) and two forbs (*Lychnis flos-cuculi* L.; *Plantago lanceolata* L.) were continuing to analyse biomass and biochemical changes. The species choice was based on their relative sensitivity in terms of stress response, survival to the changing PRs (Reynaert et al. 2021): *Lychnis flos-cuculi* and *Holcus lanatus* were two relatively sensitive species, while *Plantago lanceolata* and *Phleum pratense* were comparatively more tolerant. At the same time, these four species still yielded enough material for biochemical analyses.

2.3 Measurements of cell wall composition

After the biomass measurement, the harvested plants were further undergoing biochemical analysis to investigate the changes of cell wall composition and other biochemical components. Due to the shortage of plant material, two replicates (mesocosms) were randomly combined as one replicate for biochemical measurement (n = 6). Cell wall materials were extracted following the method of (Zhong and Lauchi 1993). 50 mg plant shoots were thoroughly homogenised in 75% ethanol for 20 min. After centrifugation at 8000 × g for 10 min, the supernatant was discarded. The pellets were homogenised and washed for 30 min with acetone, methanol: chloroform mixture (1:1, v/v) and

methanol, respectively. The supernatant was discarded, and the pellet was freeze-dried and stored at 4°C for further use. Cell wall materials were fractionated into four fractions: pectin, hemicellulose 1 (HC1), hemicellulose 2 (HC2) and cellulose. Pectin was extracted three times by hot water (100°C) for 1 h each and the supernatants were combined (pectin). Then, the pellets were subjected to triple extraction with 4% KOH containing 0.1% KBH_4 at room temperature for 8 h each and the supernatants were combined (HC1). The resulting pellets were subsequently extracted with 24% KOH containing 0.1% KBH_4 at room temperature for 8 h each and the supernatants were combined (HC2), and the residue was considered as the cellulose fraction.

Lignin was quantified according to a modified version of Iiyama and Wallis (1990). Cell wall materials (1 mg) were digested in 100 μl of 25% (v/v) acetyl bromide in acetic acid at 70°C for 30 min and cooled quickly. Then, 180 μl of 2 M NaOH was added to the mixture to terminate the digestion and mixed with 20 μl of 7.5 M hydroxylamine hydrochloride and 1 ml acetic acid. The mixtures were centrifuged at 3000 \times g for 10 min. The content of lignin was measured at 280 nm (Synergy Mx spectrophotometer, BIOTEK, Winooski, USA).

Callose was extracted and determined based on (Kohle et al. 1985). Around 50 mg plant tissue was homogenised in 0.5 ml 1 M NaOH and heated at 80°C for 30 min. After centrifugation, the 200 μl supernatant which contain callose was mixed with 1.25 ml aniline blue mixture consisting of 0.1% aniline blue in 1 M glycine at pH 9.5 and heated in a water bath at 50°C, for 20 min. Callose was quantified by fluorescence spectrophotometry (Synergy Mx spectrophotometer, BIOTEK, Winooski, USA) using an excitation wavelength of 393 nm and an emission wavelength of 484 nm.

2.4 Measurements of other biochemical components

To determine the soluble sugar content, 50 mg dry shoot tissue was extracted with 2 mL of 80% ethanol at room temperature. After centrifugation at 14000 rpm for 10 min, the soluble sugar content was determined using the anthrone reagent (Leyva et al. 2008), with glucose as a standard, and absorbance measured at 620 nm (Synergy Mx spectrophotometer, BIOTEK, Winooski, USA). To estimate starch content, the residue was digested with α -amylase (Sigma-Aldrich, EC 3.2.1.1) and amyloglucosidase (Sigma-Aldrich, EC 3.2.1.3) to hydrolyze sugar polymers and re-measure soluble sugars (Macrae 1971).

Another aliquot of 50 mg dry shoot tissue was used to extract total lipids, by applying a liquid-liquid extraction method with a mixture of chloroform, methanol and water (5:10:1 V/V/V). The extracted lipids were measured by gravimetric analysis and expressed as weight (g) per dry weight (g) of plant sample (Phillips et al. 1997). To determine total protein content, 50 mg dry shoot tissue was incubated in 1 mL 0.1 M NaOH at 60 °C overnight to extract proteins. Protein content was measured in the supernatant after centrifugation at 14000 rpm for 10 min according to the Lowry method (LOWRY et al. 1951). After reaction with the biuret reagent and Folin-Ciocalteu reagent, absorption was measured at 750 nm. Bovine Serum Albumin (BSA) was used as the standard.

2.5 Statistical analysis

All statistical analyses were performed in R (version 4.0.4). Significance was assumed for p values < 0.05. Generalized Additive Mixed Models (GAMM's) were constructed to investigate the relationship between PRs and measurements using the package mgcv (Pedersen et al. 2019) (see more info in

Table S1). Because the PR gradient is skewed, the PR durations were log transformed before fitting the models. Principle component analysis (PCA) was conducted by the R package MixOmics (Rohart et al. 2017). We used structural equation modeling (SEM) to examine the relationship between PR, soil water characteristics, biochemical components and biomass. The maximum likelihood (ML) method was used to fit models, and the best-fitted model was evaluated using p value (0.094), χ^2/df (1.59), GFI (Goodness-of-Fit Index; 0.997), CFI (Comparative Fit Index; 0.992), RMSEA (Root Mean Square Error of Approximation; 0.100) test. RMSEA showed a marginal fit, while the other indices suggested a good model fit. A random forest analysis was performed on the data of all species together using the package RandomForest (Breiman 2001) to evaluate which variable explains most variation in the aboveground biomass. The variables' importance ranking was determined by increased mean square error (%IncMSE) and node-purity percent (IncNodePurity). Finally, correlation matrices were analyzed to determine underlying drivers of the observed patterns, using the rcorr and corrplot functions of the R packages Hmisc (Harrell 2023) and corrplot (Wei T 2021), respectively.

3 Results

3.1 Effects of increasingly persistent precipitation regimes on soil water characteristics

The different PRs strongly influenced the soil water content (SWC) throughout the experiment (Table 1). More persistent PRs generally resulted in longer periods with the SWC below the permanent wilting point (PWP) (Reynaert et al. 2021; Table 1), which induces more stress. We previously demonstrated that the length of the longest consecutive period below PWP was the best predictor

of community survival, and PRs with more days below permanent wilting point had lower survival (Reynaert et al. 2021).

Table 1. Soil water characteristics including mean soil water content (SWC), coefficient of variation, the total number of days below permanent wilting point (PWP) and the longest number of consecutive days below PWP induced by different precipitation regimes (PR) during the experimental period (120 days).

PR	Mean SWC	Coef. of var.	Total days below PWP	Longest consecutive days below PWP
1W	0.125	1.99	0	0
3W	0.107	2.5	1	1
6W	0.126	2.27	5	4
10W	0.15	2.3	7	4
15W	0.158	2.16	8	4
20W	0.133	1.96	17	11
30W	0.137	2.26	25	25
60W	0.099	1.69	39	20
1D	0.115	2.28	0	0
3D	0.095	3.02	6	2
6D	0.113	2.5	5	3
10D	0.102	2.03	19	8
15D	0.151	1.87	15	10
20D	0.12	2.23	10	10
30D	0.117	1.64	30	17
60D	0.131	1.48	39	39

3.2 Effect of increasingly persistent precipitation regimes on the biomass of four grassland species

By calculating seasonal mean Fv/Fm values and survival, our previous research demonstrated that the 12 grassland species showed different sensitivity to stress. The stress sensitivity was defined by the slope of declining survival with increasing stress (lower Fv/Fm) (Reynaert et al. 2021). The stress sensitivity of the four species that we analyzed in this study were *Lychnis* > *Holcus* > *Plantago* >

Phleum, with *Phleum* also being the least sensitive species among the 12 species (Figure S12B, S13, S14 in Reynaert et al. 2021).

Different PRs induced significant changes in the biomass (dry weight) of *Holcus*, *Phleum* and *Lychnis* (Figure 1; Table S1). Under dry start regimes the biomass was reduced with more persistent PRs in the above three species, while under wet start treatments only *Lychnis* had lower biomass (Figure 1). The biomass decrease was more monotonous (linear) in *Lychnis* compared with the other three species (Figure 1; Table S1).

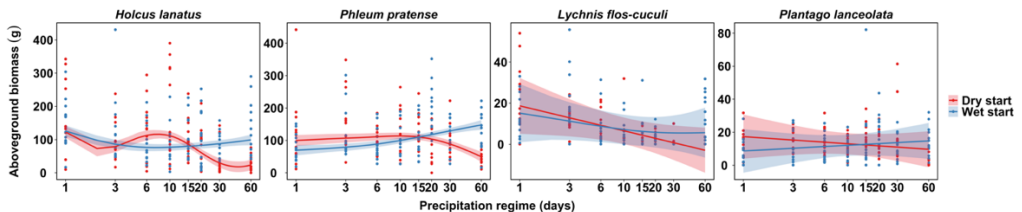


Figure 1. Effect of precipitation regimes on aboveground biomass (dry weight) of four grassland species. Lines represent fitted outcomes based on GAMM (generalized additive mixed model). The shaded areas represent 95% confidence intervals. Points indicate individual measurements ($n = 12$ per treatment).

3.3 Effect of increasingly persistent precipitation regimes on biochemical components of four grassland species

Next, we performed a principal component analysis (PCA) to gain insight into the overall effect of increasingly persistent PRs on the biochemical composition of grassland species. PC1 separated the four grassland species and explained 44% of the variance, with *Plantago* and *Phleum* located on the right and *Lychnis* and *Holcus* located on the left (Figure 2A). Persistence of the PRs exhibited separation along PC2, which explained 19% of the variance (Figure 2A). Apart from a separate position for lignin, the biochemical variables form four clusters: soluble sugar and starch, cellulose and hemicellulose, callose and pectin, and lipids and proteins (Figure 2B). Lignin, callose and pectin were more abundant

in the more persistent PRs, while soluble sugar and starch accumulated more in the less persistent PRs (Figure 2B). Lipids and protein content contributed less to the separation of samples compared with other chemical components, neither on PR nor on species level (Figure 2B). Dry and wet start regimes did not show clear separation on PC1 and PC2.

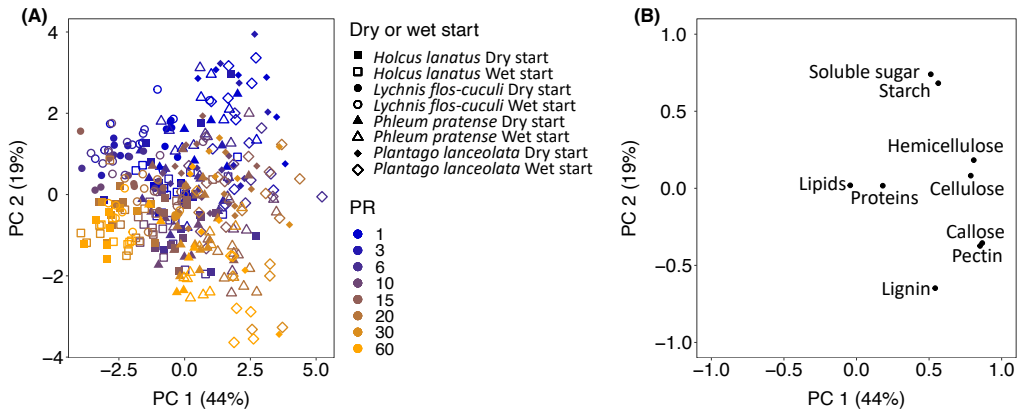


Figure 2. Global impact of increasingly persistent precipitation regimes (PRs) on biochemical components of four grassland species. Principal component analysis (PCA) conducted on biochemical variables of four species using PC1 vs PC2: (A) The samples are categorized by species, PR and dry or wet start. (B) Loadings of the biochemical variables on PC1 and PC2. Points indicate individual measurements ($n = 6$ per treatment).

We next conducted separate PCAs on the individual species. The less and more persistent PRs separated along PC1 in *Holcus*, *Phleum* and *Plantago* and along PC2, which explained less of the variance, in *Lychnis* (Figure 3A, C, E, G). The dry and wet start regimes did not clearly separate for any of these species (Figure 3A, C, E, G).

Across the four species, soluble sugar, starch, cellulose and hemicellulose were more abundant in less persistent PRs (Figure 3B, D, F, H). Under more persistent PRs, *Holcus* and *Lychnis* seemed to accumulate more lipids and protein, while *Phleum* and *Plantago* contained more lignin (Figure 3B, D, F, H).

Chapter 3

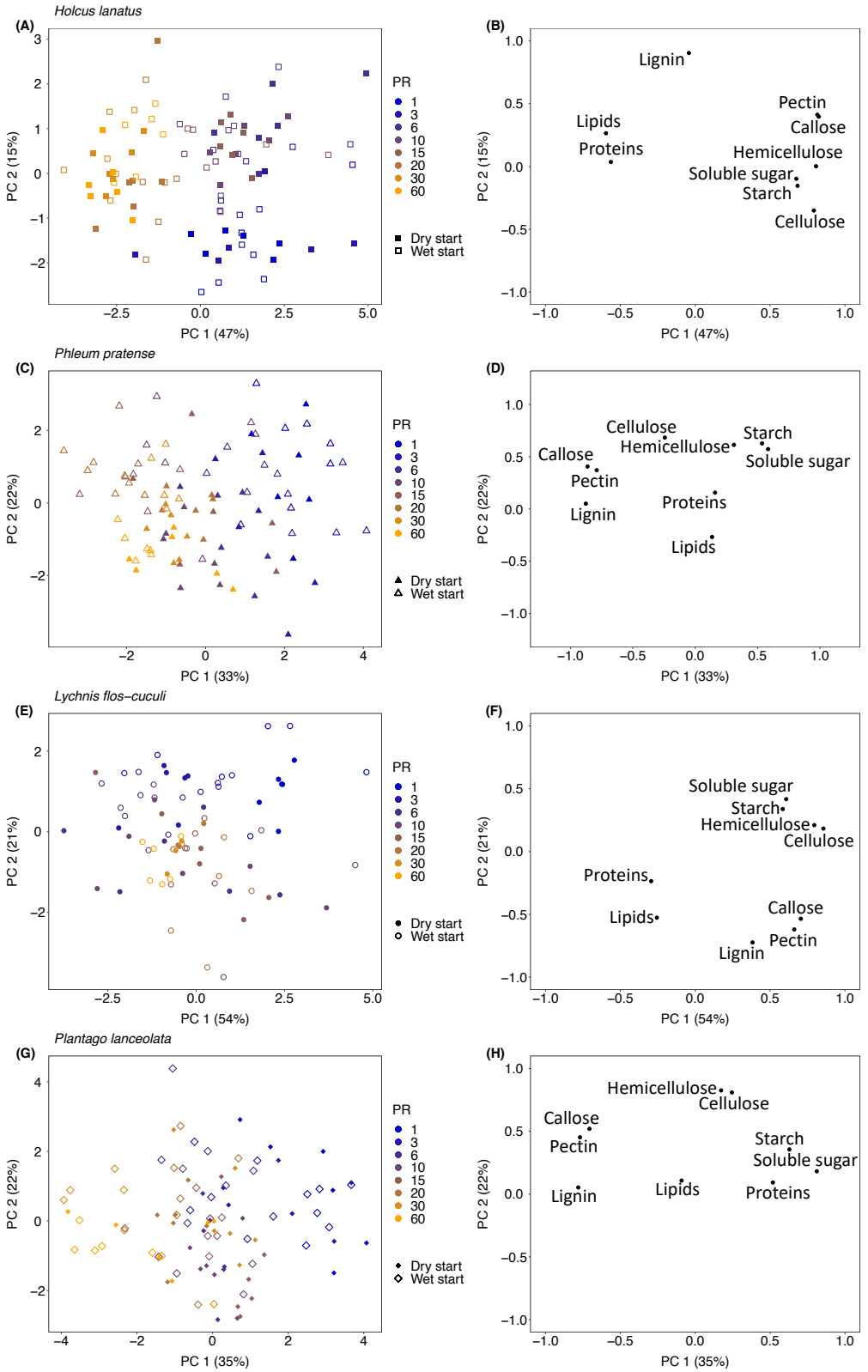


Figure 3. Impact of increasingly persistent precipitation regimes (PRs) on biochemical components of individual grassland species. Principal component analysis (PCA) conducted on biochemical variables of four species using PC1 vs PC2. (A, C, E, G). The samples are categorized by PR and dry or wet start. (B, D, F, H) Loadings of the biochemical variables on PC1 and PC2. Points indicate individual measurements ($n = 6$ per treatment).

We next evaluated the effect of PR on the individual metabolites, separating cell wall components (Figure 4) from primary metabolites (Figure 5). Except in the most resistant species *Phleum*, cellulose generally decreased with more persistent PRs under both wet and dry start (Figure 4A). As was also revealed in the PCA, the hemicellulose response was similar to that of cellulose (Figure 4B), except for a more complex pattern emerging in *Plantago*, where a slight increase between the 15 to 30 day-PR interrupted the overall decreasing trend (Figure 4B). Except *Plantago*, the other three species accumulated callose under relatively mild PRs (Figure 4C). The callose contents decreased under the most persistent PRs (30, 60 day-PR) in *Holcus*, *Phleum* and *Lychnis* (wet start), while it slightly increased in *Plantago* under the 60-day PR (Figure 4C). Pectin showed a very similar pattern as callose (Figure 4E). The lignin content generally increased under more persistent PRs in all species, most strongly in the two relatively tolerant species *Phleum* and *Plantago* (Figure 4D; Table S1).

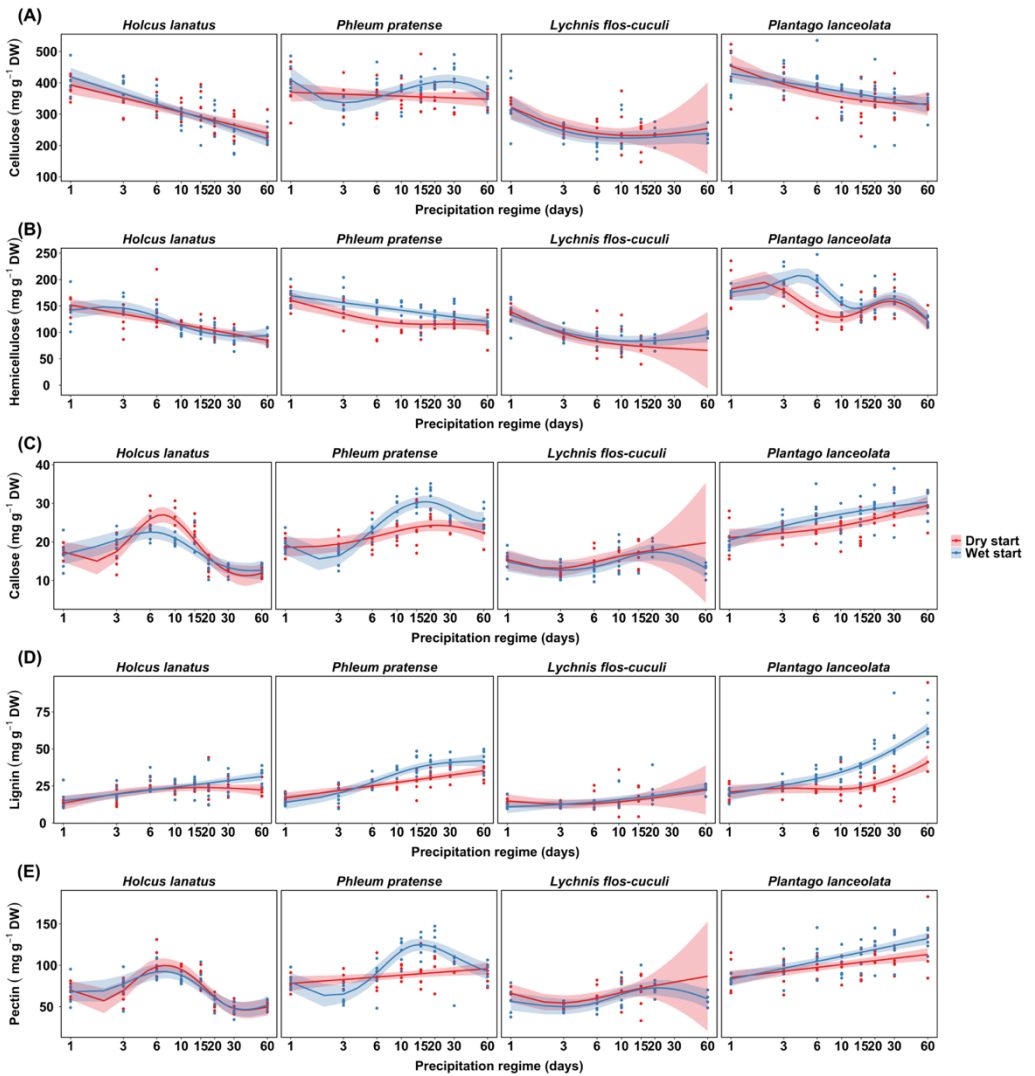


Figure 4. Impact of increasingly persistent precipitation regimes (PRs) on cell wall components of four grassland species. Lines represent fitted outcome based on GAMM (generalized additive mixed model). Shading area represents 95% confidence intervals. Points indicate individual measurements ($n = 6$ per treatment).

With respect to lipids, *Holcus* accumulated more under more persistent PRs, except at the 60-day dry start PR (Figure 5A). In *Phleum*, the lipids showed a decreasing trend along the PRs (Figure 5A). The changes in *Lychnis* and *Plantago* were subtle (Figure 5A). As also reflected in the PCA, there was no

clear pattern in the proteins (Figure 5B). For soluble sugar and starch, all four species exhibited clear declines (Figure 5C, D).

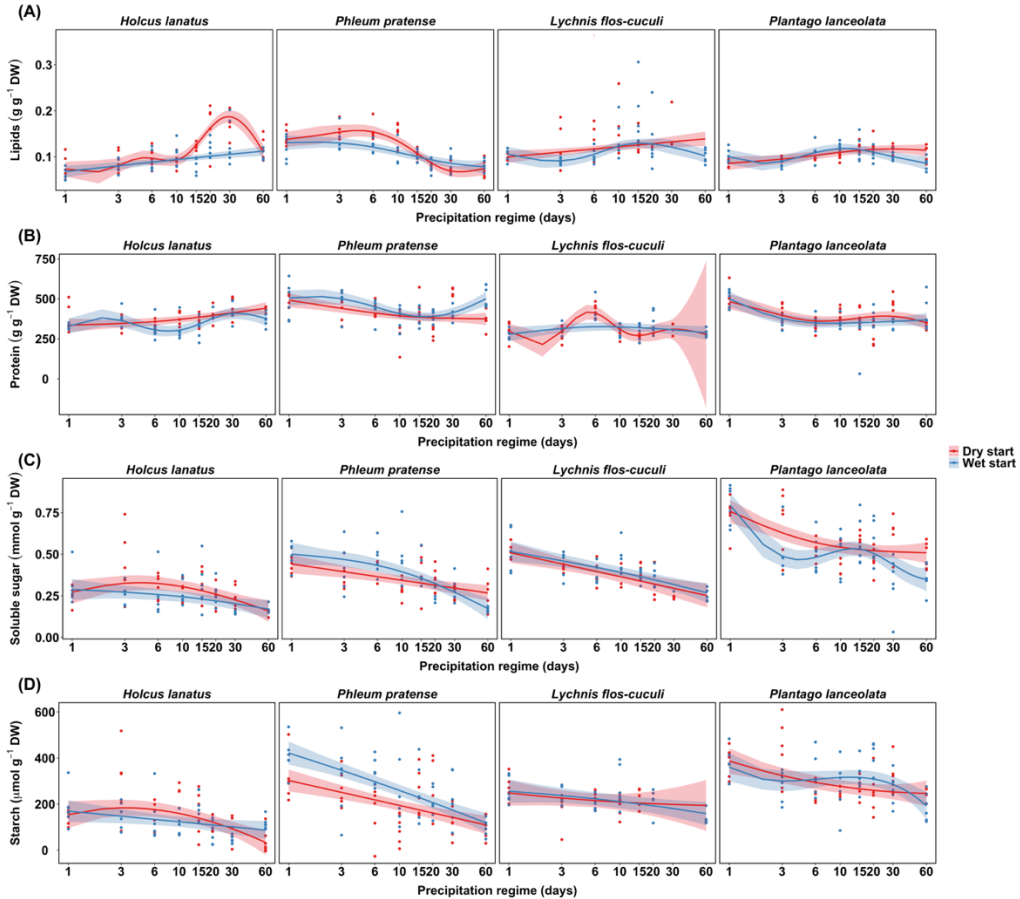


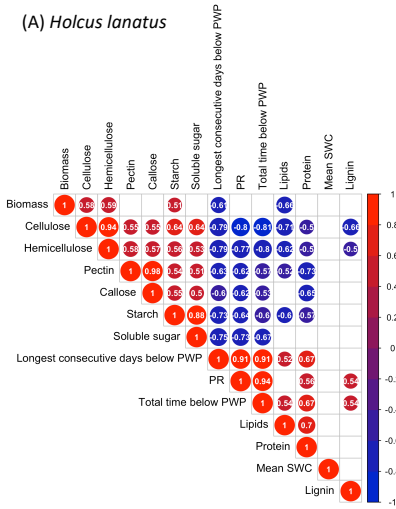
Figure 5. Impact of increasingly persistent precipitation regimes (PRs) on primary metabolites of four grassland species. Lines represent fitted outcome based on GAMM (generalized additive mixed model). Shading area represents 95% confidence intervals. Points indicate individual measurements ($n = 6$ per treatment).

3.4 Relationship between PR, soil water characteristics, biochemical components and biomass

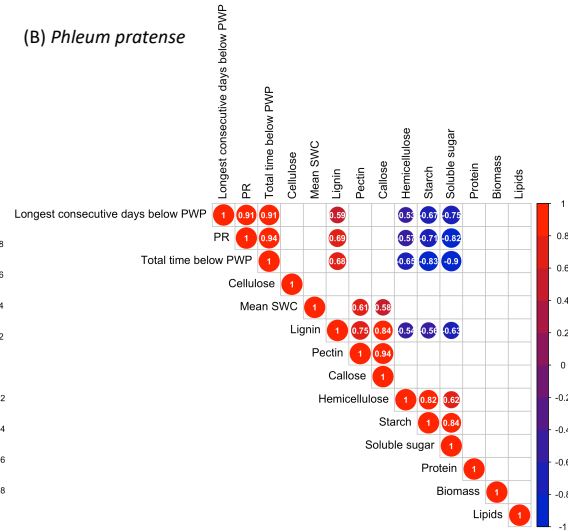
Random forests analysis suggests that the identity of the species is the most important factor to predict aboveground biomass (Figure S1), and soluble sugar the second most important factor (Figure S1). Given the primary importance of species, separate analyses were carried out by species to investigate

correlations between PR, soil water characteristics, biochemical components and biomass. A high number of significant correlations with biomass were found in the sensitive species *Holcus*. Here, cellulose, hemicellulose and starch levels correlated positively with biomass and lipids negatively (Figure 6A). The other sensitive species *Lychnis* showed a positive correlation between biomass and hemicellulose, yet the reverse relationship with lipids (Figure 6C). In the tolerant species *Phleum* and *Plantago*, no significant correlations were detected between biomass and biochemical components (Figure 6B, D). On the other hand, significant correlations were found between lignin and other components in these species. In *Phleum*, lignin correlated strongly and positively with pectin and callose, and negatively with lipids, soluble sugar, starch and hemicellulose (Figure 6B). As for *Plantago*, lignin was strongly and positively related with PR, the longest number of consecutive days below PWP and the total number of days below PWP (Figure 6D). PR, the longest number of consecutive days below PWP and the total number of days below PWP showed a higher number of correlations with biochemical components in *Holcus*, *Phleum* and *Plantago* compared with the most sensitive species *Lychnis* (Figure 6). Only a few components showed weak correlations with mean SWC in *Phleum* and *Plantago* (Figure 6B, D).

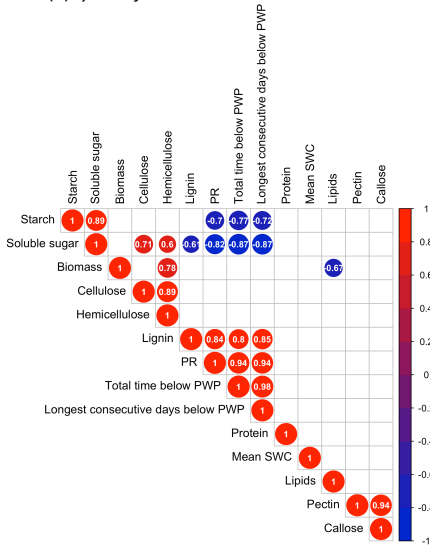
(A) *Holcus lanatus*



(B) *Phleum pratense*



(C) *Lychnis flos-cuculi*



(D) *Plantago lanceolata*

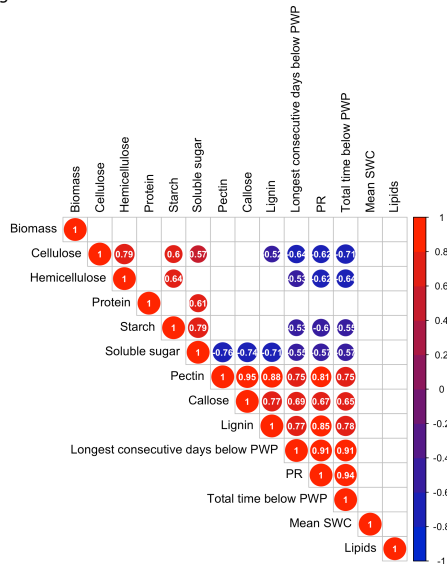


Figure 6 Correlations between PR, soil water characteristics, biochemical components and biomass of each species. Numbers are Pearson correlation coefficients (cf. colour scale). The sizes of circles represent the absolute value of corresponding coefficients. Empty cells indicate a non-significant correlation ($p > 0.05$).

Based on these correlations and plausible theory, we then constructed a SEM to quantify the strength of both the direct and indirect relationships between PR, soil water characteristics, biochemical components and biomass across all species (Figure 7). In general, PRs with longer dry and wet spells (PR) increased

the lignin content and more total days below PWP reduced the hemicellulose and starch contents (Figure 7). Cellulose and protein showed positive effects on aboveground biomass accumulation, while soluble sugar and hemicellulose exhibited negative effects on aboveground biomass (Figure 7). Particularly, soluble sugar showed a stronger negative effect on biomass compared to the other components (Figure 7), which was also suggested by the random forest analysis (Figure S1). Finally, confirming earlier observations, the length of the longest consecutive days below PWP generally reduced species biomass (Figure 7).

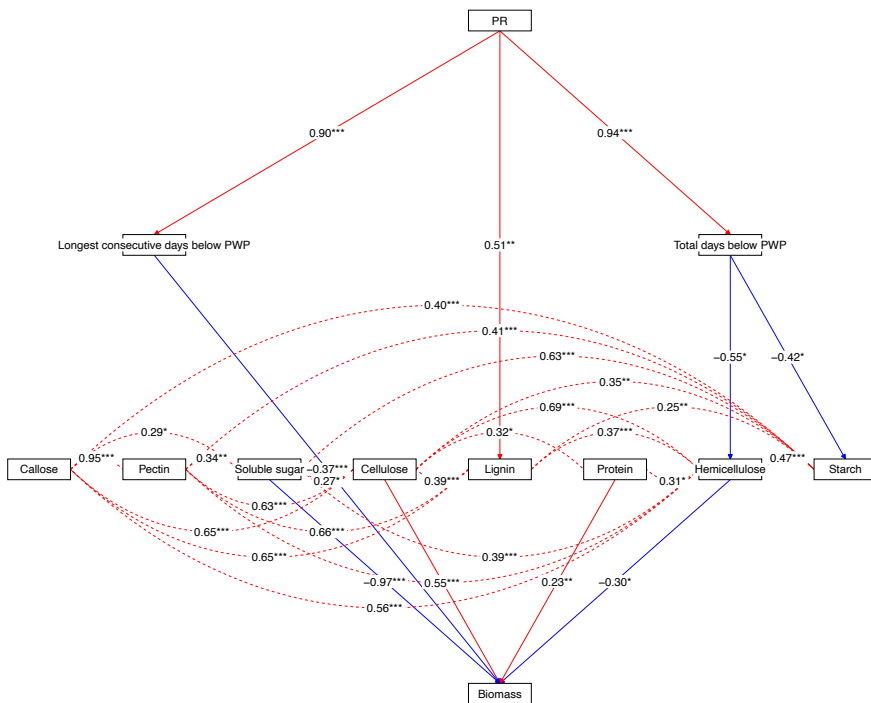


Figure 7 Structural equation model (SEM) showing the relationships between PR, soil water characteristics, biochemical components and aboveground biomass. The statistics of SEM fitting are: $\chi^2 = 17.481$, $\chi^2/df = 1.59$, $p = 0.094$, $GFI = 0.997$, $CFI = 0.992$, $RMSEA = 0.100$. The single-headed arrows indicate the hypothesized direction of causation. Dashed lines represent covariance between different biochemical components. Red lines represent positive relationships, and blue lines represent negative relationships. The values indicate standardized

*path coefficients (*p < 0.05, **p < 0.01, ***p < 0.001). Non-significant relationships were excluded to increase clarity.*

4 Discussion

In this study, we showed that increasingly persistent PRs altered the biochemistry of individual plant species. Despite the complexity of comparing data from different species and different biochemical components, we revealed both common and distinct responses related to diverging tolerances of individual species to more persistent PRs.

4.1 More persistent PRs decreased nonstructural sugars but increased lignin biosynthesis

We observed that, in all four species, the concentration of nonstructural sugars (soluble sugar and starch) decreased while lignin increased under more persistent PRs (Figure 3; 4). This likely indicates that the increasingly persistent PRs inhibited photosynthesis, while the plants simultaneously strengthened their defense responses by accumulating more lignin. Earlier studies have reported that reduced foliar nonstructural sugar during lethal drought indicates a carbon regulation role in mortality (Adams et al. 2013). Trees often increase their nonstructural sugar content at the expense of other sinks to ensure survival under drought conditions. However, this strategy comes at the cost of reduced growth and biomass (Wiley and Helliker 2012). This is consistent with our observation that the soluble sugar levels had a negative effect on biomass accumulation (Figure 7). Song et al. (2022) proposed a U-shape relationship model between nonstructural sugars and increasing aridity, with a threshold at intermediate levels of drought where an initial negative response switches to a positive response. Therefore, the decreasing trend of soluble sugar and starch with increasing persistence of PR may imply that the measurement at the end

of the experiment (120 days) may only represent a relatively short-term response and thus needs to be supplemented with longer-term data. Consistent with our results, many studies have shown that lignin biosynthesis is enhanced under various types of stress such as drought, salt and heavy metals (Q. Liu et al. 2018; Lee et al. 2007). The accumulation of lignin increases the cell wall thickness and therefore has important implications for plant lodging resistance (Q. Liu et al. 2018; Q. Li et al. 2022). Lignin can also reduce cell wall water penetration and transpiration, which helps to maintain the osmotic balance and protect membrane integrity when plants are faced with water loss (Q. Liu et al. 2018; Monties and Fukushima 2005). In our study, we did not detect an association between lignin and biomass (Figure 6; 7). Similarly, studies on *Arabidopsis* showed that growth phenotypes do not seem to be directly related to the content, composition and structure of lignin itself (Ha et al. 2021), but perhaps to other components such as flavonoids (Besseau et al. 2007). It should be noted that lignin interferes with the digestion of cell wall polysaccharides by acting as a physical barrier to microbial enzymes (Moore and Jung 2001). This suggests that the shift of nonstructural sugar to lignin would decrease the digestible energy value of grassland species under more persistent PRs.

4.2 Intrinsic and PR-induced differences between sensitive and tolerant species

Generally, the two more tolerant species, *Phleum* and *Plantago*, contained higher concentrations of soluble sugar, starch, cellulose, hemicellulose, pectin, callose and lignin compared with the two more sensitive species, *Lychnis* and *Holcus* (Figure 2). It is known that lignin, cellulose and hemicellulose enhance the mechanical strength of plant stalks and promote mineral transport through

the vascular bundles (Q. Liu et al. 2018; Q. Li et al. 2022). In addition, high soluble sugar and starch storage can be seen as an important buffer during environmental stress periods when carbon demand outweighs supply due to reduced stomatal conductance (Signori-Müller et al. 2021). In agreement, lower nonstructural sugars have been associated with increased risk of drought induced mortality (Rosas et al. 2013). Therefore, higher contents of the above-mentioned components in more tolerant species may contribute to their capacity to better withstand more persistent PRs.

The tolerant and sensitive species showed distinction in their response profile (Figure 2; Figure 3). Interestingly, the variation of biocomponents induced by altered PRs in the most sensitive species *Lychnis* (PC2: 21%), was less than in the other three species (*Holcus* PC1: 47%; *Phleum* PC1: 33%; *Plantago* PC1: 35%; Figure 3). This may reflect that the sensitive species was unable to achieve sufficient changes of biochemical components in response to altered PR. However, our earlier research showed that the metabolome of sensitive species exhibited more variation than in the relatively tolerant species (Zi et al. 2023). This difference between metabolome profile and biochemical composition can possibly be explained by the fact that the compounds reported here are generally long chain polymers, for which the synthesis and degradation is relatively time consuming. On the other hand, the metabolome is the composition of small molecular weight molecules (metabolites) which is highly dynamic in time and can be seen as a snapshot of the current status of plants. We speculate that under the altered PR, more sensitive species are less capable at inducing longer term acclimation and may hence rely more on transient defense responses that need constant reallocation of resources.

4.3 The associations between PR, soil water characteristics, biochemical components and biomass

Another goal of this study was to evaluate the associations between PRs, soil water characteristics, biochemical components and biomass. PRs strongly increase the total number of days below PWP and the longest number of consecutive days below PWP (Figure 7). As such, PR persistence primarily altered species biochemical performance indirectly by influencing soil water dynamics in relation to critical soil moisture thresholds. Similar to what we reported about survival on the same experiment (Reynaert et al. 2021), the longest number of consecutive days below PWP was the strongest predictor of aboveground biomass, stronger than PR, total number of days below PWP and mean SWC (Figure 7; S1). The fact that there were fewer correlations between soil water characteristics and biochemical components in the most sensitive species *Lychnis* (Figure 6), may further suggest that *Lychnis* was less capable to induce sufficient changes in response to the varied soil water availability. Furthermore, *Lychnis* was also the only species showing a strong decline in survival independent of the timing of wet and dry periods, suggesting a strong intrinsic non-plastic response to altered PR persistence. On the other hand, there were comparatively more correlations between biomass and biochemical composition in the relatively sensitive species *Holcus* and *Lychnis* in comparison to the more tolerant species *Phleum* and *Plantago* (Figure 6). This observation suggests that the more tolerant species may have a more robust and dynamic biochemical network, which buffers the effects of changes in individual biochemical components on biomass.

5 Conclusion

By investigating changes in biochemical composition and standing biomass along increasingly persistent PRs in different species, we showed that: a) decreased nonstructural sugars and accumulation of lignin were general responses induced by more persistent PRs across all four studied species; b) although the shift from nonstructural sugars to lignin may improve acclimation, it also decreases the nutritive value of grassland species; c) the most sensitive species *Lychnis* was less capable of inducing significant changes in macromolecular components, which may partly explain its sensitivity in response to more persistent precipitation regimes; d) the more tolerant species may have a more robust and dynamic biochemical network, which buffers the effects of changes in individual biochemical components on biomass.

6 Supplementary Data

Table S1 Generalized Additive Mixed Models (GAMM) results of each measurement and smooth term. All smooth functions were fitted using thin plate regression splines. Asterisks represent significant differences ($p < 0.05$, ** $p < 0.01$, *** $p < 0.001$).*

Measurement	Link	Smooth term	knots	edf	Chi.sq	p-value
Biomass	identity	Holcus dry start PR	8	4.567597	136.508	< 2 ^e -16 ***
	identity	Holcus wet start PR	8	3.001157	26.588	2.4 ^e -05 ***
	identity	Phleum dry start PR	8	3.213049	43.504	< 2 ^e -16 ***
	identity	Phleum wet start PR	8	2.257054	65.543	< 2 ^e -16 ***
	identity	Lychnis dry start PR	8	1.000058	4.308	0.0379 *
	identity	Lychnis wet start PR	8	1.315169	1.621	0.4516

Chapter 3

	identity	Plantago dry start PR	8	1.000244	0.558	0.4550
	identity	Plantago wet start PR	8	1.000029	0.356	0.5509
Cellulose	identity	Holcus dry start PR	4	1.009	44.51	< 2 ^e -16 ***
	identity	Holcus wet start PR	4	1.000	71.90	< 2 ^e -16 ***
	identity	Phleum dry start PR	4	1.000	0.87	0.351005
	identity	Phleum wet start PR	4	2.857	13.68	0.002578 **
	identity	Lychinis dry start PR	4	1.710	15.38	0.000720 ***
	identity	Lychinis wet start PR	4	2.264	19.91	0.000563 ***
	identity	Plantago dry start PR	4	1.853	30.54	8.82 ^e -07 ***
	identity	Plantago wet start PR	4	1.000	18.66	1.66 ^e -05 ***
Hemicellulose	identity	Holcus dry start PR	8	1.102	47.72	< 2 ^e -16 ***
	identity	Holcus wet start PR	8	3.178	55.05	< 2 ^e -16 ***
	identity	Phleum dry start PR	8	2.414	29.19	4.73 ^e -06 ***
	identity	Phleum wet start PR	8	1.001	26.08	1.41 ^e -06 ***
	identity	Lychinis dry start PR	8	1.938	44.65	< 2 ^e -16 ***
	identity	Lychinis wet start PR	8	2.483	28.91	4.52 ^e -06 ***
	identity	Plantago dry start PR	8	4.397	51.94	< 2 ^e -16 ***
	identity	Plantago wet start PR	8	4.738	72.68	< 2 ^e -16 ***
Callose	identity	Holcus dry start PR	7	4.261	119.343	< 2 ^e -16 ***

Chapter 3

	identity	Holcus wet start PR	7	3.648	55.320	< 2 ^e -16 ***
	identity	Phleum dry start PR	7	2.853	19.850	0.000259 ***
	identity	Phleum wet start PR	7	4.020	112.610	< 2 ^e -16 ***
	identity	Lychinis dry start PR	7	2.186	3.179	0.211326
	identity	Lychinis wet start PR	7	3.211	9.495	0.024463 *
	identity	Plantago dry start PR	7	1.873	26.255	3.87 ^e -06 ***
	identity	Plantago wet start PR	7	1.752	42.362	< 2 ^e -16 ***
Lignin	identity	Holcus dry start PR	6	2.13	16.542	0.000632 ***
	identity	Holcus wet start PR	6	1.000	33.430	< 2 ^e -16 ***
	identity	Phleum dry start PR	6	1.000	41.921	< 2 ^e -16 ***
	identity	Phleum wet start PR	6	2.800	112.610	< 2 ^e -16 ***
	identity	Lychinis dry start PR	6	1.624	1.169	0.473010
	identity	Lychinis wet start PR	6	1.620	15.792	0.000242 ***
	identity	Plantago dry start PR	6	2.859	39.619	< 2 ^e -16 ***
	identity	Plantago wet start PR	6	2.615	239.649	< 2 ^e -16 ***
Pectin	identity	Holcus dry start PR	8	4.502	81.297	< 2 ^e -16 ***
	identity	Holcus wet start PR	8	4.14	57.679	< 2 ^e -16 ***
	identity	Phleum dry start PR	8	1.001	7.035	0.00804 **
	identity	Phleum wet start PR	8	4.262	102.485	< 2 ^e -16 ***

Chapter 3

	identity	Lychinis dry start PR	8	2.187	4.198	0.17224
	identity	Lychinis wet start PR	8	3.168	11.792	0.01142 *
	identity	Plantago dry start PR	8	1.001	15.693	7.55 ^{e-05} ***
	identity	Plantago wet start PR	8	1.000	53.882	< 2 ^{e-16} ***
Lipids	identity	Holcus dry start PR	8	4.919	176.334	< 2 ^{e-16} ***
	identity	Holcus wet start PR	8	1.139	23.292	1.12 ^{e-05} ***
	identity	Phleum dry start PR	8	4.039	130.142	< 2 ^{e-16} ***
	identity	Phleum wet start PR	8	2.648	44.317	< 2 ^{e-16} ***
	identity	Lychinis dry start PR	8	1.000	9.285	0.002319 **
	identity	Lychinis wet start PR	8	3.468	22.696	0.000238 ***
	identity	Plantago dry start PR	8	2.258	13.631	0.002141 **
	identity	Plantago wet start PR	8	3.563	17.391	0.001991 **
Protein	identity	Holcus dry start PR	8	1.789	16.156	0.000490 ***
	identity	Holcus wet start PR	8	4.062	20.543	0.001020 **
	identity	Phleum dry start PR	8	1.994	20.506	8.43 ^{e-05} ***
	identity	Phleum wet start PR	8	3.467	34.624	7.32 ^{e-07} ***
	identity	Lychinis dry start PR	8	4.299	14.603	0.005029 **
	identity	Lychinis wet start PR	8	2.087	5.106	0.146378
	identity	Plantago dry start PR	8	3.303	20.685	0.000227 ***

Chapter 3

Soluble sugar	identity	Plantago wet start PR	8	2.844	34.196	3.85 ^{e-07} ***
	identity	Holcus dry start PR	6	2.292	17.876	0.000722 ***
	identity	Holcus wet start PR	6	1.513	6.462	0.020698 *
	identity	Phleum dry start PR	6	1.000	15.760	7.17 ^{e-05} ***
	identity	Phleum wet start PR	6	2.137	59.990	< 2 ^{e-16} ***
	identity	Lychinis dry start PR	6	1.000	19.420	1.00 ^{e-05} ***
	identity	Lychinis wet start PR	6	1.366	26.393	1.82 ^{e-06} ***
	identity	Plantago dry start PR	6	2.181	37.760	< 2 ^{e-16} ***
	identity	Plantago wet start PR	6	3.563	82.231	< 2 ^{e-16} ***
Starch	identity	Holcus dry start PR	4	2.051	19.188	0.000197 ***
	identity	Holcus wet start PR	4	1.001	4.957	0.026015 *
	identity	Phleum dry start PR	4	1.001	27.158	2.01 ^{e-07} ***
	identity	Phleum wet start PR	4	1.244	70.821	< 2 ^{e-16} ***
	identity	Lychinis dry start PR	4	1.111	0.616	0.397918
	identity	Lychinis wet start PR	4	1.262	7.222	0.031294 *
	identity	Plantago dry start PR	4	1.646	13.932	0.000585 ***
	identity	Plantago wet start PR	4	2.720	16.572	0.000621 ***

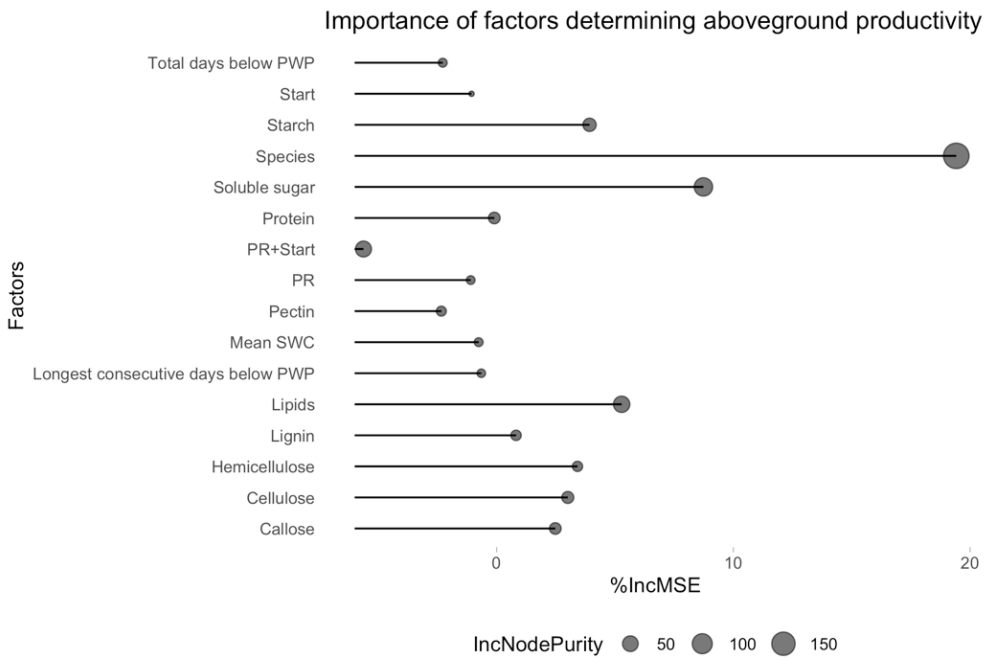


Figure S1 Results of random forest models indicating the percentage increase in the mean square error rate (%IncMSE) and the increase in node purity (IncNodePurity).

Chapter 4

Does previous exposure to extreme precipitation regimes result in acclimated grassland communities?

Published as: Reynaert, Simon, Lin Zi, Hamada AbdElgawad, Hans J. De Boeck, Olga Vindušková, Ivan Nijs, Gerrit Beemster, and Han Asard. 2022. "Does Previous Exposure to Extreme Precipitation Regimes Result in Acclimated Grassland Communities?" *Science of The Total Environment* 838 (February): 156368. <https://doi.org/10.1016/j.scitotenv.2022.156368>.

Simon Reynaert ^{a,1}, Lin Zi ^{b,1,*}, Hamada AbdElgawad ^{b,d}, Hans J. De Boeck ^a, Olga Vindušková ^{a,c}, Ivan Nijs ^a, Gerrit Beemster ^b, Han Asard ^b

a Plants and Ecosystems (PLECO), Department of Biology, University of Antwerp, B-2610 Wilrijk, Belgium

b Integrated Molecular Plant Physiology Research (IMPRES), Department of Biology, University of Antwerp, B-2020 Antwerp, Belgium

c Institute for Environmental Studies, Charles University, Prague 128 01, Czech Republic

d Botany and Microbiology Department, Faculty of Science, Beni-Suef University, Beni-Suef, 62511, Egypt

1 Shared first-author; * Corresponding author

For this chapter, L.Z performed biochemical and data analysis; L.Z and S.R wrote the manuscript as shared first authors.

Abstract

Climate change will likely increase weather persistence in the mid-latitudes, resulting in precipitation regimes (PR) with longer dry and wet periods compared to historic averages. This could affect terrestrial ecosystems substantially through the increased occurrence of repeated, prolonged drought and water logging conditions. Climate history is an important determinant of ecosystem responses to consecutive environmental extremes, through direct damage, community restructuring as well as morphological and physiological acclimation in species or individuals. However, it is unclear how community restructuring and individual metabolic acclimation effects interact to determine ecosystem responses to subsequent climate extremes. Here, we investigated, if and how, differences in exposure to extreme or historically normal PR induced long-lasting (i.e. legacy) effects at the level of community (e.g., species composition), plant (e.g., biomass), and molecular composition (e.g., sugars, lipids, stress markers). Experimental grassland communities were exposed to long (extreme) or short (historically normal) dry/wet cycles in year 1 (Y1), followed by exposure to an identical PR or the opposite PR in year 2 (Y2). Results indicate that exposure to extreme PR in Y1, reduced diversity but induced apparent acclimation effects in all climate scenarios, stimulating biomass (higher productivity and structural sugar content) in Y2. In contrast, plants pre-exposed to normal PR, showed more activated stress responses (higher proline and antioxidants) under extreme PR in Y2. Overall, Y1 acclimation effects were strongest in the dominant grasses, indicating comparatively high phenotypical plasticity. However, Y2 drought intensity also correlated with grass productivity and structural sugar findings, suggesting that responses to short-term soil water deficits contributed to the observed

patterns. Interactions between different legacy effects are discussed. We conclude that more extreme PR will likely alter diversity in the short-to midterm and select for acclimated grassland communities with increased productivity and attenuated molecular stress responses under future climate regimes.

1 Introduction

Climate change influences the intra-annual variability of precipitation patterns, including increased occurrence of precipitation regimes (PR) with both longer dry and longer wet periods in the mid-latitudes (Breinl et al. 2020; Pfliegerer et al. 2019). These changes will likely alter terrestrial ecosystems substantially by inducing prolonged environmental extremes (i.e., drought and waterlogging) more regularly compared to historic averages (Allan et al. 2020; Bardgett et al. 2013; Borke and Matzner 2009). This forces many species to rapidly adjust to novel conditions, often outside their phenotypical tolerance, or perish (Lambers 2015). The preceding range of climate conditions to which an ecosystem was subjected (i.e., climate history), plays an important role in shaping ecosystem responses to consecutive climate extremes, either through direct damage or by inducing some form of ‘ecological memory’ or ‘legacy effect’ (White et al. 2022; De Boeck, Bloor, et al. 2018; Harrison et al. 2018). Memory or legacy effects refer to carry-over effects that are still detectable in the ecosystem (on a community, plant or molecular level) after prolonged periods of time, and after the initial ‘driver’ that induced them is no longer present. In this context, the memory effect is the result of acclimation processes, that improve plant or ecosystem functioning under future stressors. For instance, there is accumulating evidence that the biomass production of formerly drought-stressed grasslands can even outperform non-stressed controls once drought stress is released (Schärer et al. 2023). However, the

diversity losses in grasslands following drought are often not recovered in subsequent years even when environmental conditions return to normal. This arises from intrinsic differences in species recovery characteristics and morphological/metabolic plasticity resulting in changes in community dynamics (e.g., competitive interactions) following the extreme(s) (De Boeck, Hiltbrunner, et al. 2018; Suttle et al. 2007; S. P. Harrison et al. 2018). However, it is not yet fully clear how interactions between direct damage caused by previous climate extremes, community restructuring and metabolic legacy effects (i.e., memory at the molecular level) together determine subsequent ecosystem responses to altered climate regimes.

When plant communities do not return to their original state following changes in PR, they may gradually adjust through community restructuring (i.e., loss of species or individuals through genotype filtering) (Engelbrecht et al. 2007; KARDOL et al. 2010) and acclimation in individual plants through phenotypic plasticity in morphology or metabolism (Becklin et al. 2016; Wellstein et al. 2017). For instance, extreme soil water depletion often filters out drought-sensitive species and selects for species with increased resistance to future droughts, thus reducing diversity but stabilizing key ecosystem processes such as, for example, productivity (De Boeck, Hiltbrunner, et al. 2018; Engelbrecht et al. 2007). This process, where primarily abiotic factors prevent the (re-)establishment or persistence of specific species (or species traits) in a particular environment, is known as 'environmental filtering' (Kraft et al. 2015; Woodward and Diament 1991). Per definition, the nature of biotic interactions also changes when species are added or removed from a community, making it difficult to fully attribute changes in community composition specifically to abiotic effects (Kraft et al. 2015). However, the principle of abiotic drivers pre-

dominantly shaping community assembly, can be more adequately tested in an experimental setting (Kraft et al. 2015; Grant et al. 2014). At the individual level, plants display a range of morphological, physiological and biochemical responses, which promote acclimation (i.e., improved functioning) to stressful environments (Buchanan et al. 2015). For instance, drought can affect stomatal morphogenesis to reduce transpiration (Onyemaobi et al. 2021) and stimulate root growth to facilitate water uptake (Farooq et al. 2009). In tandem, increased structural carbohydrate concentrations likely aid in maintaining cell wall integrity and cell wall turgor pressure (Le Gall et al. 2015), while higher concentrations of antioxidants (e.g., polyphenol) help alleviate oxidative stress (Chaudhry and Sidhu 2021), thus, facilitating continuous cell growth under drought. Conversely, flooding and soil anoxia stimulate the growth of aerenchyma and adventitious root formation at the soil surface, ensuring adequate oxygen supply to active plant tissues (Parent et al. 2008). These changes are accompanied by the maintenance of relatively high soluble sugar to generate ATP under anoxic conditions (H. Chen et al. 2005). In addition, osmotic adjustment keeps the plant water potential in balance by accumulating osmolytes such as proline and soluble sugar during climate extremes (Buchanan et al. 2015).

Whether subjection to climate extremes leads to metabolic acclimation (i.e., improved functioning) to following extremes, is species/community specific and depends on the intensity of the previous extreme event(s) (Jentsch et al. 2011; DeSoto et al. 2020; Grime et al. 2008). For example, mild drought stress could improve resistance to following water scarcity through accumulation of osmolytes, while severe drought stress, also removing the most resistant individuals, could reduce resistance to subsequent drought because of trade-

offs between resistance and recovery from direct damage (Hoover et al. 2014). Additionally, the stark contrasts in responses to prolonged drought versus prolonged periods of rainfall (and soil waterlogging) as predicted under increased weather persistence (Reynaert et al. 2021), may influence acclimation potential because long-term molecular level adaptation is likely driven by a multi-stage process involving integration of contrasting short-term responses (L. Song et al. 2022). Previous studies on metabolic acclimation to climate change have primarily focused on isolated drought (AbdElgawad et al. 2020; Menezes-Silva et al. 2017; Turner et al. 2001), high (Arora et al. 1998; Sabehat et al. 1998) or low temperatures (Sasaki et al. 1998), and (short-term) waterlogging (Phukan et al. 2016). Moreover, changes occurring at the molecular level have mostly been studied in isolated lab experiments on monocultures (C. Pinheiro and Chaves 2011; L. Zhang and Becker 2015). Therefore, the interactive effects of exposure to a history of altered precipitation regimes at multiple organizational levels of the ecosystem remain poorly understood. Hence, field studies investigating if and how PR history drives ecosystem response to altered PR regimes in multi-species assemblages, could elucidate how interactions between community restructuring and molecular acclimation effects drive ecosystem adaptation to climate change.

In this study, we investigated such potential interactions between reorganization of community structure and (molecular) acclimation in plants, resulting from exposure to a more uneven temporal distribution of equally sized rainfall events (i.e., extreme PR) compared to historic averages. The goal was to test for short- to midterm legacy (i.e., memory) effects resulting from predicted changes in intra-annual precipitation variability, i.e., weather persistence under global change (Breinl et al. 2020; Francis et al. 2020; Allan et

al. 2020). Experimental grassland communities were exposed to either long or short dry/wet (D/W) cycles in year 1 (2019), followed by exposure to an identical PR (i.e., short followed by short, or long followed by long) or to the opposite PR (i.e., short followed by long, or long followed by short) in year 2 (2020). Differences in PR were obtained by varying the duration of alternating D/W periods from 3-days consecutive dry and consecutive wet (3-day D/W) to 20-day D/W, while keeping total precipitation equal (Fig. 1). The central question was, if and how exposure to different precipitation regimes in Y1 followed by exposure to an identical PR or the opposite PR in Y2 influenced ecosystem functioning (productivity, species richness, community green cover and photosystem II efficiency) and plant metabolism (sugar, protein, lipid, proline and antioxidant content).

Because environmental filtering is thought to generally select for communities with phenotypical traits that are more suited to the abiotic conditions imposed by the particular climate regime (Cadotte and Tucker 2017; Kraft et al. 2015), we hypothesized that plant communities which were subjected to the same PR in Y2 versus Y1 would consistently outperform (in terms of productivity, richness stability, plant fitness) communities subjected to a different PR in Y2. Additionally, we expected different PR treatments to reflect different stages of the same long-term acclimation process, particularly at the molecular level (L. Song et al. 2022).

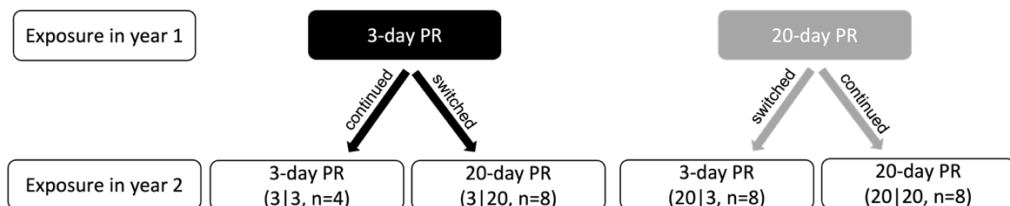


Fig.1: Overview of the precipitation regime (PR) switching experiment scheme to study the climate history effect. Mesocosms from the 3-day and 20-day PR in year 1 (Y1) were either

continued to be exposed to the same PR or were switched to another PR in year 2 (Y2). The 2-year PR is abbreviated as 'Y1/Y2' in brackets.

2 Methods & Materials

2.1 Experimental setup

The experiment was conducted at the Drie Eiken Campus of the University of Antwerp in Belgium (51°09'41"N, 04°24'9"E). The study site and experimental set-up have been described in detail in Reynaert et al. (2021). In short, 256 grassland mesocosms were distributed across eight experimental units (32 mesocosms per unit). Each experimental unit was equipped with a rain screen, automatically covering plants during rain periods, and automatic irrigation to mimic any rainfall regime (including different regimes within a single unit). The mesocosms (50 cm depth and 30 cm diameter) were filled with sandy-loam soil with a pH between 7.0 and 7.2. The field capacity (FC) of the soil was estimated at $0.26 \text{ m}^3 \text{ m}^{-3}$ and the permanent wilting point (PWP) at $0.05 \text{ m}^3 \text{ m}^{-3}$. Three individuals of 12 common perennial temperate grassland species were planted in each mesocosm. Seeds were first sown in separate seedling containers per species early April 2019, followed by transplantation into the mesocosms in the first week of May 2019 (Reynaert et al. 2021). These C3 species were planted in order to maximize interspecies interactions and covered 3 functional groups: 6 grasses (*Agrostis capillaris* L. (AC), *Anthoxanthum odoratum* L. (AO), *Deschampsia cespitosa* (L.) P. Beauv. (DC), *Phleum pratense* L. (PHP), *Poa pratensis* L. (POP), *Holcus lanatus* L. (HL)); 3 N-fixing forbs (N-fixers) (*Lotus corniculatus* L. (LC), *Trifolium pratense* L. (TP), *Trifolium medium* L. TM); and 3 non-N-fixing forbs (*Centaurea jacea* L. (CJ), *Lychnis flos-cuculi* L. (SF), *Plantago lanceolata* L. (PL)). The non-N-fixing forbs are referred to as 'forbs' from here on. We made sure the canopy was fully closed, indicating that all species had

adequately recovered from transplanting and settled before the start of the PR treatments (Reynaert et al. 2021).

From July 2, 2019, to June 25, 2020 (360 days; referred to as year 1), mesocosms were subjected to a gradient of 8 PRs, with alternating dry/wet (D/W) periods of 1, 3, 6, 10, 15, 20, 30 and 60 consecutive wet and dry days (referred to as '1-day PR', '3-day PR', etc.). As watering cycles can start with either a wet or dry period, we exposed half of the mesocosms to a wet start, and the other half to a dry start. In all treatments, a wet day received a single irrigation dose between 10:30 am and 11:00 am with 6.87 L m^{-2} water automatically applied through drippers, while a dry day received no water. This volume is 1.5 times the daily Belgian average, to account for additional evapotranspiration in the mesocosms compared to field conditions (De Boeck et al. 2006). At the end of Y1, all regimes had received the same number of irrigation days (180) and the same total water amount added (1236 L m^{-2}). To compensate for the lack of a seedbank in our mesocosms, we applied a homogenous seed rain containing equal seed contributions (92 per species per pot or >1000 per species per m^2) of all original species in the beginning of October of Y1.

From June 26, 2020, to October 23, 2020 (120 days; referred to as year 2), the 3-day PR and 20-day PR were selected as the 'short' and 'long' D/W cycles, respectively, to study climate history effects. We selected these treatments because the 3-day PR closely resembles historical Belgian weather and the 20-day PR significantly affected plant communities in comparable ways (i.e., the same species were lost) during Y1, without resulting in complete diversity collapse (Reynaert et al. 2021). Communities with a 3-day cycle history included 8 mesocosms from the 3-day wet-start treatment and 4 mesocosms from the

3-day dry-start treatment (12 total). Communities with a 20-day cycle history included 12 mesocosms from the 20-day wet-start treatment and 4 mesocosms from the 20-day dry-start treatment (16 total). The difference in the total number of replicates between the 3-day and 20-day PR resulted from an irrigation malfunction in one of the plots in the winter of Y1 causing the flooding of the plot and loss of some mesocosms.

We tested for differences between Y1 dry and wet start in both the 3-day and the 20-day regimes utilizing different LMMs (family = gaussian, link = identity), including all measured parameters on both community and functional group level as response variable, climate history (3-day/20-day with dry or wet start), functional group and their interaction as explanatory variables and plot as random effect, both at the start (June) and end (October) of the Y2 part of the experiment. Both at the start and end of the experiment, these models did not indicate any significant differences between dry and wet start treatments, except for the aboveground biomass of N-fixers with a 20-day history in October 2020 (Fig. S1) and the lipid content of N-fixers with a 20-day history in October 2020. Therefore, we maximized the number of replicates by considering mesocosms only differing in dry/wet start of Y1 to have the same climate history, knowing that this may slightly affect the interpretation of N-fixer results for biomass and lipids in mesocosms with a 20-day cycle history.

The pool of 12 mesocosms previously exposed to the 3-day PR (Y1) was split into 2 groups: 4 replicates continued to be exposed to the 3-day PR (indicated as 'Y1|Y2': 3|3), and the other 8 replicates were switched to the 20-day PR (3|20) during Y2 (Fig. 1). The 16 mesocosms exposed to the 20-day PR in Y1, were likewise split into 2 equally sized groups, and either continued to be exposed to the 20-day PR (20|20) or were switched to a 3-day PR (20|3) in Y2

(Fig. 1). Because we did not have enough replicates to incorporate dry/wet start differences in the Y2 experiment, we synchronized the timings of dry and wet spells by starting Y2 with a wet period in all PR. Total precipitation amounts per day and individual event sizes remained the same as in Y1.

2.2 Microclimate measurements

Over the course of the experiment, volumetric soil water content (SWC) averaged across 0-30 cm soil depth, and soil surface temperature, were logged automatically in 2 to 4 mesocosms per PR every half-hour by a CS650-DS Reflectometer (Campbell® Scientific INC., Logan, Utah, USA). Averaging the measurements from these sensors, we calculated SWC and soil surface temperature trajectories across the growing season for each PR (Fig. S2). Following Vicca et al. (Vicca et al. 2012), drought intensity (I_s) over the growing season of Y2 was then calculated by assigning a soil moisture stress threshold, at relative extractable water of 0.4, and calculating a cumulative sum of daily deficits below this threshold per PR (Van Sundert et al. 2021). To this end, we first calculated the maximum and daily total extractable water (TEW) over 30 cm depth (sensor depth):

$$TEW_{\max} (\%) = SWC_{FC} (\%) - SWC_{PWP} (\%);$$

$$TEW_{\text{day}} (\%) = SWC_{\text{day}} (\%) - SWC_{PWP} (\%);$$

with FC the field capacity and PWP the permanent wilting point.

The relative extractable water (REW) was then determined as $REW_{\text{day}} = TEW_{\text{day}} / TEW_{\max}$, ultimately yielding the drought intensity at daily and seasonal basis:

$$I_{s, \text{day}} = 0.4 - REW_{\text{day}} \text{ if } REW_{\text{day}} < 0.4; I_{s, \text{day}} = 0 \text{ if } REW_{\text{day}} > 0.4;$$

$$I_{s, \text{growing season}} = \sum I_{s, \text{first day of experiment}} + \dots + I_{s, \text{last day of experiment}}.$$

Photosynthetically active radiation (PAR) was also logged every 10 minutes at 2 m height in vicinity of the plots, utilizing a SKP215 Quantum Sensor (Campbell® Scientific INC., Logan, Utah, USA). Hourly values for temperature (T) and relative humidity (RH) were collected at 1.5 m height from a nearby weather station in Woensdrecht, The Netherlands. These values were further utilized to calculate average monthly vapor pressure deficit (VPD) during sunshine hours.

In each mesocosm, we visually estimated the fraction of green cover viewed from above (hereafter: canopy greenness) to the closest 5% on a weekly basis, as an indicator of plant stress and survival. Additionally, we measured chlorophyll fluorescence (F_v/F_m) in three replicates per PR every month, with a Plant Efficiency Analyser (Hansatech Ltd, King's Lynn, UK), as an indicator of photosystem II efficiency on a random green leaf of a random individual of every species per mesocosm. When none of the leaves of all the individuals of a species had any green color anymore, a zero record was assigned for F_v/F_m . Species presence was also recorded in all mesocosms once a month throughout the experiment, from which species richness was derived. When none of the individuals of a species had any green parts left, it was considered absent (i.e., zero in the presence/absence matrix). We thus used the F_v/F_m values (which also hold info about the presence or absence of species) in combination with species richness data to obtain species richness trajectories over the growing season, with a temporal resolution of approximately two weeks.

Before the start (between June 24, and June 25, 2020) and at the end of Y2 of the experiment (between October 26, and October 27, 2020), all standing biomass above 4.5 cm was cut and pooled in paper bags per functional group (grasses, non-N-fixing forbs, N-fixers) per mesocosm. Materials were oven-

dried at 70 °C for >72 h and weighed. To determine dry weights, we subtracted the average weight of 10 oven-dried empty bags. Additionally, samples for root biomass were collected at the end of Y2 using a Kopecky ring at the soil surface (0-5 cm) and at the 20-30 depth. In each layer, four rings were combined in a composite sample. Of these four rings, two were taken randomly from the inner part of the pot and two from the outer part in order to represent the total root biomass of the sampled layer. Samples were stored at 4°C until further processing. After being washed over a 1 mm sieve, all roots were collected, dried at 40°C and weighed.

2.3 Biochemical measurements

To understand the effects of PR history at the plant molecular level, we determined changes in major macromolecular components (structural sugars, proteins, lipids), as well as molecules involved in plant stress responses (non-structural sugars, proline, polyphenols, flavonoids) on a composite biomass sample per functional group at the end of Y2.

To determine the non-structural sugar content, 50 mg dry shoot tissue was extracted with 2 mL of 80% ethanol at room temperature. After centrifugation at 14000 rpm for 10 min, the soluble sugar content was determined using the anthrone reagent (Leyva et al. 2008), with glucose as a standard, and absorbance measured at 620 nm (Synergy Mx spectrophotometer, BIOTEK, Winooski, USA). To estimate starch content, the residue obtained after centrifugation at 14000 rpm for 10 min was digested with α -amylase (Sigma-Aldrich, EC 3.2.1.1) and amyloglucosidase (Sigma-Aldrich, EC 3.2.1.3) to hydrolyze sugar polymers and re-measure soluble sugars (Macrae 1971). The sum of soluble sugar and starch content represents the total non-structural sugar level. After removal of soluble sugars and starch, the remaining residue

was incubated with 1 mL 0.2 M H₂SO₄ for 2 hours at 90 °C to digest the left-over structural sugars. After centrifugation, the supernatant reacted with freshly prepared anthrone reagent (Leyva et al. 2008), and glucose was used as the reference to estimate sugar concentrations.

Another aliquot of 50 mg dry shoot tissue was used to extract total lipids, by applying a liquid-liquid extraction method with a mixture of chloroform, methanol and water (5:10:1 V/V/V). The extracted lipids were determined by gravimetric analysis and expressed as weight (g) per dry weight (g) of plant sample (Phillips et al. 1997).

To determine total protein content, 50 mg dry shoot tissue was incubated in 1 mL 0.1 M NaOH at 60 °C overnight to extract proteins. Protein content was measured in the supernatant after centrifugation at 14000 rpm for 10 min according to the Lowry method (LOWRY et al. 1951). After reaction with the biuret reagent and Folin-Ciocalteu reagent, absorption was measured at 750 nm. Bovine Serum Albumin (BSA) was used as the standard.

Proline content was measured by incubating 50 mg dry shoot tissue with 2 mL 3% aqueous sulfosalicylic acid at room temperature. The extraction was used to measure proline content by the ninhydrin colorimetric method (Bates et al. 1973). The amount of proline was calculated based on a standard curve, and absorbance was measured at 520 nm.

Polyphenols and flavonoids were extracted from 50 mg dry shoot tissue with 2 mL of 80% ethanol at room temperature. Total polyphenol content was analyzed using the Folin-Ciocalteu reagent method (Velioglu et al. 1998), with gallic acid as a standard (absorption was measured at 725 nm). The total flavonoid content was determined using the aluminum chloride colorimetric

assay (Kamal 2011), with quercetin as a standard (absorption was measured at 415 nm).

2.4 Statistical analysis

All statistical analyses were performed in R (version 4.0.4). Significance was assumed for p-values < 0.05. Graphs and figures were created utilizing the packages dplyr (Wickham et al. 2023) and ggplot2 (Wickham 2016). Linear mixed effect models (LMM's) were created with the package nlme (J. Pinheiro et al. 2018) and two-by-two differences were further explored utilizing the emmeans package (Lenth et al. 2018) with TukeyHSD post-hoc tests to correct for multiple testing. Residual plots and Shapiro-Wilk tests were utilized to check for approximate residual normality and homogeneity of variance. No data transformations were required to meet model assumptions.

To explore effects of climate history on community biomass production (above and belowground) under different PR's, we performed analysis of variance (ANOVA) on two LMM's (family = gaussian, link = identity) with community biomass as response variable, PR of Y1 (3 or 20), PR of Y2 (3 or 20) and their interaction as explanatory variables, and historical dry/wet start differences and plot as random effects. We then performed ANOVA on a second LMM (family = gaussian, link = identity) to test for differences in functional group standing biomass production. Here, model terms included biomass as response variable, PR of Y1 (3 or 20), PR of Y2 (3 or 20), functional group and their interactions as explanatory variables, and historical dry/wet start differences and plot as random effects. We applied the same analysis at functional group level utilizing different LMM's for each biochemical parameter.

Next, since soil water status was not equal at the start of the experiment for all PRs, we further explored the observed productivity responses by performing ANOVA on two different LMM's testing for the effect of average drought intensity over the Y2 growing season on total and functional group biomass or structural sugar content, respectively. Finally, we explored temporal differences in community responses (green cover, Fv/Fm and richness) by performing repeated measures ANOVA or pairwise t-tests where appropriate.

3 Results

3.1 Acclimation effects in productivity and species composition

Climate history had a significant effect on community productivity, by primarily influencing grass aboveground biomass production (Fig. 2a, b; Table S1). Communities which switched from 20-day PR in Y1, to 3-day PR in Y2 (20|3), produced more standing biomass over the course of the season compared to the continued 3-day PR treatment (3|3, $p = 0.01$). In contrast, for 3-day PR treatments that switched to 20-day PR (3|20), no strong differences were observed with the continued 20-day PR treatment (20|20), although the data tentatively suggests an opposite trend (with switched treatments producing slightly less biomass on average, $p = 0.26$). The response pattern observed at the community level originated from the grasses, while significant differences between PR history groups were absent in forbs and N-fixers. The belowground root biomass and soil C/N comparisons did not indicate any significant differences at either depth (0-5 cm vs 20-30 cm) (Fig. S3 & S4), although root biomass in the topsoil layer showed similar trends to aboveground community biomass. Together, these data indicate that, indeed, PR of the previous year,

may affect primarily the aboveground biomass production of grass communities in the subsequent year by imposing a legacy effect.

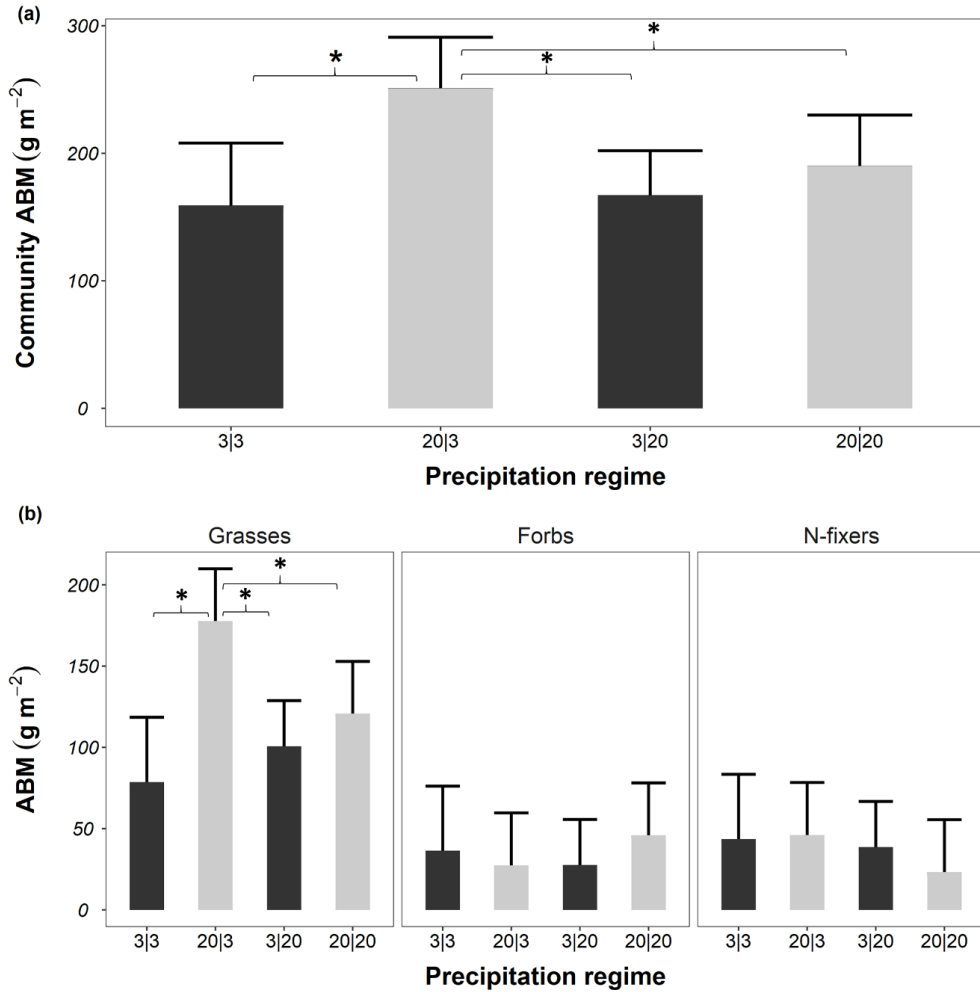


Fig. 2. Effects of precipitation regime in Y1 and Y2 on aboveground biomass. Aboveground biomass (ABM) at the end of Y2 (a: community, b: functional group) given by the LMM's testing for effects of climate history on biomass production. The error bars indicate 95% confidence intervals. Dark- and light-grey bars indicate that plants were subjected to the 3-day PR or 20-day PR in Y1, respectively. Asterisks depict significant two-by-two differences with Tukey HSD correction ("*": $p < 0.05$). The 2-year PR is abbreviated as 'Y1|Y2'. The number of replicates: 3|3 $N=4$, 20|3 $N=8$, 3|20 $N=8$ and 20|20 $N=8$.

However, aboveground biomass trends were also affected by drought intensity in year 2. Community biomass decreased significantly with increasing drought intensity over the growing season ($R^2 = 0.20$, $p = 0.009$; Fig. 3a), mostly because

grass biomass production responded negatively to decreases in mean soil water availability (Fig. 3b; effect size = -1.595, 95% CI = [-2.43, -0.761], $p < 0.001$). Mesocosms with short PR climate histories (3|3 and 3|20), experienced intermediate drought in Y2 while mesocosms with long PR climate history experienced the least (20|3) or most (20|20) drought stress in Y2 (Fig. 3; Fig. S2), indicating that ecosystems with an extreme PR history were influenced comparatively more by differences in PR during Y2.

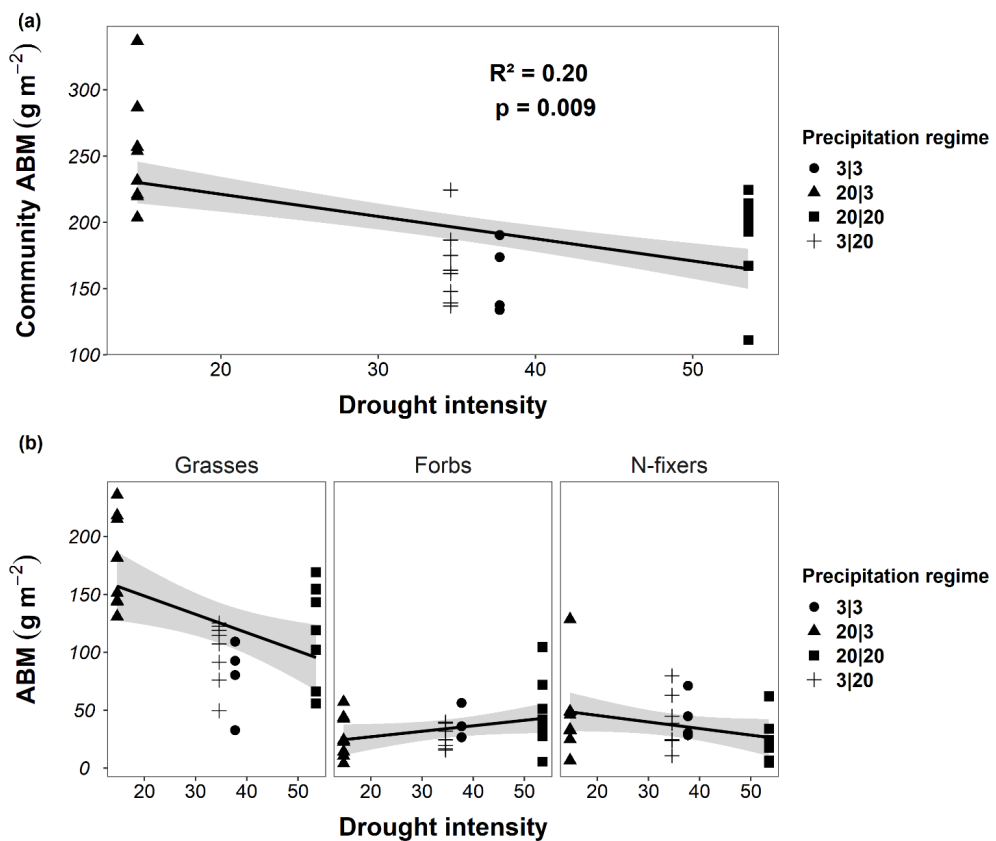


Fig. 3. Estimated relationships between end-of-season aboveground biomass (ABM) (a: community, b: functional group) and drought intensity over the growing season of Y2. Cumulative drought intensity was calculated at relative extractable water (REW) of 0.4. For full explanation on how we calculated drought intensity, see methods section 3.3. Shaded areas indicate ± 1 SE on the mean. Only the community and grasses trends were significant. The 2-year PR is abbreviated as 'Y1|Y2'. The number of replicates: 3|3 N=4, 20|3 N=8, 3|20 N=8 and 20|20 N=8.

Next, we investigated whether climate history had an influence on community composition and ecological stress responses to altered PR in Y2, as this might further explain the observed biomass responses. At the end of year 1, communities with a 3-day PR history still contained all species, while communities with a 20-day PR history had lost some of the most drought-sensitive species (i.e., forbs and N-fixers). Because the species composition did not change significantly anymore in any of the treatments after the start of Y2 (DOY = 178), we expressed it as species richness for ease of representation (Fig. S5; Table S2). With all communities retaining the richness at the end of Y1, the 20|20 and 20|3 PRs (with 20-day PR history) exhibited similar, lower species richness compared to the 3|3 and 3|20 PRs (with 3-day PR history) over the entire Y2 growing season on average (Fig. S5; Table S2). In general, no consistent differences were found between 3-day and 20-day Y2 PR treatments in terms of community F_v/F_m in Y2 (Fig. S6a, b), indicating that there were no large observable signs of PS II downregulation related to the PR in any of the treatments in Y2. However, in terms of community greenness, 20|3 communities were least stressed on average, and 20|20 communities the most, affirming the drought intensity trends (Fig. 3; Fig. S5a). The high temperatures, low humidity and high vapor pressure deficit in August (DOY 214 – 244; Table S3), seemed to only negatively affect the green cover of 3|3, 3|20 20|20 and community F_v/F_m of 20|3 (Fig. S6a, b).

3.2 Acclimation effects in plant macromolecular composition and stress-metabolism

3.2.1 Structural sugars, lipids and proteins

Similar to aboveground biomass, PR history had a significant effect on structural sugars in grasses. Grasses which switched from 20-day PR to 3-day

PR (20|3), accumulated more structural sugar over the course of the season compared to the continued 3-day PR treatment (3|3, $p < 0.05$, Fig. 4a; Table S4). Y1 PR did not induce statistically significant effects on structural sugars in forbs and N-fixers. Nevertheless, in these functional groups, a 20-day PR in Y1 (20|3 and 20|20) tended to result in slightly higher structural sugar levels, compared to the ones with 3-day PR in Y1 (3|3 and 3|20, Fig. 4a). As for the effect of Y2 PR, grasses that had 20-day PR history showed higher structural sugar when subjected to 3-day PR in Y2 (20|3) than the group subject to 20-day PR in Y2 (20|20, $p < 0.01$, Fig. 4a; Table S5), while N-fixers showed the opposite trend ($p < 0.05$, Fig. 4a; Table S5). The relationship between structural sugars and drought intensity was also estimated. In line with the biomass data (Fig. 3b), the structural sugars of grasses were negatively correlated with drought intensity (Fig. S7; effect size = -0.006; $p < 0.001$).

The Y1 PR history did not induce any significant effects on total lipids of each functional group, while PR in Y2 significantly affected the lipids levels (Fig. 4b; Table S4). For all functional groups, the groups that had 20-day PR history, showed higher lipid levels when subjected to 3-day PR in Y2 (20|3), compared to a 20-day PR in Y2 (20|20; $p < 0.01$; Fig. 4b; Table S5). Regarding proteins, neither the PR in Y1, nor that of Y2, caused significant changes in either functional group (Fig. 4c; Table S4).

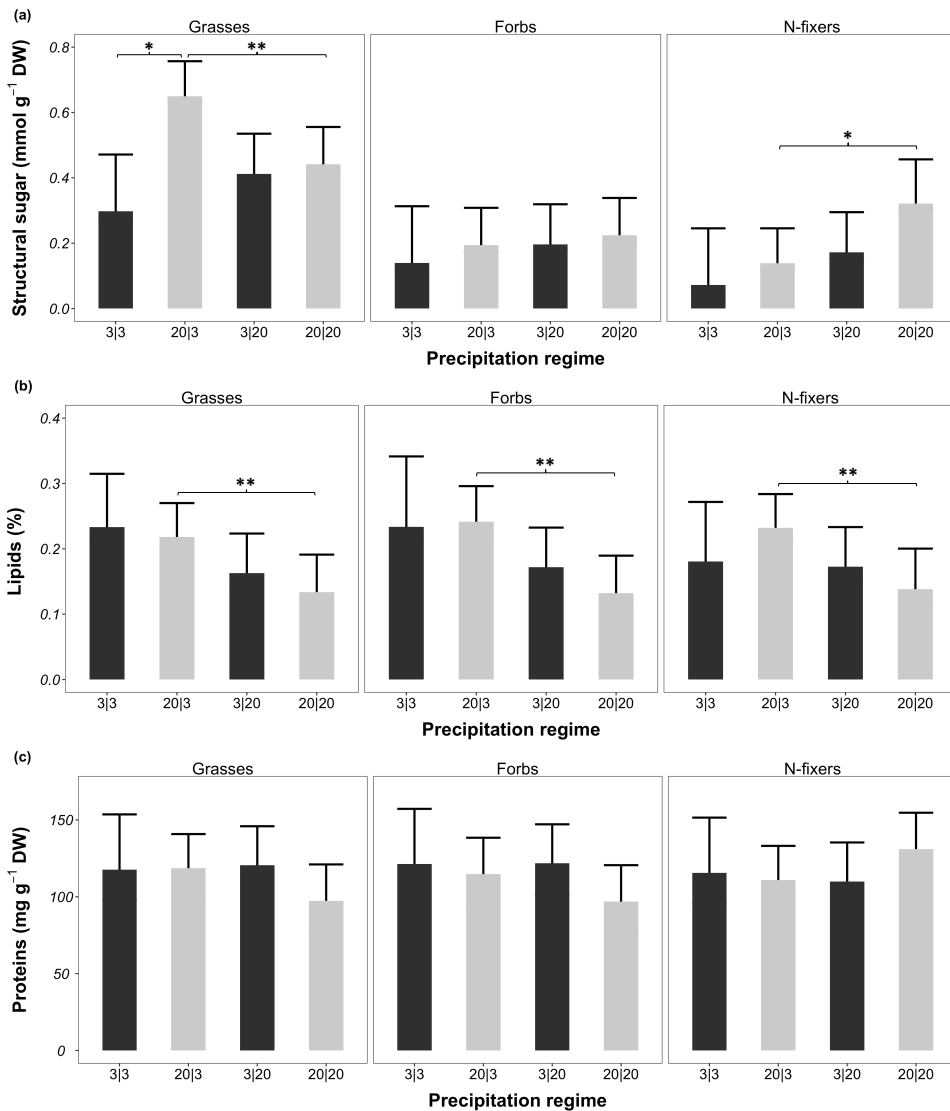


Fig. 4. Effects of precipitation regime in Y1 and Y2 on plant macromolecular components. Structural sugar (a), lipid (b), protein (c) levels per gram dry weight (DW) given by the LMM's testing for effects of climate history on plant macromolecular components. The error bars indicate 95% confidence intervals. Dark- and light-grey bars indicate that the plants were subjected to the 3-day PR or 20-day PR in Y1, respectively. Asterisks depict significant two-by-two differences with Tukey HSD correction ("*": $p < 0.05$; "***": $p < 0.01$). The 2-year PR is abbreviated as 'Y1|Y2'. The number of replicates: 3|3 N=4, 20|3 N=8, 3|20 N=8 and 20|20 N=8.

3.2.2 Non-structural sugars

Regarding the non-structural sugars level, when under the same PR in Y2, the grasses with 3-day PR history accumulated more non-structural sugars

compared to the grasses that with 20-day PR history ($p = 0.07$ under 3-day PR in Y2; $p < 0.05$ under 20-day PR in Y2; Fig. 5; Table S5). Forbs followed the same pattern as grasses, but the differences were not significant ($p = 0.23$ under 3-day PR in Y2; $p = 0.13$ under 20-day PR in Y2; Fig. 5; Table S5). Non-structural sugars of grasses and forbs were also affected by Y2 PR. The groups that were under short PR in Y2 exhibited higher non-structural sugars than the groups under long PR in Y2 (Fig. 5, Table S4). No significant differences were observed in N-fixers.

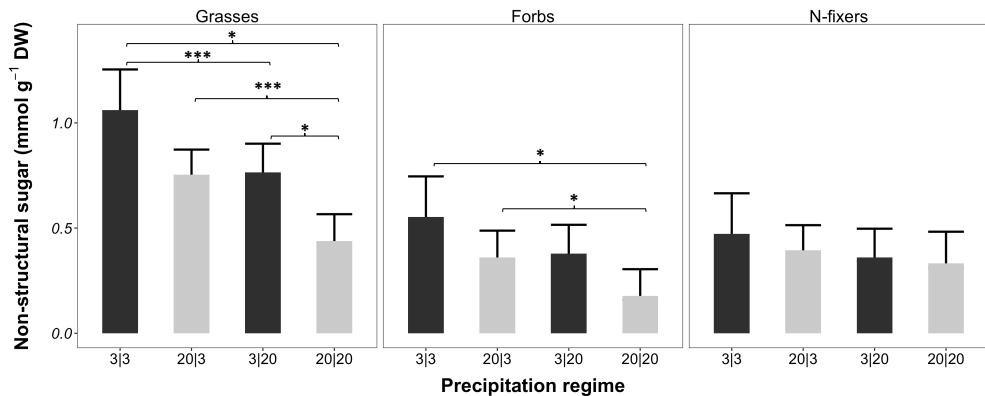


Fig 5. Effects of precipitation regime in Y1 and Y2 on plant non-structural sugars. Non-structural sugar levels per gram dry weight (DW) given by the LMM's testing for effects of climate history. The error bars indicate 95% confidence intervals. Dark- and light-grey bars indicate that the plants were subjected to the 3-day PR or 20-day PR in Y1, respectively. Asterisks depict significant two-by-two differences with Tukey HSD correction ("*": $p < 0.05$; "**": $p < 0.01$; "***": $p < 0.001$). The 2-year PR is abbreviated as 'Y1|Y2'. The number of replicates: 3|3 N=4, 20|3 N=8, 3|20 N=8 and 20|20 N=8.

3.2.3 Proline

Proline levels were on average higher in Y1 treatments with 3-day PR ($p = 0.043$), but there were no significant differences within functional groups (Fig. 6; Table S4). However, in all functional groups, for plants under long PR in Y2, the plants with a 3-day PR history (3|20) showed a tendency to accumulate more proline compared to plants with the 20-day PR history (20|20; Fig. 6; grasses: $p = 0.32$; forbs: $p = 0.14$; N-fixers: $p = 0.17$; Table S5).

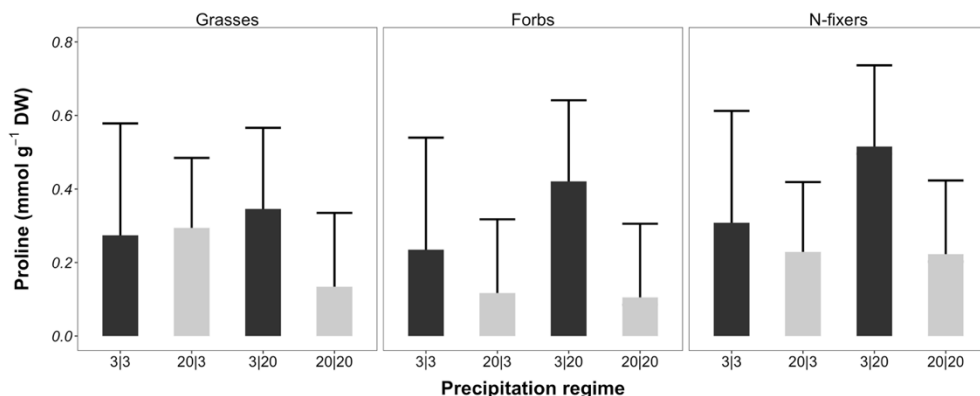


Fig 6. Effects of precipitation regime in Y1 and Y2 on plant proline. Proline levels per gram dry weight (DW) given by the LMM's testing for effects of climate history. The error bars indicate 95% confidence intervals. Dark- and light-grey bars indicate that the plants were subjected to the 3-day PR or 20-day PR in Y1, respectively. Two-by-two differences are tested by Tukey HSD correction. The 2-year PR is abbreviated as 'Y1|Y2'. The number of replicates: 3|3 N=4, 20|3 N=8, 3|20 N=8 and 20|20 N=8.

3.2.4 Polyphenols and flavonoids

For grasses, neither Y1 nor Y2 PR induced significant differences in polyphenols or flavonoids (Fig. 7; Table S5). In forbs, when both under long PR in Y2, plants with 3-day PR history (3|20) showed a tendency for higher polyphenols and flavonoids compared with the forbs that had a 20-day PR history (20|20; Fig. 7; polyphenols: $p = 0.11$; flavonoids: $p = 0.08$; Table S5). This pattern is similar to the changes in non-structural sugars (Fig. 5) and proline (Fig. 6). As for the effect of Y2 PR, forbs that had 3-day PR history exhibited higher polyphenols and flavonoids when under 20-day PR in Y2 (3|20) than the forbs under 3-day PR in Y2 (3|3; Fig. 7; polyphenols: $p < 0.05$; flavonoids: $p < 0.01$). For N-fixers, Y1 PR did not induce significant differences on polyphenols and flavonoids, while the long PR in Y2 stimulated more polyphenols than the short PR in Y2 (Fig. 7; $p < 0.05$).

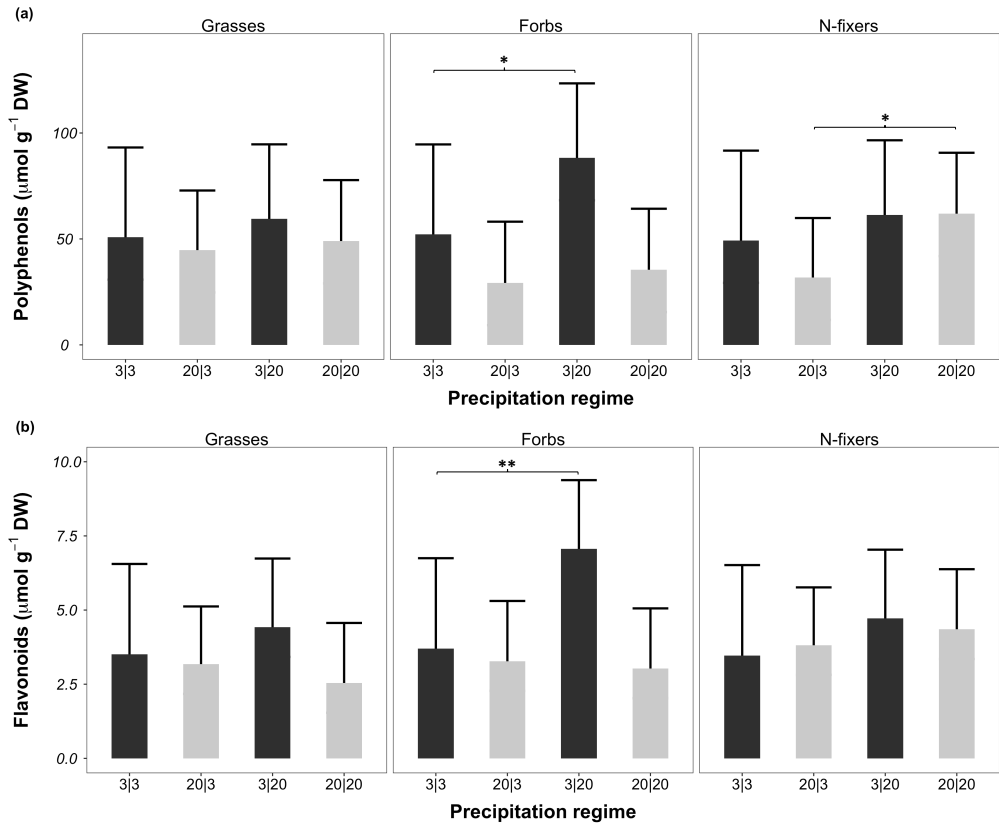


Fig 7. Effects of precipitation regime in Y1 and Y2 on plant polyphenols and flavonoids. Polyphenols (a) and flavonoids (b) levels per gram dry weight (DW) given by the LMM's testing for effects of climate history. The error bars indicate 95% confidence intervals. Dark- and light-grey bars indicate that the plants were subjected to the 3-day PR or 20-day PR in Y1, respectively. Asterisks depict significant two-by-two differences with Tukey HSD correction ("*": $p < 0.05$; "***": $p < 0.01$). The 2-year PR is abbreviated as 'Y1|Y2'. The number of replicates: 3|3 N=4, 20|3 N=8, 3|20 N=8 and 20|20 N=8.

4 Discussion

One understudied aspect of climate change is the increase in weather persistence leading to PR with longer wet and dry spells compared to historic averages (Pfleiderer et al. 2019; Francis et al. 2020). We explored to what extent such climate changes in any given year could affect plant and community properties the following year and induce historical legacy effects (Jentsch et al. 2011; Craven et al. 2018; 2016). Specifically, we investigated how exposure to

either extreme or to historically normal precipitation regimes could make grassland communities more or less vulnerable to precipitation extremes the subsequent year. By combining observations at the community level and plant macromolecular level, we tried to identify plausible mechanisms that drive the PR impact and allow ecosystem acclimation to an altered climate.

In general, we found that a history of extreme PR during Y1 appears to induce acclimation effects in these plant communities. This was apparent by persistently reduced plant diversity (Fig. S5), stimulated aboveground productivity (Fig. 2) and reduced intensity of molecular stress responses in Y2 (Fig. 5). By the end of Y2, communities with an extreme PR history in Y1 (i.e., 20|3 and 20|20), showed increased aboveground biomass (Fig. 5), higher contents of macromolecular components (Fig. 4a) and lower molecular stress levels (Fig. 5) compared to communities where rainfall had been historically normal in the previous year (3|3, 3|20). The aboveground productivity responses seemed primarily related to PR differences in Y1 and were driven by the grasses (Fig. 3). Although not significant, communities with extreme PR history had a slightly higher root biomass (Fig. S3), which may imply an ongoing morphological acclimation process. Overall, little evidence was found for legacy effects in response to periods of prolonged rainfall. These findings are in line with other climate extreme studies, indicating that previous exposure to extreme PR with longer droughts can induce above- and belowground ecosystem acclimation in temperate mesic grasslands, leading to stabilization or improvement of (aboveground) productivity in the short-to midterm (De Boeck, Hiltbrunner, et al. 2018; Jentsch et al. 2011; S. Harrison et al. 2020).

4.1 Acclimation effects in community structure

The lack of species composition changes in any of the PR treatments during Y2, contrasts with our hypothesis that switched communities would have reduced stability in terms of community structure. The Y1 diversity losses (loss of non-N-fixing forbs and N-fixers) under longer summer drought reported in Reynaert et al. (2021) were not compensated for, despite application of the seed rain. In line with other studies, this resulted in a persistent legacy effect of more grass-dominated communities with lower species richness in ecosystems with an extreme PR history compared to ecosystems with a historically normal PR history (De Boeck, Hiltbrunner, et al. 2018; S. P. Harrison et al. 2018). The lack of SWC decline below permanent wilting point in Y2, which was the main driver of diversity loss in Y1; Reynaert et al. (2021), may have precluded species losses in the unfiltered, more diverse mesocosms with a 3-day PR history when exposed to the 20-day PR (3 | 20) in the following year (Fig. S2 & S5). Additionally, temperatures and VPD (vapor pressure deficit) were generally less extreme during the Y2 summer months, compared to Y1 (Table S3). Hence, in contrast to Y1, the absence of extreme abiotic conditions may have resulted in systems where responses are better predicted by a drought index related to mean soil water availability across the entire growth season (i.e., drought intensity), rather than indices focusing on temporal differences in resource distribution (i.e., persistence of drought). This decoupling of plant survival responses from PR dynamics is reflected in the lack of extreme responses to temporal fluctuations in soil water availability for both green cover and F_v/F_m (Fig. S5 & S6). However, it is also possible that 1-year-old established plant communities are generally less sensitive to perturbations in PR, i.e., independent of their rainfall history. Established plants may, for instance, be more deep rooting (P.

Li et al. 2020; H. Liu et al. 2018) or have better-developed plant-soil networks (Radujković et al. 2020) leading to improved drought resistance (J. Li et al. 2019) and limited changes in their performance under environmental fluctuations.

4.2 Acclimation effects in productivity and stress-metabolism

The biomass changes in these ecosystems, driven by the PR of the previous year, could result from the persistent historical PR differences in species composition as well as from changes in species performance, or both (Felton and Smith 2017; S. Harrison et al. 2020). Additionally, soil legacy properties in terms of microbial community, water and nutrient availability, should be taken into account (Jentsch et al. 2011).

In line with previous studies, the observed inverse relationship between productivity and diversity could be related to environmental filtering to more drought resistant/resilient species (S. Harrison et al. 2020; De Boeck, Bloor, et al. 2018) in combination with competitive release of highly productive species under extreme PR (Kraft et al. 2015; Hallett et al. 2019). Indeed, only the dominant grasses, which made up a larger proportion of individuals in the 20-day PR history ecosystems, were affected by differences in drought intensity during Y2. This indicates that they can rapidly respond to changes in the environment, likely because of comparatively high phenotypical plasticity (Troelstra and Berendse 1982; Van Sundert et al. 2021; Zeiter et al. 2016). In addition, differences in the ‘spikiness’ of SWC curves (Fig. S2) suggest that species in historically ‘filtered’ ecosystems (i.e., 20|20 and 20|3), used to more extreme temporal variation in water availability, take up added (irrigation) water more rapidly than their unfiltered counterparts (Stampfli et al. 2018). Moreover, given that the total administered precipitation amounts were equal for all communities in Y2, the difference in end-of-season productivity

responses could indicate that filtered ecosystems also had the highest water-to-biomass conversion efficiency (water-use efficiency). However, the realized effects of increases in water-use efficiency on end-of-season biomass do not only depend on total water supply but also on the temporal dynamics of actual soil water content, since water becomes increasingly difficult to extract from drier soils (Gardner 1965; Jentsch et al. 2011; Vicca et al. 2012). In that regard, although 20|20 also showed a tendency to accumulate more biomass compared to 3|20, the correlation between drought index and plant productivity could suggest that the 'climate legacy effect' in aboveground plant productivity may primarily have been caused by differences in soil water status and community composition at the start of Y2, cascading throughout temporal soil water dynamics in the following months. Given these uncertainties, observations at the (macro)-molecular level may further clarify realized acclimation effects related to plant and community performance.

First, differences in structural sugar accumulation further affirm that a history of extreme PR may increase aboveground productivity through stimulation of long-term structural sugar accumulation, which is central to cell growth and reproduction, particularly in grasses (Fig. 4a). However, other macromolecular components measured here, namely lipids and proteins, were unaffected by PR history at the functional group level. These two groups of molecules carry out a wide range of functions, and their synthesis and degradation are adjusted rapidly in response to fluctuating environments (Obata 2019). Therefore, lipids and proteins may more likely reflect short-term responses instead of historical imprints. Indeed, the extreme PR in Y2 significantly decreased the lipid contents of all three functional groups (Fig. 4b), which may be due to higher Y2 drought intensity in the continued 20-day PR (20|20) compared to the switched 3-day

PR (20|3). This is consistent with previous studies, which reported that higher temperatures and drought decreased lipid contents in *Leymus chinensis* and soybean (Damatta et al. 2010; Z. Z. Xu and Zhou 2006).

In addition, reduced molecular stress responses may indicate that plants are able to grow better under a given PR, since the synthesis of defensive molecules is energy intensive, and regulated by the trade-off between growth and defense due to carbon limitation (Bolton 2009). However, because plant defenses against abiotic stresses are orchestrated by complex regulatory networks (He et al. 2018), it can be expected that the molecular acclimation process to altered PR involves several stages, complicating interpretation of effects. When plants were exposed to extreme PR for the first time and/or short time (3|20), they showed a tendency to accumulate more stress-responsive osmoregulation metabolites such as proline, and increased antioxidants (e.g., polyphenols, flavonoids) compared to the plants that were exposed to normal PR (3|3; Fig. 6,7) (Weng 2014; Tugizimana et al. 2018). This is in line with previous studies suggesting that an increase of proline, polyphenols and flavonoids plays a critical role in acclimation to various abiotic stresses (Abdelgawad et al. 2015; Parida et al. 2007; Khedr et al. 2003). Specifically, the increased contents of polyphenols and flavonoids were more evident in forbs compared to grasses and N-fixers (Fig. 7), implying that the stimulation of antioxidants is an important strategy of forbs in response to climate extremes. This is supported by previous phytochemical studies, which have shown that the forbs *Plantago* and *Centaurea* have considerable antioxidant synthesis capability (Tugizimana et al. 2018), and some *Plantago* species are even considered as medicinal plants for this reason (Lukova et al. 2017).

After 480 days (Y1 + Y2) of exposure to extreme PR (20|20), plants exhibited less contents of defensive molecules (e.g., non-structural sugars, proline, polyphenols and flavonoids; Fig. 5;6;7) compared with plants that had pre-exposure to normal PR (3|20). Given that these effects contrast with the short-term drought intensity trend in these communities, they are the most convincing evidence for realized molecular level acclimation. These observations possibly reflect the different stages of molecular plant acclimation in response to altered PR (L. Song et al. 2022). In the beginning of exposure to extreme PR (acclimation stage A, which is ongoing for the group 3|20), the production of anti-stress molecules would be stimulated. Simultaneously, other longer-term acclimation mechanisms such as epigenetic modifications and/or chromatin remodeling may improve plant functioning under extreme PR (Bruce et al. 2007; Jacques et al. 2021; van Loon 2016), resulting in gradually more acclimated plants. In a later stage, the contents of the protective components may then reduce back to a 'normal' level (stage B, which happened in 20|20). This could help to allocate more energy and resources to plant primary metabolism such as structural sugar accumulation, thus facilitating constant growth, which eventually results in a higher biomass of grasses. These findings are in line with Song et al. (2022), who recently suggested that after the short-term plastic responses under drought (phase A), non-structural sugars decline with increasing aridity (phase B) until they reach a vulnerable threshold.

Finally, differences in available soil nutrients (particularly N, P, K) and/or soil microbial communities related to historical PR may also have contributed to the observed responses (Jentsch et al. 2011). Although end-of-season soil CN ratios did not differ (Fig. S4), regimes with longer droughts could have induced stronger birch-effects upon rewetting (Van Sundert et al. 2020), leading to

potentially higher nutrient supply at the start of Y2 in extreme regimes. In that case, increased nutrient availability under historically extreme PR could not only have boosted productivity, but also explain the differences in molecular stress responses as more available soil nutrients may lower observable plant stress (da Silva et al. 2011). Additionally, several studies have indicated that differences in soil microbial community can improve plant resistance to recurring drought (J. Li et al. 2019). However, data on soil nutrients and microbiota at the start of Y2 were not available.

4.3 Interactions between acclimation effects

In contrast to the generality implied by the environmental filtering hypothesis, we did not find that communities with previous exposure to a historically normal rainfall pattern outperformed their extreme PR history counterparts under mutual subjection to ‘normal’ regimes in Y2, rather, we observed the opposite. This could indicate that climate change acclimation in mesic plant communities driven by changes in rainfall regimes only occurs when the community restructures (Suttle et al. 2007), although the short timescale of the experiment may have resulted in ecosystems that have not yet reached a steady state in which plants are optimally acclimated to their given climate regime (White et al. 2021). In fact, all acclimation processes outlined in this study should be considered initial, short- to midterm responses to recent changes in precipitation regimes. Nonetheless, this link between diversity changes and acclimation effects is in line with most other studies (Grant et al. 2014; S. Harrison 2020; Grime et al. 2008).

Integrating these observations, we propose a conceptual model outlining how interactive effects at multiple organizational levels of the ecosystem may lead to improved ecosystem functioning (i.e. increased productivity and reduced

stress response) in temperate mesic grasslands previously subjected to extreme PR (Fig. 8). When soil water fluctuations become extreme under altered PR (Reynaert et al. 2021), it is reasonable to assume that some species with low stress tolerance (e.g., *Lychnis flos-cuculi*) disappear through environmental filtering (and/or shifts in community dynamics), selecting for less diverse yet more stress resistant communities (e.g., with increased belowground C investment, different plant drought tolerance strategies, etc.)(Felton and Smith 2017). This community restructuring could lead to changes of the overall molecular composition of functional groups and result in increased water-use efficiency of the community. Simultaneously, metabolic stress acclimation in surviving individuals and/or species likely also improves plant functioning, leading to higher C-to-biomass allocation due to reduced investment in stress metabolism under environmental fluctuations. Hence, PR changes which induce community restructuring and observable short- to midterm metabolic acclimation effects may select for more stress-resistant plant communities with improved ecosystem functioning (in terms of productivity) under future precipitation regimes.

However, interactions between long(er) and short-term responses to changes in PR at multiple levels of the ecosystem complicate attribution to species-level acclimation within the studied plant communities. The visible differences at the molecular level (particularly non-structural sugars in 3|20 vs 20|20) within functional groups that did not change in diversity over the entirety of the experiment (i.e., grasses), suggest that at least part of the observed productivity response is attributable to phenotypical plasticity (i.e., priming effects) within species and/or individuals leading to long(er)-term metabolic legacy effects that fundamentally altered plant functioning. Nonetheless, shifts

in species richness and/or relative species composition (e.g., species that survive but that produce very little biomass), may have also led to a higher contribution to total biomass by species that acclimated better under extreme climate regimes (Jentsch et al. 2011; Song et al. 2022). In combination with short-term drought effects and potential nutrient or microbial differences, this could have resulted in similar observations at the molecular level. Hence, future monoculture studies on the same species used in this experiment could further elucidate long-lasting molecular acclimation effects to altered PR at the species level.

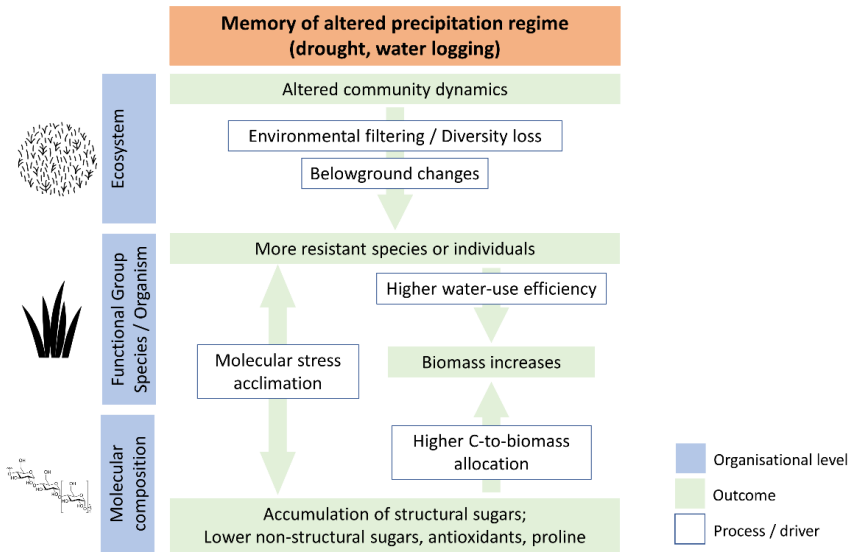


Fig. 8. Conceptual diagram indicating how the memory of exposure to altered (extreme) PR may affect different organizational levels of the ecosystem, leading to improved ecosystem functioning (i.e., increased productivity and reduced stress responses) in a future climate.

5 Conclusion

We demonstrated that previous subjection to more extreme precipitation regimes may result in acclimated grassland communities during the following year with altered diversity but improved stress responses and increased aboveground productivity under future climate extremes. Our findings indicate

that such short- to midterm ecosystem adjustment to changes in precipitation regimes is orchestrated by the interaction of short vs long(er) term acclimation processes influencing multiple organizational levels of the ecosystem simultaneously (Felton and Smith 2017). However, despite the clear link between diversity changes and molecular acclimation effects, it is difficult to fully attribute molecular level responses to particular species within functional groups. Hence, future studies should focus on elucidating acclimation processes in species and individuals within plant communities, to better understand the relative importance of different processes driving ecosystem adaptation to global change.

6 Supplementary

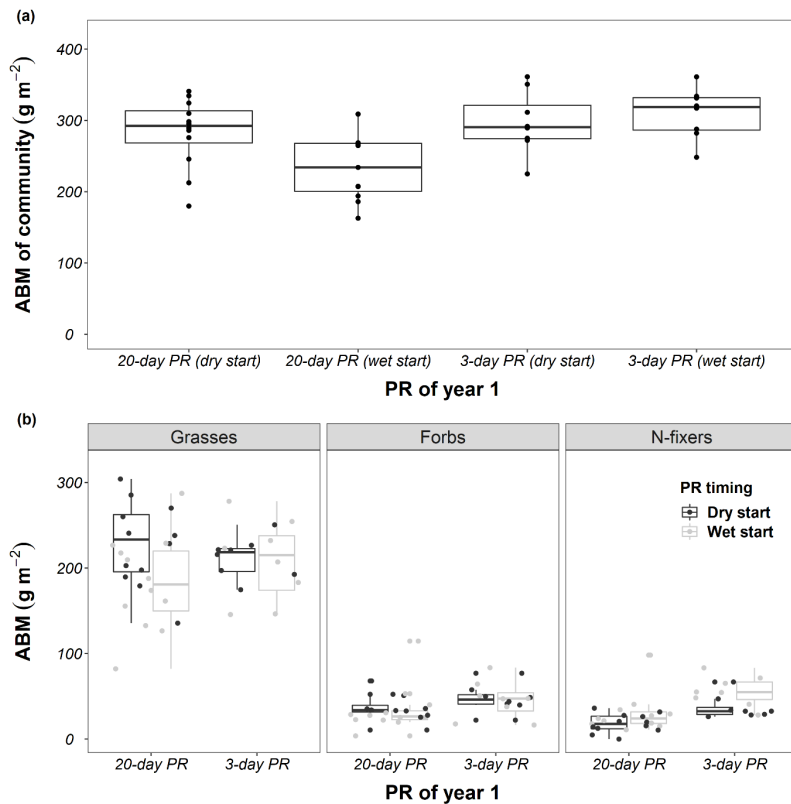


Fig. S1 Aboveground biomass (ABM) at the end of year 1 (DOY = 177) for (a) the community and (b) per functional group. Precipitation regime is abbreviated by 'PR'. PR treatments with a dry or wet start are indicated in dark grey or light grey, respectively. No significant differences were found between historical PR treatments in terms of aboveground biomass.

Table S1. Results from ANOVAs testing the effects of precipitation regime of year 1, year 2 and their interaction on plant community biomass and the effects of precipitation regime of year 1, precipitation regime of year 2, functional group and their interactions on biomass of the functional groups, root biomass (0-5 cm and 20-30 cm) and soil C/N (0-5 cm and 20-30 cm).

Model	Effect	F - test	p - value
Biomass of the Community	Precipitation regime (PR) of Y1	F (1, 3) = 17.18	0.0260
	PR of Y2	F (1, 21) = 5.94	0.0238
	PR of Y1 x PR of Y2	F (1, 21) = 6.07	0.0225
Biomass of the functional groups	PR of Y1	F (1, 3) = 8.87	0.060
	PR of Y2	F (1, 69) = 3.07	0.084
	Functional group	F (2, 69) = 91.68	<0.001
	PR of Y1 x PR of Y2	F (1, 69) = 3.14	0.08
	PR of Y1 x Functional group	F (2, 69) = 8.88	<0.001
	PR of Y2 x Functional group	F (2, 69) = 2.34	0.104
	PR of Y1 x PR of Y2 x Functional group	F (2, 69) = 5.57	0.006
Root biomass at 0-5 cm layer	PR of Y1	F (1, 3) = 2.46122	0.2147
	PR of Y2	F (1, 16) = 0.01898	0.8921
	PR of Y1 x PR of Y2	F (1, 16) = 0.00488	0.9452
Root biomass at 20-30 cm layer	PR of Y1	F (1, 3) = 3.20242	0.1715
	PR of Y2	F (1, 15) = 0.06097	0.8083
	PR of Y1 x PR of Y2	F (1, 15) = 1.34417	0.2644
C/N at 0-5 cm layer	PR of Y1	F (1, 2) = 1.0308	0.4168
	PR of Y2	F (1, 14) = 1.5969	0.2270
	PR of Y1 x PR of Y2	F (1, 2) = 0.4415	0.5747
C/N at 20-30 cm layer	PR of Y1	F (1, 3) = 0.9254	0.4070
	PR of Y2	F (1, 17) = 0.0117	0.9153
	PR of Y1 x PR of Y2	F (1, 17) = 0.3009	0.5905

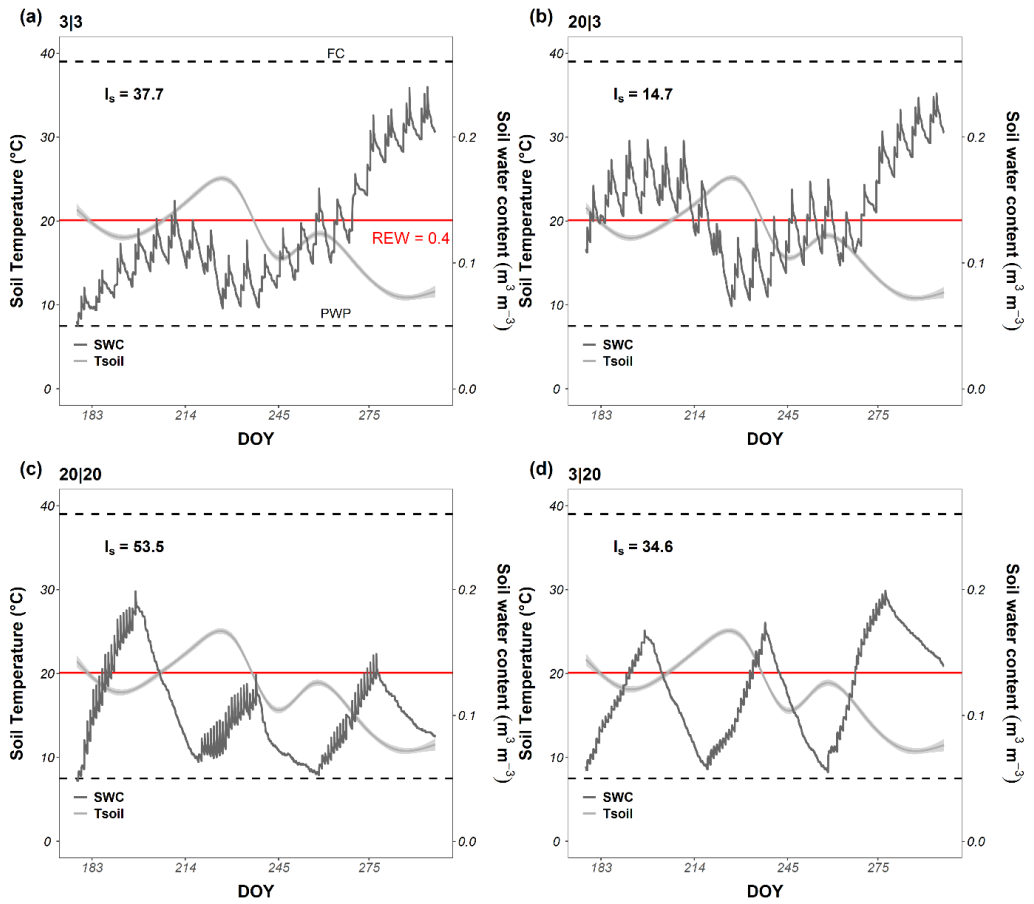


Fig. S2. Volumetric soil water content (dark grey) and soil surface temperature (light grey) trajectories over the course of year 2 per treatment (a: 3|3, b: 20|3, c: 20|20, d: 3|20). The soil surface temperature graph has been smoothed with the standard “loess”- fit +/- 1 SE in ggplot2 for clarity. The dashed lines highlight the permanent wilting point (PWP) and field capacity (FC). The drought threshold at relative extractable water (REW) of 0.4 is indicated in red and cumulative drought intensity is abbreviated by I_s. Soil water and soil surface temperature are abbreviated by SWC (dark grey) and Tsoil (light grey), respectively.

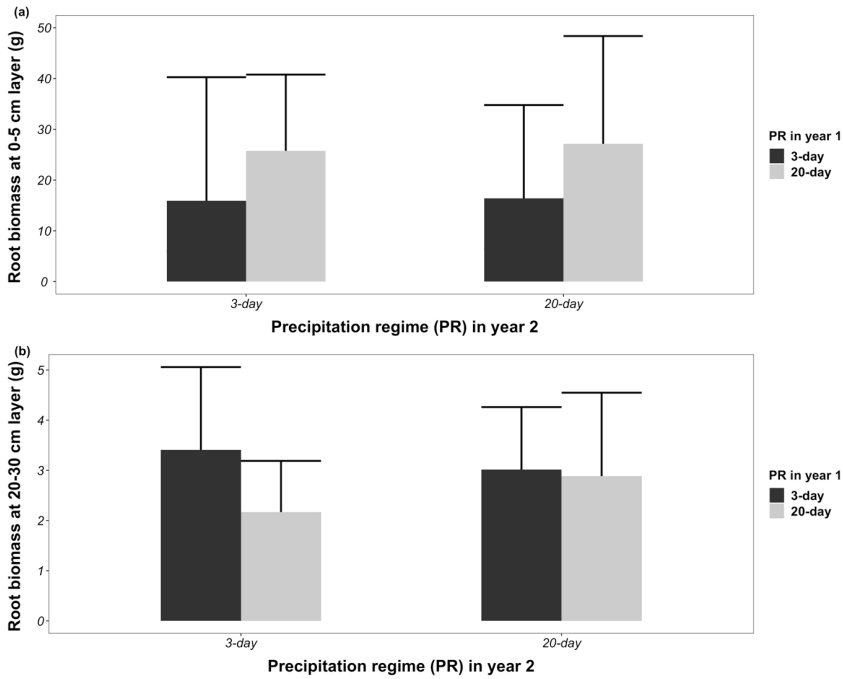


Fig. S3. Effects of precipitation regime in year 1 and year 2 on root biomass. Root biomass at top layer (a), bottom layer (b) and approximate 95% CI's given by the LMM's testing for effects of climate history. Dark- and light-grey bars indicate that the plants were subjected to the 3-day PR or 20-day PR in year 1, respectively.

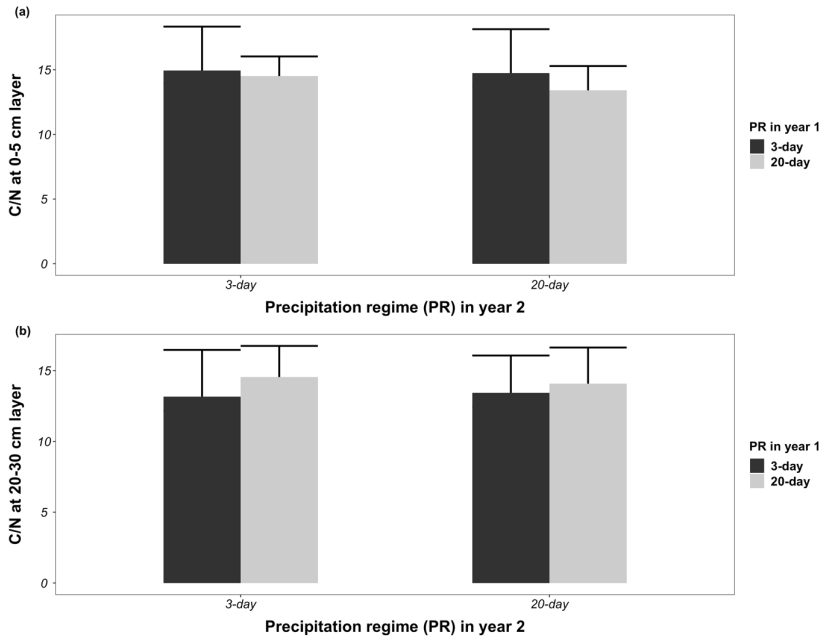


Fig. S4. Effects of precipitation regime in year 1 and year 2 on C/N. C/N at 0-5 cm layer of soil (a), 20-30 cm layer of soil (b) and approximate 95% CI's given by the LMM's testing for effects of climate history. Dark- and light-grey bars indicate that the plants were subjected to the 3-day PR or 20-day PR in year 1, respectively.

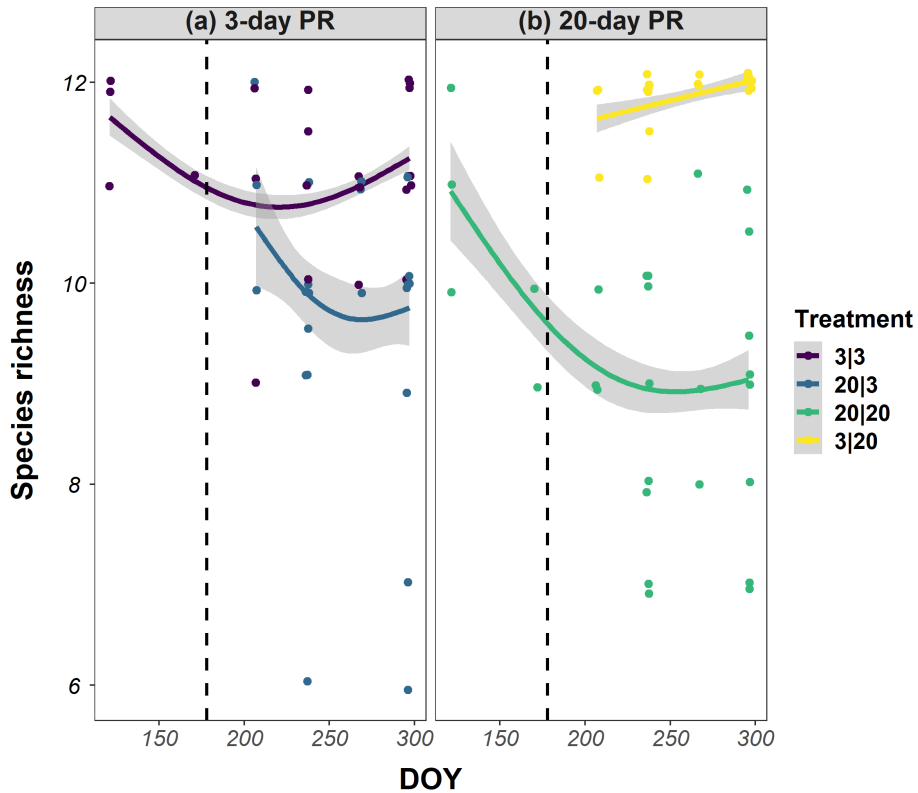


Fig. S5. Evolution of species richness over time in year 1 (DOY 121 - 177) and year 2 (DOY 178 - 297) in ecosystems subjected to (a) 3-day PR during Y1 and (b) 20-day PR during Y1. The dashed line indicates the start of the year 2 (DOY = 178). Full lines are gam smoother functions as specified in ggplot2 (3 knots), to correct for variation in sample size between points in time (see methods 3.2). Shaded areas represent +/- 1 SE on the mean. Day of the year is abbreviated by DOY.

Table S2. P-values of t-tests comparing the average richness between treatments at the end of August 2020 and the end of October 2020. Significant differences are highlighted in bold. These time-points were the only two timepoints where richness in all replicates of all treatments was assessed, hence allowing the best comparison of average richness per treatment. The table confirms the trends of Figure S5, indicating that 20|20 and 20|3 have the same lower diversity compared to 3|3 and 3|20, which also have the same diversity.

	24/08/2020			22/10/2020		
	3 20	20 3	20 20	3 20	20 3	20 20
3 3	0.4	0.03	0.009	0.29	0.03	0.006
3 20		0.003	<0.001		0.004	<0.001
20 3			0.54			0.55

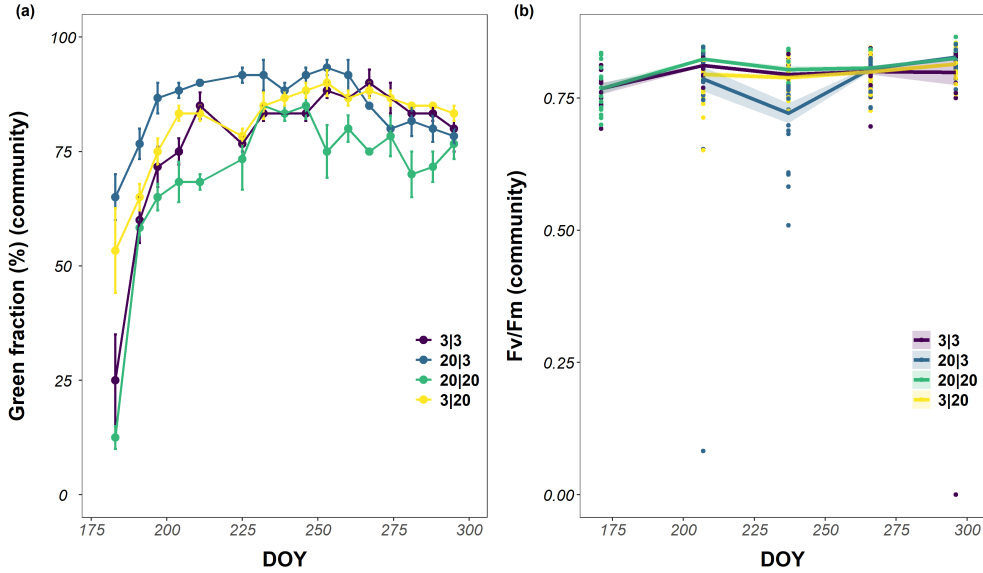


Fig. S6. Evolution of community green fraction and F_v/F_m in year 2 of the experiment. Error bars and shaded areas represent ± 1 SE on the mean. Day of the year is abbreviated by DOY.

Table S3. Monthly averages of daily mean, maximum and minimum air temperature (T_{air}), and relative humidity and vapour pressure deficit (VPD) during sunshine hours for each month in Y2 of the experiment (26th June 2020- 27th October 2020). The long-term T averages (1981-2010) are given in parentheses.

Month	T_{air} mean (°C)	T_{air} max. (°C)	T_{air} min. (°C)	Relative humidity (%)	VPD (kPa)
July	18.4 (18.5)	23.6 (23.2)	13.3 (13.8)	65.8	0.91
August	21.5 (18.2)	28.0 (23.1)	15.9 (13.2)	62.3	1.34
September	16.7 (15.1)	23.0 (19.7)	11.4 (10.6)	64.4	0.92
October	12.1 (11.3)	15.7 (15.3)	9.5 (7.4)	77.4	0.36

Table S4. Results from ANOVAs testing the effects of precipitation regime of year 1, precipitation regime of year 2, functional group and their interactions on metabolic changes. Significant effects ($p < 0.05$) are indicated in bold.

Model	Effect	F - test	p - value
Structural sugar	PR of Y1	F (1, 3) = 16.7543	0.0264
	PR of Y2	F (1, 63) = 2.1558	0.1470
	Functional group	F (2, 63) = 60.5153	<0.001
	PR of Y1 x PR of Y2	F (1, 63) = 3.9011	0.0526
	PR of Y1 x Functional group	F (2, 63) = 3.2079	0.0471
	PR of Y2 x Functional group	F (2, 63) = 5.8409	0.0047
	PR of Y1 x PR of Y2 x Functional group	F (2, 63) = 5.5901	0.0058
Lipids	PR of Y1	F (1, 3) = 0.1825	0.6981
	PR of Y2	F (1, 58) = 39.1261	<0.001
	Functional group	F (2, 58) = 0.3219	0.7261
	PR of Y1 x PR of Y2	F (1, 58) = 3.9063	0.0529
	PR of Y1 x Functional group	F (2, 58) = 0.2616	0.7707
	PR of Y2 x Functional group	F (2, 58) = 0.6687	0.5163
	PR of Y1 x PR of Y2 x Functional group	F (2, 58) = 0.9064	0.4096
Proteins	PR of Y1	F (1, 3) = 1.3617	0.3276
	PR of Y2	F (1, 65) = 0.5989	0.4418
	Functional group	F (2, 65) = 0.1862	0.8305
	PR of Y1 x PR of Y2	F (1, 65) = 0.2765	0.6008
	PR of Y1 x Functional group	F (2, 65) = 2.1071	0.1298
	PR of Y2 x Functional group	F (2, 65) = 1.6638	0.1974
	PR of Y1 x PR of Y2 x Functional group	F (2, 65) = 2.2538	0.1131
Non-structural sugars	PR of Y1	F (1, 3) = 25.2254	0.0152
	PR of Y2	F (1, 63) = 47.2307	<0.001
	Functional group	F (2, 63) = 80.6276	<0.001
	PR of Y1 x PR of Y2	F (1, 63) = 0.0126	0.9108
	PR of Y1 x Functional group	F (2, 63) = 5.0847	0.0090
	PR of Y2 x Functional group	F (2, 63) = 5.2499	0.0078
	PR of Y1 x PR of Y2 x Functional group	F (2, 63) = 0.1394	0.8701
Proline	PR of Y1	F (1, 3) = 11.28542	0.0438
	PR of Y2	F (1, 65) = 0.56562	0.4547

Chapter 4

	Functional group	F (2, 65) = 2.29595	0.1088
	PR of Y1 x PR of Y2	F (1, 65) = 6.03069	0.0167
	PR of Y1 x Functional group	F (2, 65) = 1.29427	0.2811
	PR of Y2 x Functional group	F (2, 65) = 1.38742	0.2570
	PR of Y1 x PR of Y2 x Functional group	F (2, 65) = 0.01509	0.9850
Polyphenols	PR of Y1	F (1, 3) = 3.37793	0.1634
	PR of Y2	F (1, 65) = 9.82254	0.0026
	Functional group	F (2, 65) = 0.02571	0.9746
	PR of Y1 x PR of Y2	F (1, 65) = 0.28806	0.5933
	PR of Y1 x Functional group	F (2, 65) = 7.15929	0.0015
	PR of Y2 x Functional group	F (2, 65) = 1.40122	0.2536
	PR of Y1 x PR of Y2 x Functional group	F (2, 65) = 2.55653	0.0854
Flavonoids	PR of Y1	F (1, 3) = 4.69268	0.1189
	PR of Y2	F (1, 65) = 3.38666	0.0703
	Functional group	F (2, 65) = 2.77936	0.0695
	PR of Y1 x PR of Y2	F (1, 65) = 5.47460	0.0224
	PR of Y1 x Functional group	F (2, 65) = 4.26890	0.0181
	PR of Y2 x Functional group	F (2, 65) = 1.04010	0.3592
	PR of Y1 x PR of Y2 x Functional group	F (2, 65) = 1.33932	0.2692

Table S5. Adjusted *P*-values of pairwise comparison between different precipitation regimes (year 1|year 2) within (a) community biomass responses (b) grasses, (c) forbs, (d) N-fixers using Tukey's HSD method. Significant differences are indicated in bold.

(a) Community	20 20 - 3 20	20 20 - 20 3	20 20 - 3 3	3 20 - 20 3	3 20 - 3 3	20 3 - 3 3
Standing biomass	0.2867	0.0024	0.2184	0.0098	0.9081	0.0241

(b) Grasses	20 20 - 3 20	20 20 - 20 3	20 20 - 3 3	3 20 - 20 3	3 20 - 3 3	20 3 - 3 3
Standing biomass	0.5770	0.0009	0.2573	0.0374	0.5967	0.0328
Structural sugar	0.9510	0.0025	0.3264	0.0654	0.3246	0.0395
Lipids	0.7472	0.0072	0.1583	0.3321	0.0684	0.9598
Non-structural sugar	0.0411	<.0001	0.0115	0.9976	0.0009	0.0747
Proline	0.3233	0.3268	0.6838	0.9468	0.9123	0.9978

Chapter 4

Polyphenols	0.8945	0.9782	0.9995	0.7708	0.8845	0.9813
Flavonoids	0.4084	0.8876	0.8497	0.6515	0.8024	0.9908

(c) Forbs	20 20 - 3 20	20 20 - 20 3	20 20 - 3 3	3 20 - 20 3	3 20 - 3 3	20 3 - 3 3
Standing biomass	0.6264	0.5705	0.9427	1.0000	0.9427	0.9505
Structural sugar	0.9566	0.9542	0.6504	1.0000	0.8298	0.8548
Lipids	0.5697	0.0004	0.2262	0.2261	0.3206	0.9963
Non-structural sugar	0.1376	0.0298	0.0471	0.9895	0.0970	0.2307
Proline	0.1436	0.9993	0.7196	0.1567	0.3321	0.7666
Polyphenols	0.1140	0.9391	0.7653	0.0873	0.0179	0.5941
Flavonoids	0.0858	0.9927	0.9383	0.1004	0.0076	0.9823

(d) N-fixers	20 20 - 3 20	20 20 - 20 3	20 20 - 3 3	3 20 - 20 3	3 20 - 3 3	20 3 - 3 3
Standing biomass	0.7267	0.3868	0.6846	0.9474	0.9917	0.9988
Structural sugar	0.2565	0.0233	0.1201	0.9197	0.4425	0.7635
Lipids	0.6794	0.0038	0.6829	0.2946	0.9940	0.5307
Non-structural sugar	0.9735	0.8005	0.4447	0.9367	0.4341	0.7404
Proline	0.1696	0.9999	0.8869	0.1673	0.2354	0.9006
Polyphenols	1.0000	0.0292	0.8738	0.3610	0.7401	0.7392
Flavonoids	0.9817	0.9297	0.8792	0.8116	0.6054	0.9896

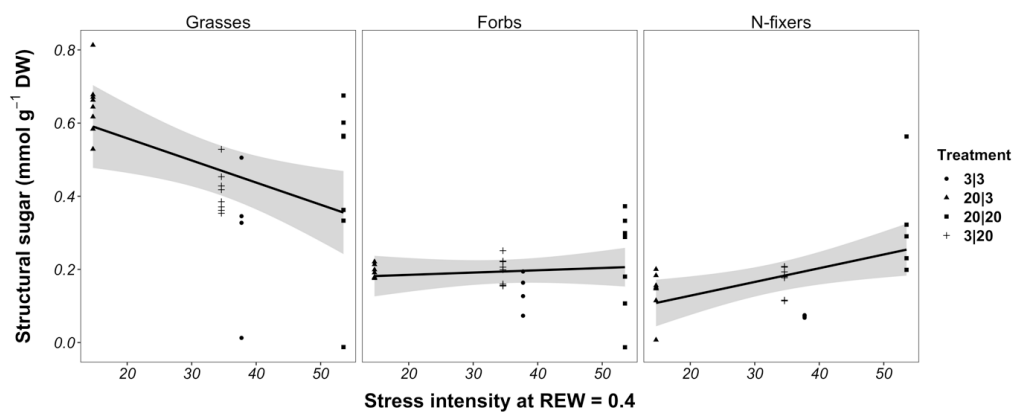


Fig. S7. Estimated relationships between structural sugar levels of each functional group and cumulative stress intensity over the growing season of year 2. Cumulative stress intensity was calculated at relative extractable water (REW) of 0.4. Shaded areas indicate ± 1 SE on the mean. Drought intensity during Y2 only had a significant effect on the structural sugars composition of grasses.

Chapter 5

Soil microbiome legacy shifts cell wall composition and hormonal response to more persistent precipitation regimes across multiple northern European grassland species

Lin Zi^{a,1}, Chase Donnelly^{b,1}, Lingjuan Li^c, Bart Cuypers^b, Kris Laukens^b, Erik Verbruggen^c, Els Prinsen^a, Han Asard^a, Gerrit Beemster^a, Hamada AbdElgawad^a

a Integrated Molecular Plant Physiology Research (IMPRES), Department of Biology, University of Antwerp, B-2020 Antwerp, Belgium

b Adrem Data Lab (Adrem), Department of Computer Science, University of Antwerp, B-2020 Antwerp, Belgium

c Plants and Ecosystems (PLECO), Department of Biology, University of Antwerp, B-2610 Wilrijk, Belgium

1 Shared first co-authors

For this chapter, L.Z performed the experiment, physiological and biochemical analysis; C.D carried out the transcriptomic analysis with the help of L.Z. L.Z and C.D wrote the manuscript together.

Abstract

Climate change is leading to more persistent precipitation regimes (PRs) featuring prolonged dry and wet periods. Exposure to more persistent PRs affects soil microbial communities, but how this affects plant responses to future PRs is largely unknown. We exposed grassland mesocosms to either a historical normal PR (1-day wet/dry cycle) or a persistent PR (30-day wet/dry cycle) for 120 days. Next, the conditioned soil became the inoculum to study the effect of soil history on the growth response of four grassland species: *Holcus lanatus*, *Phleum pratense*, *Plantago lanceolata*, and *Lotus corniculatus* to subsequent increasingly persistent PRs. The more persistent PR significantly reduced plants' survival, productivity, and photosynthetic activity. Transcriptomic analysis revealed pathways related to hormone signaling (e.g. jasmonic acid, abscisic acid, salicylic acid, ethylene), oxidative stress, cell wall modification (e.g. callose and pectin metabolic process, lignin synthesis), chitin catabolic process to be upregulated under more persistent PR in four grassland species, with soil history of 30-day PR exposure enhancing these findings. *Holcus lanatus* responded the least at the transcriptome level compared to the other three species, which may partially explain its sensitivity towards the altered PR. Notably, the transcriptomic responses increased due to the 30-day PR soil history probably shows that the soil microbiome legacy likely plays an important role in ecosystem acclimation to more persistent PRs.

1 Introduction

Climate change is leading to increasingly persistent precipitation regimes (PRs), characterized by severe rainfall events and extended intervening dry periods in northern Europe (Knapp et al. 2002; Pfliegerer et al. 2019; Breinl et al. 2020;

Tuel et al. 2022; Knapp et al. 2008). The shift to more persistent precipitation patterns significantly increases the temporal variability of soil water content, affecting ecosystems at multiple organization levels, such as plant and soil microbial communities and their interactions (Arca et al. 2021; Barnard et al. 2013). Extreme rainfall patterns can rapidly alter plant community composition and key carbon cycling processes independent of changes in total precipitation (Knapp et al. 2002). Reducing the frequency of rainfall events without a change in the amount of rainfall resulted in lower ecosystem level net CO₂ uptake (Arca et al. 2021). Our recent studies on open-air grassland mesocosms showed that more persistent precipitation regimes alter grassland community compositions (Reynaert et al. 2021), induce changes in the metabolome and biochemical components of grassland species at different magnitudes (Zi et al. 2023), and results in a soil microbial community that is less predictable (L. Li, Nijs, et al. 2023). Due to the high variability of the environment and the competition between species under natural conditions, it is challenging to decipher the responses of individual species at the transcriptome level. Therefore, it is critical to study these responses in growth room experiments with a controlled environment to further depict the impact of the altered PRs on individual grassland species.

Plant traits and soil characteristics are plastic in response to climate extremes, and their modifications may maintain for long periods even after the initial 'driver' ceases. These persisting effects are called legacy effects or stress memory (Wurst and Ohgushi 2015; Cuddington 2011). Multiple studies have found that legacy effects play a vital role in shaping how ecosystems function under future stressors through community restructuring, plant acclimation, plant-soil interactions (Gessler et al. 2020; Meisner et al. 2018; Xiliang Li et al.

2022; Barnard et al. 2013; Walter et al. 2013). Studies investigating plant stress memory have shown that multiple consecutive exposures to drought enable plants to respond rapidly to a water deficit when compared to plants encountering drought for the first time (Xiliang Li et al. 2022; Ramírez et al. 2015). Our recent study showed that previous exposure to extreme PRs resulted in acclimated grassland communities through community restructuring and plant metabolic changes (Reynaert et al. 2022). Climate history also induces a significant impact on soil microbiome community assembly (Xiaogang Li et al. 2019). This soil biotic legacy effect, in turn, can influence plant-soil interactions, affecting individual plants' performance (Kardol et al. 2007; Ristok et al. 2019). This study looks to expand the knowledge on the role of the soil microbiomes' legacy effect on individual plants in response to subsequent persistent PR events.

Environmental stress factors such as drought, flooding, or a combination of the two significantly impact all aspects of plant health (Ahuja et al. 2010). To understand the impact of the legacy effect of soil under different PR, it is important to conduct a comprehensive analysis encompassing physiological, biochemical, and transcriptional responses. The transcriptomic response of plants to drought stress has been extensively researched. Multiple genetic pathways have been implicated to play an important role in drought responses. Transcriptomic studies have also found links to signal transduction, amino acids, carbohydrate metabolism, hormones, and secondary metabolites (X. Ma et al. 2016; Hongyan Wang et al. 2016; Avramova et al. 2015). The upregulation of genes involved in jasmonic acids and ethylene has been linked to drought tolerance in plants (Egea et al. 2018). The abscisic acid (ABA) signaling pathway has been found to have a vital role in drought response in plants, as ABA

accumulation has been shown to lead to stomatal closure to guard against water loss (Munemasa et al. 2015; Zhu 2016). Cell wall synthesis is also thought to play a vital role in plant drought response (Dalal et al. 2018; Lenk et al. 2019; Q. Zhang et al. 2020). The effect of drought on grassland specific species has also been studied with similar results. The main pathways include ABA signaling, mitogen-activated protein kinase (MAPK) signaling, transcription factors (TFs) such as WRKY (Min et al. 2020; Xiqiang Liu et al. 2022). Previous studies have shown that rhizosphere microbial communities can mitigate the effects of drought on plants (Bogati et al. 2022). However, the transcriptomic response of non-model species to more persistent PRs with soil legacy effect has not yet been studied.

For this study, four common grassland species were chosen based on findings from our previous study to cover a diverse set of functional groups and sensitivities (Reynaert et al. 2021). *Holcus lanatus* and *Phleum pratense* represent a sensitive and tolerant grass species respectively, while *Plantago lanceolata* and *Lotus corniculatus* represent a forb and nitrogen fixer. The four species were then exposed to increasingly persistent PRs ranging from 1-day dry/wet cycle to 20-day dry/wet cycle. We examine soil microbiome legacy effects by using 1-day PR and 30-day PR exposed soil collected from a previous grassland mesocosm experiment (Reynaert et al. 2021). To our knowledge, little is known about the transcriptome changes of these four species induced by environmental stress, except a study revealed the effect of pH extremes on *Holcus lanatus* and its interaction with the microbiome by Young et al. (2018). Here we perform an integrated analysis of physiological, biochemical, and transcriptional responses to determine 1) How do different non model grassland species respond to increasingly long dry and wet periods? 2) Does an

adaptation of soil microbial community to previous PR (legacy) modify plant responses to the subsequent more persistent PR?

2 Material and methods

2.1 Experimental Design

This study involves the use of soil conditioned from our previous experiment to investigate the potential soil microbial legacy effect and the plant responses towards altered watering regimes (Reynaert et al. 2021). The soil from that experiment were subjected to a range of 8 PRs, with alternating dry/wet periods of 1, 3, 6, 10, 15, 20, 30 and 60 consecutive wet and dry days (referred to as '1-day PR', '3-day PR', etc.). PRs started with dry or wet period are shorted as 'D' and 'W', respectively. The detailed experimental set-up can be found in our previous publication (Reynaert et al. 2021). After 120 days, soil samples were collected from six randomly chosen replicate containers per treatment by combining five randomly distributed samples (1 cm diameter, 0–5 cm depth) from each container. The soil from 1W and 30W regimes were selected as normal and extreme PR for this study to investigate microbial legacy effect.

This study was conducted in a climate chamber with controlled conditions: 16/8 h day/night photoperiod, 21/18 °C air temperature, and 60/70% humidity. Non inoculum soils were sterilized before use in the experiment. The soil composition in each pot (1.5 L) is composed of 90% sterile soil and 10% soil from 1W or 30W from the outdoor experiment. Seeds of four common C3 grassland species *Holcus lanatus* L., *Phleum pratense* L., *Plantago lanceolata* L., *Lotus corniculatus* L. were first germinated in separate trays per species, followed by transplantation of homogeneous seedlings into the pot for further experiment. The plants were under a range of alternating dry/wet cycle,

starting from a 1-day dry/wet cycle, 5-day dry/wet cycle, 10-day dry/wet cycle, and ending with a 20-day dry/wet cycle. The total duration of the experiment was 40 days. There were four replicates (pots) per water regime and soil type combination, and each pot contained five individuals from the same species (Figure 1a). On wet days, 70 mL of water was irrigated into the pot. All watering regimes had the same number of wet and dry days (20 days) and total irrigation amount (1.4 L; Figure 1b).

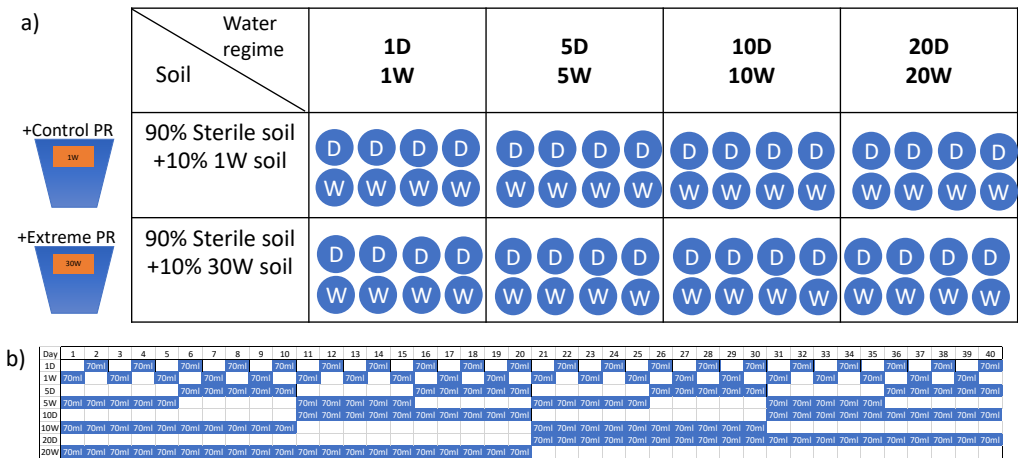


Figure 1 The experiment design for each species. a) The plants in “+Control PR” and “+Extreme PR” soils are under a gradient of alternating dry/wet cycle, ranging from 1-day dry/wet cycle, 5-day dry/wet cycle to 20-day dry/wet cycle. The soil is composed of 90% sterile soil and inoculated with 10% soil from the 1W or 30W in the outdoor experiment, respectively. ‘D’, ‘W’ represents the dry and wet start, respectively. Each group contains four replicates (pots), and each pot contains five individual plants from same species. b) The total duration of the experiment is 40 days. The blocks in blue represent wet days.

2.2 Soil water content measurement

During the experiment, the soil weight (together with pot) was measured every day at the same time, just before watering. On wet days, the soil weight after watering was also measured. After the experiment was finished, the soil was dried in the oven at 60 °C for 72 h until completely dry and the dried soil was weighed. The gravimetric water content θ_g is calculated as follows:

$$\theta g = \frac{m_{water}}{m_{soil}} = \frac{m_{wet} - m_{dry}}{m_{dry}}$$

Volumetric water content θv is the volume of liquid water per volume of soil (Bilskie 2001), and is calculated as follows:

$$\theta v = \frac{volumewater}{volumesoil} = \frac{\frac{m_{water}}{\rho_{water}}}{\frac{m_{soil}}{\rho_{bulk}}} = \frac{\theta g \times \rho_{bulk}}{\rho_{water}}$$

The ρ_{bulk} is the ratio of soil dry mass to sample volume (1.5 L):

$$\rho_{bulk} = \frac{m_{dry}}{volume}$$

2.3 Biomass, DW/FW and Fv/Fm measurement

At the end of the experiment (day 41), the five individuals per pot were weighed to obtain the fresh weight. In order to determine the dry weight/fresh weight ratio, 3 to 5 random leaves from five individuals were weighed to have their fresh weight (FW), then placed in an oven at 60 °C for 72 h to obtain the dry weight (DW) and calculate the FW/DW ratio. To determine the photochemical efficiency of photosystem II, Fv/Fm was measured by applying a fluorometer PEA (Hansatech, Britain) after 30 min of dark adaptation.

2.4 RNA Extraction and Next-Generation Sequencing

After the completion of the experiment (day 41), four replicates were collected for PRs of 1W and 5W and for each soil inoculum of 1W and 30W. This yielded a total of 16 samples per species or 64 total samples for transcriptomics analysis. Leaf samples from each plant were collected and frozen in liquid nitrogen and kept at -80°C until used for RNA extraction.

Total RNA was extracted using the RNeasy Plant Mini Kit (Qiagen) following the manufacturer's protocols. RNA concentration and purity were then checked using a NanoDrop ND-1000 UV-VIS (Thermo Fisher Scientific) and Qubit RNA Assay Kit 4.0 (Thermo Fisher Scientific). Preparation of the RNA library using standard protocols and 2x150BP PE transcriptome sequencing was conducted on an Illumina sequencer by Novogene Co., LTD (Cambridge, UK).

2.5 Data Acquisition and Quality Control

Raw data from the sequencing facility for all species were first run through FastQC v0.11.9 (Andrews 2010) to check the quality of sequencing reads. Data was then trimmed (LEADING:20 TRAILING:20 ILLUMINACLIP:\$adapters:2:40:15 SLIDINGWINDOW:4:20 MINLEN:36) to remove low-quality reads in Trimmomatic v0.36 (Bolger, Lohse, and Usadel 2014).

2.6 Creating De Novo Transcriptomes

As no reference genome is available for any of the species, a de novo transcriptome was created for all four species. Multiple de novo assembly tools are available and have been previously compared for use across different species datasets (Hölzer and Marz 2019; Chopra et al. 2014). Based on these comparisons, Trinity v2.15 Assembler (--seqType fq--SS_lib_type RF --trimmomatic) was chosen for its ability to work across a large range of data sets and reproducibility across all four species used in this study (Grabherr et al. 2011). Bowtie2 v2.5.0 (Langmead and Salzberg 2012) was used to map reads to the assembled transcriptomes to access read representation of the transcriptomes.

2.7 Annotation of Transcriptomes

The assembled contigs were annotated using Trinotate v4.0.0 software package for each species (Bryant et al. 2017) Trinotate was run using the recommended parameters. First, open reading frames (ORFs) were translated from the previously generated Trinity.fasta files using the TransDecoder.LongOrfs and predicted with TransDecoder.Predict. Protein sequences were then used to generate trinotate files with the following commands (blastp -query protein.fasta -db uniprot_sprot.pep -num_threads 32 -max_target_seqs 1 -outfmt 6 > blastp.out, blastx -query Trinity.fasta -db uniprot_sprot.pep -num_threads 32 -max_target_seqs 1 -outfmt 6 > blastx.out, hmmscan—cpu 32 --domtblou PFAM.out Pfam-A.hmm protein.fasta, signalp -f short -n signalp.out protein.fasta, tmhmm—short < protein.fasta > tmhmm.out, Program versions: BLAST++ v2.2.28; HMMER v3.1b2; SignalP v4.1; TMHMM v2.0). The Uniprot protein database was downloaded via the trinotate website (https://data.broadinstitute.org/Trinity/Trinotate_v2.0_RESOURCES/). All recovered data was placed into a SQLITE database and a trinotate.xls annotation table was created. All go assignments per gene were extracted using `extract_GO_assignments_from_Trinotate_xls` (-G—include_ancestral_terms) and a gene lengths file was created using `fasta_seq_length.pl` and `TPM_weighted_gene_length.py` both using the default parameters.

2.8 Differential Expression and GO enrichment analysis

Trinity generated gene transcript abundance was quantified using Kallisto V0.46.1. First, a kallisto index file was generated using the index command and default parameters. Then, each sample file is run in kallisto using the trinity

script `align_and_estimate_abundance.pl` (`--seqType fq--est_method kallisto--gene_trans_map--SS_lib_type RF`). The results for all samples were then combined into a matrix file using `abundance_estimates_to_matrix.pl` (`--est_method kallisto`). Differential expression analysis was then performed using DESeq2v1.40 to look into the differentially expressed genes (DEGs) caused by contrasts in the water regime, inoculum soil, and the interaction between the two. DEGs were chosen using a cutoff value of $FDR < 0.01$ and \log_2 fold change of > 4 . GOSeq v1.52 was used to conduct GO enrichment analysis on the data to find which terms were overrepresented in the data. GOSeq was selected for this study as it considers gene lengths to remove bias from long transcripts (M. D. Young et al. 2010).

2.9 Clustering analysis and interpretation

We performed quality threshold clustering (Heyer et al. 1999) on the DEGs from all four species to investigate gene expression patterns of interest and to determine transcriptional profiles across the species. Clustering was performed using the Multiple Experiment Viewer (MEV v4.9.0) software tool (Howe et al. 2011). Prior to clustering, data was normalized in MEV to obtain expression values in a similar range to allow for overlapping patterns during clustering. Quality threshold clustering was performed on the significant genes for all zones using Pearson correlation with 0.5 cluster diameter and minimum cluster density of 50 (Heyer et al. 1999).

Clusters were then compared across the four species to find similar expression patterns of genes for the four species. Similar profiles were placed into groups containing clusters for all species. The genes in these groups then underwent over expression analysis with GOSeq in order to see which genes produced

similar patterns across species. These pathways were then validated by biochemical tests to confirm their significance.

2.10 Plant cell wall composition analysis

Cell wall materials were extracted following the method of (Zhong and Lauchli 1993). 50 mg plant shoots were thoroughly homogenized in 75% ethanol for 20 min. After centrifugation at $8000 \times g$ for 10 min, the supernatant was discarded. The pellets were homogenized and washed for 30 min with acetone, methanol: chloroform mixture (1:1, v/v) and methanol, respectively. The supernatant was discarded, and the pellet was freeze-dried and stored at 4°C for further use. Cell wall materials were fractionated into four fractions: pectin, hemicellulose 1 (HC1), hemicellulose 2 (HC2) and cellulose. Pectin was extracted three times with hot water (100°C) for 1 h each and the supernatants were combined (pectin). Then, the pellets were subjected to triple extraction with 4% KOH containing 0.1% KBH_4 at room temperature for 8 h each and the supernatants were combined (HC1). The resulting pellets were subsequently extracted with 24% KOH containing 0.1% KBH_4 at room temperature for 8 h each and the supernatants were combined (HC2), and the residue was considered as the cellulose fraction.

Lignin was quantified according to a modified version of Liyama and Wallis (1990). Cell wall materials (1 mg) were digested in $100 \mu\text{l}$ of 25% (v/v) acetyl bromide in acetic acid at 70°C for 30 min and cooled quickly. Then, $180 \mu\text{l}$ of 2 M NaOH was added to the mixture to terminate the digestion and mixed with $20 \mu\text{l}$ of 7.5 M hydroxylamine hydrochloride and 1 ml acetic acid. The mixtures were centrifuged at $3000 \times g$ for 10 min. The content of lignin was measured at 280 nm (Synergy Mx spectrophotometer, BIOTEK, Winooski, USA).

Callose was extracted and determined based on (Kohle et al. 1985). Around 50 mg of plant tissue was homogenised in 0.5 ml 1 M NaOH and heated at 80°C for 30 min. After centrifugation, the 200 µl supernatant, which contains callose, was mixed with 1.25 ml aniline blue mixture consisting of 0.1% aniline blue in 1 M glycine at pH 9.5 and heated in a water bath at 50°C, for 20 min. Callose was quantified by fluorescence spectrophotometry (Synergy Mx spectrophotometer, BIOTEK, Winooski, USA) using an excitation wavelength of 393 nm and an emission wavelength of 484 nm.

To perform xyloglucan extractions, five milligrams of cell wall residue were resuspended in a 400 µL solution of 10 mM pyridine-acetate buffer at pH 4.5, followed by four subsequent washes. The extraction of accessible xyloglucan was achieved using 4 units of endocellulase obtained from *Trichoderma longibranchiatum* (Megazyme) through an overnight digestion process at 37°C. Any undigested material was washed twice with water and then extracted for 24 hours with 900 µL of a solution containing 24% KOH and 0.1% NaBH₄. After centrifugation, the supernatant was neutralized using 300 µL of acetic acid. The extracted cell wall material was filtered through a 10K centrifugal filter, subjected to repeated washes with 10 mM pyridine-acetate buffer at pH 4.5, and digested overnight with 4 units of endocellulase. The determination of reducing sugars was accomplished through the p-hydroxybenzoic acid hydrazide assay (Lever 1972). Finally, the samples were dried and resuspended in a 20 mM Na-acetate buffer at pH 5.0, achieving a concentration of 3 mM reducing sugars.

2.11 Analysis of enzymes related to cell wall composition

2.11.1 Cinnamyl alcohol dehydrogenase (CAD) activity

CAD activity was analyzed according to the method of Mansell et al. (1974). 50 mg frozen samples were extracted in 100 mM of phosphate buffer (pH 7.3) containing 4% (w/v) polyvinylpyrrolidone (PVP), 20 μ M phenylmethylsulfonyl fluoride and EDTA (2 mM), followed by centrifugation at 4 °C at 1400 rpm for 20 min. CAD activity was assayed in reaction mixture of 100 mM phosphate buffer (pH 6.5) containing 20 mM coniferyl alcohol and 5 mM NADP⁺ and monitoring the absorbance at 340 nm. The amount causing a change of 0.001 in absorbance per min at 340 nm was defined as one unit (U) of CAD activity.

2.11.2 Peroxidase (POD) activity

Peroxidase enzyme activity was assayed following the method described by Childs and Bardsley (1975). 50 mg of frozen samples were homogenized with phosphate buffer (50 mM, pH 7) contains 0.4% (w/v) polyvinylpyrrolidone (PVP) and EDTA (2 mM). The homogenized mixture was centrifuged (10000g, 15 min at 4 °C) and the supernatant was used as an extract of the enzyme. The reaction was carried in reaction mixture of 0.1 M (pH 6) phosphate buffer, containing 50 mM solution of caffeic acid and 50 μ l enzymatic extract. The reaction started with the addition of 0.92 mM hydrogen peroxide. The changes in absorbance were read at 470 nm. The amount causing a change of 1.0 in absorbance per min at 470 nm was defined as one unit (U) of POD activity.

2.11.3 Chitinase activity assay

The chitinase activity was determined by measuring the release of fluorescence from one of four 4-methylumbelliferyl glycosides of 4MU-(GlcNAc) according to a previously described method (L. Sun et al. 1999). The reactions were

conducted in 50 μL of 0.1 M PBS (pH 6.0) containing 20 μg of protein and 5 μM 4MU-(GlcNAc). The mixtures were incubated for 90 min at 37°C. Reactions were stopped by adding 2 mL of 0.2 M Na_2CO_3 . Fluorescence was measured with excitation at 350 nm, and emission was monitored at 440 nm in a microplate reader.

2.11.4 Callose synthase assay

Callose synthase activity was measured in 96-well microtiter plates according to Shedletzky et al. (1997) with modifications. 50 mg frozen samples were extracted in 100 mM of phosphate buffer (pH 7.3) containing 4% (w/v) polyvinylpyrrolidone (PVP), 20 μM phenylmethylsulfonyl fluoride and EDTA (2 mM), followed by centrifugation at 4 °C at 1400 rpm for 20 min. Twenty microliters of the extracted protein (content: 2–2.5 μg) were incubated with 70 μL reaction buffer (50 mM Tris/HCl (pH 7.3), 0.02% digitonin (Sigma), 2 mM CaCl_2 , 20 mM cellobiose, 0.5 mM UDP-glc (Sigma)) for 1 h at 25 °C. The addition of 10 μL 10 N NaOH terminated the reactions. The produced (1,3)- β -glucan was solubilized by shaking the microtiter plate at 80 °C for 30 min.

2.12 Plant Hormone analysis

50-100 mg of frozen plant material was dissolved in 800 μL 80% (v/v) methanol (HiPerSolv CHROMANORM®; VWR, Leuven, Belgium), followed by a 15 minute sonication and overnight metabolite extraction at - 20°C. Internal standards were added after overnight extraction: 1000 pmol [$^2\text{H}_4$]1-aminocyclopropanecarboxylic acid ([$^2\text{H}_4$]-ACC) (OlchemIm, Olomouc, Czech Republic), and 300 pmol (\pm)-3-oxo-2-pentyl-cyclopentane-1-acetic acid (DHJA) (OlchemIm, Olomouc, Czech Republic). Oasis® HLB Sorbent (Waters, Deerfield, IL, USA) was also added. Afterwards, the sample was centrifuged by an

Eppendorf Centrifuge 5810R (14000 RPM, 4°C, 15 min; Eppendorf, Hamburg, Germany).

The supernatant was filtered with a size-based Chromafil® AO-20/3 filter (nylon, pore size 0,20µm, diameter 3 mm; Macherey-Nagel, Düren, Germany). The filtrate was divided into 2 fractions, ACC and JA, and was dried under nitrogen gas with a Zymark TurboVap LV.

The dried acc fraction was resolved in 70µl 10% MeOH and transferred to UPLC-MS/MS vial. The concentration of ACC was obtained with an ACQUITY UPLC system combined with a Waters ACQUITY TQD Tandem Quadrupole UPLC/MS/MS. The analytical column was an ACQUITY UPLC BEH Amide 130Å, 1.7 µm, 2.1 mm X 100 mm with an ACQUITY UPLC BEH Amide VanGuard Pre-column, 130Å, 1.7 µm, 2.1 mm X 5 mm, Waters. Compounds of interest were eluted from the column by a solvent composition of 99,9:0,1 A:B with A being 0,1% (v/v) FA in ACN and B 0,1% (v/v) FA in water to A:B 1:99 for 6,5 minutes under a linear gradient. Both the flow rate of 0,300 µl min⁻¹ and the column temperature of 40°C remained constant. The column was rinsed with 99% ACN and equilibrated by 99,9:0,1 A:B for one minute each. ES⁺-MRM was used for detecting the tACC-fraction. Compounds of interest and it's corresponding data and parameters can be found in table 2. Chromatograms were analyzed using Waters® TargetLynx™ 4.2. 2 (Waters, Milford, MA, USA).

The JA fraction was resolved and derivatized in 70 µl of 1-Ethyl-3-(3'-dimethylaminopropyl) carbodiimide (EDAC) solution (5 mg EDAC (Sigma-Aldrich, Saint-Louis, MO, USA) dissolved in 1 ml 100% methanol (HiPerSolv CHROMANORM®; VWR, Leuven, Belgium)). The solution was heated and shaken by an Eppendorf Thermomixer Compact (900 RPM, 38°C, 60 min;

Eppendorf, Hamburg, Germany). The samples were dried under a nitrogen gas stream and resolved in 70 µl 10% (v/v) methanol.

The concentration of JA was obtained with an ACQUITY UPLC system combined with a Waters ACQUITY TQD Tandem Quadrupole UPLC/MS/MS. The analytical column was a reverse-phase BEH C18 Column (130Å, 1.7 µm, 2.1 mm X 50 mm), guarded by a BEH C18 VanGuard Pre-column (130Å, 1.7 µm, 2.1 mm X 5 mm). Samples were eluted from the column by a solvent composition of 92:8 A:B with A 0,1% (v/v) FA in water and B 0,1% (v/v) FA in ACN to A:B 60:40 for 4,2 minutes under a linear gradient. This was followed by a transition from 60:40 to 10:90 in 0,5 minutes, also under a linear gradient. Both the flow rate of 0,420 µl min⁻¹ and column temperature of 40°C were kept constant. The column was rinsed with 90% ACN for 0,6 minutes and equilibrated with 92:8 A:B for 1,4 minutes. ES⁺-MRM was used for detection of analytes. Chromatograms were analyzed using Waters® TargetLynx™ 4.2.

To determine the content of abscisic acid (ABA), we followed a previously established protocol (Q. Qi et al. 1998). In short, the plant tissue extracts were subjected to drying and then methylated by the addition of diazomethane. Subsequent analyses were conducted utilizing a GC-MS SIM (6890N network GC system) in conjunction with a 5973-network mass selective detector, both supplied by Agilent Technologies in Palo Alto, CA, USA. The quantification of ABA signals was performed using the Lab-Base data software provided by ThermoQuaset in Manchester, UK.

2.13 Statistical analysis

All statistical analyses were performed in R (version 4.0.4). Significance was assumed for p -values < 0.05 . Figures were created utilizing the packages dplyr (Wickham H 2023), ggplot2 (Wickham 2016) and plotrix (Lemon et al. 2022).

Plant survival, FW, DW/FW, DW, Fv/Fm were analyzed by ANOVAS with species, watering regimes, dry or wet start, soil background and their interactions as fixed factors. Cell wall compositions, enzymes, hormones of each species were analyzed by two-way ANOVA with watering regimes, soil background and their interactions as factors. Significant differences between each group were further determined by Tukey HSD test ($p < 0.05$).

3 Results

3.1 Patterns of soil water content induced by different precipitation regimes

The SWC effectively reflected the different watering regimes during the experiment (Figure 2). The soil under 10W and 20W reached waterlogging status during the wet period, with 20W having more days under the waterlogging condition (Figure 2f; h). 20D and 20W showed the longest continues days of drought (SWC $< 0.05 \text{ m}^3\text{m}^{-3}$). As expected, the 1D and 1W showed the least SWC fluctuation (Figure 2a; b), and the variation of SWC increased with the more persistent precipitation regimes (Figure 2).

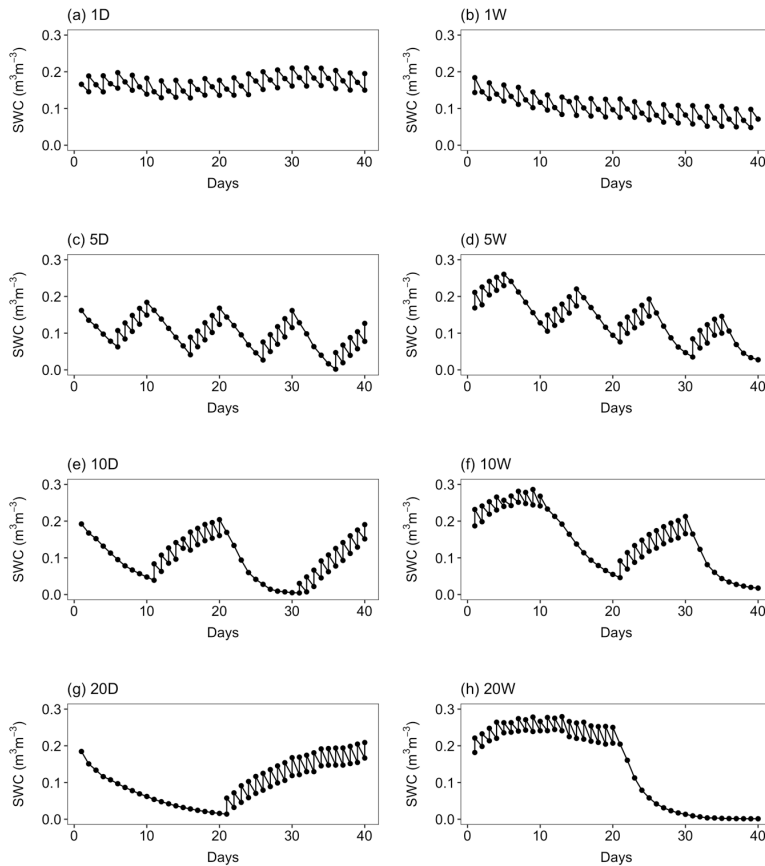


Figure 2 Soil water content during the 40 days experiment of each watering regime. 'D' and 'W' represent dry or wet start, respectively. Total water content was identical for each PR. During the wet days, the SWC before and after watering were measured.

3.2 Plant phenotypes in response to different precipitation regimes and soil background

Generally, four species showed progressive deterioration (size/wilting) with increasingly persistent PR (Figure 3). Plants exhibited better appearance under dry start treatment (harvest after wet period), particularly for 10D *Lotus* and 20D *Plantago*. *Holcus* and *Plantago* showed decreased survival from 5D/W compared with 1D/W (Figure 3). *Phleum* and *Lotus* presented wilted leaves and less biomass from 10D/W (Figure 3). Except for *Plantago*, the species showed

the most seriously wilted shoots and least biomass in the 20D/W regimes. *Plantago* showed higher biomass (recovered more) at 20D compared with 10D, though less biomass than seen in the 1D and 5D samples (Figure 3). Under 20D, *Plantago* grown with 30W soil has accumulated more biomass than when grown with 1W soil (Figure 3). For the other species, there were no evident visible differences between two types of soils at the end of the experiment (Figure 3).

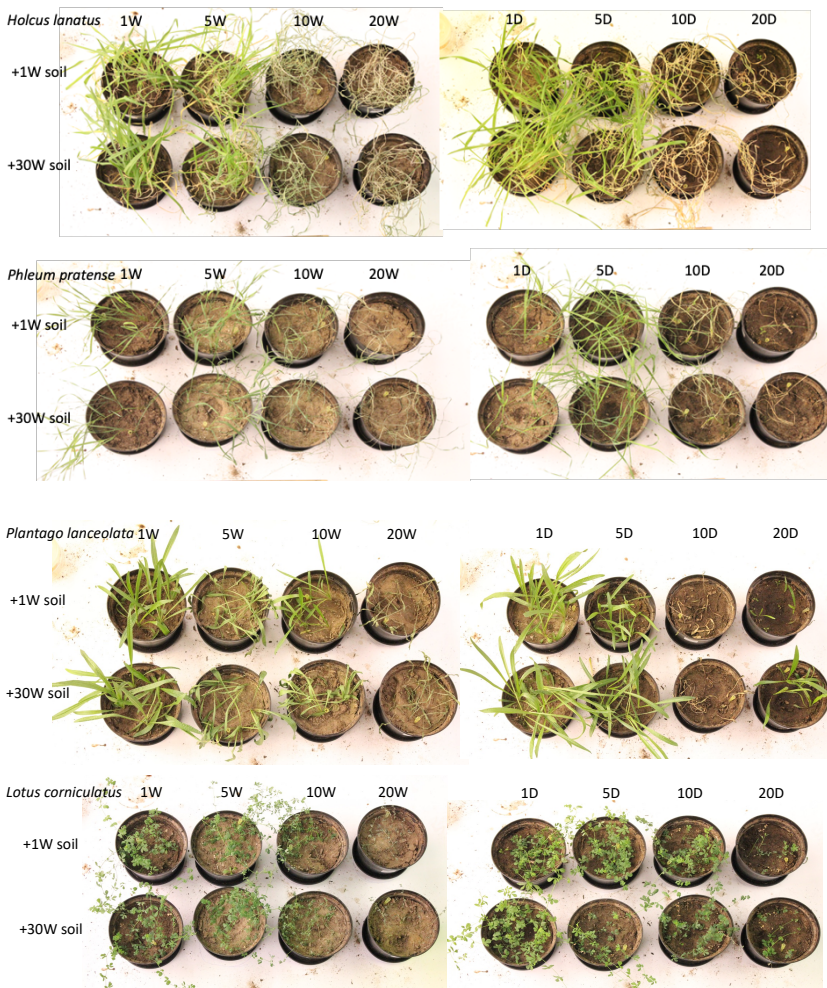


Figure 3 Representative photographs visualizing four species under different watering regimes and soil background at the end of experiment.

The more persistent PRs resulted in reductions in survival in four species (Figure 4a). The wet start watering regimes significantly reduced the survival at 20W in four species, while the dry start regimes significantly reduced the survival from 10D (Figure 4a). There were no living *Holcus* and *Plantago* under 10D, while *Phleum* and *Lotus* showed 25% and 75% of living plants, respectively (Figure 4a). *Plantago* showed a higher survival rate at 20D compared with 10D; specifically, the *Plantago* inoculated with 30W soil showed a higher survival than inoculated with 1W soil under 20D regime (Figure 4a; $p < 0.01$).

Fresh weight was reduced with the increasing persistency of watering regimes in four species, and the decrease was more moderate in *Lotus* compared with the other three species (Figure 4b). Consistent with the visualization and survival, *Plantago* exhibited higher fresh weight at 20D than 10D. Under 20D, *Plantago* inoculated with 30W soil accumulated more fresh weight than inoculated with 1W soil (Figure 4b; $p < 0.001$).

Four species showed divergent patterns on DW/FW. The DW/FW of *Holcus* increased with more persistent watering regimes under dry start and wet start. In *Phleum*, the DW/FW was higher in 10-day watering regime compared to 1-day watering regime but seemed to decrease under the 20-day regime. In *Plantago*, dry start and wet start regimes showed opposite trends, which means the harvesting time (the plants under dry or wet period) significantly influences the water content of *Plantago* tissue. In *Lotus*, the DW/FW increased with more persistent wet start regimes, whereas no evident trend was exhibited under dry start regimes (Figure 4c). Generally, the DW decreased under more persistent watering regimes (Figure 4d).

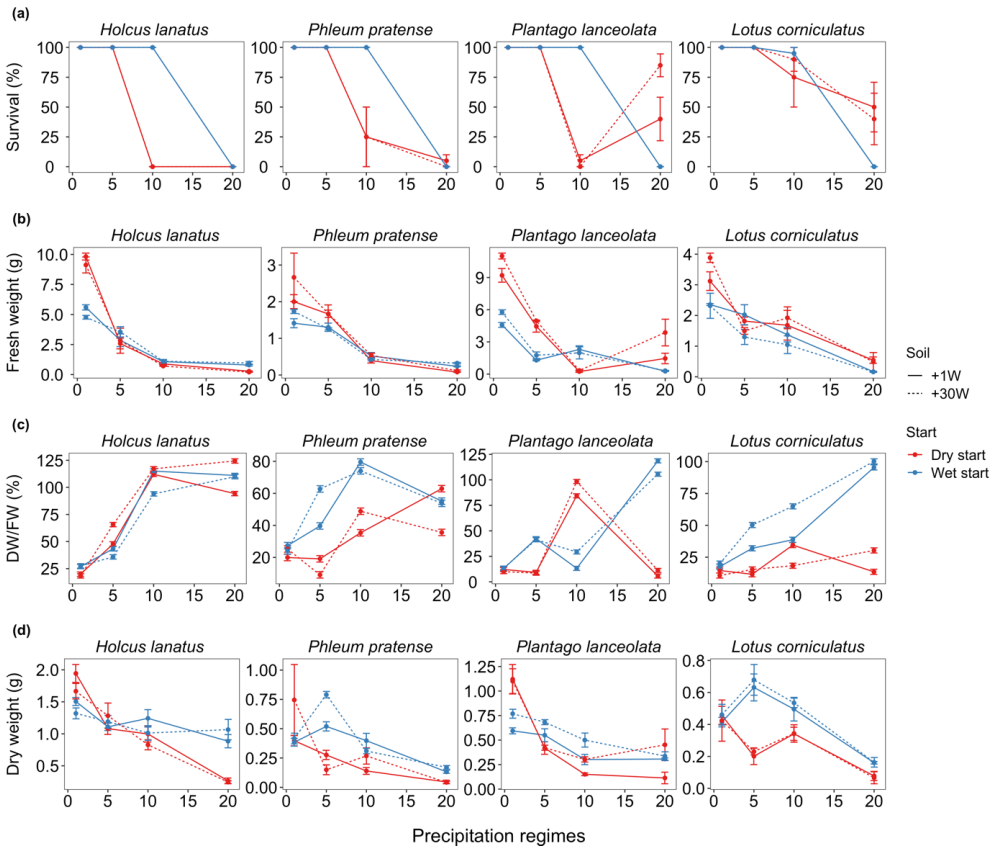


Figure 4 Survival, fresh weight (FW), dry weight (DW), DW/FW of each species at the end of experiment. Data are represented as mean \pm SE (n=4).

The global pattern for the four species found the 5-day regime did not induce significant changes in Fv/Fm compared with 1-day regime (Figure 5). 10-day regime significantly reduced the Fv/Fm in *Holcus*, and the value was almost 0 under 10-day and 20-day regimes. 10-day regime also significantly reduced the Fv/Fm of the other three species, but the magnitude was less than *Holcus* (Figure 5). Under 20-day wet start regime (20W), there was no detectable change in Fv/Fm for the four species. On the other hand, *Plantago* showed increased Fv/Fm under 20-day dry start regime (20D) compared with 10-day dry start regime (10D), consistent with the visual results (Figure 3). Under 20D, *Plantago* inoculated with 30W soil showed higher Fv/Fm than inoculated with

1W soil (Figure 5). There were no significant differences between the 20-day dry start regime (20D) when compared with the 10-day dry start regime (10D) in *Lotus*.

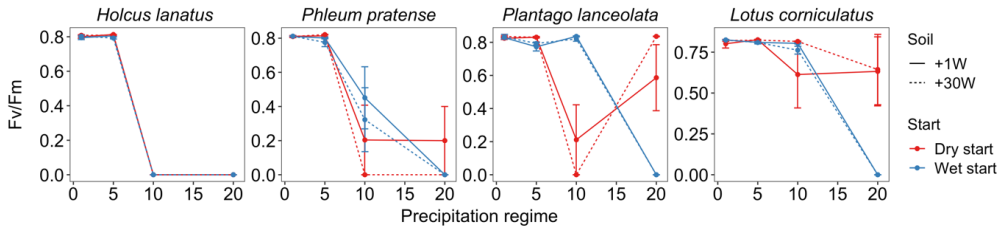


Figure 5 Fv/Fm of each species at the end of experiment. Data are represented as mean \pm SE ($n=4$).

3.3 RNA Seq

3.3.1 Transcriptome Assembly

To further understand the effect of PR and soil microbiome legacy on the four species, we set out to perform a genome-wide transcriptome analysis. Because this technique is highly sensitive it would result in changes in nearly all genes during more severe responses. Therefore, in order to identify the more specific responses and adaptations from soil legacy, we focused on the 1W and 5W regimes grown on 1W and 30W soil inoculate. Sequencing Reads were obtained for 16 samples from each of the four species for a total of 64 samples. Reads were trimmed and quality checked prior to assembly. A total of \sim 450 million reads were obtained from each species: \sim 28 million per sample. These cleaned reads were then assembled with Trinity to generate de novo transcriptomes from each species, as no species had publicly available genomes available for mapping at the time of this study. The assemblies therefore resulted in four de novo transcriptomes; the complete breakdown of the four transcriptome assemblies is shown in Table 1.

Table 1: Transcriptome Assembly statistics per species

Species	Bases	Transcriptome Size (MB)	Genes	Contig N50	Bowtie Mapping %
<i>Holcus lanatus</i>	3.27E+08	753.307	4.82E+05	1537	88
<i>Lotus corniculatus</i>	2.64E+08	710.797	3.98E+05	1304	85
<i>Plantago lanceolata</i>	4.94E+08	583.368	8.67E+05	1510	87
<i>Phleum pratense</i>	2.24E+08	1242.61	3.14E+05	969	86

3.3.2 Annotation

Annotation of the de novo transcriptome assemblies was completed with trinotate as described by (Bryant et al. 2017). All results of transcriptome annotation are reported in a transcript annotation summary file available for download (Data S1). Gene Ontology ids were then assigned to transcripts by using the best matching Swiss-Prot entries at the time of this experiment (2023) and are also available in the data files (Data S2).

3.3.3 Differential Expression

Differential expression analysis was performed on the 16 samples per species to find the effect of PR and soil inoculum using DeSeq2. Differentially expressed genes (DEGs) were stated to be significant for all species at $\log_2\text{fold} > 4$ and $\text{FDR} < 0.001$ to compare results between species. The most DEGs were found for *Phleum*, with 7296 DEGs found, while the least DEGs were found in *Holcus* with only 606 differentially expressed genes. The total breakdown per species and contrast can be found in Figure 6.

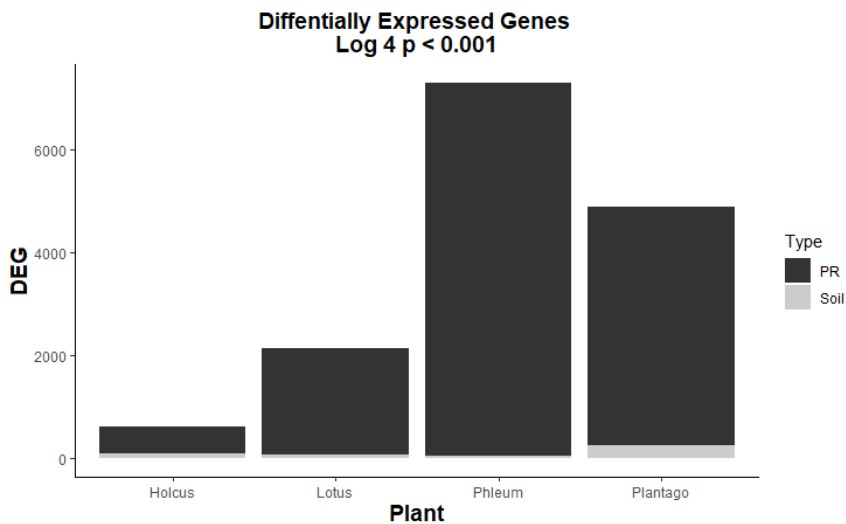


Figure 6: Comparison of differentially expressed genes across species after normalization and setting a significance cutoff of \log_2 fold greater than 4 and FDR value of 0.001. Significant genes are listed for both precipitation regime and soil legacy effect.

3.4 Clustering

The DEGs of each species for both water and soil were combined for clustering analysis to look for patterns across species. QT Clustering resulted in 46 clusters, 15 for *Plantago*, 10 for *Phleum*, 10 for *Lotus*, and 11 for *Holcus*. Three patterns were found in all four species: PR (drought) effect with no effect of inoculum soil (Figure 7), inoculum effect on plants with 1W water regime but no effect on 5W plants (Figure 8), and inoculum effect on plants with 5W water regime (drought) but no effect on 1W plants (Figure 9).

3.4.1 Effect of drought

Before the end of the experiment (40 days), 5W samples were under 5 days dry period and exhibited lower SWC when compared with 1W samples (Figure 2). Therefore, 5W samples experience a moderate drought effect at the time of harvest. The effect of drought on plants has been extensively studied across multiple species, and to confirm that our species showed a similar drought

response, we first investigated the six clusters that showed the effect of drought but no effect of soil inoculum (Figure 7). Therefore, we performed over-representation analysis (ORA) with GOSep on the DEGs from each cluster affected by 5W across the species. The top 20 overrepresented GO terms are listed in Table S1. The clusters labeled *Lotus 3* and *Phleum 4* were upregulated due to the effect of drought, while a single cluster from each of the species in this study showed a downregulation effect due to drought (*Lotus 4*, *Phleum 2*, *Holcus 3*, & *Plantago 2*; Figure 7). When looking into the overexpression of the upregulated genes, we find genes related to stress/defense response that are known to confer drought resistance in some species, such as MYB108, 1-Cys peroxiredoxin PER1, and WRKY40 (Baldoni et al. 2015; Pulido et al. 2009; Hongxia Wang et al. 2018). Multiple genes for photosynthesis, sugar metabolism, peroxidase, flavonoid biosynthesis, and heat stress transcription factors were overrepresented among the DEGs across all species. These processes have previously been studied across multiple species. (Niu et al. 2023; Shinozaki and Yamaguchi-Shinozaki 2007).

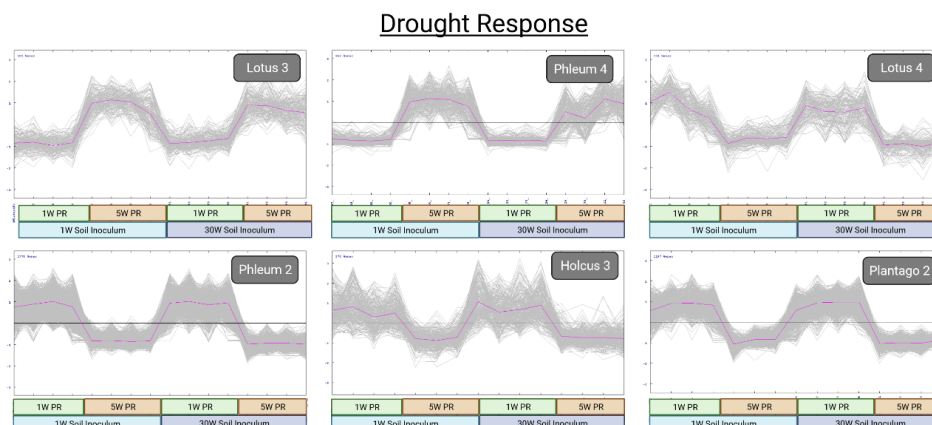


Figure 7: Clusters representing drought response with no effect of soil inoculum. An increase in expression due to drought was found in two clusters (Lotus 3 & Phleum 4), while a decrease in expression was found in four clusters representing all four species in this study (Lotus 4, Phleum 2, Holcus 3, and Plantago 2).

3.4.2 Shift in 1W plants induced by soil history

The effect of soil inoculum with 30W history on the 1W regime is seen in 6 clusters representing all species except for *Holcus* (Figure 8). As with the previous analysis the genes comprising the top 20 overrepresented GO terms are seen in Table S1. Two clusters, labeled *Lotus* 8 and *Phleum* 6 (Figure 8), showed a decrease in expression due to the 30W soil inoculum. Photosynthesis decreased the most out of the major pathways, with an overrepresentation for genes relating to chlorophyll a-b and photosystem I found in both species. The remaining four clusters showed an increase in expression due to 30W soil inoculum. *Lotus* and *Phleum* both showed an enrichment in genes relating to nucleotide processes, while *Plantago* had an enrichment for genes relating to cell wall modification such as caffeic acid 3-O-methyltransferase (Q. H. Ma and Xu 2008).

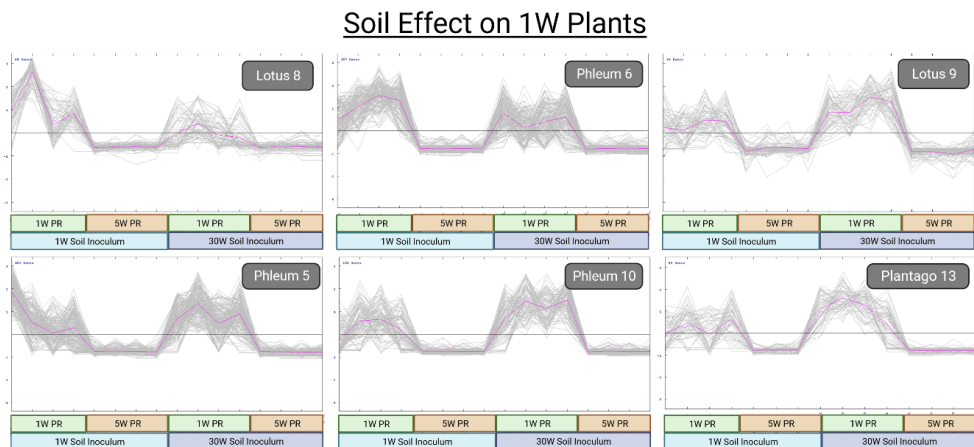


Figure 8: Matching cluster patterns for all species where an effect of soil inoculum can be seen on 1W plants but no soil effect can be seen on 5W plants. *Lotus* 8 and *Phleum* 6 are seen to have a decrease in expression, while *Lotus* 9, *Phleum* 5 & 10, and *Plantago* 13 show an increase in expression due to soil inoculum with drought history.

3.4.3 Shift in 5W plants induced by soil history

Holcus 1 & 4 showed a decrease in gene expression due to the 30W soil inoculum effect on 5W samples (Figure 9). This pattern represents the primary response of *Holcus* to the 30W soil inoculum. The ORA GO terms found for the genes in these clusters showed soil legacy effected an increase in amino acid metabolic processes, responses to oxidative stress, and biological regulatory processes (Table S2). Looking further into the common genes for these clusters shows genes for regulating defense response and disease resistance, chitinase, sugar transport, and multiple transcription factors such as *MAPK 3, 9, 10, & 17, MYB4, and WRK 6, 9, 19, 24, 72*.

The major response found across all four species (13 clusters) was an increase in the upregulation of DEGs due to the 30W soil inoculum under 5W regime (Figure 9). As with the previous patterns, clusters underwent ORA to determine which pathways were changed more due to the 30W soil inoculum under 5W regime (Table S1; S3). Looking into the effects of this pattern from the ORAs; cell wall composition, antioxidant regulation, pathogen response, and hormonal activity such as abscisic acid (ABA), ethylene, jasmonic acid, and salicylic acid increased across all four species. *Holcus* contained the least amount of ORA genes across the four species, while *Phleum* and *Lotus* contained the most. To further determine the effects of soil on 5W regime of each species, the genes shifting the ORA pathways are detailed in Table S2.

3.4.3.1 Cell Wall Composition

Cell wall composition pathways were affected across all species, and genes for multiple cell wall components were upregulated more with 30W soil under 5W regime. *Endoglucanases 5, 13, 4, 6, & 14*, which affect cell wall development, cellulose, and cell wall extensibility, were found as well as

Galacturonosyltransferases 2 & 9, pectate lyase A, D, F which are involved in pectin metabolic process in cell walls (Glass et al. 2015; Kong et al. 2011). Other cell wall related genes in *Holcus* include *Xyloglucan glycosyltransferase 7, cell wall monoprotein's*, and *endo- β -1,4-glucanase's*. *Plantago* similarly contained genes relating to cell wall composition such as *beta-xylosidase, Beta-glucosidase BoGH3B, callose synthase 9*, and *BC1 COMPLEX KINASE 1. WAK 1 & 2*, which have a known role as a pectin receptor in the cell wall (Kohorn and Kohorn 2012), are also upregulated. *Lotus* shows an overexpression of multiple cell wall genes such as *Xyloglucan's*, also seen in *Holcus*. Genes that are involved in the lignin biosynthesis pathway were also found, such as *CAD 1, CSE, Peroxidase 4, UGT 74B1 & 72B1* and *CCoAOMT* which is involved in drought tolerance by promoting lignin biosynthesis (D. Zhao et al. 2021). *WAK 1, 2, & 3*, seen in *Plantago*, are also seen in *Lotus*, along with cellulose synthesis genes, such as *KOBITO1* (Pagant et al. 2002). In *Phleum*, cell wall genes seen in previous species related to *Xyloglucan* and lipid biosynthesis genes are also upregulated, such as *CsCSE1 & LACS6*.

3.4.3.2 Antioxidant Regulation

In our four species, multiple genes related to antioxidant regulation increased the most for 30W soil under 5W regime. In *Holcus*, genes such as *peroxiredoxin PRX1, peroxisomal catalase*, and *superoxide dismutase* were overly expressed. In *Plantago*, redox genes such as *glutamate—cysteine ligase* and *Glyoxalase I-4* are enriched as well (Jez, Cahoon, and Chen 2004; T. Li et al. 2021). *Lotus* showed the most redox genes in the ORA data, with genes such as *Peroxidase 4 & 52, Glyoxylase I 4, L-ascorbate oxidase, GPX 2 & 3, PHGPx, GST U22, GSTparcA, GSTparcC, & ALDH3H1* showing an increase due to the 30W

inoculum soil under 5W. Finally, *Phleum* contained redox genes such as *GST23*, *Peroxygenase* and *Glyoxylase I 4*.

Pathways related to sugar metabolism increased due to 30W soil inoculum under drought across all four species. Genes related to glycolysis such as *Glucose-6-phosphate isomerase 1* increased in *Holcus*. In *Plantago* starch and sugar metabolic pathway gene *lysosomal beta glucosidase* increased (Bhogireddy et al. 2020). *Lotus* showed genes relating to sugars such as *Beta-glucosidase*, *glucosyltransferase*, *MST4*, and *SWEET 10, 13, & 15* which mediate sucrose uptake (L.-Q. Chen et al. 2015). Sugar related genes such as *Beta-glucosidase 7*, *Alkaline/neutral invertase A*, *Neutral/alkaline invertase 1* increased in *Lotus*.

3.4.3.3 Pathogen Response

Response to pathogens also increased more with 30W soil inoculum under drought across species (Table S1; S3). Although *Holcus* notably shows no related genes in the ORA, it does have significant DEGs for pathogen response when looking through the data. *Plantago* showed an increase in genes relating to Chitin such as *Endochitinase A, 4, & EP3*, and *chitinase 6 & CHIT5* and pathogen response genes such as *Protein EDR2*, *ATAF2*, *HSPRO2*, *BDA1*, and *WRKY33*. *RLK Xa21* and *GsSRK SD1-13* also increased, promoting disease resistance and have been linked to drought response (W. Y. Song et al. 1995; Shamsunnaher et al. 2020; X. L. Sun et al. 2013). Chitin related genes seen in other species such as *class V chintase* and *endochitinase* also increased in *Lotus*. *Lotus* had a further upregulation of genes involved in plant defense/pathogen response such as *ATAF2*, *ABCG 11, 15, & 35*, *PR-1*, *PR10.1*, *PR10.2A*, *ICE1*, *PTDTH-2*, *UGT74B1*, *Xanthotoxin synthase*, *CRK12*, *HSPRO2*, and *SAM22*. Chitinase genes increased in *Phleum* such as *Chitinase 1, 5, & CLP*. As with *Lotus*,

multiple RLKs increased in expression for *Phleum* such as *SAPK6*, *SAPK4*, *LECRKSIT2*, *SIK1*, and *CRK2*.

3.4.3.4 Hormonal Regulation

Hormonal regulation plays an important role in drought response and genes relating to hormonal regulation pathways increased under 30W soil legacy across species. Plantago showed increased expression for genes such as MACPF domain-containing protein At1g14780 and RNA-binding protein BRN1 which are involved in salicylic acid response to drought (Thatcher et al. 2016). F-box, NRT1, TIFY 9, SOAR1 proteins, Ubiquitin Ligases RGLG1, ERF ABR1 that regulate jasmonic acid and ABA also increased for the 5W samples in 30W soil (Gonzalez et al. 2017; Chiba et al. 2015; Ye et al. 2009; Wu et al. 2016; Jiang et al. 2015). Multiple hormonal regulator genes increased in Lotus that regulate ethylene, salicylic and jasmonic acids, and ABA such as: RING BRH1, ERFs 1B, 12, 13, 53, 96, 106, 110, ABR1, & RAP2-6, NDR1 10 & 3, F-box, UNE112, MYB 2, 44, 74, 78, 102, & 108, WRKY 6, 24, 40 & 76, TIGY 10A & 5B, JAZ1, ACS 1, 2, & 3, PT1, MBF1C, ABI3, IOS1, ABI5, JA2L, GsSRK, JMJ30, AFP3, & SRM1. Similarly, for Phleum, hormonal regulating genes such as RING BRH1, ERF 1B, 53, 110, 113, 114, 115, ABR1, & RAP2-6, RAP2-13, PUB18, F-BOX, RGLG1, NRT1, MYB 2 & 4, 78 & 102, TIFY 9, TIFY11, OsOPR7 are upregulated more with 30W soil inoculum under 5W regime.

3.4.3.5 Drought Stress

Drought tolerance and stress related genes upregulated further by the soil inoculum. In *Plantago*, multiple transcription factors increased, such as *MYB44* which regulates drought tolerance and ERFs such as *113*, which increases drought tolerance were found to be overly expressed (X. Fang et al. 2022; B. Zhao et al. 2022). Flavonoid related genes increased in *Plantago* such as *UDP-*

glycosyltransferase 79B6 and *anthocyanidin 3GGT*. In *Lotus* multiple zinc finger proteins increased such as *ZAT10*, *11*, *18*, *AZF1*, *AZF2* which have a known role in plant tolerance to stressors such as drought (Mittler et al. 2006; Yin et al. 2017). *Lotus* also contained dehydration responsive element binding proteins, which have a known role in enhancing plant drought response (B. Huang and Liu 2006). RLKs in *Lotus* such as *SD1-7* and *SD1-8* and multiple mitogen-activated protein kinases, such as *MKKK 17*, *18*, & *20* increased. As with *Lotus* multiple zinc finger proteins in *Phleum* such as *ZAT 1*, *7*, *10*, & *12* and transcription factors such as *MAPK 17* & *18*, which positively regulate drought stress resistance, increased from the soil legacy (Y. Li et al. 2017). *Phleum* also contained multiple genes with possible roles in plant stress response such as such as *NAC1*, *2* & *48*, *ABC C3*, *G14*, & *G25*, *CDPK 30*, *ICE*, *DHCOR410*, *DHN1*, *DHN3*, *DHRAB26*, *DHRAB 15*, *DHRAB16b*, *LEA 5*, *6*, *17* & *18*, and *Galactinol synthase 1*.

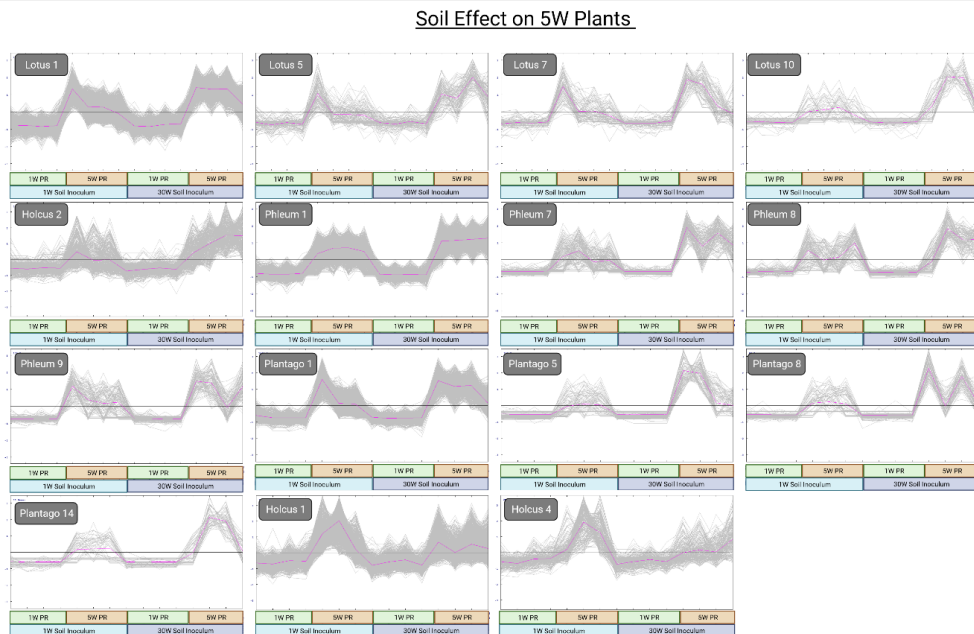


Figure 9: Matching cluster patterns for all species where an effect of soil inoculum can be seen on 5W plants but no soil effect can be seen on 1W plants. An increase in expression due to 30W

inoculum is seen in 13 clusters (*Lotus* 1, 5, 7, 10; *Holcus* 2; *Phleum* 1, 7, 8, 9; *Plantago* 1, 5, 8, 14). While a decrease in expression is seen in two clusters for *Holcus* (1 & 4).

3.5 Cell wall modification and plant hormone changes induced by different precipitation regimes and soil legacy

As seen in the transcriptomic results, multiple cell wall, hormone related genes were increased due to the soil legacy. We therefore selected multiple metabolites/compounds to study based on the pathways with the most related DEGs. For instance, multiple genes relating to the lignin biosynthesis pathway are over expressed in *Lotus*, so we measured lignin content to see if the transcriptional changes corresponded with metabolite and biochemical changes. These genes were not found in *Holcus* and hence a shift in cell wall composition is expected to be seen in these biochemical validation experiments, with differing effects for each species.

In *Holcus* and *Lotus* we found no significant differences between 1W, 5W and different soil types on cellulose concentration (Figure 10a). In *Phleum* and *Plantago*, cellulose was significantly decreased under 5W compared with 1W ($p < 0.01$), but no significant effects of different soil types were detected (Figure 10a). Hemicellulose contents were significantly decreased under 5W compared 1W in *Holcus* ($p < 0.001$), *Phleum* ($p < 0.01$) and *Lotus* ($p < 0.05$), but no evident changes were found between different soils in four species (Figure 10b). Callose contents significantly accumulated under 5W compared with 1W in *Phleum* ($p < 0.01$), *Plantago* ($p < 0.001$) and *Lotus* ($p < 0.001$) (Figure 10c). Regarding the soil effect, under 5W treatment, *Plantago* that grew in 30W soil accumulated more callose than those that grew in 1W soil, which is consistent with transcriptional findings that *Plantago* had the most genes relating to callose synthesis pathways (Figure 10c). Pectin was significantly reduced under 5W

compared with 1W in *Holcus* ($p < 0.01$; Figure 10d), but no significant soil effect was observed. There were no significant differences between watering regimes and soil background in the other three species (Figure 10d). Regarding to xyloglucan, *Holcus* and *Lotus* accumulated more xyloglucan under 5W compared with 1W ($p < 0.001$ and $p < 0.01$, respectively; Figure 10e). Specifically, under 5W, plants that grew under 30W soil showed more accumulation than those that grew under 1W soil (Figure 10e). All four species showed higher lignin concentration under 5W compared with 1W (Figure 10f). Under 5W, *Plantago* and *Lotus* exhibited higher concentration of lignin when grown with 30W soil when compared with those grown on 1W soil (Figure 10f).

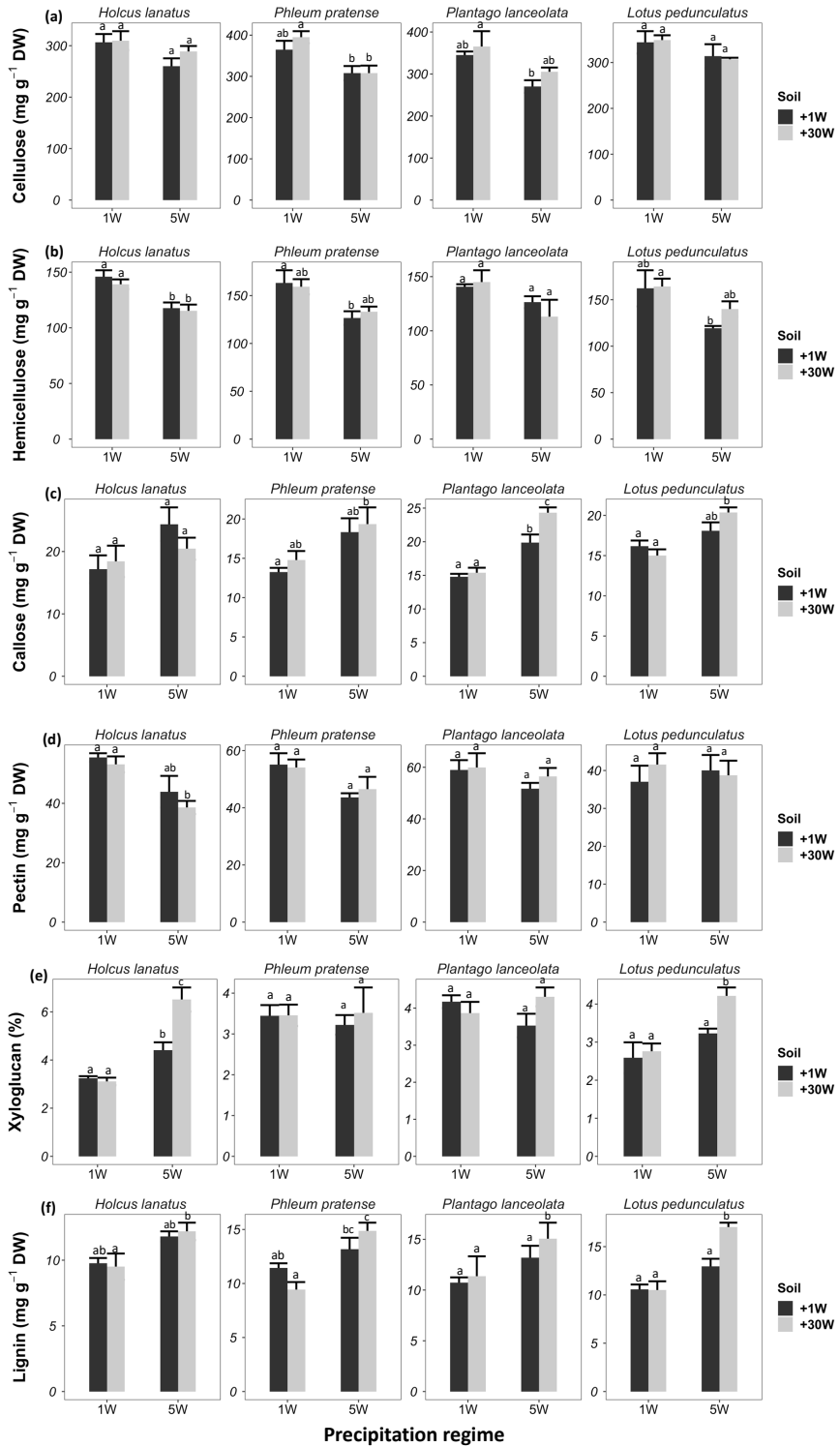


Figure 10 Cell wall compositions per dry weight (DW) of each species under different watering regimes and soil background. Data are represented as mean \pm SE ($n=4$). Different letters represent the significant differences between groups (Tukey HSD test; $p < 0.05$).

Enzymes related to cell wall modification were also measured in this study. Generally, the three species *Holcus*, *Phleum* and *Plantago* exhibited higher activities of CAD, peroxidase, callose synthase and chitinase under the 5W than under the 1W regime (Figure 11). Under the 5W regime, the enzyme activity in these three species consistently trended to be higher on 30W soil samples compared to the 1W soil samples, though this shift was not always significant (Figure 11).

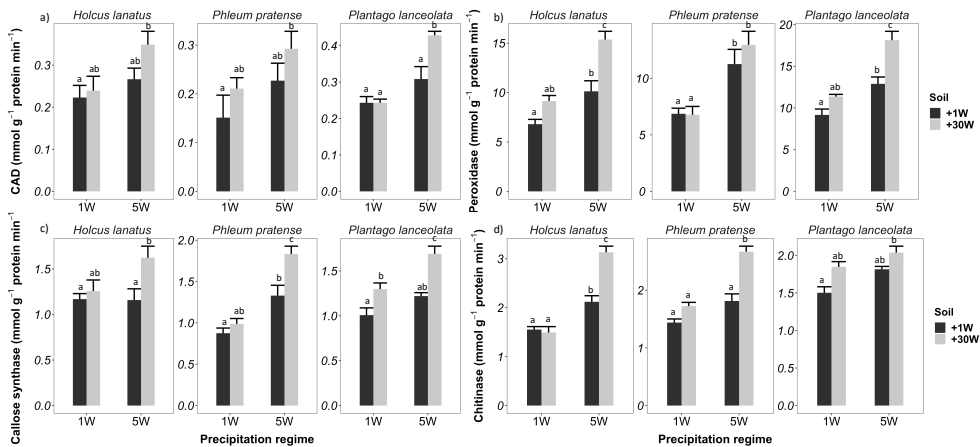


Figure 11 Enzymes related to cell wall modification under different precipitation regimes and soil background. Data are represented as mean \pm SE ($n=4$). Different letters represent the significant differences between groups (Tukey HSD test; $p < 0.05$).

Significant evidence in the transcriptional results showed differing regulation of hormones under drought stress due to the soil inoculum. For instance, TIFY genes were found across species that are known to influence jasmonic acids regulation. In *Holcus*, there were no significant differences in jasmonic acid concentration between different watering regimes and soil, however jasmonic acid was increased under 5W compare with 1W in *Phleum* ($p < 0.01$), *Plantago* ($p < 0.01$) and *Lotus* ($p < 0.001$; Figure 12a). Under 5W treatment, *Phleum* and

Lotus accumulated more jasmonic acid when grown with 30W soil when compared with 1W soil (Figure 12a). All four species accumulated more abscisic acid under 5W than 1W (Figure 12b); under 5W, although not significant, four species showed a tendency to accumulate more abscisic acid on 30W soil than 1W soil (Figure 12b). As for ACC (ethylene precursor), there were no significant effects between different watering regimes and soil in *Holcus* and *Lotus*; while it increased under 5W compare 1W in *Phleum* and *Plantago* (Figure 12c).

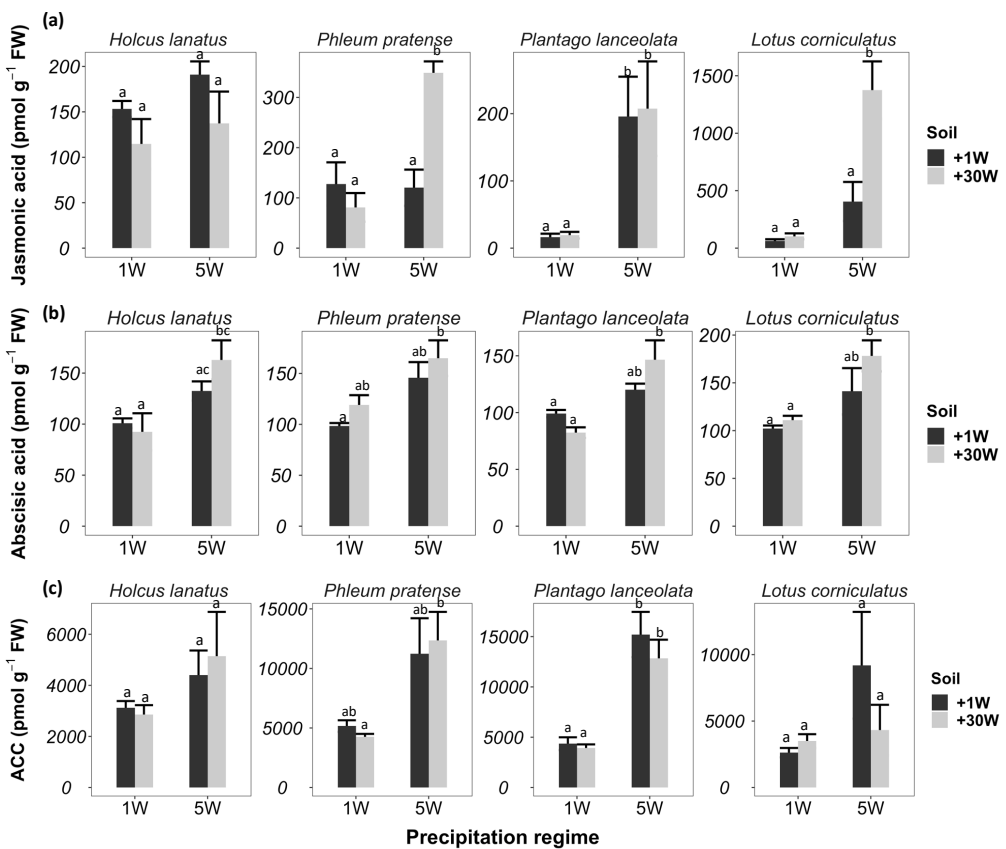


Figure 12 Plant hormone of each species under different precipitation regimes and soil background. Data are represented as mean \pm SE (n=4). Different letters represent the significant differences between groups (Tukey HSD test; $p < 0.05$).

4 Discussion

In this study, we investigated the soil microbiome legacy induced four common grassland species responses to subsequent PR, across whole plant, physiology, transcriptome and biochemical levels.

4.1 More persistent PR reduced plant productivity and fitness

Our previous research on a multispecies open-air experiment has shown that increasingly persistent PRs significantly reduced grassland diversity (Reynaert et al. 2021). This reduced species richness is probably due to the combined effect of PRs and interspecific competition. Our current monoculture experiment demonstrates that the increasingly persistent PRs significantly reduced each species survival, fresh weight, and photosynthetic activity (Figure 4; 5). Consistent with the findings from the outdoor experiment (Reynaert et al. 2021), we find *Holcus* to be more sensitive towards increasingly persistent PRs compared to *Phleum* when comparing Fv/Fm from 10-day PR (Figure 5). *Plantago* differed from the other three species (especially the two grasses, *Holcus* and *Phleum*) under 20D regime by exhibiting recovery at the end of the experiment (wet period) by generating new leaves (Figure 4). This is consistent with Morales et al. (2021), who reported that *Plantago* is able to fully regenerate its above-ground biomass through renewed growth once the stress has ceased. However, since *Plantago* has undergone only one 20-day dry/wet cycle, it would be interesting to know the performance of *Plantago* under an extended 20-day dry and wet cycle. It can be expected that although *Plantago* may still regenerate during the wet period, the overall yield will not be able to reach the overall growth under a regular PR. *Lotus* and *Phleum* are relatively small sized plants. This conservative growth/resource strategy likely led to their

increased survival and lowered stress under mild PR conditions (e.g., 10D) compared to *Holcus* and *Plantago*. However, it should be noted that although a conservative resource strategy may help plants cope with drought stress, our previous multispecies experiment showed that N-fixers such as *Lotus* exhibited a lower baseline competitive success (lower survival rate under normal PR) compared with fast-growing grasses such as *Holcus* (Reynaert et al. 2021), therefore, both the baseline competitive ability and stress sensitivity need to be taken into consideration when evaluating the performance of grassland species in response to the altered PR.

4.2 Soil legacy affected plant responses to the subsequent PR at transcriptome and biochemical level

In our recent outdoor study, we found that more persistent PR causes a pronounced soil microbial legacy but no significant impact on the aboveground biomass of subsequent plant communities (L. Li, Lin, et al. 2023). In this study, where competition between species was removed, at 5W PR we observed differences in plant productivity for three of the four species studied due to soils with different climate histories. *Holcus* and *Plantago* seems benefited from the soil history, while *lotus* had a detrimental effect, and no effect was observed for *Phleum* (Figure 4). Transcriptome analyses are genome-wide and highly sensitive and therefore an ideal method to identify responses that do not directly relate to profound overall growth responses. We found PR to be the main factor influencing the transcriptomic and biochemical changes across these four species (Figure 6). However, soil microbiome legacy also induced significant differences at the transcriptomic and biochemical levels of each species (Figure 8; 9). We are particularly interested in how soil with a more persistent PR (30W) history stimulates plant responses to the subsequent more

persistent PR (5W) (Figure 9). We found that upregulation of pathways related to hormone synthesis, oxidative stress, cell wall modification, and chitin catabolic process under 5W conditions in four species were enhanced by soils with a more persistent PR history (Figure 13). The upregulation of these processes should help us understand how plants can adjust to recurring extended PR regimes.

Chitin is a specific component of fungal cell walls (Wan et al. 2008). The enhanced response of chitinase and endochitinase under 5W PR with 30W soil indicated the activation of the plants' defense against fungal pathogens attack (Grover 2012; Wan et al. 2008). Our study also found that *MAPK* (20, 17, & 18) and *WRKY* (24, 33, 76, & 40) showed an enhanced response to 5W PR with 30W soil. *MAPK18* and *WRKY33* have been directly connected to chitin response in rice and Arabidopsis (Yamada et al. 2017; Wan et al. 2004). The TFs *WRKY* have been shown to be activated by *MAPK* cascade, suggesting that TFs are highly involved in chitin signaling (Wan et al. 2004). That the 30W soil stimulates this increase in chitin response is likely due to a significant shift in the fungal community composition in 30W soil compared to 1W soil (L. Li, Nijs, et al. 2023). Significant shifts in cell wall response were seen across all four species in this study (Figure 9), consistent with previous studies on biotic and abiotic stressors that found cell wall modification is a common response (Bacete et al. 2018; Novaković et al. 2018). In our study, we found that Receptor Like Kinases (RLKs) such as *SAPK6*, *SAPK4*, *LECRKSIT2*, *SIK1*, and *CRK2* showed highest upregulation under 5W PR with 30W soil. These RLKs act as cell wall integrity (CWI) sensors, which detect molecules originating from pathogens or cell wall damage induced by abiotic stress (Bacete et al. 2018; Baez, Tichá, and Hamann 2022; Novaković et al. 2018). Although RLK signaling during abiotic stress remains

largely unknown (Novaković et al. 2018), it has been shown that over-expression *SAPK6* improves drought and temperature tolerance in rice (Chang et al. 2017), *SAPK4* regulate salt stress acclimation (Diédhiou et al. 2008). The cell wall damage signals, in turn, can trigger ROS response (Tenhaken 2015) and hormone pathways such as jasmonic acid (Mielke and Gasperini 2019), ethylene, abscisic acid (ABA) and salicylic acid (SA)(Bacete et al. 2018). Consistently, we find several Ethylene Response Factors (ERFs), jasmonic acid response genes *TIFY 9*, & *11*, and genes involved in salicylic acid pathway *MACPF* & *BRN1* were upregulated most under 5W PR with 30W soil legacy (Y. Qi et al. 2010). Over-expression of *TIFY11* and *MACPF* may have a similar response in our study as compared with previous studies which found *TIFY11* to be related to increased tolerance to salt and dehydration stresses in rice (Ye et al. 2009) and that *MACPF* genes play significant roles during plant vegetative growth and environmental stress adaptation in *Poaceae* (L. Yu et al. 2020). Here, we also show that all four species exhibited the highest concentration of abscisic acid under 5W PR with 30W soil legacy (Figure 12b). This further indicates that soil with a more persistent PR history may enhance plant responses towards subsequent persistent PR by activating hormone signaling pathways, especially jasmonic acid and abscisic acids. The ROS pathway can further regulate cell wall remodeling and integrity maintenance (Figure 13)(Didi et al. 2015; Denness et al. 2011; Novaković et al. 2018). ROS-induced activity of peroxidases is the primary mechanism involved in wall modification during stress (Novaković et al. 2018) . Peroxidases are proposed to polymerize lignin molecules by cross-linking cell wall aromatic compounds; therefore, they are tightly associated with cell wall loosening and stiffening (Francoz et al. 2015; Q. Liu et al. 2018. In our research, *peroxidase 4*, *52*, *2*, *3*, & *CAD 1* were enhanced

under 5W PR with 30W soil legacy. We conclude based on the results that all four species showed the highest peroxidase levels under 5W PR with 30W soil legacy (Figure 11b) and the known association of these genes with lignin biosynthesis (Warinowski et al. 2016), that the enhanced response of peroxidase genes activates the lignin biosynthesis pathway. Specifically, *Plantago* and *Lotus* exhibited the highest content of lignin under 5W PR with 30W soil legacy (Figure 10f). Increased accumulation of lignin provides a barrier against pathogen attack and reduces the infiltration of fungal enzymes and toxins into plant cell walls (Q. Liu et al. 2018; Santiago et al. 2013); it also reduces cell water penetration and transpiration, which helps to maintain cell osmotic balance and protective membrane integrity (Q. Liu et al. 2018; Monties and Fukushima 2005). In our previous open-air experiment, we found the phenylalanine/tyrosine metabolic pathway, which acts upstream of lignin biosynthesis, is enhanced in more persistent PR responses and is thought to play an important role in the tolerance capacity of different grassland species (Zi et al. 2023). Except lignin, genes related to other cell wall components such as pectate lyase (*A, D, & F*), callose synthase (*9*), and endoglucanase (*5, 13, 4, 6, & 14b*) were enhanced due to 30W soil microbiome mediated legacy effects (Figure 13). These genes have played a central role in modulating cell wall extensibility and plasticity, which is an adaptive mechanism to water deficit and growth adjustment (Le Gall et al. 2015).

It should be noted that the inoculation responses observed in this research can't be completely attributed to soil microbiome. By using a soil dilution (e.g. 10% in a 90% sterilized soil), differences in nutrients and other chemical compounds are strongly diluted out, whereas inoculants only need a low concentration to multiply from. Hence, any subsequent effects are more likely

to be of microbial origin than anything else. Furthermore, the dilute chemical compounds are also likely to have been microbially metabolized in the meantime (between training and experimental phases). Still, we can't completely rule out the role of plant signals in the responses.

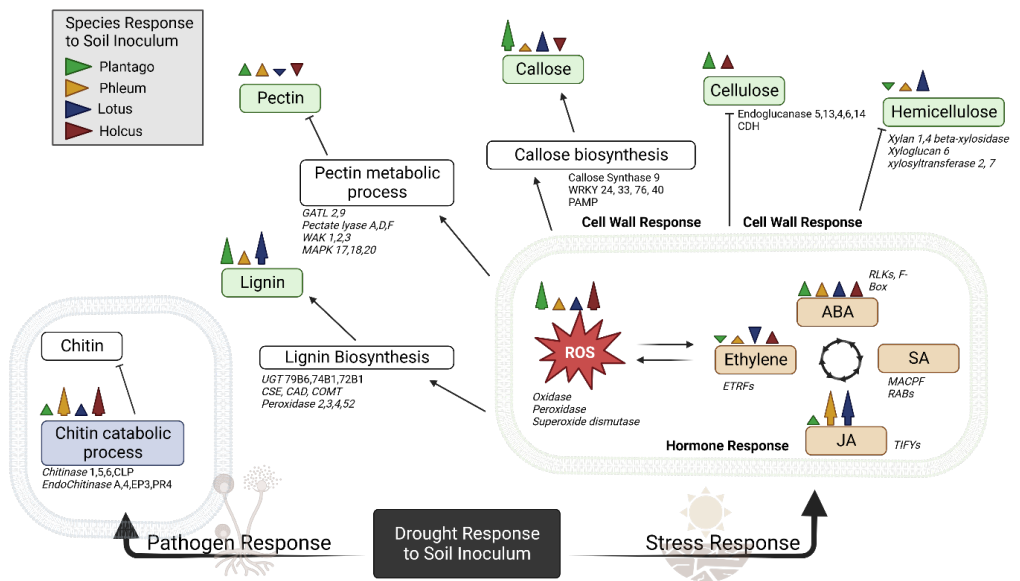


Figure 13 Summary and proposed pathways for transcriptional regulation of 5W PR in combination with 30W inoculated soil in four grassland species. Highlighted boxes represent levels that were measured with biochemical analysis. The arrows above indicate the increase (up arrow) or decrease (down arrow) as well as significance of the shift (larger or smaller arrow). Genes that were found to be overly expressed are shown under their respective pathways.

4.3 Comparisons between different functional group and species

As discussed in the earlier sections, different species showed similarities in their response to the soil legacy mediated PR effects in terms of productivity and transcriptome shifts. However, there are notable differences which might relate to tolerance capacity and functional group dominated responses. *Holcus* was found to be a relatively sensitive species in our previous multispecies study in response to more persistent PRs (Zi et al. 2023; Reynaert et al. 2021). In this study, *Holcus* also exhibited high sensitivity towards altered PR (faster

reduction of survival, biomass and photosynthesis activity) compared with the other grass *Phleum*. Particularly, we found that *Holcus* exhibited much less DEGs compared with the other three species (Figure 6), which suggests that *Holcus* is less capable of re-programming its transcriptome under more persistent PRs, and this may be part of the reason for being sensitive to the altered PR. Although chitinase activity was also enhanced under 5W PR with 30W soil in *Holcus*, the chitinase catabolic pathway was not overrepresented, unlike the other three species (TableS3). The lignin biosynthesis pathway is overrepresented in *Lotus* and *Plantago*, which is confirmed by biochemical analysis that lignin is significantly increased under the 5WPR with 30W soil legacy in the two species (Figure 10). *Holcus* showed no overrepresentation or significant changes in lignin content across the study, a possible explanation for its sensitivity to shifting PR. The reason that *Lotus* could accumulate more lignin in a stress event is possibly because *Lotus* is a nitrogen-fixing plant, which have a higher nitrogen usage efficiency, and it is reported that a higher nitrogen concentration in the soil can increase plant lignin content (Basyal et al. 2022).

5 Conclusion

To the best of our knowledge, this study is the first to examine the effect of a soil microbiome with climate legacy on the growth of non-model grassland species under subsequent more persistent PRs. We found that more persistent PRs significantly reduced the plants survival, productivity and photosynthesis, but that soil legacy shifted the effects of more persistent PR. Transcriptomic and biochemical analysis revealed that pathways related to hormone synthesis (e.g. jasmonic acid, abscisic acid, salicylic acid, ethylene), oxidative stress, cell wall modification, and chitin catabolic processes were affected under 5W PR. Moreover, soil with a more persistent PR history promoted the upregulation of

these processes, which may provide potential beneficial effects for plants in response to the more persistent PR. We previously showed that exposure to more persistent PRs significantly shifted the soil microbial community. The results in this study suggest this increases the amount of positive symbiotic interactions during the subsequent persistent PR stress events. Although, the changes at plant transcriptomic and biochemical level under these conditions may not be able to induce a significant, systematic change on plant survival or biomass during this short-term experiment, these effects may become more significant under a prolonged study. We also found *Holcus lanatus* to be less capable of significant changes at transcriptomic level under persistent PR, which may partially explain its sensitivity towards the altered PRs. Currently the changes of soil microbial community composition are being analyzed, which will provide greater evidence and possibly a more detailed mechanism about the soil legacy mediated responses of grassland species to the increasingly persistent PRs.

6 Supplementary

Supplementary is available at:

<https://data.mendeley.com/datasets/9mp843mss4/1>

Chapter 6

Discussion

1 Discern potential tipping point (threshold) in plant responses to prolonged dry/wet period

The weather pattern is becoming more persistent as predicted by climate change models, with one of the main features being both the prolonged dry and wet period (IPCC 2021; Knapp et al. 2008; Zeppel et al. 2014; Breinl et al. 2020). The dry and wet spell induce contradictory stress to ecosystems and are considered as major risks in many areas if it became extreme (Zandalinas et al. 2018; Kreienkamp et al. 2021). However, the alternated longer dry and wet spell are still scarcely studied so far; therefore, it is important to explore at which degree of combined dry and wet period induce irreversible damages to the ecosystem (Smith 2011).

By applying a gradient approach (increased longer dry and wet period) in this study, possible thresholds or tipping points may be identified (De Boeck, Bloor, et al. 2018). The ecosystem responses to climate extremes contain multiple layers. In this study, I found that the sensitive species *Centaurea jacea* showed a tipping point of metabolome changes at 10-days dry/wet PR, while the other three species *Holcus*, *Phleum* and *Plantago* showed significant changes at 20-days dry/wet PR. Interestingly, regarding to the soil microbiome, we have found that the fungal diversity and connectivity tended to change most from 10-days dry/wet PR (L. Li, Nijs, et al. 2023). From 20-day PR onwards, plant species diversity was significantly decreased (Reynaert et al. 2021). This reflects that the increasingly persistent PRs may first affect the sensitive individual through molecular, physiological, morphological changes. Except plants, the microbiome community properties were strongly affected by more persistent PRs, and even earlier than plant responses. These changes will have a positive or negative effect on ecosystem processes (such as productivity, nutrient

cycling, etc.), and results in higher-order responses for instance shifts in species abundances (Smith 2011).

It should be noted that the discussed potential tipping point of different levels highly depends on the temperature. As predicted by the intergovernmental panel on climate change, a global temperature will increase 1.5 °C in the early 2030s (IPCC 2021). Exceeding 1.5 °C global warming could trigger multiple climate tipping points according to Armstrong McKay et al. (2022). According to our study, the soil water content decreased significantly during heatwaves in July and August 2019, even under the wet period (Reynaert et al. 2021). Therefore, it can be foreseen that the rising temperature will exacerbate the effect of longer dry spell in the more persistent PRs, and the ecosystem would be more vulnerable even under a mild PR.

2 Amino acids, cell wall modification, and hormone signaling pathways are highly involved in responses to more persistent PRs

According to the open-air mesocosm experiment and growth room experiment, we have found that amino acids metabolism, cell wall modification and hormone signaling pathway are highly related to the more persistent PR responses in multiple species (Figure 1). Amino acids are precursors of several secondary metabolites; therefore, the changes of these compounds can produce alterations of secondary metabolism (Romero et al. 2021). Particularly, phenylalanine, alanine accumulation is a general response across several grassland species under more persistent PRs (Chapter 2). Phenylalanine serves as the substrate of phenylalanine ammonia-lyase (PAL), the key enzyme in the phenylpropanoid pathway (Romero et al. 2021). Phenylpropanoids contribute to almost all aspects of plant responses towards biotic and abiotic stimuli.

Lignin, suberin, tannins are phenylpropanoid-based polymers, which contribute substantially to the stability and robustness of plants towards mechanical or environmental damage, such as drought or wounding (Vogt 2010; Moura et al. 2010). Consistently, several species showed higher concentration of lignin under more persistent PRs (Chapter 3; Figure 1). The increase of lignin and related enzymes such as peroxidase and cinnamyl alcohol dehydrogenase were further confirmed through transcriptomic and biochemical analysis in the growth room experiment (Chapter 5; Figure 1). The increased lignin deposition not only improves cell wall rigidity, but also can reduce plant cell wall water penetration and transpiration, which helps to maintain cell osmotic balance and protective membrane integrity when plants under persistent PRs (Q. Liu et al. 2018). Except lignin, the other cell wall components such as cellulose, hemicellulose, pectin have also been significantly affected by persistent PRs (Chapter 3; 5). Although the modified cell wall structure and composition may enhance the tolerance of plants to the changed PR, it should be noted that the increased lignin may reduce the biomass quality (Johnson et al. 2018), as lignin interferes with the digestion of cell wall polysaccharides by acting as a physical barrier to microbial enzymes (Moore and Jung 2001). The cell wall damage signals can further activate hormone signaling pathways (Mielke and Gasperini 2019). Through transcriptomic analysis, we found that jasmonic acid, ethylene, abscisic acid and salicylic acid pathways were upregulated under more persistent PRs, which were confirmed by biochemical analysis (chapter 5; Figure 1). By increasing the organic osmoprotectants and antioxidative enzyme activity, jasmonic acid effectively improves the drought tolerance of plants (Ali and Baek 2020). Under drought stress, it is well known that ABA can mediate stomatal closure which reduces water loss by decreasing transpiration rate (Muhammad Aslam et al.

2022). Moreover, ABA progressively increases hydraulic conductivity and stimulates root cell elongation, enabling plants recovery from water-limited conditions (Daszkowska-Golec 2016). The effect of SA on drought tolerance remains to be determined; it has been suggested that low concentrations of applied SA increase drought tolerance, whereas high concentrations decrease drought tolerance (Miura et al. 2014). As one of the most diversified signaling molecules, ethylene acclimates plants under adverse conditions. It promotes adventitious root formation, regulates opening and closing of stomatal aperture, etc (Husain et al. 2020). These hormones interact with other signaling molecules and initiates a cascade of adaptive responses of plants towards the altered PR.

3 Different strategies of species with varied sensitivity in response to more persistent PRs

In this study, I found that the metabolome of sensitive species exhibited higher variation than in the relatively tolerant species, and the metabolome of sensitive species significantly changed at a mild PR while the tolerant species changed at more persistent PR (chapter 2). On the other hand, the variation of biochemical components induced by altered PRs in the most sensitive species was less than in the other three species (chapter 3). The biochemical components such as lignin, cellulose, hemicellulose are long chain polymers, for which the synthesis and degradation is relatively time-consuming. On the other hand, the metabolome is the composition of small molecular weight molecules (metabolites) which is highly dynamic in time and can be seen as a snapshot of the current status of plants (Hong et al. 2016; Almeida et al. 2020). We speculate that under the altered PR, more sensitive species are less capable at inducing longer term acclimation but rely more on transient defense

responses that need constant reallocation of resources. I have also found that on some key metabolites/compounds such as phenylalanine, alanine, lignin, the magnitude of accumulation in tolerant species is higher than in sensitive species (chapter 2; 3). These results suggest that the accumulation of these metabolites/compounds may be key factors limiting acclimation of sensitive species in response to more persistent PRs.

4 Acclimation potential of grassland ecosystem to more persistent weather

Climate history is an important determinant of ecosystem responses to repeated environmental extremes, through direct damage, community restructuring, changed soil properties and microbiome community, as well as acclimation in plant species and individuals (Reynaert et al. 2022; Menezes-Silva et al. 2017). In this study, we aimed to elucidate climate history effects at multiple levels, including community, species, soil microbiome and plant molecular changes. The grassland community exhibited acclimation potential after pre-exposure to extreme PR, by showing stimulated biomass and structural sugar content in the following growing season (Chapter 4; Figure 1). This outcome probably is the result of environmental filtering (selected the tolerant species/individuals), changed molecular, physiology stress responses of individual plant, and the possible below ground changes such as soil nutrition, microbiome community. However, it should be noted that this acclimation potential is at the cost of filter out the sensitive species/individuals, the ecosystem is at a risk of biodiversity loss. On the other hand, plants pre-exposed to normal PR showed more activated molecular stress responses (higher proline and antioxidants) under extreme PR in the next growing season, which repressed the carbon allocation to biomass (Chapter 4). We further

investigated the soil microbiome history effect in chapter 5. Transcriptomic and biochemical analysis revealed that the soil with more persistent PR history enhancing plant stress and immune responses such as hormone signaling, oxidative stress, cell wall modification, chitin catabolic process under more persistent PR (Figure 1), probably provide potential beneficial effect to plants (Ali and Baek 2020; Miedes et al. 2014). However, this soil microbiome legacy effect is not strong enough to induce profound changes at plant biomass and survival level, maybe because of the short-time scale of this growth room study, but more likely reflect that a sufficient acclimation is the combination and interaction effect of multiple organizational levels.

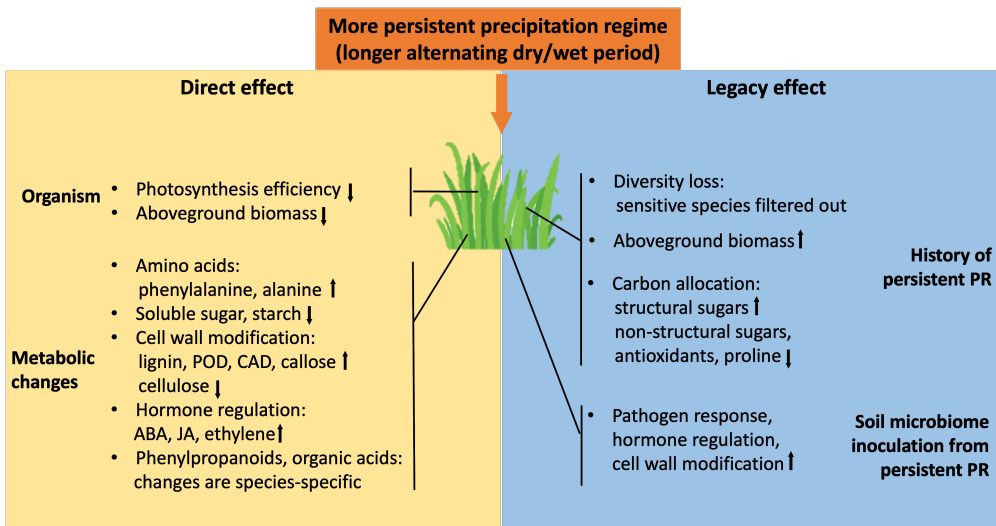


Figure 1 Schematic overview of the most important conclusions found in this PhD study. An arrow up (↑) indicates increased values, while an arrow down (↓) indicates decreased values.

5 Soil-plant interactions

Water availability is a key driver of both plant and soil microorganism functions, including soil C and N cycling (Engelhardt et al. 2021). According to my colleague Lingjuan’s research, under wet start regimes, the total C, total N and C/N showed a tendency to decline with more persistent PRs (L. Li, Nijs, et al.

2023). Variations in the availability of C and N have serious impacts on plants, as these elements are essential nutrients for plant development (Elbasiouny et al. 2022). Nitrogen is one of the main regulators for the changes in photosynthesis and quantum yield (Fv/Fm) of the plant, because up to 75% of leaf N is present in the chloroplasts (Tantray et al. 2020; J. Tang et al. 2019). The decreased N in the soil may partially explain the reduced Fv/Fm observed under the more persistent PRs (Chapter 2). Furthermore, cell walls accumulate a significant amount of N, at up to 10% of cell wall materials (J. Tang et al. 2019). I have found that cell wall remodeling is highly activated under the more persistent PRs (Chapter 3 and 5), potentially accelerating nitrogen consumption from the soil. On the other hand, the total C, N did not exhibit significant differences among dry start regimes which ended with wet period, possibly associated with the 'Birch effect': a burst of CO₂ and release of inorganic nitrogen when rewetting a dry soil (Jarvis et al. 2007; Singh et al. 2023). The Birch effect may potentially diminish the differences induced by different dry start regimes. The non-significant changes in soil C and N among dry start regimes may contribute to the observation that the more persistent dry start regimes induced less changes in certain metabolites (e.g., phenylalanine, alanine, as discussed in Chapter 2) compared to the wet start regimes.

Based on Lingjuan's study, except affect soil nutrients, more persistent PRs also reduced the fungal diversity (L. Li, Nijs, et al. 2023). Among the fungal phyla, Ascomycota exhibited a slight increase under more persistent dry start PRs, while other phyla did not show clear patterns (L. Li, Nijs, et al. 2023). Ascomycota exhibits a broad range of lifestyles, including pathogenic, saprobic, and endophytic (Wijayawardene et al. 2021), and is involved in both beneficial and negative plant interactions (Challacombe et al. 2019; Priyashantha et al. 2023). When a plant fails to induce effective defense responses, the pathogenic

fungi can infect plants and causing disease (Priyashantha et al. 2023). On the other hand, if the host's defense mechanisms effectively stop the spread of the pathogen, the pathogen attack can even be seen as 'priming', that the plants acquire enhanced resistance to both biotic and abiotic stress, as observed in Chapter 5. The exact nature of plant-fungi interactions under more persistent PRs still needs further study in the future.

6 Challenges

In this thesis, both outdoor mesocosms and a controlled growth room were utilized to study the effects of altered PRs. Both approaches have their advantages and limitations due to the inherent trade-offs between experimental realism (facilitating extrapolation) and control (facilitating the attribution of observed responses)(De Boeck et al. 2015; Kröel-Dulay et al. 2022). The outdoor mesocosm experiment provides a more realistic condition, including natural variations in temperature, light, as well as interactions with pollinators and microorganisms. In addition, the outdoor experiment is suitable for long-term, large-scale study, allowing us to study acclimation at ecosystem level. However, it is impossible to avoid some artifacts; for instance, the humidity of the external environment will impact the results of PR treatments. On the other hand, there were moments of high air humidity coinciding with drought treatment periods, as well as moments of low humidity during drought treatment. Therefore, humidity could exert both positive and negative effects on the treatments, potentially may neutralize the outcome. Heatwave is another factor that affect the soil water contents (SWC) induced by PRs. The summer of 2019, corresponding to the period of the mesocosms experiment, experienced unusually high temperatures. It was marked by two heatwaves in the latter part of July and August, with a daily maximum temperature of 39.7°C

recorded on 25/07 (KMI 2019). The two heatwaves intensified the impact of the dry period and also led to a decrease in SWC even during the wet period (Figure S2, chapter 2), resulting in some non-evident patterns. For instance, 10D PR was under dry period in the first heatwave, causing a decrease in SWC below the permanent wilting point (PWP) until the end of July. This extremely dry period could alter soil characteristics. According to my colleague's unpublished work, soils become more water repellent with a build-up period of 7 days, leading to reduced infiltration rates and decreased water use efficiency during the subsequent wet period. Muhr et al. (2010) also reported that rewetting could not restore soil moisture of the dry soil as before, presumably because of preferential flow and water repellency of soil organic matter. Therefore, the 10D treatment exhibited lower SWC compared to its counterpart 10W, which was under wet conditions during the first heatwave period (Figure S2, Chapter 2). This highlights the intricate interplay among PR, humidity, temperature, and the timing of irrigation in the outdoor experiment setting.

In Chapter 2, untargeted metabolomic analysis was applied to study the comprehensive profile of several grassland species. It is a powerful tool to analyze diverse sample types without the prior knowledge of the expected metabolites (Sardans et al. 2011). This is especially advantageous in our research, as it is an exploratory study and have limited plant material. However, many benefits of untargeted analysis accompanied with limitations, including the lower precision compared with the targeted analysis, bias towards detection of high-abundance molecules (Gertsman and Barshop 2018). For instance, plant hormones and some important signaling molecules such as GABA, betaines were barely detected in our untargeted metabolomic analysis (Chapter 2). Moreover, the relatively subtle changes in low-abundance

molecules between different PRs may be challenging to capture through untargeted metabolomics, potentially resulting in the oversight of certain biomarkers. Hence, it is crucial to complement the study with targeted metabolite analysis, and confirm the differences identified through untargeted metabolomics.

7 Perspectives

To compensate for the constraints of outdoor experiments and to precisely attribute the effects of PR, a growth room experiment in chapter 5 with a controlled environment is essential. It is particularly advantageous for transcriptomic and other delicate molecular analyses. In addition, the growth room provides the opportunity for more rapid experiments to explore the PR effects on other species. In fact, I have already conducted a preliminary experiment to test the effect of more persistent PRs on the growth of a model crop plant, maize. I found that the increasingly prolonged dry/wet cycles significantly inhibited the maize growth (Figure 2). Unlike the non-model grassland species which I studied in this project, maize has a well-characterized and sequenced genome, and benefit from well-established resources including a vast collection of mutants (Strable and Scanlon 2009). This allows us to continue in-depth studies on specific genes and pathways, for instance the pathways related to amino acids, cell wall modification and hormone regulation that I found in this research. Besides, maize exhibits significant genetic diversity with various cultivars. Therefore, it will be interesting to screen and select sensitive and tolerant maize lines and identify potential biomarkers in the future study.

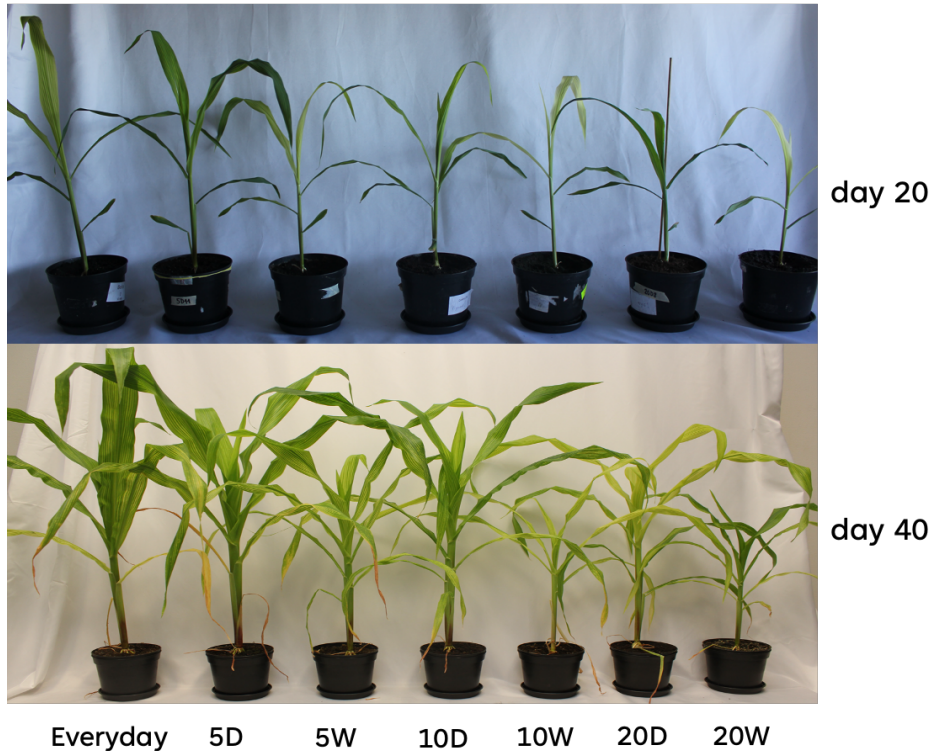


Figure 2 Illustration of the effect of increasingly prolonged dry/wet cycles on maize growth. Maize plants were under different dry/wet cycles, ranging from watered every day, 5-day dry/wet cycle until 20-day dry/wet cycle. The experiment lasts 40 days, and all the plants received the same amount of water at the end of experiment. 'D' and 'W' represents dry start and wet start treatment, respectively.

In this thesis, I focused on studying the metabolome and biochemical composition changes of plant aboveground material. Another very important aspect is the changes of below ground organs in response to the altered PR. Alterations in the composition of root exudates may influence not only the plant itself but also neighboring plants, soil properties (such as the amount of nutrients), and soil microbiome community (Gargallo-Garriga et al. 2018). Studies have shown that root exudate metabolomes change under drought and show limited capacity for recovery (Gargallo-Garriga et al. 2018); shoots and root showed opposite metabolic response to drought (Gargallo-Garriga et al. 2014) and warming (Gargallo-Garriga et al. 2015). Wedeking et al. (2018) found

that leaves and roots responded with different dynamics to rewatering. The different complementary responses of shoots and roots together buffering the effects of the complex environmental conditions (Gargallo-Garriga et al. 2014; 2015). According to one of the colleague Dr. Olga Vindušková's research, total mesocosm root biomass decreased under more persistent PRs. Given the multispecies environment of the mesocosm experiment, distinguishing and analyzing the roots of each species pose challenges. In the future, creating a monoculture environment would be valuable for a more in-depth exploration of root metabolomic changes under more persistent PRs. This approach will enhance our understanding of plant stress responses, biotic interactions, biomarker discovery, and ecosystem conservation.

Acknowledgement

First and foremost, I want to express my sincere gratitude to my supervisors, Prof. Han Asard and Prof. Hamada AbdElgawad for your expertise, insightful guidance and constant support. Your encouragement and belief in my abilities throughout the journey of my PhD are invaluable to me. It was you gave me the opportunity to pursue my study in Belgium, and I deeply appreciated the four years under your supervision.

Special thanks to Prof. Gerrit Beemster, who consistently provides instructive suggestions and feedback during group meetings. Your calmness and enthusiasm for science are a great inspiration to me.

I am deeply thankful to the other PIs and postdocs of the 'Regime Shift' project, Prof. Ivan Nijs, Prof. Kris Laukens, Prof. Erik Verbruggen, Dr. Hans De Boeck, and Dr. Olga Vindušková. Your expertise in different aspects has been an invaluable asset to the accomplishment and success of the project.

I also want to thank my committee members, Prof. Els Prinsen, Prof. Matteo Campioli, Dr. Otmar Urban, Prof. Hilde Nelissen and Prof. Ann Cuypers. Thank you all for taking time to read my thesis, gave me constructive suggestions to improve my thesis.

I want to thank Dr. Otmar Urban, Dr. Albert Gargallo-Garriga and Michal Oravec for the nice collaborations on metabolomic analysis. Your help and guidance made this research possible and resulted in a nice outcome.

I would like to thank my colleagues Simon, Chase and Lingjuan, it's my great pleasure to work with all of you in this project. Your insights, dedication on the project is a great help for me. I will remember the time that we spent together

on harvesting, transplanting, installing tubes, moving soils...it's all of you make the work less tough and with more fun.

I would like to thank Romain and Cindy in IMPRES group. Whenever I need help on harvesting, I can always count on Romain. You brought me many nice memories during these four years: beers, raclette, video games, board games...hope we can still have raclette together this winter. Cindy, you are the best officemate. I love our little chats, it gave us so much happiness and energy, released our stress especially when we encountered some tough moments during the PhD.

I also would like to thank all the other members in IMPRES (and beyond): Julie, Chiara, Jesper, Jonas, Sevgi, Sophie, Sébastjen, Daria, Naomi, Ahmad, Renato and the students I met and supervised. Thank you all for the help and fun we had together.

I want to express my deepest thanks to my parents, Fengqin, Qinghe and my sister Jing. Your support, love, wisdom are the source for me to grow and become the person I am today. You are always there when I want to talk and need support. I am grateful for being your daughter, Mum and Dad, and for the values you have imparted to me.

In addition to my family members, I would like to thank my boyfriend, Chris. You brought me so much happiness, rest and support, make the journey of completing this thesis much more fun.

Finally, I want to thank myself for keep pursuing my goal and taking challenges, to decide to do my master in Germany, continue my PhD in Belgium...It was a wonderful and meaningful period in my life.

Bibliography

- AbdElgawad, Hamada, Viktoriya Avramova, Geert Baggerman, Geert Van Raemdonck, Dirk Valkenburg, Xaveer Van Ostade, Yves Guisez, et al. 2020. "Starch Biosynthesis Contributes to the Maintenance of Photosynthesis and Leaf Growth under Drought Stress in Maize." *Plant, Cell & Environment* 43 (9): 2254–71. <https://doi.org/10.1111/PCE.13813>.
- AbdElgawad, Hamada, Darin Peshev, Gaurav Zinta, Wim Van Den Ende, Ivan A. Janssens, and Han Asard. 2014. "Climate Extreme Effects on the Chemical Composition of Temperate Grassland Species under Ambient and Elevated CO₂: A Comparison of Fructan and Non-Fructan Accumulators." *PLOS ONE* 9 (3): e92044. <https://doi.org/10.1371/JOURNAL.PONE.0092044>.
- Abdelgawad, Hamada, Dirk De Vos, Gaurav Zinta, Malgorzata A. Domagalska, Gerrit T.S. Beemster, and Han Asard. 2015. "Grassland Species Differentially Regulate Proline Concentrations under Future Climate Conditions: An Integrated Biochemical and Modelling Approach." *New Phytologist* 208 (2): 354–69. <https://doi.org/10.1111/nph.13481>.
- Adams, Henry D., Matthew J. Germino, David D. Breshears, Greg A. Barron-Gafford, Maite Guardiola-Claramonte, Chris B. Zou, and Travis E. Huxman. 2013. "Nonstructural Leaf Carbohydrate Dynamics of *Pinus Edulis* during Drought-Induced Tree Mortality Reveal Role for Carbon Metabolism in Mortality Mechanism." *New Phytologist* 197 (4): 1142–51. <https://doi.org/10.1111/nph.12102>.
- Ahuja, Ishita, Ric C.H. de Vos, Atle M. Bones, and Robert D. Hall. 2010. "Plant Molecular Stress Responses Face Climate Change." *Trends in Plant Science* 15 (12): 664–74. <https://doi.org/10.1016/j.tplants.2010.08.002>.
- Ali, Md Sarafat, and Kwang Hyun Baek. 2020. "Jasmonic Acid Signaling Pathway in Response to Abiotic Stresses in Plants." *International Journal of Molecular Sciences* 21 (2). <https://doi.org/10.3390/ijms21020621>.
- Allan, Richard P., Mathew Barlow, Michael P. Byrne, Annalisa Cherchi, Hervé Douville, Hayley J. Fowler, Thian Y. Gan, et al. 2020. "Advances in Understanding Large-Scale Responses of the Water Cycle to Climate Change." *Annals of the New York Academy of Sciences* 1472 (1): 49–75. <https://doi.org/10.1111/NYAS.14337>.
- Allen, Craig D., Alison K. Macalady, Haroun Chenchouni, Dominique Bachelet, Nate McDowell, Michel Vennetier, Thomas Kitzberger, et al. 2010. "A Global Overview of Drought and Heat-Induced Tree Mortality Reveals Emerging Climate Change Risks for Forests." *Forest Ecology and Management* 259 (4): 660–84. <https://doi.org/10.1016/J.FORECO.2009.09.001>.
- Almeida, Tânia, Gloria Pinto, Barbara Correia, Sónia Gonçalves, Mónica Meijón, and Mónica Escandón. 2020. "In-Depth Analysis of the *Quercus Suber* Metabolome under Drought Stress and Recovery Reveals Potential Key Metabolic Players." *Plant Science* 299 (October): 110606. <https://doi.org/10.1016/J.PLANTSCI.2020.110606>.

Bibliography

Andrews, S. 2010. "FastQC: A Quality Control Tool for High Throughput Sequence Data [Online]."

Araújo, Wagner L., Takayuki Tohge, Kimitsune Ishizaki, Christopher J. Leaver, and Alisdair R. Fernie. 2011. "Protein Degradation – an Alternative Respiratory Substrate for Stressed Plants." *Trends in Plant Science* 16 (9): 489–98. <https://doi.org/10.1016/J.TPLANTS.2011.05.008>.

Arca, Valentina, Sally A. Power, Manuel Delgado-Baquerizo, Elise Pendall, and Raúl Ochoa-Hueso. 2021. "Seasonal Effects of Altered Precipitation Regimes on Ecosystem-Level CO₂ Fluxes and Their Drivers in a Grassland from Eastern Australia." *Plant and Soil* 460 (1–2): 435–51. <https://doi.org/10.1007/S11104-020-04811-X/FIGURES/9>.

Armstrong McKay, David I., Arie Staal, Jesse F. Abrams, Ricarda Winkelmann, Boris Sakschewski, Sina Loriani, Ingo Fetzer, Sarah E. Cornell, Johan Rockström, and Timothy M. Lenton. 2022. "Exceeding 1.5°C Global Warming Could Trigger Multiple Climate Tipping Points." *Science (New York, N.Y.)* 377 (6611): eabn7950. <https://doi.org/10.1126/SCIENCE.ABN7950>.

Arora, Rajeev, Dharmalingam S Pitchay, and Bradford C Bearce. 1998. "Water-Stress-Induced Heat Tolerance in Geranium Leaf Tissues: A Possible Linkage through Stress Proteins?" *Physiologia Plantarum* 103 (1): 24–34. <https://doi.org/https://doi.org/10.1034/j.1399-3054.1998.1030104.x>.

Avramova, Viktoriya, Hamada Abdelgawad, Zhengfeng Zhang, Bartosz Fotschki, Romina Casadevall, Lucia Vergauwen, Dries Knapen, et al. 2015. "Drought Induces Distinct Growth Response, Protection, and Recovery Mechanisms in the Maize Leaf Growth Zone." *Plant Physiology* 169 (2): 1382. <https://doi.org/10.1104/PP.15.00276>.

Bacete, Laura, Hugo Mérida, Eva Miedes, and Antonio Molina. 2018. "Plant Cell Wall-Mediated Immunity: Cell Wall Changes Trigger Disease Resistance Responses." *Plant Journal* 93 (4): 614–36. <https://doi.org/10.1111/tpj.13807>.

Baez, Luis Alonso, Tereza Tichá, and Thorsten Hamann. 2022. "Cell Wall Integrity Regulation across Plant Species." *Plant Molecular Biology* 2022 109:4 109 (4): 483–504. <https://doi.org/10.1007/S11103-022-01284-7>.

Baldoni, Elena, Annamaria Genga, and Eleonora Cominelli. 2015. "Plant MYB Transcription Factors: Their Role in Drought Response Mechanisms." *International Journal of Molecular Sciences* 16 (7): 15811. <https://doi.org/10.3390/IJMS160715811>.

Barchet, Genoa L.H., Rebecca Dauwe, Robert D. Guy, William R. Schroeder, Raju Y. Soolanayakanahally, Malcolm M. Campbell, and Shawn D. Mansfield. 2014. "Investigating the Drought-Stress Response of Hybrid Poplar Genotypes by Metabolite Profiling." *Tree Physiology* 34 (11): 1203–19. <https://doi.org/10.1093/TREEPHYS/TPT080>.

Bardgett, Richard D., Pete Manning, Elly Morriën, and Franciska T. De Vries. 2013. "Hierarchical Responses of Plant-Soil Interactions to Climate Change: Consequences for the Global Carbon Cycle." *Journal of Ecology* 101 (2): 334–43. <https://doi.org/10.1111/1365-2745.12043>.

Barnard, Romain L., Catherine A. Osborne, and Mary K. Firestone. 2013. "Responses of Soil Bacterial and Fungal Communities to Extreme Desiccation and Rewetting." *The ISME Journal* 2013 7:11 7 (11): 2229–41. <https://doi.org/10.1038/ismej.2013.104>.

- Barriopedro, David, Erich M. Fischer, Jürg Luterbacher, Ricardo M. Trigo, and Ricardo García-Herrera. 2011. "The Hot Summer of 2010: Redrawing the Temperature Record Map of Europe." *Science* 332 (6026): 220–24. <https://doi.org/10.1126/SCIENCE.1201224>.
- Basyal, Binod, Cliff Foster, Katherine L. Gross, and Sarah M. Emery. 2022. "Nitrogen Fertilizer, Arbuscular Mycorrhizal Fungi, and Soil Nematodes Affect Lignin Quality and Quantity in Switchgrass (*Panicum Virgatum* L.)." *Bioenergy Research* 15 (2): 1033–41. <https://doi.org/10.1007/s12155-021-10284-2>.
- Bates, L. S., R. P. Waldren, and I. D. Teare. 1973. "Rapid Determination of Free Proline for Water-Stress Studies." *Plant and Soil* 1973 39:1 39 (1): 205–7. <https://doi.org/10.1007/BF00018060>.
- Becklin, Katie M., Jill T. Anderson, Laci M. Gerhart, Susana M. Wadgyamar, Carolyn A. Wessinger, and Joy K. Ward. 2016. "Examining Plant Physiological Responses to Climate Change through an Evolutionary Lens." *Plant Physiology* 172 (2): 635–49. <https://doi.org/10.1104/pp.16.00793>.
- Benson-Evans, K. 1950. "Effect of Microclimate on the Establishment of Timothy Grass." *Nature* 4191 (4191): 325.
- Besseau, Sébastien, Laurent Hoffmann, Pierrette Geoffroy, Catherine Lapierre, Brigitte Pollet, and Michel Legrand. 2007. "Flavonoid Accumulation in Arabidopsis Repressed in Lignin Synthesis Affects Auxin Transport and Plant Growth." *Plant Cell* 19 (1): 148–62. <https://doi.org/10.1105/tpc.106.044495>.
- Bhogireddy, Sailaja, Abishek Xavier, Vanika Garg, Nancy Layland, Renee Arias, Paxton Payton, Spurthi N. Nayak, Manish K. Pandey, Naveen Puppala, and Rajeev K. Varshney. 2020. "Genome-Wide Transcriptome and Physiological Analyses Provide New Insights into Peanut Drought Response Mechanisms." *Scientific Reports* 2020 10:1 10 (1): 1–16. <https://doi.org/10.1038/s41598-020-60187-z>.
- Bilskie, J. 2001. "Soil Water Status: Content and Potential: Campbell Scientific." *Inc. App. Note 2S-1 1784* (435): 84321.
- Boeck, H. J. De, C. M.H.M. Lemmens, H. Bossuyt, S. Malchair, M. Carnol, R. Merckx, I. Nijs, and R. Ceulemans. 2006. "How Do Climate Warming and Plant Species Richness Affect Water Use in Experimental Grasslands?" *Plant and Soil* 288 (1–2): 249–61. <https://doi.org/10.1007/S11104-006-9112-5/FIGURES/6>.
- Boeck, Hans J. De, Seraina Bassin, Maya Verlinden, Michaela Zeiter, and Erika Hiltbrunner. 2016. "Simulated Heat Waves Affected Alpine Grassland Only in Combination with Drought." *New Phytologist* 209 (2): 531–41. <https://doi.org/10.1111/NPH.13601>.
- Boeck, Hans J. De, Juliette M.G. Bloor, Juergen Kreyling, Johannes C.G. Ransijn, Ivan Nijs, Anke Jentsch, and Michaela Zeiter. 2018. "Patterns and Drivers of Biodiversity–Stability Relationships under Climate Extremes." *Journal of Ecology* 106 (3): 890–902. <https://doi.org/10.1111/1365-2745.12897>.
- Boeck, Hans J. De, Erika Hiltbrunner, Maya Verlinden, Seraina Bassin, and Michaela Zeiter. 2018. "Legacy Effects of Climate Extremes in Alpine Grassland." *Frontiers in Plant Science* 871. <https://doi.org/10.3389/fpls.2018.01586>.
- Boeck, Hans J. De, Sara Vicca, Jacques Roy, Ivan Nijs, Alexandru Milcu, Juergen Kreyling, Anke Jentsch, et al. 2015. "Global Change Experiments: Challenges and Opportunities." *BioScience* 65 (9): 922–31. <https://doi.org/10.1093/biosci/biv099>.

Bibliography

- Bogati, K ;, M Walczak, Nikolaos Monokrousos, Kalisa Bogati, and Maciej Walczak. 2022. "The Impact of Drought Stress on Soil Microbial Community, Enzyme Activities and Plants." *Agronomy* 2022, Vol. 12, Page 189 12 (1): 189. <https://doi.org/10.3390/AGRONOMY12010189>.
- Bolger, Anthony M., Marc Lohse, and Bjoern Usadel. 2014. "Trimmomatic: A Flexible Trimmer for Illumina Sequence Data." *Bioinformatics* 30 (15): 2114–20. <https://doi.org/10.1093/BIOINFORMATICS/BTU170>.
- Bolton, Melvin D. 2009. "Primary Metabolism and Plant Defense-Fuel for the Fire." / 487 *MPMI* 22 (5): 487–97. <https://doi.org/10.1094/MPMI>.
- Borken, Werner, and Egbert Matzner. 2009. "Reappraisal of Drying and Wetting Effects on C and N Mineralization and Fluxes in Soils." *Global Change Biology* 15 (4): 808–24. <https://doi.org/10.1111/j.1365-2486.2008.01681.x>.
- Breiman, Leo. 2001. "Random Forests" 45: 5–32.
- Breinl, Korbinian, Giuliano Di Baldassarre, Maurizio Mazzoleni, David Lun, and Giulia Vico. 2020. "Extreme Dry and Wet Spells Face Changes in Their Duration and Timing." *Environmental Research Letters* 15 (7): 074040. <https://doi.org/10.1088/1748-9326/AB7D05>.
- Britten, James. 1871. "Holcus Lanatus." *Notes and Queries* s4-VII (172): 323. <https://doi.org/10.1093/nq/s4-VII.172.323-b>.
- Brookshire, E. N.J., and T. Weaver. 2015. "Long-Term Decline in Grassland Productivity Driven by Increasing Dryness." *Nature Communications* 2015 6:1 6 (1): 1–7. <https://doi.org/10.1038/ncomms8148>.
- Bruce, Toby J.A., Michaela C. Matthes, Johnathan A. Napier, and John A. Pickett. 2007. "Stressful 'Memories' of Plants: Evidence and Possible Mechanisms." *Plant Science* 173 (6): 603–8. <https://doi.org/10.1016/J.PLANTSCI.2007.09.002>.
- Bryant, Donald M., Kimberly Johnson, Tia DiTommaso, Timothy Tickle, Matthew Brian Couger, Duygu Payzin-Dogru, Tae J. Lee, et al. 2017. "A Tissue-Mapped Axolotl De Novo Transcriptome Enables Identification of Limb Regeneration Factors." *Cell Reports* 18 (3): 762–76. <https://doi.org/10.1016/J.CELREP.2016.12.063/ATTACHMENT/B24F06B8-7AC7-45AF-B605-ODA3B55AE55E/MMC11.ZIP>.
- Buchanan, Bob B., Wilhelm Gruissem, and Russell L. Jones. 2015. *Biochemistri & Molecular Biology of Plants*. American Society of Plant Biologists. <https://doi.org/10.1192/bjp.112.483.211-a>.
- Cadotte, Marc W., and Caroline M. Tucker. 2017. "Should Environmental Filtering Be Abandoned?" *Trends in Ecology and Evolution* 32 (6): 429–37. <https://doi.org/10.1016/j.tree.2017.03.004>.
- Cavagnaro, Timothy R. 2016. "Soil Moisture Legacy Effects: Impacts on Soil Nutrients, Plants and Mycorrhizal Responsiveness." *Soil Biology and Biochemistry* 95: 173–79. <https://doi.org/10.1016/j.soilbio.2015.12.016>.
- Cavers, P.B, I.J Bassett, and C.W Crompton. 1980. "THE BIOLOGY OF CANADIAN WEEDS. 47. Plantago Lanceolata L.P." *Canadian Journal of Plant Science* 60: 1269–82.
- Challacombe, Jean F., Cedar N. Hesse, Lisa M. Bramer, Lee Ann McCue, Mary Lipton, Samuel Purvine, Carrie Nicora, La Verne Gallegos-Graves, Andrea Porras-Alfaro, and

- Cheryl R. Kuske. 2019. "Genomes and Secretomes of Ascomycota Fungi Reveal Diverse Functions in Plant Biomass Decomposition and Pathogenesis." *BMC Genomics* 20 (1): 1–27. <https://doi.org/10.1186/s12864-019-6358-x>.
- Chang, Yu, Ba Hoanh Nguyen, Yongjun Xie, Benze Xiao, Ning Tang, Wenliu Zhu, Tongmin Mou, and Lizhong Xiong. 2017. "Co-Overexpression of the Constitutively Active Form of OsZIP46 and ABA-Activated Protein Kinase SAPK6 Improves Drought and Temperature Stress Resistance in Rice." *Frontiers in Plant Science* 8 (June): 1–16. <https://doi.org/10.3389/fpls.2017.01102>.
- Chaudhry, Smita, and Gagan Preet Singh Sidhu. 2021. "Climate Change Regulated Abiotic Stress Mechanisms in Plants: A Comprehensive Review." *Plant Cell Reports*. <https://doi.org/10.1007/S00299-021-02759-5>.
- Chen, Hongjun, Robert G Qualls, and Robert R Blank. 2005. "Effect of Soil Flooding on Photosynthesis, Carbohydrate Partitioning and Nutrient Uptake in the Invasive Exotic *Lepidium Latifolium*." *Aquatic Botany* 82 (4): 250–68. <https://doi.org/https://doi.org/10.1016/j.aquabot.2005.02.013>.
- Chen, Li-Qing, I Winnie Lin, Xiao-Qing Qu, Davide Sosso, Heather E. McFarlane, Alejandra Londoño, A. Lacey Samuels, and Wolf B. Frommer. 2015. "A Cascade of Sequentially Expressed Sucrose Transporters in the Seed Coat and Endosperm Provides Nutrition for the *Arabidopsis* Embryo." *The Plant Cell* 27 (3): 607–19. <https://doi.org/10.1105/TPC.114.134585>.
- Cheng, An Po, Szu Yu Chen, Ming Hsin Lai, Dong Hong Wu, Shih Shun Lin, Chieh Yi Chen, and Chia Lin Chung. 2020. "Transcriptome Analysis of Early Defenses in Rice against *Fusarium Fujikuroi*." *Rice* 13 (1). <https://doi.org/10.1186/s12284-020-00426-z>.
- Chevilly, Sergio, Laura Dolz-Edo, José M. López-Nicolás, Luna Morcillo, Alberto Vilagrosa, Lynne Yenush, and José M. Mulet. 2021. "Physiological and Molecular Characterization of the Differential Response of Broccoli (*Brassica Oleracea* var. *Italica*) Cultivars Reveals Limiting Factors for Broccoli Tolerance to Drought Stress." *Journal of Agricultural and Food Chemistry* 69 (35): 10394–404. <https://doi.org/10.1021/acs.jafc.1c03421>.
- Chiba, Yasutaka, Takafumi Shimizu, Shinya Miyakawa, Yuri Kanno, Tomokazu Koshiba, Yuji Kamiya, and Mitsunori Seo. 2015. "Identification of *Arabidopsis* Thaliana NRT1/PTR FAMILY (NPF) Proteins Capable of Transporting Plant Hormones." *Journal of Plant Research* 128 (4): 679–86. <https://doi.org/10.1007/S10265-015-0710-2>.
- Childs, R. E., and W. G. Bardsley. 1975. "The Steady State Kinetics of Peroxidase with 2,2' Azino Di (3 Ethylbenzthiazoline 6 Sulphonic Acid) as Chromogen." *Biochemical Journal* 145 (1): 93–103. <https://doi.org/10.1042/bj1450093>.
- Chopra, Ratan, Gloria Burow, Andrew Farmer, Joann Mudge, Charles E. Simpson, and Mark D. Burow. 2014. "Comparisons of De Novo Transcriptome Assemblers in Diploid and Polyploid Species Using Peanut (*Arachis* Spp.) RNA-Seq Data." *PLOS ONE* 9 (12): e115055. <https://doi.org/10.1371/JOURNAL.PONE.0115055>.
- Cohen, J., X. Zhang, J. Francis, T. Jung, R. Kwok, J. Overland, T. J. Ballinger, et al. 2019. "Divergent Consensuses on Arctic Amplification Influence on Midlatitude Severe Winter Weather." *Nature Climate Change* 2019 10:1 10 (1): 20–29. <https://doi.org/10.1038/s41558-019-0662-y>.

- Cornic, Gabriel, and Angelo Massacci. 1996. "Leaf Photosynthesis Under Drought Stress BT - Photosynthesis and the Environment." In , edited by Neil R Baker, 347–66. Dordrecht: Springer Netherlands. https://doi.org/10.1007/0-306-48135-9_14.
- Coumou, D., G. Di Capua, S. Vavrus, L. Wang, and S. Wang. 2018. "The Influence of Arctic Amplification on Mid-Latitude Summer Circulation." *Nature Communications* 9 (1): 1–12. <https://doi.org/10.1038/s41467-018-05256-8>.
- Craine, Joseph M., Jesse B. Nippert, Andrew J. Elmore, Adam M. Skibbe, Stacy L. Hutchinson, and Nathaniel A. Brunsell. 2012. "Timing of Climate Variability and Grassland Productivity." *Proceedings of the National Academy of Sciences of the United States of America* 109 (9): 3401–5. <https://doi.org/10.1073/pnas.1118438109>.
- Craven, Dylan, Nico Eisenhauer, William D. Pearse, Yann Hautier, Forest Isbell, Christiane Roscher, Michael Bahn, et al. 2018. "Multiple Facets of Biodiversity Drive the Diversity–Stability Relationship." *Nature Ecology & Evolution* 2:10 2 (10): 1579–87. <https://doi.org/10.1038/s41559-018-0647-7>.
- Craven, Dylan, Forest Isbell, Pete Manning, John Connolly, Helge Bruelheide, Anne Ebeling, Christiane Roscher, et al. 2016. "Plant Diversity Effects on Grassland Productivity Are Robust to Both Nutrient Enrichment and Drought." *Philosophical Transactions of the Royal Society B: Biological Sciences* 371 (1694). <https://doi.org/10.1098/RSTB.2015.0277>.
- Crisp, Peter A., Diep Ganguly, Steven R. Eichten, Justin O. Borevitz, and Barry J. Pogson. 2016. "Reconsidering Plant Memory: Intersections between Stress Recovery, RNA Turnover, and Epigenetics." *Science Advances* 2 (2). <https://doi.org/10.1126/SCIADV.1501340/ASSET/07CA86E6-2B18-4DEE-80FB-15670B1FCD98/ASSETS/GRAPHIC/1501340-F6.JPEG>.
- Cuddington, Kim. 2011. "Legacy Effects: The Persistent Impact of Ecological Interactions." *Biological Theory* 6 (3): 203–10. <https://doi.org/10.1007/S13752-012-0027-5>.
- Dalal, Monika, Sarika Sahu, Sneha Tiwari, Atmakuri R. Rao, and Kishor Gaikwad. 2018. "Transcriptome Analysis Reveals Interplay between Hormones, ROS Metabolism and Cell Wall Biosynthesis for Drought-Induced Root Growth in Wheat." *Plant Physiology and Biochemistry* 130 (September): 482–92. <https://doi.org/10.1016/J.PLAPHY.2018.07.035>.
- Damatta, Fábio M, Adriana Grandis, Bruna C Arenque, and Marcos S Buckeridge. 2010. "Impacts of Climate Changes on Crop Physiology and Food Quality." *Food Research International* 43: 1814–23. <https://doi.org/10.1016/j.foodres.2009.11.001>.
- Daszkowska-Golec, Agata. 2016. "The Role of Abscisic Acid in Drought Stress: How ABA Helps Plants to Cope with Drought Stress BT - Drought Stress Tolerance in Plants, Vol 2: Molecular and Genetic Perspectives." In , edited by Mohammad Anwar Hossain, Shabir Hussain Wani, Soumen Bhattacharjee, David J Burritt, and Lam-Son Phan Tran, 123–51. Cham: Springer International Publishing. https://doi.org/10.1007/978-3-319-32423-4_5.
- Denness, Lucinda, Joseph Francis McKenna, Cecile Segonzac, Alexandra Wormit, Priya Madhou, Mark Bennett, John Mansfield, Cyril Zipfel, and Thorsten Hamann. 2011. "Cell Wall Damage-Induced Lignin Biosynthesis Is Regulated by a Reactive Oxygen Species- and Jasmonic Acid-Dependent Process in Arabidopsis." *Plant Physiology* 156 (3): 1364–74. <https://doi.org/10.1104/pp.111.175737>.
- DeSoto, Lucía, Maxime Cailleret, Frank Sterck, Steven Jansen, Koen Kramer, Elisabeth M.R. Robert, Tuomas Aakala, et al. 2020. "Low Growth Resilience to Drought Is Related to

- Future Mortality Risk in Trees.” *Nature Communications* 11 (1): 1–9. <https://doi.org/10.1038/s41467-020-14300-5>.
- Didi, Vojtěch, Phil Jackson, and Jan Hejáltko. 2015. “Hormonal Regulation of Secondary Cell Wall Formation.” *Journal of Experimental Botany* 66 (16): 5015–27. <https://doi.org/10.1093/jxb/erv222>.
- Diédhiou, Calliste J., Olga V. Popova, Karl Josef Dietz, and Dortje Golldack. 2008. “The SNF1-Type Serine-Threonine Protein Kinase SAPK4 Regulates Stress-Responsive Gene Expression in Rice.” *BMC Plant Biology* 8: 1–13. <https://doi.org/10.1186/1471-2229-8-49>.
- Doblin, Monika S, Filomena Pettolino, and Antony Bacic. 2010. “Plant Cell Walls: The Skeleton of the Plant World.” *Functional Plant Biology* 37. <https://doi.org/10.1071/FP09279>.
- Easterling, D. R., G. A. Meehl, C. Parmesan, S. A. Changnon, T. R. Karl, and L. O. Mearns. 2000. “Climate Extremes: Observations, Modeling, and Impacts.” *Science* 289 (5487): 2068–74. <https://doi.org/10.1126/SCIENCE.289.5487.2068>.
- Egea, Isabel, Irene Albaladejo, Victoriano Meco, Belén Morales, Angel Sevilla, Maria C. Bolarin, and Francisco B. Flores. 2018. “The Drought-Tolerant *Solanum Pennellii* Regulates Leaf Water Loss and Induces Genes Involved in Amino Acid and Ethylene/Jasmonate Metabolism under Dehydration.” *Scientific Reports* 2018 8:1 8 (1): 1–14. <https://doi.org/10.1038/s41598-018-21187-2>.
- Elbasiouny, Heba, Hassan El-Ramady, Fathy Elbehiry, Vishnu D. Rajput, Tatiana Minkina, and Saglara Mandzhieva. 2022. “Plant Nutrition under Climate Change and Soil Carbon Sequestration.” *Sustainability (Switzerland)* 14 (2): 1–20. <https://doi.org/10.3390/su14020914>.
- Elst, Evelyne M., Hans J. De Boeck, Lisa Vanmaele, Maya Verlinden, Pauline Dhliwayo, and Ivan Nijs. 2017. “Impact of Climate Extremes Modulated by Species Characteristics and Richness.” *Perspectives in Plant Ecology, Evolution and Systematics* 24 (February): 80–92. <https://doi.org/10.1016/J.PPEES.2016.12.007>.
- Engelbrecht, Bettina M J, Liza S Comita, Richard Condit, Thomas A Kursar, Melvin T Tyree, Benjamin L Turner, and Stephen P Hubbell. 2007. “Drought Sensitivity Shapes Species Distribution Patterns in Tropical Forests.” *Nature* 447 (7140): 80–82. <https://doi.org/10.1038/nature05747>.
- Engelhardt, Ilonka C., Pascal A. Niklaus, Florian Bizouard, Marie Christine Breuil, Nadine Rouard, Florence Deau, Laurent Philippot, and Romain L. Barnard. 2021. “Precipitation Patterns and N Availability Alter Plant-Soil Microbial C and N Dynamics.” *Plant and Soil* 466 (1–2): 151–63. <https://doi.org/10.1007/S11104-021-05015-7>.
- Ereful, Nelzo C., Li Yu Liu, Andy Greenland, Wayne Powell, Ian Mackay, and Hei Leung. 2020. “RNA-Seq Reveals Differentially Expressed Genes between Two *Indica* Inbred Rice Genotypes Associated with Drought-Yield QTLs.” *Agronomy* 10 (5). <https://doi.org/10.3390/agronomy10050621>.
- Fàbregas, Norma, and Alisdair R. Fernie. 2019. “The Metabolic Response to Drought.” *Journal of Experimental Botany* 70 (4): 1077–85. <https://doi.org/10.1093/JXB/ERY437>.
- Fang, Xin, Jia Ma, Fengcai Guo, Dongyue Qi, Ming Zhao, Chuangzhong Zhang, Le Wang, et al. 2022. “The AP2/ERF GmERF113 Positively Regulates the Drought Response by

- Activating GmPR10-1 in Soybean." *International Journal of Molecular Sciences* 23 (15). <https://doi.org/10.3390/IJMS23158159/S1>.
- Fang, Yujie, and Lizhong Xiong. 2015. "General Mechanisms of Drought Response and Their Application in Drought Resistance Improvement in Plants." *Cellular and Molecular Life Sciences* 72 (4): 673–89. <https://doi.org/10.1007/s00018-014-1767-0>.
- Farfan-Vignolo, Evelyn Roxana, and Han Asard. 2012. "Effect of Elevated CO₂ and Temperature on the Oxidative Stress Response to Drought in *Lolium Perenne* L. and *Medicago Sativa* L." *Plant Physiology and Biochemistry* 59 (2012): 55–62. <https://doi.org/10.1016/j.plaphy.2012.06.014>.
- Farooq, M., A.Wahid, N. Kobayashi, D. Fujita, and S.M.A. Basra. 2009. "Plant Drought Stress: Effects, Mechanisms and Management." *Agron. Sustain. Dev* 29: 185–212.
- Felton, Andrew J., Ingrid J. Slette, Melinda D. Smith, and Alan K. Knapp. 2020. "Precipitation Amount and Event Size Interact to Reduce Ecosystem Functioning during Dry Years in a Mesic Grassland." *Global Change Biology* 26 (2): 658–68. <https://doi.org/10.1111/GCB.14789>.
- Felton, Andrew J., and Melinda D. Smith. 2017. "Integrating Plant Ecological Responses to Climate Extremes from Individual to Ecosystem Levels." *Philosophical Transactions of the Royal Society B: Biological Sciences* 372 (1723). <https://doi.org/10.1098/rstb.2016.0142>.
- Fiehn, Oliver. 2002. "Metabolomics – the Link between Genotypes and Phenotypes." *Plant Molecular Biology* 2002 48:1 48 (1): 155–71. <https://doi.org/10.1023/A:1013713905833>.
- Foyer, C H, and J M Fletcher. 2001. "Plant Antioxidants: Colour Me Healthy." *Biologist (London, England)* 48 (3): 115–20.
- Francis, Jennifer A., Natasa Skific, and Stephen J. Vavrus. 2020. "Increased Persistence of Large-Scale Circulation Regimes over Asia in the Era of Amplified Arctic Warming, Past and Future." *Scientific Reports* 2020 10:1 10 (1): 1–13. <https://doi.org/10.1038/s41598-020-71945-4>.
- Francoz, Edith, Philippe Ranocha, Huan Nguyen-Kim, Elisabeth Jamet, Vincent Burlat, and Christophe Dunand. 2015. "Roles of Cell Wall Peroxidases in Plant Development." *Phytochemistry* 112 (1): 15–21. <https://doi.org/10.1016/j.phytochem.2014.07.020>.
- Fry, Ellen L., Emma S. Pilgrim, Jerry R.B. Tallwin, Roger S. Smith, Simon R. Mortimer, Deborah A. Beaumont, Janet Simkin, et al. 2017. "Plant, Soil and Microbial Controls on Grassland Diversity Restoration: A Long-Term, Multi-Site Mesocosm Experiment." *Journal of Applied Ecology* 54 (5): 1320–30. <https://doi.org/10.1111/1365-2664.12869>.
- Gachara, Grace, Jihane Kenfaoui, Rashid Suleiman, Beatrice Kilima, Mohammed Taoussi, Kamal Aberkani, Zineb Belabess, et al. 2023. "The Role of Soil Microbiome in Driving Plant Performance: An Overview Based on Ecological and Ecosystem Advantages to the Plant Community." *Gesunde Pflanzen*. <https://doi.org/10.1007/s10343-023-00935-z>.
- Gall, Hyacinthe Le, Florian Philippe, Jean Marc Domon, Françoise Gillet, Jérôme Pelloux, and Catherine Rayon. 2015. "Cell Wall Metabolism in Response to Abiotic Stress." *Plants* 4 (1): 112–66. <https://doi.org/10.3390/plants4010112>.

- Gallego-Giraldo, Lina, Gail Shadle, Hui Shen, Jaime Barros-Rios, Sandra Fresquet Corrales, Huanzhong Wang, and Richard A. Dixon. 2016. "Combining Enhanced Biomass Density with Reduced Lignin Level for Improved Forage Quality." *Plant Biotechnology Journal* 14 (3): 895–904. <https://doi.org/10.1111/pbi.12439>.
- Garcia-Herrera, R., J. Díaz, R. M. Trigo, J. Luterbacher, and E. M. Fischer. 2010. "A Review of the European Summer Heat Wave of 2003." *Critical Reviews in Environmental Science and Technology* 40 (4): 267–306. <https://doi.org/10.1080/10643380802238137>.
- Gardner, W. R. 1965. "Dynamic Aspects of Soil-Water Availability to Plants." *Annual Review of Plant Physiology* 16 (1): 323–42. <https://doi.org/10.1146/annurev.pp.16.060165.001543>.
- Gargallo-Garriga, Albert, Catherine Preece, Jordi Sardans, Michal Oravec, Otmar Urban, and Josep Peñuelas. 2018. "Root Exudate Metabolomes Change under Drought and Show Limited Capacity for Recovery." *Scientific Reports* 8 (1). <https://doi.org/10.1038/S41598-018-30150-0>.
- Gargallo-Garriga, Albert, Jordi Sardans, Victor Granda, Joan Llusà, Guille Peguero, Dolores Asensio, Romà Ogaya, et al. 2020. "Different 'Metabolomic Niches' of the Highly Diverse Tree Species of the French Guiana Rainforests." *Scientific Reports* 10 (1). <https://doi.org/10.1038/s41598-020-63891-y>.
- Gargallo-Garriga, Albert, Jordi Sardans, Míriam Pérez-Trujillo, Michal Oravec, Otmar Urban, Anke Jentsch, Juergen Kreyling, Carl Beierkuhnlein, Teodor Parella, and Josep Peñuelas. 2015. "Warming Differentially Influences the Effects of Drought on Stoichiometry and Metabolomics in Shoots and Roots." *New Phytologist* 207 (3): 591–603. <https://doi.org/10.1111/nph.13377>.
- Gargallo-Garriga, Albert, Jordi Sardans, Míriam Pérez-Trujillo, Albert Rivas-Ubach, Michal Oravec, Kristyna Vecerova, Otmar Urban, et al. 2014. "Opposite Metabolic Responses of Shoots and Roots to Drought." *Scientific Reports* 4: 1–7. <https://doi.org/10.1038/srep06829>.
- Gertsman, Ilya, and Bruce A. Barshop. 2018. "Promises and Pitfalls of Untargeted Metabolomics." *Journal of Inherited Metabolic Disease* 41 (3): 355–66. <https://doi.org/10.1007/S10545-017-0130-7>.
- Gessler, Arthur, Alessandra Bottero, John Marshall, and Matthias Arend. 2020. "The Way Back: Recovery of Trees from Drought and Its Implication for Acclimation." *New Phytologist* 228 (6): 1704–9. <https://doi.org/10.1111/nph.16703>.
- Gherardi, Laureano A., and Osvaldo E. Sala. 2015. "Enhanced Precipitation Variability Decreases Grass- and Increases Shrub-Productivity." *Proceedings of the National Academy of Sciences of the United States of America* 112 (41): 12735–40. https://doi.org/10.1073/PNAS.1506433112/SUPPL_FILE/PNAS.1506433112.SAPP.DOCX.
- Glass, Magdalena, Sarah Barkwill, Faride Unda, and Shawn D. Mansfield. 2015. "Endo- β -1,4-Glucanases Impact Plant Cell Wall Development by Influencing Cellulose Crystallization." *Journal of Integrative Plant Biology* 57 (4): 396–410. <https://doi.org/10.1111/JIPB.12353>.
- Gonzalez, Lauren E., Kristen Keller, Karen X. Chan, Megan M. Gessel, and Bryan C. Thines. 2017. "Transcriptome Analysis Uncovers Arabidopsis F-BOX STRESS INDUCED 1 as a

Regulator of Jasmonic Acid and Abscisic Acid Stress Gene Expression." *BMC Genomics* 18 (1). <https://doi.org/10.1186/S12864-017-3864-6>.

Grabherr, Manfred G., Brian J. Haas, Moran Yassour, Joshua Z. Levin, Dawn A. Thompson, Ido Amit, Xian Adiconis, et al. 2011. "Trinity: Reconstructing a Full-Length Transcriptome without a Genome from RNA-Seq Data." *Nature Biotechnology* 29 (7): 644. <https://doi.org/10.1038/NBT.1883>.

Grace, Stephen C., and Dane A. Hudson. 2016. "Processing and Visualization of Metabolomics Data Using R." *Metabolomics - Fundamentals and Applications*, December. <https://doi.org/10.5772/65405>.

Grant, Kerstin, Juergen Kreyling, Hermann Heilmeyer, Carl Beierkuhnlein, and Anke Jentsch. 2014. "Extreme Weather Events and Plant-Plant Interactions: Shifts between Competition and Facilitation among Grassland Species in the Face of Drought and Heavy Rainfall." *Ecological Research* 29 (5): 991-1001. <https://doi.org/https://doi.org/10.1007/s11284-014-1187-5>.

Grieu, P., D. W. Lucero, R. Ardiani, and J. R. Ehleringer. 2001. "The Mean Depth of Soil Water Uptake by Two Temperate Grassland Species over Time Subjected to Mild Soil Water Deficit and Competitive Association." *Plant and Soil* 230 (2): 197-209. <https://doi.org/10.1023/A:1010363532118>.

Grime, J Philip, Jason D Fridley, Andrew P Askew, Ken Thompson, John G Hodgson, and Chris R Bennett. 2008. "Long-Term Resistance to Simulated Climate Change in an Infertile Grassland." *Proceedings of the National Academy of Sciences* 105 (29): 10028-32. <https://doi.org/10.1073/pnas.0711567105>.

Grimoldi, Agustín A., Pedro Insausti, Viviana Vasellati, and Gustavo G. Striker. 2005. "Constitutive and Plastic Root Traits and Their Role in Differential Tolerance to Soil Flooding among Coexisting Species of a Lowland Grassland." *International Journal of Plant Sciences* 166 (5): 805-13. <https://doi.org/10.1086/431805>.

Grover, Anita. 2012. "Plant Chitinases: Genetic Diversity and Physiological Roles." *Critical Reviews in Plant Sciences* 31 (1): 57-73. <https://doi.org/10.1080/07352689.2011.616043>.

Guo, Rui, Lian Xuan Shi, Yang Jiao, Ming Xia Li, Xiu Li Zhong, Feng Xue Gu, Qi Liu, Xu Xia, and Hao Ru Li. 2018. "Metabolic Responses to Drought Stress in the Tissues of Drought-Tolerant and Drought-Sensitive Wheat Genotype Seedlings." *AoB PLANTS* 10 (2): 1-13. <https://doi.org/10.1093/aobpla/ply016>.

Gurrieri, Libero, Martina Merico, Paolo Trost, Giuseppe Forlani, and Francesca Sparla. 2020. "Impact of Drought on Soluble Sugars and Free Proline Content in Selected Arabidopsis Mutants." *Biology* 9 (11): 1-14. <https://doi.org/10.3390/biology9110367>.

Ha, Chan Man, Xiaolan Rao, Garima Saxena, and Richard A. Dixon. 2021. "Growth-Defense Trade-Offs and Yield Loss in Plants with Engineered Cell Walls." *New Phytologist* 231 (1): 60-74. <https://doi.org/10.1111/nph.17383>.

Hallett, Lauren M., Lauren G. Shoemaker, Caitlin T. White, and Katharine N. Suding. 2019. "Rainfall Variability Maintains Grass-Forb Species Coexistence." *Ecology Letters* 22 (10): 1658-67. <https://doi.org/10.1111/ELE.13341>.

Harb, Amal, Craig Simpson, Wenbin Guo, Ganesan Govindan, Vijaya Gopal Kakani, and Ramanjulu Sunkar. 2020. "The Effect of Drought on Transcriptome and Hormonal Profiles

- in Barley Genotypes With Contrasting Drought Tolerance." *Frontiers in Plant Science* 11 (December): 1–23. <https://doi.org/10.3389/fpls.2020.618491>.
- Harrell, Frank E. 2023. "Harrell Miscellaneous [R Package Hmisc Version 4.8-0]," February.
- Harrison, Susan P., Marina L. LaForgia, and Andrew M. Latimer. 2018. "Climate-Driven Diversity Change in Annual Grasslands: Drought plus Deluge Does Not Equal Normal." *Global Change Biology* 24 (4): 1782–92. <https://doi.org/10.1111/gcb.14018>.
- Harrison, Susan, Marko J Spasojevic, and Daijiang Li. 2020. "Climate and Plant Community Diversity in Space and Time." *Proceedings of the National Academy of Sciences* 117 (9): 4464–70. <https://doi.org/10.1073/pnas.1921724117>.
- He, Mei, and Nai Zheng Ding. 2020. "Plant Unsaturated Fatty Acids: Multiple Roles in Stress Response." *Frontiers in Plant Science* 11 (September): 1378. <https://doi.org/10.3389/FPLS.2020.562785/BIBTEX>.
- He, Mei, Cheng-Qiang He, and Nai-Zheng Ding. 2018. "Abiotic Stresses: General Defenses of Land Plants and Chances for Engineering Multistress Tolerance." <https://doi.org/10.3389/fpls.2018.01771>.
- Heisler-White, Jana L., John M. Blair, Eugene F. Kelly, Keith Harmony, and Alan K. Knapp. 2009. "Contingent Productivity Responses to More Extreme Rainfall Regimes across a Grassland Biome." *Global Change Biology* 15 (12): 2894–2904. <https://doi.org/10.1111/J.1365-2486.2009.01961.X>.
- Heyer, Laurie J., Semyon Kruglyak, and Shibu Yooseph. 1999. "Exploring Expression Data: Identification and Analysis of Coexpressed Genes." *Genome Research* 9 (11): 1106. <https://doi.org/10.1101/GR.9.11.1106>.
- Hilker, Monika, and Thomas Schmölling. 2019. "Stress Priming, Memory, and Signalling in Plants." *Plant, Cell & Environment* 42 (3): 753–61. <https://doi.org/10.1111/PCE.13526>.
- Hölzer, Martin, and Manja Marz. 2019. "De Novo Transcriptome Assembly: A Comprehensive Cross-Species Comparison of Short-Read RNA-Seq Assemblers." *GigaScience* 8 (5): 1–16. <https://doi.org/10.1093/GIGASCIENCE/GI2039>.
- Hong, Jun, Litao Yang, Dabing Zhang, and Jianxin Shi. 2016. "Plant Metabolomics: An Indispensable System Biology Tool for Plant Science." *International Journal of Molecular Sciences* 17 (6). <https://doi.org/10.3390/ijms17060767>.
- Hoover, David L, Alan K Knapp, and Melinda D Smith. 2014. "Resistance and Resilience of a Grassland Ecosystem to Climate Extremes." *Ecology* 95 (9): 2646–56. <https://doi.org/https://doi.org/10.1890/13-2186.1>.
- Howe, Eleanor A., Raktim Sinha, Daniel Schlauch, and John Quackenbush. 2011. "RNA-Seq Analysis in MeV." *Bioinformatics* 27 (22): 3209. <https://doi.org/10.1093/BIOINFORMATICS/BTR490>.
- Huang, Bo, and Jin Yuan Liu. 2006. "A Cotton Dehydration Responsive Element Binding Protein Functions as a Transcriptional Repressor of DRE-Mediated Gene Expression." *Biochemical and Biophysical Research Communications* 343 (4): 1023–31. <https://doi.org/10.1016/J.BBRC.2006.03.016>.
- Huang, Tengfang, and Georg Jander. 2017. "Abscisic Acid-Regulated Protein Degradation Causes Osmotic Stress-Induced Accumulation of Branched-Chain Amino Acids in

Arabidopsis Thaliana." *Planta* 246 (4): 737–47. <https://doi.org/10.1007/S00425-017-2727-3>.

Husain, Tajammul, Abreeq Fatima, Mohammad Suhel, Samiksha Singh, Anket Sharma, Sheo Mohan Prasad, and Vijay Pratap Singh. 2020. "A Brief Appraisal of Ethylene Signaling under Abiotic Stress in Plants." *Plant Signaling and Behavior* 15 (9). <https://doi.org/10.1080/15592324.2020.1782051>.

Ihsan, Muhammad Z., Fathy S. El-Nakhrawy, Saleh M. Ismail, Shah Fahad, and Ihsanullah Daur. 2016. "Wheat Phenological Development and Growth Studies as Affected by Drought and Late Season High Temperature Stress under Arid Environment." *Frontiers in Plant Science* 7 (June 2016): 191357. <https://doi.org/10.3389/FPLS.2016.00795/BIBTEX>.

Iiyama, Kenji, and Adrian F.A. Wallis. 1990. "Determination of Lignin in Herbaceous Plants by an Improved Acetyl Bromide Procedure." *Journal of the Science of Food and Agriculture* 51 (2): 145–61. <https://doi.org/10.1002/JSFA.2740510202>.

IPCC. 2021. *IPCC. Climate Change 2021: The Physical Science Basis. Future Global Climate: Scenario-42 Based Projections and Near-Term Information*; Cambridge University Press: Cambridge, UK.

Jacques, Cécile, Christophe Salon, Romain L. Barnard, Vanessa Vernoud, and Marion Prudent. 2021. "Drought Stress Memory at the Plant Cycle Level: A Review." *Plants* 2021, Vol. 10, Page 1873 10 (9): 1873. <https://doi.org/10.3390/PLANTS10091873>.

Janiak, Agnieszka, Mirosław Kwasniewski, Marta Sowa, Anetta Kuczyńska, Krzysztof Mikołajczak, Piotr Ogrodowicz, and Iwona Szarejko. 2019. "Insights into Barley Root Transcriptome under Mild Drought Stress with an Emphasis on Gene Expression Regulatory Mechanisms." *International Journal of Molecular Sciences* 20 (24). <https://doi.org/10.3390/ijms20246139>.

Jarvis, Paul, Ana Rey, Charalampos Petsikos, Lisa Wingate, Mark Rayment, João Pereira, João Banza, et al. 2007. "Drying and Wetting of Mediterranean Soils Stimulates Decomposition and Carbon Dioxide Emission: The 'Birch Effect.'" *Tree Physiology* 27 (7): 929–40. <https://doi.org/10.1093/treephys/27.7.929>.

Jeandet, Philippe, Magda Formela-Luboińska, Mateusz Labudda, and Iwona Morkunas. 2022. "The Role of Sugars in Plant Responses to Stress and Their Regulatory Function during Development." *International Journal of Molecular Sciences* 23 (9). <https://doi.org/10.3390/ijms23095161>.

Jentsch, Anke, Juergen Kreyling, Michael Elmer, Ellen Gellesch, Bruno Glaser, Kerstin Grant, Roman Hein, Marco Lara, Heydar Mirzae, Stefanie E Nadler, Laura Nagy, Denis Otieno, Karin Pritsch, Uwe Rascher, Martin Schädl er Schädl er, et al. 2011. "SPECIAL FEATURE ECOLOGICAL CONSEQUENCES OF CLIMATE EXTREMES Climate Extremes Initiate Ecosystem-Regulating Functions While Maintaining Productivity." *British Ecological Society Journal of Ecology* 99: 689–702. <https://doi.org/10.1111/j.1365-2745.2011.01817.x>.

Jentsch, Anke, Juergen Kreyling, Michael Elmer, Ellen Gellesch, Bruno Glaser, Kerstin Grant, Roman Hein, Marco Lara, Heydar Mirzae, Stefanie E Nadler, Laura Nagy, Denis Otieno, Karin Pritsch, Uwe Rascher, Martin Schädl er, et al. 2011. "Climate Extremes Initiate Ecosystem-Regulating Functions While Maintaining Productivity." *Journal of*

- Ecology* 99 (3): 689–702. <https://doi.org/https://doi.org/10.1111/j.1365-2745.2011.01817.x>.
- Jez, Joseph M., Rebecca E. Cahoon, and Sixue Chen. 2004. "Arabidopsis Thaliana Glutamate-Cysteine Ligase: Functional Properties, Kinetic Mechanism, and Regulation of Activity." *The Journal of Biological Chemistry* 279 (32): 33463–70. <https://doi.org/10.1074/JBC.M405127200>.
- Jiang, Shang Chuan, Chao Mei, Shan Liang, Yong Tao Yu, Kai Lu, Zhen Wu, Xiao Fang Wang, and Da Peng Zhang. 2015. "Crucial Roles of the Pentatricopeptide Repeat Protein SOAR1 in Arabidopsis Response to Drought, Salt and Cold Stresses." *Plant Molecular Biology* 88 (4–5): 369–85. <https://doi.org/10.1007/S11103-015-0327-9/FIGURES/8>.
- Johnson, Kim L., Michael J. Gidley, Antony Bacic, and Monika S. Doblin. 2018. "Cell Wall Biomechanics: A Tractable Challenge in Manipulating Plant Cell Walls 'Fit for Purpose!'" *Current Opinion in Biotechnology* 49 (February): 163–71. <https://doi.org/10.1016/J.COPBIO.2017.08.013>.
- Jonavičienė, K., B. Studer, T. Asp, L. B. Jensen, V. Paplauskienė, S. Lazauskas, and G. Brazauskas. 2012. "Identification of Genes Involved in a Water Stress Response in Timothy and Mapping of Orthologous Loci in Perennial Ryegrass." *Biologia Plantarum* 56 (3): 473–83. <https://doi.org/10.1007/s10535-012-0110-6>.
- Kamal, Javed. 2011. "Quantification of Alkaloids, Phenols and Flavonoids in Sunflower (*Helianthus Annuus* L.)." *African Journal of Biotechnology* 10 (16): 3149–51. <https://doi.org/10.5897/AJB09.1270>.
- Kambona, Carolyn Mukiri, Patrice Ahossi Koua, Jens Léon, and Agim Ballvora. 2023. "Stress Memory and Its Regulation in Plants Experiencing Recurrent Drought Conditions." *Theoretical and Applied Genetics* 136 (2): 1–21. <https://doi.org/10.1007/s00122-023-04313-1>.
- Kang, Won Hee, Young Mi Sim, Namjin Koo, Jae Young Nam, Junesung Lee, Nayoung Kim, Hakgi Jang, Yong Min Kim, and Seon In Yeom. 2020. "Transcriptome Profiling of Abiotic Responses to Heat, Cold, Salt, and Osmotic Stress of *Capsicum Annuum* L." *Scientific Data* 7 (1): 1–7. <https://doi.org/10.1038/s41597-020-0352-7>.
- KARDOL, PAUL, COURTNEY E. CAMPANY, LARA SOUZA, RICHARD J. NORBY, JAKE F. WELTZIN, and AIMEE T. CLASSEN. 2010. "Climate Change Effects on Plant Biomass Alter Dominance Patterns and Community Evenness in an Experimental Old-Field Ecosystem." *Global Change Biology* 16 (10): 2676–87. <https://doi.org/10.1111/J.1365-2486.2010.02162.X>.
- Kardol, Paul, Nelleke J. Cornips, Monique M.L. Van Kempen, J. M.Tanja Bakx-Schotman, and Wim H. Van Der Putten. 2007. "Microbe-Mediated Plant-Soil Feedback Causes Historical Contingency Effects in Plant Community Assembly." *Ecological Monographs* 77 (2): 147–62. <https://doi.org/10.1890/06-0502>.
- Khedr, Abdel Hamid A, Mohammad A Abbas, Amal A Abdel Wahid, W Paul Quick, and Gaber M Abogadallah. 2003. "Proline Induces the Expression of Salt-stress-responsive Proteins and May Improve the Adaptation of *Pancreaticum Maritimum* L. to Salt-stress." *Journal of Experimental Botany* 54 (392): 2553–62. <https://doi.org/10.1093/jxb/erg277>.

Bibliography

- Kinoshita, Tetsu, and Motoaki Seki. 2014. "Epigenetic Memory for Stress Response and Adaptation in Plants." *Plant and Cell Physiology* 55 (11): 1859–63. <https://doi.org/10.1093/PCP/PCU125>.
- KMI. 2019. "Klimatologisch Seizoenoverzicht, Zomer 2019.," no. september: 1–9.
- Knapp, Alan K., Claus Beier, David D. Briske, Aimée T. Classen, Luo Yiqi, Markus Reichstein, Melinda D. Smith, et al. 2008. "Consequences of More Extreme Precipitation Regimes for Terrestrial Ecosystems." *BioScience* 58 (9): 811–21. <https://doi.org/10.1641/B580908>.
- Knapp, Alan K., Philip A. Fay, John M. Blair, Scott L. Collins, Melinda D. Smith, Jonathan D. Carlisle, Christopher W. Harper, Brett T. Danner, Michelle S. Lett, and James K. McCarron. 2002. "Rainfall Variability, Carbon Cycling, and Plant Species Diversity in a Mesic Grassland." *Science* 298 (5601): 2202–5. <https://doi.org/10.1126/science.1076347>.
- Kohle, Harald, Wolfgang Jeblick, Frauke Poten, Wolfgang Blaschek, Heinrich Kauss, Fachbereich Biologie, Universität Kaiserslautern, D- Kaiserslautern, and Federal Republic. 1985. "Chitosan-Elicited Callose Synthesis in Soybean Cells as a." *Plant Physiology*, 544–51.
- Kohorn, Bruce D., and Susan L. Kohorn. 2012. "The Cell Wall-Associated Kinases, WAKs, as Pectin Receptors." *Frontiers in Plant Science* 3 (MAY): 25457. <https://doi.org/10.3389/FPLS.2012.00088/BIBTEX>.
- Kolde, Raivo. 2012. "Pheatmap: Pretty Heatmaps." *R Package Version* 1 (2): 726.
- Kong, Yingzhen, Gongke Zhou, Yanbin Yin, Ying Xu, Sivakumar Pattathil, and Michael G. Hahn. 2011. "Molecular Analysis of a Family of Arabidopsis Genes Related to Galacturonosyltransferases." *Plant Physiology* 155 (4): 1791. <https://doi.org/10.1104/PP.110.163220>.
- Kornhuber, Kai, and Talia Tamarin-Brodsky. 2021. "Future Changes in Northern Hemisphere Summer Weather Persistence Linked to Projected Arctic Warming." *Geophysical Research Letters* 48 (4): 1–12. <https://doi.org/10.1029/2020GL091603>.
- Kraft, Nathan J.B., Peter B. Adler, Oscar Godoy, Emily C. James, Steve Fuller, and Jonathan M. Levine. 2015. "Community Assembly, Coexistence and the Environmental Filtering Metaphor." *Functional Ecology* 29 (5): 592–99. <https://doi.org/10.1111/1365-2435.12345>.
- Krasensky, Julia, and Claudia Jonak. 2012. "Drought, Salt, and Temperature Stress-Induced Metabolic Rearrangements and Regulatory Networks." *Journal of Experimental Botany* 63 (4): 1593–1608. <https://doi.org/10.1093/JXB/ERR460>.
- Kreienkamp, Frank, Sjoukje Y Philip, Jordis S Tradowsky, Sarah F Kew, Philip Lorenz, Julie Arrighi, Alexandre Belleflamme, et al. 2021. "Rapid Attribution of Heavy Rainfall Events Leading to the Severe Flooding in Western Europe during July 2021." *Royal Netherlands Meteorological Institute (KNMI)* 13 (July): 1–51.
- Kreienkamp, Frank, Sjoukje Y Philip, Jordis S Tradowsky, Sarah F Kew, Philip Lorenz, Alexandre Belleflamme, Thomas Bettmann, et al. 2021. "Rapid Attribution of Heavy Rainfall Events Leading to the Severe Flooding in Western Europe during July 2021 Contributors," no. July.
- Kröel-Dulay, György, Andrea Mojzes, Katalin Sztár, Michael Bahn, Péter Batáry, Claus Beier, Mark Bilton, et al. 2022. "Field Experiments Underestimate Aboveground Biomass

- Response to Drought.” *Nature Ecology and Evolution* 6 (5): 540–45. <https://doi.org/10.1038/s41559-022-01685-3>.
- Lambers, Janneke Hille Ris. 2015. “Extinction Risks from Climate Change: How Will Climate Change Affect Global Biodiversity?” *Science* 348 (6234): 501–2. <https://doi.org/10.1126/science.aab2057>.
- Langmead, Ben, and Steven L. Salzberg. 2012. “Fast Gapped-Read Alignment with Bowtie 2.” *Nature Methods* 2012 9:4 9 (4): 357–59. <https://doi.org/10.1038/nmeth.1923>.
- Lee, Bok Rye, Kil Yong Kim, Woo Jin Jung, Jean Christophe Avice, Alain Ourry, and Tae Hwan Kim. 2007. “Peroxidases and Lignification in Relation to the Intensity of Water-Deficit Stress in White Clover (*Trifolium Repens* L.)” *Journal of Experimental Botany* 58 (6): 1271–79. <https://doi.org/10.1093/jxb/erl280>.
- Lemon, Jim, Ben Bolker, Sander Oom, Eduardo Klein, Barry Rowlingson, Hadley Wickham, Anupam Tyagi, et al. 2022. “Package ‘plotrix’ Title Various Plotting Functions.”
- Lenk, Ingo, Lorraine H.C. Fisher, Martin Vickers, Aderemi Akinyemi, Thomas Didion, Martin Swain, Christian Sig Jensen, Luis A.J. Mur, and Maurice Bosch. 2019. “Transcriptional and Metabolomic Analyses Indicate That Cell Wall Properties Are Associated with Drought Tolerance in *Brachypodium Distachyon*.” *International Journal of Molecular Sciences* 2019, Vol. 20, Page 1758 20 (7): 1758. <https://doi.org/10.3390/IJMS20071758>.
- Lenth, Russell, Henrik Singmann, Jonathon Love, Paul Buerkner, and Maxime Herve. 2018. “Emmeans: Estimated Marginal Means.” AKA *Least-Squares Means*, 1–2.
- Lever, M. 1972. “A New Reaction for Colorimetric Determination of Carbohydrates.” *Analytical Biochemistry* 47 (1): 273–79. [https://doi.org/10.1016/0003-2697\(72\)90301-6](https://doi.org/10.1016/0003-2697(72)90301-6).
- Leyva, Alberto, Anelis Quintana, Meily Sánchez, Elias N. Rodríguez, José Cremata, and Julio C. Sánchez. 2008. “Rapid and Sensitive Anthrone–Sulfuric Acid Assay in Microplate Format to Quantify Carbohydrate in Biopharmaceutical Products: Method Development and Validation.” *Biologicals* 36 (2): 134–41. <https://doi.org/10.1016/J.BIOLOGICALS.2007.09.001>.
- Li, Junqin, Bo Meng, Hua Chai, Xuechen Yang, Wenzheng Song, Shuixiu Li, Ao Lu, Tao Zhang, and Wei Sun. 2019. “Arbuscular Mycorrhizal Fungi Alleviate Drought Stress in C3 (*Leymus Chinensis*) and C4 (*Hemarthria Altissima*) Grasses via Altering Antioxidant Enzyme Activities and Photosynthesis.” *Frontiers in Plant Science* 10 (April): 1–12. <https://doi.org/10.3389/fpls.2019.00499>.
- Li, Lingjuan, Qiang Lin, Ivan Nijs, Hans De Boeck, Gerrit T.S. Beemster, Han Asard, and Erik Verbruggen. 2023. “More Persistent Weather Causes a Pronounced Soil Microbial Legacy but Does Not Impact Subsequent Plant Communities.” *Science of The Total Environment* 903 (December): 166570. <https://doi.org/10.1016/J.SCITOTENV.2023.166570>.
- Li, Lingjuan, Ivan Nijs, Hans De Boeck, Olga Vindušková, Simon Reynaert, Chase Donnelly, Lin Zi, and Erik Verbruggen. 2023. “Longer Dry and Wet Spells Alter the Stochasticity of Microbial Community Assembly in Grassland Soils.” *Soil Biology and Biochemistry* 178 (March): 108969. <https://doi.org/10.1016/J.SOILBIO.2023.108969>.
- Li, Mingqian, Hainan Li, Anni Sun, Liwei Wang, Chuanyou Ren, Jiang Liu, and Xining Gao. 2022. “Transcriptome Analysis Reveals Key Drought-Stress-Responsive Genes in Soybean.” *Frontiers in Genetics* 13 (November): 1–17. <https://doi.org/10.3389/fgene.2022.1060529>.

- Li, Peilin, Dan Zhu, Yilong Wang, and Dan Liu. 2020. "Elevation Dependence of Drought Legacy Effects on Vegetation Greenness over the Tibetan Plateau." *Agricultural and Forest Meteorology* 295: 108190. <https://doi.org/https://doi.org/10.1016/j.agrformet.2020.108190>.
- Li, Qing, Canfang Fu, Chengliang Liang, Xiangjiang Ni, Xuanhua Zhao, Meng Chen, and Lijun Ou. 2022. "Crop Lodging and The Roles of Lignin, Cellulose, and Hemicellulose in Lodging Resistance." *Agronomy* 12 (8): 1–18. <https://doi.org/10.3390/agronomy12081795>.
- Li, Tiemei, Xin Cheng, Xiaowei Wang, Guanggui Li, Bianbian Wang, Wenyuan Wang, Na Zhang, et al. 2021. "Glyoxalase I-4 Functions Downstream of NAC72 to Modulate Downy Mildew Resistance in Grapevine." *The Plant Journal : For Cell and Molecular Biology* 108 (2): 394–410. <https://doi.org/10.1111/TPJ.15447>.
- Li, Xiaogang, Alexandre Jousset, Wietse de Boer, Víctor J. Carrión, Taolin Zhang, Xingxiang Wang, and Eiko E. Kuramae. 2019. "Legacy of Land Use History Determines Reprogramming of Plant Physiology by Soil Microbiome." *ISME Journal* 13 (3): 738–51. <https://doi.org/10.1038/s41396-018-0300-0>.
- Li, Xiliang, Saheed Olaide Jimoh, Yuanheng Li, Junjie Duan, Yanwei Cui, Ke Jin, Zhen Wang, and Yong Zhang. 2022. "Stress Memory and Phyllosphere/Soil Legacy Underlie Tolerance and Plasticity of *Leymus Chinensis* to Periodic Drought Risk." *Agricultural and Forest Meteorology* 312 (November 2021): 108717. <https://doi.org/10.1016/j.agrformet.2021.108717>.
- Li, Yuanyuan, Huixian Cai, Pu Liu, Chunyan Wang, Huiyang Gao, Changai Wu, Kang Yan, Shizhong Zhang, Jinguang Huang, and Chengchao Zheng. 2017. "Arabidopsis MAPKKK18 Positively Regulates Drought Stress Resistance via Downstream MAPKK3." *Biochemical and Biophysical Research Communications* 484 (2): 292–97. <https://doi.org/10.1016/J.BBRC.2017.01.104>.
- Liang, Qianyan, Bicheng Dun, Linbao Li, Xiaobo Ma, Haibo Zhang, Yang Su, and Di Wu. 2023. "Metabolomic and Transcriptomic Responses of *Adiantum* (*Adiantum Nelumboides*) Leaves under Drought, Half-Waterlogging, and Rewater Conditions." *Frontiers in Genetics* 14 (April): 1–20. <https://doi.org/10.3389/fgene.2023.1113470>.
- Liu, Huiying, Zhaorong Mi, Li Lin, Yonghui Wang, Zhenhua Zhang, Fawei Zhang, Hao Wang, et al. 2018. "Shifting Plant Species Composition in Response to Climate Change Stabilizes Grassland Primary Production." *Proceedings of the National Academy of Sciences* 115 (16): 4051–56. <https://doi.org/10.1073/pnas.1700299114>.
- Liu, Qingquan, Le Luo, and Luqing Zheng. 2018. "Lignins: Biosynthesis and Biological Functions in Plants." *International Journal of Molecular Sciences* 19 (2). <https://doi.org/10.3390/IJMS19020335>.
- Liu, Xiqiang, Aiping Chen, Yuxiang Wang, Guili Jin, Yanhui Zhang, Lili Gu, Chenjian Li, Xinqing Shao, and Kun Wang. 2022. "Physiological and Transcriptomic Insights into Adaptive Responses of *Seriphidium Transiliense* Seedlings to Drought Stress." *Environmental and Experimental Botany* 194 (February): 104736. <https://doi.org/10.1016/J.ENVEXPBOT.2021.104736>.

- Liu, Xuebang, Bin He, Lanlan Guo, Ling Huang, and Deliang Chen. 2020. "Similarities and Differences in the Mechanisms Causing the European Summer Heatwaves in 2003, 2010, and 2018." *Earth's Future* 8 (4): e2019EF001386. <https://doi.org/10.1029/2019EF001386>.
- Llanes, Analía, Andrea Andrade, Sergio Alemano, and Virginia Luna. 2018. "Metabolomic Approach to Understand Plant Adaptations to Water and Salt Stress." *Plant Metabolites and Regulation under Environmental Stress*, January, 133–44. <https://doi.org/10.1016/B978-0-12-812689-9.00006-6>.
- Long, Jonathan R. De, Robin Heinen, Johannes Heinze, Elly Morriën, G. Kenny Png, Sarah J. Sapsford, François P. Teste, and Ellen L. Fry. 2023. "Plant-Soil Feedback: Incorporating Untested Influential Drivers and Reconciling Terminology." *Plant and Soil* 2023 485:1 485 (1): 7–43. <https://doi.org/10.1007/S11104-023-05908-9>.
- Loon, Leendert C. van. 2016. "The Intelligent Behavior of Plants." *Trends in Plant Science* 21 (4): 286–94. <https://doi.org/10.1016/j.tplants.2015.11.009>.
- LOWRY, Oliver H, ROSEBROUGH NJ, FARR AL, and RANDALL RJ. 1951. "Protein Measurement with the Folin Phenol Reagent." *The Journal of Biological Chemistry* 193 (1): 265–75.
- Lukova, Paolina, Ivanka Dimitrova-Dyulgerova, Diana Karcheva-Bahchevanska, Rumen Mladenov, Iliia Iliev, and Mariana Nikolova. 2017. "Comparative Morphological and Qualitative Phytochemical Analysis of Plantago Media L. Leaves with P. Major L. and P. Lanceolata L. Leaves." *International Journal of Medical Research and Pharmaceutical Sciences* 4 (6): 20–26. <https://doi.org/10.5281/zenodo.810782>.
- Luo, Wentao, Wang Ma, Lin Song, Niwu Te, Jiaqi Chen, Taofeek O. Muraina, Kate Wilkins, et al. 2023. "Compensatory Dynamics Drive Grassland Recovery from Drought." *Journal of Ecology*, no. November 2022: 1281–91. <https://doi.org/10.1111/1365-2745.14096>.
- Luo, Yiqi, Jerry Melillo, Shuli Niu, Claus Beier, James S. Clark, Aimée T. Classen, Eric Davidson, et al. 2011. "Coordinated Approaches to Quantify Long-Term Ecosystem Dynamics in Response to Global Change." *Global Change Biology* 17 (2): 843–54. <https://doi.org/10.1111/J.1365-2486.2010.02265.X>.
- Ma, Qing Hu, and Yang Xu. 2008. "Characterization of a Caffeic Acid 3-O-Methyltransferase from Wheat and Its Function in Lignin Biosynthesis." *Biochimie* 90 (3): 515–24. <https://doi.org/10.1016/J.BIOCHI.2007.09.016>.
- Ma, Xiaosong, Hui Xia, Yunhua Liu, Haibin Wei, Xiaoguo Zheng, Congzhi Song, Liang Chen, Hongyan Liu, and Lijun Luo. 2016. "Transcriptomic and Metabolomic Studies Disclose Key Metabolism Pathways Contributing to Well-Maintained Photosynthesis under the Drought and the Consequent Drought-Tolerance in Rice." *Frontiers in Plant Science* 7 (DECEMBER2016): 1886. <https://doi.org/10.3389/FPLS.2016.01886/BIBTEX>.
- Macrae, J C. 1971. "Quantitative Measurement of Starch in Very Small Amounts of Leaf Tissue." *Planta (Berl.)*. Vol. 96.
- Mansell, Richard L., Georg G. Gross, Joachim Stöckigt, Heinz Franke, and Meinhard H. Zenk. 1974. "Purification and Properties of Cinnamyl Alcohol Dehydrogenase from Higher Plants Involved in Lignin Biosynthesis." *Phytochemistry* 13 (11): 2427–35. [https://doi.org/10.1016/S0031-9422\(00\)86917-4](https://doi.org/10.1016/S0031-9422(00)86917-4).
- Meisner, Annelein, Gerlinde B. De Deyn, Wietse De Boer, and Wim H. Van Der Putten. 2013. "Soil Biotic Legacy Effects of Extreme Weather Events Influence Plant Invasiveness."

- Proceedings of the National Academy of Sciences of the United States of America* 110 (24): 9835–38. <https://doi.org/10.1073/pnas.1300922110>.
- Meisner, Annelein, Samuel Jacquioid, Basten L. Snoek, Freddy C. Ten Hooven, and Wim H. van der Putten. 2018. “Drought Legacy Effects on the Composition of Soil Fungal and Prokaryote Communities.” *Frontiers in Microbiology* 9 (MAR): 1–12. <https://doi.org/10.3389/fmicb.2018.00294>.
- Melandri, Giovanni, Hamada Abdelgawad, David Riewe, Jos A Hageman, Han Asard, Gerrit T S Beemster, Niteen Kadam, et al. 2020. “Biomarkers for Grain Yield Stability in Rice under Drought Stress.” *Journal of Experimental Botany* 71 (2): 669–83. <https://doi.org/10.1093/jxb/erz221>.
- Menezes-Silva, Paulo E., Lilian M.V.P. Sanglard, Rodrigo T. Ávila, Leandro E. Morais, Samuel C.V. Martins, Priscilla Nobres, Camila M. Patreze, et al. 2017. “Photosynthetic and Metabolic Acclimation to Repeated Drought Events Play Key Roles in Drought Tolerance in Coffee.” *Journal of Experimental Botany* 68 (15): 4309–22. <https://doi.org/10.1093/jxb/erx211>.
- Miedes, Eva, Ruben Vanholme, Wout Boerjan, and Antonio Molina. 2014. “The Role of the Secondary Cell Wall in Plant Resistance to Pathogens.” *Frontiers in Plant Science* 5 (AUG): 1–13. <https://doi.org/10.3389/fpls.2014.00358>.
- Mielke, Stefan, and Debora Gasperini. 2019. “Interplay between Plant Cell Walls and Jasmonate Production.” *Plant and Cell Physiology* 60 (12): 2629–37. <https://doi.org/10.1093/PCP/PCZ119>.
- Min, Xueyang, Xiaoshan Lin, Boniface Ndayambaza, Yanrong Wang, and Wenxian Liu. 2020. “Coordinated Mechanisms of Leaves and Roots in Response to Drought Stress Underlying Full-Length Transcriptome Profiling in *Vicia Sativa* L.” *BMC Plant Biology* 20 (1): 1–21. <https://doi.org/10.1186/S12870-020-02358-8/FIGURES/12>.
- Mittler, Ron, Yong Sig Kim, Luhua Song, Jesse Coutu, Alicia Coutu, Sultan Ciftci-Yilmaz, Hojong Lee, Becky Stevenson, and Jian Kang Zhu. 2006. “Gain- and Loss-of-Function Mutations in *Zat10* Enhance the Tolerance of Plants to Abiotic Stress.” *FEBS Letters* 580 (28–29): 6537. <https://doi.org/10.1016/J.FEBSLET.2006.11.002>.
- Miura, Kenji, Yasuomi Tada, and Kenji * Miura. 2014. “Regulation of Water, Salinity, and Cold Stress Responses by Salicylic Acid.” <https://doi.org/10.3389/fpls.2014.00004>.
- Monties, Bernard, and Kazuhiko Fukushima. 2005. “Occurrence, Function and Biosynthesis of Lignins.” In *Biopolymers Online*. <https://doi.org/https://doi.org/10.1002/3527600035.bpol1001>.
- Moore, Kenneth J, and Hans-joachim G Jung. 2001. “Lignin and Fiber Digestion.” *JOURNAL OF RANGE MANAGEMENT* 54 (July): 420–30.
- Morales, Melanie, Ot Pasques, and Sergi Munné-Bosch. 2021. “English Plantain Deploys Stress Tolerance Mechanisms at Various Organization Levels across an Altitudinal Gradient in the Pyrenees.” *Physiologia Plantarum* 173 (4): 2350–60. <https://doi.org/10.1111/ppl.13586>.
- Moura, Jullyana Cristina Magalhães Silva, Cesar Augusto Valencise Bonine, Juliana de Oliveira Fernandes Viana, Marcelo Carnier Dornelas, and Paulo Mazzafera. 2010. “Abiotic and Biotic Stresses and Changes in the Lignin Content and Composition in Plants.” *Journal*

of *Integrative Plant Biology* 52 (4): 360–76. <https://doi.org/10.1111/J.1744-7909.2010.00892.X>.

Muhammad Aslam, Mehtab, Muhammad Waseem, Bello Hassan Jakada, Eyalira Jacob Okal, Zuliang Lei, Hafiz Sohaib Ahmad Saqib, Wei Yuan, Weifeng Xu, and Qian Zhang. 2022. “Mechanisms of Abscisic Acid-Mediated Drought Stress Responses in Plants.” *International Journal of Molecular Sciences* 23 (3). <https://doi.org/10.3390/ijms23031084>.

Muhr, Jan, Janine Franke, and Werner Borken. 2010. “Drying-Rewetting Events Reduce C and N Losses from a Norway Spruce Forest Floor.” *Soil Biology and Biochemistry* 42 (8): 1303–12. <https://doi.org/10.1016/j.soilbio.2010.03.024>.

Munemasa, Shintaro, Felix Hauser, Jiyoung Park, Rainer Waadt, Benjamin Brandt, and Julian I. Schroeder. 2015. “Mechanisms of Abscisic Acid-Mediated Control of Stomatal Aperture.” *Current Opinion in Plant Biology* 28 (December): 154–62. <https://doi.org/10.1016/j.PBI.2015.10.010>.

Mutava, Raymond N., Silvas Jebakumar K. Prince, Naeem Hasan Syed, Li Song, Babu Valliyodan, Wei Chen, and Henry T. Nguyen. 2015. “Understanding Abiotic Stress Tolerance Mechanisms in Soybean: A Comparative Evaluation of Soybean Response to Drought and Flooding Stress.” *Plant Physiology and Biochemistry* 86 (January): 109–20. <https://doi.org/10.1016/j.plaphy.2014.11.010>.

Muthamilarasan, Mehanathan, Nagendra Kumar Singh, and Manoj Prasad. 2019. “Chapter One - Multi-Omics Approaches for Strategic Improvement of Stress Tolerance in Underutilized Crop Species: A Climate Change Perspective.” In , edited by Dhavendra B T - *Advances in Genetics* Kumar, 103:1–38. Academic Press. <https://doi.org/https://doi.org/10.1016/bs.adgen.2019.01.001>.

Naudts, K., J. Van den Berge, E. Farfan, P. Rose, H. AbdElgawad, R. Ceulemans, I. A. Janssens, H. Asard, and I. Nijs. 2013. “Future Climate Alleviates Stress Impact on Grassland Productivity through Altered Antioxidant Capacity.” *Environmental and Experimental Botany* 99 (2014): 150–58. <https://doi.org/10.1016/j.envexpbot.2013.11.003>.

Niu, Yufei, Jingyu Li, Fanting Sun, Taiyu Song, Baojia Han, Zijie Liu, and Peisen Su. 2023. “Comparative Transcriptome Analysis Reveals the Key Genes and Pathways Involved in Drought Stress Response of Two Wheat (*Triticum Aestivum* L) Varieties.” *Genomics* 115 (5): 110688. <https://doi.org/10.1016/J.YGENO.2023.110688>.

Novaković, Lazar, Tingting Guo, Antony Bacic, Arun Sampathkumar, and Kim L. Johnson. 2018. “Hitting the Wall—Sensing and Signaling Pathways Involved in Plant Cell Wall Remodeling in Response to Abiotic Stress.” *Plants* 7 (4): 1–25. <https://doi.org/10.3390/plants7040089>.

Obata, Toshihiro. 2019. “Metabolons in Plant Primary and Secondary Metabolism.” *Phytochemistry Reviews* 18 (6): 1483–1507. <https://doi.org/10.1007/S11101-019-09619-X>.

Obata, Toshihiro, Sandra Witt, Jan Lisec, Natalia Palacios-Rojas, Igor Florez-Sarasa, Salima Yousfi, Jose Luis Araus, Jill E. Cairns, and Alisdair R. Fernie. 2015. “Metabolite Profiles of Maize Leaves in Drought, Heat, and Combined Stress Field Trials Reveal the Relationship

Bibliography

- between Metabolism and Grain Yield.” *Plant Physiology* 169 (4): 2665–83. <https://doi.org/10.1104/PP.15.01164>.
- OKSANEN, J. 2007. “Vegan : Community Ecology Package. R Package Version 1.8-5.” <Http://Www.Cran.r-Project.Org>.
- Oladosu, Yusuff, Mohd Y. Rafii, Chukwu Samuel, Arolu Fatai, Usman Magaji, Isiaka Kareem, Zarifh Shafika Kamarudin, Isma’ila Muhammad, and Kazeem Kolapo. 2019. “Drought Resistance in Rice from Conventional to Molecular Breeding: A Review.” *International Journal of Molecular Sciences* 20 (14). <https://doi.org/10.3390/ijms20143519>.
- O’Mara, F. P. 2012. “The Role of Grasslands in Food Security and Climate Change.” *Annals of Botany* 110 (6): 1263–70. <https://doi.org/10.1093/aob/mcs209>.
- Onyemaobi, Olive, Harriet Sangma, Gagan Garg, Xiaomei Wallace, Sue Kleven, Pipob Suwanchaikasem, Ute Roessner, and Rudy Dolferus. 2021. “Reproductive Stage Drought Tolerance in Wheat: Importance of Stomatal Conductance and Plant Growth Regulators.” *Genes* 12 (11). <https://doi.org/10.3390/genes12111742>.
- Orians, Colin M, Rabea Schweiger, Jeffrey S Dukes, Eric R Scott, and Caroline Müller. 2019. “Combined Impacts of Prolonged Drought and Warming on Plant Size and Foliar Chemistry.” *Annals of Botany* 124: 41–52. <https://doi.org/10.1093/aob/mcz004>.
- Osvaldo, Susanne Schwinning, and E Sala. 2004. “PULSE EVENTS AND ARID ECOSYSTEMS Hierarchy of Responses to Resource Pulses in Arid and Semi-Arid Ecosystems.” *Oecologia* 141: 211–20. <https://doi.org/10.1007/s00442-004-1520-8>.
- Pagant, Silvère, Adeline Bichet, Keiko Sugimoto, Olivier Lerouxel, Thierry Desprez, Maureen McCann, Patrice Lerouge, Samantha Vernhettes, and Herman Höfte. 2002. “KOBITO1 Encodes a Novel Plasma Membrane Protein Necessary for Normal Synthesis of Cellulose during Cell Expansion in Arabidopsis.” *The Plant Cell* 14 (9): 2001. <https://doi.org/10.1105/TPC.002873>.
- Parent, Claire, Nicolas Capelli, Audrey Berger, Michèle Crèvecoeur, and James F Dat. 2008. “An Overview of Plant Responses to Soil Waterlogging.” *Plant Stress* 2: 20–27.
- Parida, Asish Kumar, Vipin S Dagaonkar, Manoj S Phalak, G V Umalkar, and Laxman P Aurangabadkar. 2007. “Alterations in Photosynthetic Pigments, Protein and Osmotic Components in Cotton Genotypes Subjected to Short-Term Drought Stress Followed by Recovery.” *Plant Biotechnology Reports* 1 (1): 37–48. <https://doi.org/10.1007/s11816-006-0004-1>.
- Pedersen, Eric J., David L. Miller, Gavin L. Simpson, and Noam Ross. 2019. “Hierarchical Generalized Additive Models in Ecology: An Introduction with MgcV.” *PeerJ* 2019 (5): e6876. <https://doi.org/10.7717/PEERJ.6876/SUPP-1>.
- Petermann, Jana S., and Oksana Y. Buzhdygan. 2021. “Grassland Biodiversity.” *Current Biology* 31 (19): R1195–1201. <https://doi.org/10.1016/j.cub.2021.06.060>.
- Peters, Kristian, Anja Worrich, Alexander Weinhold, Oliver Alka, Gerd Balcke, Claudia Birkemeyer, Helge Bruelheide, et al. 2018. “Current Challenges in Plant Eco-Metabolomics.” *International Journal of Molecular Sciences* 19 (5). <https://doi.org/10.3390/IJMS19051385>.

Bibliography

- Pfleiderer, Peter, Carl Friedrich Schleussner, Kai Kornhuber, and Dim Coumou. 2019. "Summer Weather Becomes More Persistent in a 2 °C World." *Nature Climate Change* 2019 9:9 9 (9): 666–71. <https://doi.org/10.1038/s41558-019-0555-0>.
- Phillips, Katherine M., Maria Teresa Tarragó-Trani, Tina M. Grove, Ingolf Grün, Rita Lugogo, Robert F. Harris, and Kent K. Stewart. 1997. "Simplified Gravimetric Determination of Total Fat in Food Composites after Chloroform-Methanol Extraction." *JAOCs, Journal of the American Oil Chemists' Society* 74 (2): 137–42. <https://doi.org/10.1007/s11746-997-0158-1>.
- Phukan, Ujjal J, Sonal Mishra, and Rakesh Kumar Shukla. 2016. "Waterlogging and Submergence Stress: Affects and Acclimation." *Critical Reviews in Biotechnology* 36 (5): 956–66. <https://doi.org/10.3109/07388551.2015.1064856>.
- Pinheiro, C., and M. M. Chaves. 2011. "Photosynthesis and Drought: Can We Make Metabolic Connections from Available Data?" *Journal of Experimental Botany* 62 (3): 869–82. <https://doi.org/10.1093/jxb/erq340>.
- Pinheiro, J., D. Bates, S. DebRoy, D. Sarkar, and R Core Team. 2018. "nlme: Linear and Nonlinear Mixed Effects Models. R Package Version 3.1-163."
- Pluskal, Tomáš, Sandra Castillo, Alejandro Villar-Briones, and Matej Orešič. 2010. "MZmine 2: Modular Framework for Processing, Visualizing, and Analyzing Mass Spectrometry-Based Molecular Profile Data." *BMC Bioinformatics* 11 (July). <https://doi.org/10.1186/1471-2105-11-395>.
- Prasad, P V V, S A Staggenborg, and Z Ristic. 2008. "Impacts of Drought and/or Heat Stress on Physiological, Developmental, Growth, and Yield Processes of Crop Plants." In *Response of Crops to Limited Water*, 301–55. Advances in Agricultural Systems Modeling. <https://doi.org/https://doi.org/10.2134/advagricsystmodel1.c11>.
- Priyashantha, A. K.Hasith, Dong Qin Dai, Darbhe J. Bhat, Steven L. Stephenson, Itthayakorn Promputtha, Prashant Kaushik, Saowaluck Tibpromma, and Samantha C. Karunarathna. 2023. "Plant–Fungi Interactions: Where It Goes?" *Biology* 12 (6): 1–22. <https://doi.org/10.3390/biology12060809>.
- Pulido, Pablo, Roland Cazalis, and Francisco Javier Cejudo. 2009. "An Antioxidant Redox System in the Nucleus of Wheat Seed Cells Suffering Oxidative Stress." *The Plant Journal* 57 (1): 132–45. <https://doi.org/10.1111/J.1365-3113X.2008.03675.X>.
- Qi, Qungang, Patricia A. Rose, Garth D. Abrams, David C. Taylor, Suzanne R. Abrams, and Adrian J. Cutler. 1998. "(+)-Abscisic Acid Metabolism, 3-Ketoacyl-Coenzyme a Synthase Gene Expression, and Very-Long-Chain Monounsaturated Fatty Acid Biosynthesis in Brassica Napus Embryos." *Plant Physiology* 117 (3): 979–87. <https://doi.org/10.1104/pp.117.3.979>.
- Qi, Yiping, Kenichi Tsuda, Anna Joe, Masanao Sato, Le V. Nguyen, Jane Glazebrook, James R. Alfano, Jerry D. Cohen, and Fumiaki Katagiri. 2010. "A Putative RNA-Binding Protein Positively Regulates Salicylic Acid-Mediated Immunity in Arabidopsis." <https://doi.org/10.1094/MPMI-05-10-0106> 23 (12): 1573–83. <https://doi.org/10.1094/MPMI-05-10-0106>.
- Radujković, Dajana, Rudy van Diggelen, Roland Bobbink, Maaïke Weijters, Jim Harris, Mark Pawlett, Sara Vicca, and Erik Verbruggen. 2020. "Initial Soil Community Drives

Bibliography

- Heathland Fungal Community Trajectory over Multiple Years through Altered Plant–Soil Interactions.” *New Phytologist* 225 (5): 2140–51. <https://doi.org/10.1111/nph.16226>.
- Ramírez, D. A., J. L. Rolando, W. Yactayo, P. Monneveux, V. Mares, and R. Quiroz. 2015. “Improving Potato Drought Tolerance through the Induction of Long-Term Water Stress Memory.” *Plant Science* 238 (September): 26–32. <https://doi.org/10.1016/J.PLANTSCI.2015.05.016>.
- Rangani, Jaykumar, Ashok Panda, and Asish Kumar Parida. 2020. “Metabolomic Study Reveals Key Metabolic Adjustments in the Xerohalophyte *Salvadora Persica* L. during Adaptation to Water Deficit and Subsequent Recovery Conditions.” *Plant Physiology and Biochemistry* 150 (January): 180–95. <https://doi.org/10.1016/j.plaphy.2020.02.036>.
- Revenga, Carmen. 2001. *Pilot Analysis of Global Ecosystems: Freshwater Systems*.
- Reyer, C, S Leuzinger, A Rammig, A Wolf, R P Bartholomeus, A Bonfante, F de Lorenzi, et al. 2013. “A Plant’s Perspective of Extremes: Terrestrial Plant Responses to Changing Climatic Variability Europe PMC Funders Group.” *Glob Chang Biol* 19 (1). <https://doi.org/10.1111/gcb.12023>.
- Reynaert, Simon, Hans J. De Boeck, Erik Verbruggen, Maya Verlinden, Nina Flowers, and Ivan Nijs. 2021. “Risk of Short-Term Biodiversity Loss under More Persistent Precipitation Regimes.” *Global Change Biology* 27 (8): 1614–26. <https://doi.org/10.1111/GCB.15501>.
- Reynaert, Simon, Lin Zi, Hamada AbdElgawad, Hans J. De Boeck, Olga Vindušková, Ivan Nijs, Gerrit Beemster, and Han Asard. 2022. “Does Previous Exposure to Extreme Precipitation Regimes Result in Acclimated Grassland Communities?” *Science of The Total Environment* 838 (February): 156368. <https://doi.org/10.1016/j.scitotenv.2022.156368>.
- Ristok, Christian, Yvonne Poeschl, Jan Hendrik Dudenhöffer, Anne Ebeling, Nico Eisenhauer, Fredd Vergara, Cameron Wagg, Nicole M. van Dam, and Alexander Weinhold. 2019. “Plant Species Richness Elicits Changes in the Metabolome of Grassland Species via Soil Biotic Legacy.” *Journal of Ecology* 107 (5): 2240–54. <https://doi.org/10.1111/1365-2745.13185>.
- Rivas-Ubach, Albert, Albert Gargallo-Garriga, Jordi Sardans, Michal Oravec, Laia Mateu-Castell, Míriam Pérez-Trujillo, Teodor Parella, Romà Ogaya, Otmar Urban, and Josep Peñuelas. 2014. “Drought Enhances Folivory by Shifting Foliar Metabolomes in *Quercus Ilex* Trees.” *New Phytologist* 202 (3): 874–85. <https://doi.org/10.1111/NPH.12687>.
- Rohart, Florian, Benoît Gautier, Amrit Singh, and Kim Anh Lê Cao. 2017. “MixOmics: An R Package for ‘omics Feature Selection and Multiple Data Integration.” *PLOS Computational Biology* 13 (11): e1005752. <https://doi.org/10.1371/JOURNAL.PCBI.1005752>.
- Romero, Helena, Delphine M. Pott, José G. Vallarino, and Sonia Osorio. 2021. “Metabolomics-Based Evaluation of Crop Quality Changes as a Consequence of Climate Change.” *Metabolites* 2021, Vol. 11, Page 461 11 (7): 461. <https://doi.org/10.3390/METABO11070461>.
- Rosa, Mariana, Carolina Prado, Griselda Podazza, Roque Interdonato, Juan A. González, Mirna Hilal, and Fernando E. Prado. 2009. “Soluble Sugars-Metabolism, Sensing and Abiotic Stress a Complex Network in the Life of Plants.” *Plant Signaling and Behavior* 4 (5): 388–93. <https://doi.org/10.4161/psb.4.5.8294>.
- Rosas, Teresa, Lucía Galiano, Romà Ogaya, Josep Peñuelas, and Jordi Martínez-Vilalta. 2013. “Dynamics of Non-Structural Carbohydrates in Three Mediterranean Woody

- Species Following Long-Term Experimental Drought." *Frontiers in Plant Science* 4 (OCT). <https://doi.org/10.3389/FPLS.2013.00400>.
- Sabehat, Adnan, David Weiss, and Susan Lurie. 1998. "Heat-Shock Proteins and Cross-Tolerance in Plants." *Physiologia Plantarum* 103 (3): 437–41. <https://doi.org/https://doi.org/10.1034/j.1399-3054.1998.1030317.x>.
- Sala, Osvaldo E. 2001. "Temperate Grasslands BT - Global Biodiversity in a Changing Environment: Scenarios for the 21st Century." In , edited by F Stuart Chapin, Osvaldo E Sala, and Elisabeth Huber-Sannwald, 121–37. New York, NY: Springer New York. https://doi.org/10.1007/978-1-4613-0157-8_7.
- Sala, Osvaldo E., Lucía Vivanco, and Pedro Flombaum. 2013. "Grassland Ecosystems." *Encyclopedia of Biodiversity: Second Edition*, January, 1–7. <https://doi.org/10.1016/B978-0-12-384719-5.00259-8>.
- Salazar, Osvaldo, Juan Vargas, Francisco Nájera, Oscar Seguel, and Manuel Casanova. 2014. "Monitoring of Nitrate Leaching during Flush Flooding Events in a Coarse-Textured Floodplain Soil." *Agricultural Water Management* 146 (3): 218–27. <https://doi.org/10.1016/j.agwat.2014.08.014>.
- Santiago, Rogelio, Jaime Barros-Rios, and Rosa A. Malvar. 2013. "Impact of Cell Wall Composition on Maize Resistance to Pests and Diseases." *International Journal of Molecular Sciences* 14 (4): 6960–80. <https://doi.org/10.3390/ijms14046960>.
- Santos, Tiago Benedito dos, Alessandra Ferreira Ribas, Silvia Graciele Hülse de Souza, Ilara Gabriela Frasson Budzinski, and Douglas Silva Domingues. 2022. "Physiological Responses to Drought, Salinity, and Heat Stress in Plants: A Review." *Stresses* 2 (1): 113–35. <https://doi.org/10.3390/STRESSES2010009/S1>.
- Sardans, Jordi, Albert Gargallo-Garriga, Otmar Urban, Karel Klem, Tom W.N. Walker, Petr Holub, Ivan A. Janssens, and Josep Peñuelas. 2020. "Ecometabolomics for a Better Understanding of Plant Responses and Acclimation to Abiotic Factors Linked to Global Change." *Metabolites* 10 (6): 1–20. <https://doi.org/10.3390/METABO10060239>.
- Sardans, Jordi, Josep Peñuelas, and Albert Rivas-Ubach. 2011. "Ecological Metabolomics: Overview of Current Developments and Future Challenges." *Chemoecology* 21 (4): 191–225. <https://doi.org/10.1007/S00049-011-0083-5/TABLES/4>.
- Sasaki, Hidekazu, Kazuo Ichimura, Kunihiro Okada, and Masayuki Oda. 1998. "Freezing Tolerance and Soluble Sugar Contents Affected by Water Stress during Cold-Acclimation and de-Acclimation in Cabbage Seedlings." *Scientia Horticulturae* 76 (3): 161–69. [https://doi.org/https://doi.org/10.1016/S0304-4238\(98\)00143-5](https://doi.org/https://doi.org/10.1016/S0304-4238(98)00143-5).
- Schärer, Marie Louise, Andreas Lüscher, and Ansgar Kahmen. 2023. "Post-Drought Compensatory Growth in Perennial Grasslands Is Determined by Legacy Effects of the Soil and Not by Plants." *New Phytologist*, 2265–75. <https://doi.org/10.1111/nph.19291>.
- Schmitz, E., E. Nordberg Karlsson, and P. Adlercreutz. 2020. "Warming Weather Changes the Chemical Composition of Oat Hulls." *Plant Biology* 22 (6): 1086–91. <https://doi.org/10.1111/PLB.13171>.
- Schweiger, Rabea, Markus C. Baier, Marcus Persicke, and Caroline Müller. 2014. "High Specificity in Plant Leaf Metabolic Responses to Arbuscular Mycorrhiza." *Nature Communications* 2014 5:1 5 (1): 1–11. <https://doi.org/10.1038/ncomms4886>.

Bibliography

- Seago, James L., Leland C. Marsh, Kevin J. Stevens, Aleš Soukup, Olga Votrubová, and Daryl E. Enstone. 2005. "A Re-Examination of the Root Cortex in Wetland Flowering Plants with Respect to Aerenchyma." *Annals of Botany* 96 (4): 565–79. <https://doi.org/10.1093/aob/mci211>.
- Sebastiania, M., A. Gargallo-Garriga, J. Sardans, M. Pérez-Trujillo, F. Monteiro, A. Figueiredo, M. Maia, et al. 2021. "Metabolomics and Transcriptomics to Decipher Molecular Mechanisms Underlying Ectomycorrhizal Root Colonization of an Oak Tree." *Scientific Reports* 11 (1). <https://doi.org/10.1038/S41598-021-87886-5>.
- Shahbazy, Mohammad, Parviz Moradi, Gokhan Ertaylan, Ali Zahraei, and Mohsen Kompany-Zareh. 2020. "FTICR Mass Spectrometry-Based Multivariate Analysis to Explore Distinctive Metabolites and Metabolic Pathways: A Comprehensive Bioanalytical Strategy toward Time-Course Metabolic Profiling of *Thymus Vulgaris* Plants Responding to Drought Stress." *Plant Science* 290 (January): 110257. <https://doi.org/10.1016/J.PLANTSCI.2019.110257>.
- Shamsunnaher, Xiuhua Chen, Xiaoxuan Zhang, Xiao Xia Wu, Xiaoen Huang, and Wen Yuan Song. 2020. "Rice Immune Sensor XA21 Differentially Enhances Plant Growth and Survival under Distinct Levels of Drought." *Scientific Reports* 2020 10:1 10 (1): 1–11. <https://doi.org/10.1038/s41598-020-73128-7>.
- Shedletzky, Esther, Christoph Unger, and Deborah P Delmer. 1997. "A Microtiter-Based Fluorescence Assay for (1, 3) - b -Glucan Synthases" 93 (249): 88–93.
- Shen, Jiazhi, Shuangshuang Wang, Litao Sun, Yu Wang, Kai Fan, Chen Li, Hui Wang, Caihong Bi, Fen Zhang, and Zhaotang Ding. 2022. "Dynamic Changes in Metabolic and Lipidomic Profiles of Tea Plants during Drought Stress and Re-Watering." *Frontiers in Plant Science* 13 (September): 1–16. <https://doi.org/10.3389/fpls.2022.978531>.
- Shinozaki, Kazuo, and Kazuko Yamaguchi-Shinozaki. 2007. "Gene Networks Involved in Drought Stress Response and Tolerance." *Journal of Experimental Botany* 58 (2): 221–27. <https://doi.org/10.1093/JXB/ERL164>.
- Signarbieux, Constant, and Urs Feller. 2012. "Effects of an Extended Drought Period on Physiological Properties of Grassland Species in the Field." *Journal of Plant Research* 125 (2): 251–61. <https://doi.org/10.1007/s10265-011-0427-9>.
- Signori-Müller, Caroline, Rafael S. Oliveira, Fernanda de Vasconcellos Barros, Julia Valentim Tavares, Martin Gilpin, Francisco Carvalho Diniz, Manuel J. Marca Zevallos, et al. 2021. "Non-Structural Carbohydrates Mediate Seasonal Water Stress across Amazon Forests." *Nature Communications* 12 (1). <https://doi.org/10.1038/s41467-021-22378-8>.
- Silva, Elizamar Ciríaco da, RJMC Nogueira, Marcelle Almeida da Silva, and Manoel Bandeira de Albuquerque. 2011. "Drought Stress and Plant Nutrition." *Plant Stress* 5 (1): 32–41.
- Singh, Shikha, Melanie A. Mayes, Stephanie N. Kivlin, and Sindhu Jagadamma. 2023. "How the Birch Effect Differs in Mechanisms and Magnitudes Due to Soil Texture." *Soil Biology and Biochemistry* 179 (September 2022): 108973. <https://doi.org/10.1016/j.soilbio.2023.108973>.
- Smith, Melinda D. 2011. "An Ecological Perspective on Extreme Climatic Events: A Synthetic Definition and Framework to Guide Future Research." *Journal of Ecology* 99 (3): 656–63. <https://doi.org/10.1111/J.1365-2745.2011.01798.X>.

- Soliman, Wagdi Saber, Shu ichi Sugiyama, and Ahmed M. Abbas. 2018. "Contribution of Avoidance and Tolerance Strategies towards Salinity Stress Resistance in Eight C3 Turfgrass Species." *Horticulture Environment and Biotechnology* 59 (1): 29–36. <https://doi.org/10.1007/s13580-018-0004-4>.
- Song, Lin, Wentao Luo, Robert J. Griffin-Nolan, Wang Ma, Jiangping Cai, Xiaon Zuo, Qiang Yu, et al. 2022. "Differential Responses of Grassland Community Nonstructural Carbohydrate to Experimental Drought along a Natural Aridity Gradient." *Science of The Total Environment* 822: 153589. <https://doi.org/10.1016/j.scitotenv.2022.153589>.
- Song, Wen Yuan, Guo Liang Wang, Li Li Chen, Han Suk Kim, Li Ya Pi, Tom Holsten, J. Gardner, et al. 1995. "A Receptor Kinase-Like Protein Encoded by the Rice Disease Resistance Gene, Xa21." *Science* 270 (5243): 1804. <https://doi.org/10.1126/SCIENCE.270.5243.1804>.
- Soniya, E. V., Asha Srinivasan, Athira Menon, and Divya Kattupalli. 2022. *Transcriptomics in Response of Biotic Stress in Plants. Transcriptome Profiling: Progress and Prospects*. INC. <https://doi.org/10.1016/B978-0-323-91810-7.00018-2>.
- Stampfli, Andreas, Juliette M G Bloor, Markus Fischer, and Michaela Zeiter. 2018. "High Land-Use Intensity Exacerbates Shifts in Grassland Vegetation Composition after Severe Experimental Drought." *Global Change Biology* 24 (5): 2021–34. <https://doi.org/https://doi.org/10.1111/gcb.14046>.
- Stewart, Rebecca I.A., Matteo Dossena, David A. Bohan, Erik Jeppesen, Rebecca L. Kordas, Mark E. Ledger, Mariana Meerhoff, et al. 2013. *Mesocosm Experiments as a Tool for Ecological Climate-Change Research. Advances in Ecological Research*. Vol. 48. Elsevier Ltd. <https://doi.org/10.1016/B978-0-12-417199-2.00002-1>.
- Strable, Josh, and Michael J. Scanlon. 2009. "Maize (Zea Mays): A Model Organism for Basic and Applied Research in Plant Biology." *Cold Spring Harbor Protocols* 4 (10). <https://doi.org/10.1101/PDB.EMO132>.
- Striker, Gustavo Gabriel. 2012. "Flooding Stress on Plants : Anatomical , Morphological and Physiological Responses." *Botany*, no. March 2012: 3–28.
- Sun, Liangwu, Byron Adams, James R. Gurnon, Yen Ye, and James L. Van Etten. 1999. "Characterization of Two Chitinase Genes and One Chitosanase Gene Encoded by Chlorella Virus PBCV-1." *Virology* 263 (2): 376–87. <https://doi.org/10.1006/viro.1999.9958>.
- Sun, Xiao Li, Qing Yue Yu, Li Li Tang, Wei Ji, Xi Bai, Hua Cai, Xiao Fei Liu, Xiao Dong Ding, and Yan Ming Zhu. 2013. "GsSRK, a G-Type Lectin S-Receptor-like Serine/Threonine Protein Kinase, Is a Positive Regulator of Plant Tolerance to Salt Stress." *Journal of Plant Physiology* 170 (5): 505–15. <https://doi.org/10.1016/J.JPLPH.2012.11.017>.
- Sundert, Kevin Van, Mohammed A S Arfin Khan, Siddharth Bharath, Yvonne M Buckley, Maria C Caldeira, Ian Donohue, Maren Dubbert, et al. 2021. "Fertilized Graminoids Intensify Negative Drought Effects on Grassland Productivity." *Global Change Biology* 27 (11): 2441–57. <https://doi.org/https://doi.org/10.1111/gcb.15583>.
- Sundert, Kevin Van, Veronika Brune, Michael Bahn, Mario Deutschmann, Roland Hasibeder, Ivan Nijs, and Sara Vicca. 2020. "Post-Drought Rewetting Triggers Substantial K Release and Shifts in Leaf Stoichiometry in Managed and Abandoned Mountain

- Grasslands." *Plant and Soil* 448 (1): 353–68. <https://doi.org/10.1007/s11104-020-04432-4>.
- Suttle, K. B., Meredith A. Thomsen, and Mary E. Power. 2007. "Species Interactions Reverse Grassland Responses to Changing Climate." *Science* 315 (5812): 640–42. https://doi.org/10.1126/SCIENCE.1136401/SUPPL_FILE/SUTTLE.SOM.REV1.PDF.
- Tang, Jingchao, Baodi Sun, Ruimei Cheng, Zuomin Shi, Da Luo, Shirong Liu, and Mauro Centritto. 2019. "Effects of Soil Nitrogen (N) Deficiency on Photosynthetic N-Use Efficiency in N-Fixing and Non-N-Fixing Tree Seedlings in Subtropical China." *Scientific Reports* 9 (1): 1–14. <https://doi.org/10.1038/s41598-019-41035-1>.
- Tang, Sha, Lin Li, Yongqiang Wang, Qiannan Chen, Wenying Zhang, Guanqing Jia, Hui Zhi, Baohua Zhao, and Xianmin Diao. n.d. "Genotype-Specific Physiological and Transcriptomic Responses to Drought Stress in *Setaria Italica* (an Emerging Model for Panicoideae Grasses) OPEN." Accessed May 2, 2023. <https://doi.org/10.1038/s41598-017-08854-6>.
- Tantray, Aadil Yousuf, Sheikh Shanawaz Bashir, and Altaf Ahmad. 2020. "Low Nitrogen Stress Regulates Chlorophyll Fluorescence in Coordination with Photosynthesis and Rubisco Efficiency of Rice." *Physiology and Molecular Biology of Plants* 26 (1): 83–94. <https://doi.org/10.1007/s12298-019-00721-0>.
- Tebaldi, Claudia, Katharinec Hayhoe, Julie M. Arblaster, and Gerald A. Meehl. 2006. "Going to the Extremes: An Intercomparison of Model-Simulated Historical and Future Changes in Extreme Events." *Climatic Change* 79 (3–4): 185–211. <https://doi.org/10.1007/s10584-006-9051-4>.
- Tenhaken, Raimund. 2015. "Cell Wall Remodeling under Abiotic Stress." *Frontiers in Plant Science* 5 (JAN): 771. <https://doi.org/10.3389/FPLS.2014.00771/BIBTEX>.
- terHorst, Casey P., and Peter C. Zee. 2016. "Eco-Evolutionary Dynamics in Plant–Soil Feedbacks." *Functional Ecology* 30 (7): 1062–72. <https://doi.org/10.1111/1365-2435.12671>.
- Thatcher, Shawn R., Olga N. Danilevskaya, Xin Meng, Mary Beatty, Gina Zastrow-Hayes, Charlotte Harris, Brandon Van Allen, Jeffrey Habben, and Bailin Li. 2016. "Genome-Wide Analysis of Alternative Splicing during Development and Drought Stress in Maize." *Plant Physiology* 170 (1): 586. <https://doi.org/10.1104/PP.15.01267>.
- Todaka, Daisuke, Yu Zhao, Takuya Yoshida, Madoka Kudo, Satoshi Kidokoro, Junya Mizoi, Ken Suke Kodaira, et al. 2017. "Temporal and Spatial Changes in Gene Expression, Metabolite Accumulation and Phytohormone Content in Rice Seedlings Grown under Drought Stress Conditions." *The Plant Journal : For Cell and Molecular Biology* 90 (1): 61–78. <https://doi.org/10.1111/TPJ.13468>.
- Troelstra, Sep R, and Frank Berendse. 1982. "Root CEC Determinations to Establish Root Biomasses of Two Plant Species Grown in Mixtures." *Plant and Soil* 64 (2): 277–81. <https://doi.org/10.1007/BF02184262>.
- Tuel, A., D. Steinfeld, S. M. Ali, M. Sprenger, and O. Martius. 2022. "Large-Scale Drivers of Persistent Extreme Weather During Early Summer 2021 in Europe." *Geophysical Research Letters* 49 (18): 1–11. <https://doi.org/10.1029/2022GL099624>.

- Tugizimana, Fidele, Msizi I. Mhlongo, Lizelle A. Piater, and Ian A. Dubery. 2018. "Metabolomics in Plant Priming Research: The Way Forward?" *International Journal of Molecular Sciences* 19 (6). <https://doi.org/10.3390/ijms19061759>.
- Turner, Neil C, Graeme C Wright, and K H M B T - Advances in Agronomy Siddique. 2001. "Adaptation of Grain Legumes (Pulses) to Water-Limited Environments." In , 71:193–231. Academic Press. [https://doi.org/https://doi.org/10.1016/S0065-2113\(01\)71015-2](https://doi.org/https://doi.org/10.1016/S0065-2113(01)71015-2).
- Ummenhofer, Caroline C., and Gerald A. Meehl. 2017. "Extreme Weather and Climate Events with Ecological Relevance: A Review." *Philosophical Transactions of the Royal Society B: Biological Sciences* 372 (1723). <https://doi.org/10.1098/rstb.2016.0135>.
- UNDRR. 2020. "The Human Cost of Disasters: An Overview of the Last 20 Years (2000–2019)." *Human Cost of Disasters*. <https://doi.org/10.18356/79b92774-en>.
- Upchurch, Robert G. 2008. "Fatty Acid Unsaturation, Mobilization, and Regulation in the Response of Plants to Stress." *Biotechnology Letters* 2008 30:6 30 (6): 967–77. <https://doi.org/10.1007/S10529-008-9639-Z>.
- Velioglu, Y. S., G. Mazza, L. Gao, and B. D. Oomah. 1998. "Antioxidant Activity and Total Phenolics in Selected Fruits, Vegetables, and Grain Products." *Journal of Agricultural and Food Chemistry* 46 (10): 4113–17. <https://doi.org/10.1021/JF9801973>.
- Vicca, S., A. K. Gilgen, M. Camino Serrano, F. E. Dreesen, J. S. Dukes, M. Estiarte, S. B. Gray, et al. 2012. "Urgent Need for a Common Metric to Make Precipitation Manipulation Experiments Comparable." *New Phytologist* 195 (3): 518–22. <https://doi.org/10.1111/J.1469-8137.2012.04224.X>.
- Vogt, Thomas. 2010. "Phenylpropanoid Biosynthesis." *Molecular Plant* 3 (1): 2–20. <https://doi.org/10.1093/MP/SSP106>.
- Walter, Julia, Anke Jentsch, Carl Beierkuhnlein, and Juergen Kreyling. 2013. "Ecological Stress Memory and Cross Stress Tolerance in Plants in the Face of Climate Extremes." *Environmental and Experimental Botany* 94: 3–8. <https://doi.org/10.1016/j.envexpbot.2012.02.009>.
- Wan, Jinrong, Shuqun Zhang, and Gary Stacey. 2004. "Activation of a Mitogen-Activated Protein Kinase Pathway in Arabidopsis by Chitin." *Molecular Plant Pathology* 5 (2): 125–35. <https://doi.org/10.1111/J.1364-3703.2004.00215.X>.
- Wan, Jinrong, Xue-cheng Zhang, and Gary Stacey. 2008. "Chitin Signaling and Plant Disease Resistance." *Molecular Plant Pathology* 6 (October): 831–33. <https://doi.org/10.1199/tab.002>.
- Wang, Hongxia, Chengyuan Wang, Weijuan Fan, Jun Yang, Ingo Appelhagen, Yinliang Wu, and Peng Zhang. 2018. "A Novel Glycosyltransferase Catalyses the Transfer of Glucose to Glucosylated Anthocyanins in Purple Sweet Potato." *Journal of Experimental Botany* 69 (22): 5444. <https://doi.org/10.1093/JXB/ERY305>.
- Wang, Hongyan, Honglei Wang, Hongbo Shao, and Xiaoli Tang. 2016. "Recent Advances in Utilizing Transcription Factors to Improve Plant Abiotic Stress Tolerance by Transgenic Technology." *Frontiers in Plant Science* 7 (FEB2016): 67. <https://doi.org/10.3389/FPLS.2016.00067/BIBTEX>.
- Wang, Mingxun, Jeremy J Carver, Vanessa V Phelan, Laura M Sanchez, Neha Garg, Yao Peng, Don Duy Nguyen, et al. 2016. "Sharing and Community Curation of Mass

- Spectrometry Data with Global Natural Products Social Molecular Networking." *Nature Publishing Group*. <https://doi.org/10.1038/nbt.3597>.
- Wang, Xiaoxia, Rui Guo, Mingxia Li, Yuan Liu, Mingli Zhao, · Hui Fu, Xueying Liu, Shiyao Wang, and Lianxuan Shi. 2019. "Metabolomics Reveals the Drought-Tolerance Mechanism in Wild Soybean (Glycine Soja)" 41: 161. <https://doi.org/10.1007/s11738-019-2939-1>.
- Warinowski, Tino, Sanna Koutaniemi, Anna Kärkönen, Ilari Sundberg, Merja Toikka, Liisa Kaarina Simola, Ilkka Kilpeläinen, and Teemu H. Teeri. 2016. "Peroxidases Bound to the Growing Lignin Polymer Produce Natural like Extracellular Lignin in a Cell Culture of Norway Spruce." *Frontiers in Plant Science* 7 (OCTOBER2016): 215595. <https://doi.org/10.3389/FPLS.2016.01523/BIBTEX>.
- Warren, Charles R., Ismael Aranda, and F. Javier Cano. 2012. "Metabolomics Demonstrates Divergent Responses of Two Eucalyptus Species to Water Stress." *Metabolomics* 8 (2): 186–200. <https://doi.org/10.1007/s11306-011-0299-y>.
- Wedeking, Rita, Mickaël Maucourt, Catherine Deborde, Annick Moing, Yves Gibon, Heiner E. Goldbach, and Monika A. Wimmer. 2018. "1H-NMR Metabolomic Profiling Reveals a Distinct Metabolic Recovery Response in Shoots and Roots of Temporarily Drought-Stressed Sugar Beets." *PLoS ONE* 13 (5): 1–21. <https://doi.org/10.1371/journal.pone.0196102>.
- Wei T, Simko V. 2021. "R Package 'Corrplot': Visualization of a Correlation Matrix. (Version 0.92)." <https://doi.org/https://github.com/taiyun/corrplot>.
- Wellstein, Camilla, Peter Poschlod, Andreas Gohlke, Stefano Chelli, Giandiego Campetella, Sergey Rosbakh, Roberto Canullo, Jürgen Kreyling, Anke Jentsch, and Carl Beierkuhnlein. 2017. "Effects of Extreme Drought on Specific Leaf Area of Grassland Species: A Meta-Analysis of Experimental Studies in Temperate and Sub-Mediterranean Systems." *Global Change Biology* 23 (6): 2473–81. <https://doi.org/10.1111/gcb.13662>.
- Weng, Jing Ke. 2014. "The Evolutionary Paths towards Complexity: A Metabolic Perspective." *The New Phytologist* 201 (4): 1141–49. <https://doi.org/10.1111/NPH.12416>.
- White, Hannah J., Willson Gaul, Lupe León-Sánchez, Dinara Sadykova, Mark C. Emmerson, Paul Caplat, and Jon M. Yearsley. 2021. "Ecosystem Stability at the Landscape Scale Is Primarily Associated with Climatic History." *Functional Ecology* 00 (October): 1–13. <https://doi.org/10.1111/1365-2435.13957/SUPPINFO>.
- White, Hannah J., Willson Gaul, Lupe León-Sánchez, Dinara Sadykova, Mark C. Emmerson, Paul Caplat, and Jon M. Yearsley. 2022. "Ecosystem Stability at the Landscape Scale Is Primarily Associated with Climatic History." *Functional Ecology* 36 (3): 622–34. <https://doi.org/10.1111/1365-2435.13957>.
- Wickham H, François R, Henry L, Müller K, Vaughan D. 2023. "Dplyr: A Grammar of Data Manipulation." <https://dplyr.tidyverse.org>.
- Wickham, Hadley. 2016. "Data Analysis." In *Ggplot2*, 189–201. Springer.
- Wickham, Hadley, Romain François, Lionel Henry, Kirill Müller, and Davis Vaughan. 2023. "Dplyr: A Grammar of Data Manipulation."

Bibliography

- Wijayawardene, Nalin N., Kevin D. Hyde, and Dong Qin Dai. 2021. "Outline of Ascomycota." *Encyclopedia of Mycology: Volume 1,2 1* (January): 246–54. <https://doi.org/10.1016/B978-0-12-819990-9.00064-0>.
- Wiley, Erin, and Brent Helliker. 2012. "A Re-Evaluation of Carbon Storage in Trees Lends Greater Support for Carbon Limitation to Growth." *New Phytologist* 195 (2): 285–89. <https://doi.org/10.1111/j.1469-8137.2012.04180.x>.
- Woodward, F I, and A D Diament. 1991. "Functional Approaches to Predicting the Ecological Effects of Global Change." *Functional Ecology* 5 (2): 202–12. <https://doi.org/10.2307/2389258>.
- Wright, A. J., L. Mommer, K. Barry, and J. van Ruijven. 2021. "Stress Gradients and Biodiversity: Monoculture Vulnerability Drives Stronger Biodiversity Effects during Drought Years." *Ecology* 102 (1). <https://doi.org/10.1002/ecy.3193>.
- Wu, Qian, Xu Zhang, Marta Peirats-Llobet, Borja Belda-Palazon, Xiaofeng Wang, Shao Cui, Xiangchun Yu, Pedro L. Rodriguez, and Chengcai An. 2016. "Ubiquitin Ligases RGLG1 and RGLG5 Regulate Abscisic Acid Signaling by Controlling the Turnover of Phosphatase PP2CA." *The Plant Cell* 28 (9): 2178. <https://doi.org/10.1105/TPC.16.00364>.
- Wurst, Susanne, and Takayuki Ohgushi. 2015. "Do Plant-and Soil-Mediated Legacy Effects Impact Future Biotic Interactions?" <https://doi.org/10.1111/1365-2435.12456>.
- Xia, Jianguo, Nick Psychogios, Nelson Young, and David S. Wishart. 2009. "MetaboAnalyst: A Web Server for Metabolomic Data Analysis and Interpretation." *Nucleic Acids Research* 37 (suppl_2): W652–60. <https://doi.org/10.1093/NAR/GKP356>.
- Xu, Zhen Zhu, and Guang Sheng Zhou. 2006. "Combined Effects of Water Stress and High Temperature on Photosynthesis, Nitrogen Metabolism and Lipid Peroxidation of a Perennial Grass *Leymus Chinensis*." *Planta* 224 (5): 1080–90. <https://doi.org/10.1007/S00425-006-0281-5/TABLES/1>.
- Xu, Zhenzhu, Guangsheng Zhou, and Hideyuki Shimizu. 2010. "Plant Responses to Drought and Rewatering." *Plant Signaling and Behavior* 5 (6): 649–54. <https://doi.org/10.4161/psb.5.6.11398>.
- Yamada, Kenta, Koji Yamaguchi, Satomi Yoshimura, Akira Terauchi, and Tsutomu Kawasaki. 2017. "Conservation of Chitin-Induced MAPK Signaling Pathways in Rice and Arabidopsis." *Plant and Cell Physiology* 58 (6): 993–1002. <https://doi.org/10.1093/PCP/PCX042>.
- Yang, Fan, Chunyu Han, Zhen Li, Yangnan Guo, and Zhulong Chan. 2015. "Dissecting Tissue- and Species-Specific Responses of Two *Plantago* Species to Waterlogging Stress at Physiological Level." *Environmental and Experimental Botany* 109: 177–85. <https://doi.org/10.1016/j.envexpbot.2014.07.011>.
- Yang, Yaodong, Mumtaz Ali Saand, Liyun Huang, Walid Badawy Abdelaal, Jun Zhang, Yi Wu, Jing Li, Muzafar Hussain Sirohi, and Fuyou Wang. 2021. "Applications of Multi-Omics Technologies for Crop Improvement." *Frontiers in Plant Science* 12 (September): 1–22. <https://doi.org/10.3389/fpls.2021.563953>.
- Ye, Haiyan, Hao Du, Ning Tang, Xianghua Li, and Lizhong Xiong. 2009. "Identification and Expression Profiling Analysis of TIFY Family Genes Involved in Stress and Phytohormone Responses in Rice." *Plant Molecular Biology* 71 (3): 291–305. <https://doi.org/10.1007/S11103-009-9524-8/METRICS>.

Bibliography

- Yin, Mingzhu, Yanping Wang, Lihua Zhang, Jinzhu Li, Wenli Quan, Li Yang, Qingfeng Wang, and Zhulong Chan. 2017. "The Arabidopsis Cys2/His2 Zinc Finger Transcription Factor ZAT18 Is a Positive Regulator of Plant Tolerance to Drought Stress." *Journal of Experimental Botany* 68 (11): 2991–3005. <https://doi.org/10.1093/JXB/ERX157>.
- Yobi, Abou, Bernard W.M. Wone, Wenxin Xu, Danny C. Alexander, Lining Guo, John A. Ryals, Melvin J. Oliver, and John C. Cushman. 2013. "Metabolomic Profiling in Selaginella Lepidophylla at Various Hydration States Provides New Insights into the Mechanistic Basis of Desiccation Tolerance." *Molecular Plant* 6 (2): 369–85. <https://doi.org/10.1093/MP/SSS155>.
- Young, Ellen, Manus Carey, Andrew A. Meharg, and Caroline Meharg. 2018. "Microbiome and Ecotypic Adaption of *Holcus Lanatus* (L.) to Extremes of Its Soil PH Range, Investigated through Transcriptome Sequencing." *Microbiome* 6 (1): 48. <https://doi.org/10.1186/s40168-018-0434-3>.
- Young, Matthew D., Matthew J. Wakefield, Gordon K. Smyth, and Alicia Oshlack. 2010. "Gene Ontology Analysis for RNA-Seq: Accounting for Selection Bias." *Genome Biology* 11 (2): 1–12. <https://doi.org/10.1186/GB-2010-11-2-R14/TABLES/4>.
- Yu, Lujun, Di Liu, Shiyi Chen, Yangshuo Dai, Wuxiu Guo, Xue Zhang, Linna Wang, et al. 2020. "Evolution and Expression of the Membrane Attack Complex and Perforin Gene Family in the Poaceae." *International Journal of Molecular Sciences* 21 (16): 1–20. <https://doi.org/10.3390/ijms21165736>.
- Yu, Shen, and Joan G. Ehrenfeld. 2009. "The Effects of Changes in Soil Moisture on Nitrogen Cycling in Acid Wetland Types of the New Jersey Pinelands (USA)." *Soil Biology and Biochemistry* 41 (12): 2394–2405. <https://doi.org/10.1016/J.SOILBIO.2009.06.012>.
- Zandalinas, Sara I, Ron Mittler, Damián Balfagón, Vicent Arbona, and Aurelio Gómez-Cadenas. 2018. "Plant Adaptations to the Combination of Drought and High Temperatures." *Physiologia Plantarum* 162: 2–12. <https://doi.org/10.1111/ppl.12540>.
- Zeiter, Michaela, Sara Schärer, Roman Zweifel, David M Newbery, and Andreas Stampfli. 2016. "Timing of Extreme Drought Modifies Reproductive Output in Semi-Natural Grassland." *Journal of Vegetation Science* 27 (2): 238–48. <https://doi.org/https://doi.org/10.1111/jvs.12362>.
- Zeppel, M. J.B., J. V. Wilks, and J. D. Lewis. 2014. "Impacts of Extreme Precipitation and Seasonal Changes in Precipitation on Plants." *Biogeosciences* 11 (11): 3083–93. <https://doi.org/10.5194/bg-11-3083-2014>.
- Zhang, Lu, and Donald F. Becker. 2015. "Connecting Proline Metabolism and Signaling Pathways in Plant Senescence." *Frontiers in Plant Science* 6 (JULY): 1–8. <https://doi.org/10.3389/fpls.2015.00552>.
- Zhang, Meng, Rivka Barg, Mingan Yin, Yardena Gueta-Dahan, Alicia Leikin-Frenkel, Yehiam Salts, Sara Shabtai, and Gozal Ben-Hayyim. 2005. "Modulated Fatty Acid Desaturation via Overexpression of Two Distinct Omega-3 Desaturases Differentially Alters Tolerance to Various Abiotic Stresses in Transgenic Tobacco Cells and Plants." *The Plant Journal: For Cell and Molecular Biology* 44 (3): 361–71. <https://doi.org/10.1111/J.1365-313X.2005.02536.X>.
- Zhang, Qinbin, Hui Liu, Xiaolin Wu, and Wei Wang. 2020. "Identification of Drought Tolerant Mechanisms in a Drought-Tolerant Maize Mutant Based on Physiological,

- Biochemical and Transcriptomic Analyses.” *BMC Plant Biology* 20 (1): 1–14. <https://doi.org/10.1186/S12870-020-02526-W/FIGURES/7>.
- Zhao, Bo, Zhengyao Shao, Likai Wang, Fan Zhang, Daveraj Chakravarty, Wei Zong, Juan Dong, Liang Song, and Hong Qiao. 2022. “MYB44-ENAP1/2 Restricts HDT4 to Regulate Drought Tolerance in Arabidopsis.” *PLOS Genetics* 18 (11): e1010473. <https://doi.org/10.1371/JOURNAL.PGEN.1010473>.
- Zhao, Daqiu, Yuting Luan, Wenbo Shi, Xiayan Zhang, Jiasong Meng, and Jun Tao. 2021. “A Paeonia Ostii Caffeoyl-CoA O-Methyltransferase Confers Drought Stress Tolerance by Promoting Lignin Synthesis and ROS Scavenging.” *Plant Science* 303 (February): 110765. <https://doi.org/10.1016/J.PLANTSCI.2020.110765>.
- Zhao, Yuanyuan, Zhifeng Liu, and Jianguo Wu. 2020. “Grassland Ecosystem Services: A Systematic Review of Research Advances and Future Directions.” *Landscape Ecology* 35 (4): 793–814. <https://doi.org/10.1007/s10980-020-00980-3>.
- ZHONG, HAILIN, and ANDRÉ LAUCHLI. 1993. “Changes of Cell Wall Composition and Polymer Size in Primary Roots of Cotton Seedlings Under High Salinity.” *Journal of Experimental Botany* 44 (4): 773–78. <https://doi.org/10.1093/jxb/44.4.773>.
- Zhu, Jian Kang. 2016. “Abiotic Stress Signaling and Responses in Plants.” *Cell* 167 (2): 313–24. <https://doi.org/10.1016/J.CELL.2016.08.029>.
- Zi, Lin, Albert Gargallo-garriga, Michal Oravec, Hamada Abdelgawad, Ivan Nijs, Hans J De Boeck, Simon Reynaert, et al. 2023. “Ecometabolomic Analysis of the Effect of More Persistent Precipitation Regimes Reveals Common and Tolerance Related Metabolic Adjustments in Four Grassland Species.” *Environmental and Experimental Botany* 215 (August): 105489. <https://doi.org/10.1016/j.envexpbot.2023.105489>.